University of Stavanger

Faculty of Science and Technology

MASTER'S THESIS

Study program/ Specialization: Offshore Technology/ Subsea Technology	Spring semester, 2013 Open / ~~Restricted access~~
Writer: Indra Permana	..... (Writer's signature)

Faculty supervisor:
Dr. Daniel Karunakaran (Adjunct Professor)
(University of Stavanger, Subsea 7 Norway)

External supervisor(s):
Dr. Dasharatha Achani (Subsea 7 Norway)

Title of thesis:

A Study on Engineering Critical Assessment (ECA) of Subsea Pipeline Girth Welds for Reeling Installation

Credits (ECTS):
30

Key words: ECA, CTOD, J-Integral, Reeling Installation, pipeline, LINKpipe, CRACKWISE, Fracture Mechanics, Girth Welds, clad pipes.	Pages: xxiv + 112 + attachment/other: 74 Stavanger, June 15, 2013 Date/year

ABSTRACT

Reeling is offshore pipeline installation method which delivers fast and cost effective pipeline laying. Each of the pipeline segment are welded onshore, the long section of pipeline then spooled onto a large diameter of reel. However, reeling installation method causes large plastic strain to the pipeline girth welds. Due to the existing cracks commonly found in the girth welds, the plastic strain will cause possible crack growth.

To derive the acceptance criteria for pipeline girth weld defects and sustain the integrity of pipeline during reeling installation, an Engineering Critical Assessment (ECA) is required.

The objective of this thesis is to perform Engineering Critical Assessment (ECA) of pipeline girth welds during reeling installation particularly in spooling on and reeling off stages using LINKpipe and CRACKWISE software and also to perform the ECA for clad/lined pipes using LINKpipe.

CRACKWISE is one of the software that can be used for the flaw assessment of pipeline girth welds during reeling installation. In order to reduce the conservatism of existing failure assessment methods, SINTEF recently have developed a new failure assessment approach which depends on finite element calculations of pipeline model.

LINKpipe is based on four-node ANDES shell elements and a non-linear line-spring element. The software established an efficient and adequately accurate model even for large level of strain, thus it has potential as an alternative ECA tool for pipelines subjected to plastic strains. Moreover, the new bi-metallic shell elements that were developed in LINKpipe making it capable analyzing defect assessments on clad and lined pipes.

Based on the analyses performed for the thesis work the influence of misalignment for the critical crack size curve is less significant compared to the effect of residual stress. On the contrary, pipe misalignment in LINKpipe ECA simulations can show the effect of increasing the Crack Driving Force very significantly, which makes the critical crack size, became smaller. Whereas the residual stress showed little influence in the prediction of the critical crack size using LINKpipe.

When the maximum possible misalignment (which is 1.95mm) along with the residual stress is applied, the critical crack size curves resulted from CRACKWISE and LINKpipe, are relatively close to each other. However, CRACKWISE tends to be conservative for long crack lengths (>90mm) compared to LINKpipe, whereas for short crack lengths (<90mm) CRACKWISE yields less conservative critical crack sizes.

Key words : ECA, CTOD, J-Integral, Reeling Installation, pipeline, LINKpipe, CRACKWISE, Fracture Mechanics, Girth Welds, clad pipes.

ACKNOWLEDGEMENT

This thesis is the final work to fulfill the requirement for Master of Science degree in the Offshore Technology at the Department of Mechanical and Structural Engineering and Materials Science, Faculty of Science and Technology, University of Stavanger, Norway. This thesis work is carried out in the premises of the company, Subsea7 Norway during spring, academic year 2013.

I would like to acknowledge and express my sincere gratitude to the following persons who have made the completion of this thesis possible:

My faculty supervisor, Dr. Daniel Karunakaran (Adjunct Professor), for giving me the opportunity to work for the thesis under his supervision, and also for his advice, guidances and support.

My supervisor from Subsea7, Dr. Dasharatha Achani, for his guidances, support, his willingness to spend time to review the thesis. His advice and knowledge are very valuable for this thesis.

Dr. Zhengmao Yang from Subsea7, for his advice and valuable discussion during the thesis work.

Subsea7 Norway, for providing me an office space, computer system, full support and access to the software used for the thesis work.

My loving, supportive, encouraging, and patient wife, Rika Afriana for her endless support, prayers and help. This thesis would not have been possible without her contributions.

Last but not least, I would like to thank my family in Indonesia, my mother, my brother and sister for their love, prayers and support.

Stavanger, 15th June 2013

Indra Permana

TABLE OF CONTENTS

LIST OF FIGURES

LIST OF TABLES

DEFINITION OF SYMBOLS

SYMBOL - LATIN CHARACTERS

a	Crack depth
A	Area
a_0	Initial crack depth
A_0	Original cross sectional area
a_{eff}	Effective crack tip
a_g	Limit tearing flaw extension
a_j	Intermediate value of tearing flaw extension
B	Specimen Width
BM	Base Material
c	Half of the crack length
C	Clad Layer
C_1, C_2	Fitting parameter in crack growth resistance equation
C_e	The elastic compliance
CTOD	Crack Tip Opening Displacement
d_n	A dimensionless constant
e_{yo}	Reference Strain,
E	Elastic modulus of the material
E’	Young’s modulus for plane strain
F_w	Finite width correction factor
FW	Filler Weld
G	The strain-energy release rate
H	The length of the specimen between the grips
H_s	Significant Wave Height
J	The elastic-plastic field in the vicinity of at the crack tip
J_e	Elastic part of the J-Integral
J_p	Plastic part of the J-Integral
J_{p0}	Plastic part of the J-Integral without crack growth correction
K	Stress Intensity Factor
K_c	Critical stress intensity factor
K_I	The stress intensity factor (Mode I - tensile opening load)
K_m	Misalignment

K_{mat}	Material toughness measured by stress intensity factor
K_r	Fracture ratio of applied elastic K value to Kmat
K_t	Elastic stress concentration factor (SCF)
$K_{tm/tb}$	Membrane/bending stress SCF
L	Width of girth weld cap
L_r	Ratio of applied load to yield load
$L_{r\ max}$	The cut off level
m	Constraint parameter according to ASTM E1290-02
$M_{km/kb}$	Membrane/bending stress intensity magnification factors for weld toe
$M_{m/b}$	Membrane/bending stress intensity magnification factors
n	Strain Hardening Exponent
OD	Pipe Outside Diameter
OW	Overlay Weld
P	Tension Load
P_b	Primary bending stress
P_m	Primary membrane stress
PP	Parent Pipe
Q_b	Secondary bending stress
Q_m	Secondary membrane stress
r	The distance in front of the crack tip
r_c	Radius of the cylinder
RH	Root/hot passes
R_{reel}	Reel drum radius
r_y	The distance between actual and effective crack tip
s	Arc length along Γ
S	Nominal stress (excluding SCF)
s_{yo}	Reference Stress,
T and t	Wall thickness of the pipes on each side of the girth weld, T > t
$\vec{T}$	The force vector normal to Γ
t_c	Overall coating thickness
T_{Sw}	Tensile strength of the weld filler metal
T_{Spp}	Tensile strength of the parent pipe material
$\vec{u}$	The displacement vector
U	The pseudopotential energy
U_p	The plastic part of the area under the load vs. CMOD curve
UTS	The tensile strength at the test temperature
v	Poisson's ratio

w	The strain-energy density
W	Plate Thickness
WM	Weld Metal
WT	Wall Thickness
x	The fraction of the length of the localized ligament deformation passing through the weld metal
y	The fraction of the length of the localized ligament deformation passing through the clad material
YS	The engineering yield stress at test temperature
Y_{Sw}	Yield strength of the weld filler metal
Y_{Spp}	Yield strength of the parent pipe material
$(Y\sigma)_p$	Contributions from primary stresses
$(Y\sigma)_s$	Contributions from secondary stresses

SYMBOL - GREEK CHARACTERS

α	Elastic parameter
Γ	Any contour surrounding the crack tip
δ	The displacement at the crack tip
δ_{mat}	Material toughness measured by CTOD method
$\delta_t + \delta_m$	Eccentricities from wall thickness differences and misalignment
Δa	Tearing Length
$\Delta\sigma_b$	Bending component of stress range
$\Delta\sigma_m$	Membrane component of stress range
ε_1	Actual strain (including SCF)
ε_{nom}	Nominal strain (excluding SCF)
$\varepsilon_{1,nom}$	Total Nominal Strain
ε_C	Strain where stress-strain curve of the weld filler metal crosses the stress-strain curve of the parent pipe
ε_p	Accumulated Plastic Strain
ε_{pl}	True Plastic strain
$\varepsilon_{TS,W}$	Strain value at tensile strength of the weld filler metal
$\varepsilon_{TS,PP}$	Strain value at tensile strength of the parent pipe material

η_p	Dimensionless function of the geometry
v	Crack opening displacement
ρ	A plasticity correction factor
$\sigma_{BM}(\varepsilon)$	The stress strain curve for the base material
σ_C	Stress where stress-strain curve of the weld filler metal crosses the stress-strain curve of the parent pipe
$\sigma_{clad}(\varepsilon)$	The stress-strain curve for the clad material
$\sigma_{eff}(\varepsilon)$	The equivalent stress strain curve
$\sigma_{WM}(\varepsilon)$	The stress strain curve of the weld material
σ	Stress Level
σ_1	Actual stress (including SCF)
σ_o	Initial yield stress
σ_e	Engineering Stress
σ_L	Lower Yield Stress
σ_t	True Stress
σ_U	Lower Yield Stress
σ'_Y	The appropriate material yield strength at the given temperature for analysis
σ_{yy}	The local stress near the crack tip
σ_{ys}	Yield Strength
σ_{uts}	Ultimate Tensile Strength
σ'_f	The appropriate flow strength

1. INTRODUCTION

1.1 Background

Reeling is offshore pipeline installation method (**Figure 1.1**) which delivers fast and cost effective pipeline laying. Each of the pipeline segment are welded onshore, the long section of pipeline then spooled onto a large diameter of reel.

The reductions in terms of installation time and overall cost is possible due to the continuity of the method and all of the fabrication processes such as assembly, welding, inspection, and coating was completed on shore.

However, reeling installation method caused large plastic strain to the pipeline girth welds. Due to the existing cracks commonly found in the girth welds, the plastic strain will cause possible crack growth. To derive the acceptance criteria for pipeline girth weld defects and sustain the integrity of pipeline during reeling installation, an Engineering Critical Assessment (ECA) is required. ECA is based on fracture mechanics and has the objective to generate the allowable cracks size in the girth welds.

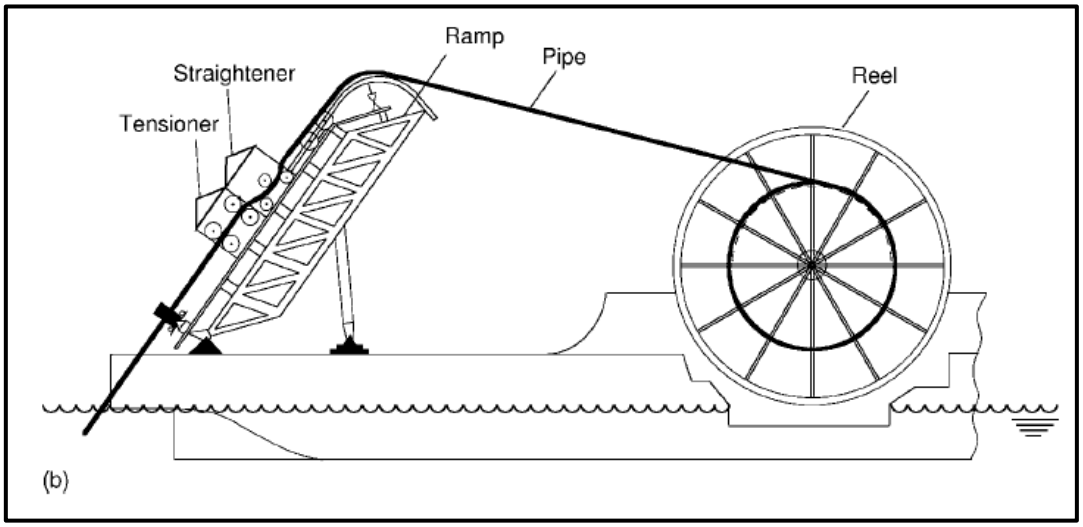

Figure 1.1 Configuration of pipeline reeling installation (Ref., photograph courtesy Technip cited in Kyriakides, 2007).

ECA can be conducted as described in several standards such as BS7910 (Guide to methods for assessing the acceptability of flaws in metallic structures), DNV-OS-F101 Appendix A (Structural Integrity of Girth Welds in Offshore Pipelines) and DNV-RP-F108 (Fracture Control for Pipeline Installation Methods Introducing Cyclic Plastic Strain).

BS7910 is a common industry practice for flaw assessment procedures. However, BS7910 is not developed for pipeline condition with large plastic strain. The recommended practice DNV-RP-F108 is therefore established to provide guidance for defect assessment of pipeline subjected to cyclic plastic strain e.g. reeling installation method. CRACKWISE is one of the software that can be used for the flaw assessment of pipeline girth welds during reeling installation. In order to reduce the conservatism of existing failure assessment methods, SINTEF recently have developed a new failure assessment approach which depends on finite element calculations of pipeline model.

LINKpipe is based on four-node ANDES shell elements and a non-linear line-spring element (*Olsø* et al., 2008). The software established an efficient and adequately accurate model even for large level of strain, thus it has potential as an alternative ECA tool for pipelines subjected to plastic strains.

The implementation of clad/lined pipes combined with reeling installation is considered to be cost effective in situation where the products transported through pipeline are highly corrosive. Clad pipe is pipeline in which the CRA (Corrosion Resistance Alloy) metallurgically bonded to the backing steel, whereas lined pipe is pipeline in which the CRA is mechanically bonded to the backing steel.

The new feature from LINKpipe to assess defects in clad/lined pipes is very useful for the present industry. The new bi-metallic shell elements that were developed in LINKpipe making it capable analyzing defect assessments on clad and lined pipes which is not covered by former method.

1.2 Problem Description

The thesis emphasizes on the Engineering Critical Assessment for pipeline subjected to plastic strain deformation during reeling installation and determining the acceptable flaw size in girth welds. It is important to remark some of the challenges for the assessments:

1. Defects in the pipeline Girth welds is a common occurrence and it can be a big challenges for pipeline integrity assessments, especially when the pipeline subjected to large plastic strain in order of ~2% during reeling installation (Espen et al., 2007);
2. Traditional ECA procedure tend to yield “over-conservative” results and the assessment of pipeline girth welds subjected to plastic strain may have very small acceptable defect size for weld flaws (Cosham and Macdonald, 2008);
3. There is currently no common recognized ECA procedure for clad and lined pipes subjected to plastic strain (Olsø et al., 2011);
4. Clad pipes have common problem of partial weld undermatch in which the weld metal will undermatching the base metal (Olsø et al., 2011);
5. There are several conditions that have to consider in the ECA analysis such as misalignment at the girth welds, effect of weld residual stress, and strength mismatch between base metal and weld metal.

1.3 Thesis Objectives

The objective of this thesis is to perform Engineering Critical Assessment (ECA) of pipeline girth welds during reeling installation particularly in spooling on and reeling off stages using LINKpipe and CRACKWISE software.

The Scopes of this thesis are as follows:

1. To perform ECA analyses using the tools CRACKWISE and LINKpipe and compare the results;
2. To carry out sensitivity analyses considering misalignment at the girth welds, effect of weld residual stress, and strength mismatch between base and weld metal in LINKpipe;
3. To perform an ECA for clad/lined pipes using LINKpipe and discuss the results against those from previous work.

1.4 Outline of Thesis

The outline of the thesis is describes as follows:

Chapter 2: (State of the art)

Contains all the relevant publications of existing developments related to ECA for subsea pipelines during reeling installation with the corresponding citations.

Chapter 3: (Theoretical Background)

The chapter includes theoretical background relevant for ECA for subsea pipelines.

Chapter 4: (Modeling Tools)

The chapter includes general description of modeling tools (LINKpipe and CRACKWISE) used in the analyses.

Chapter 5: (Analysis Methodology)

The chapter describes the analysis methodology using CRACKWISE and LINKpipe for ECA of Pipelines.

Chapter 6: (Case Study)

The chapter describes the case study including the necessary input such as geometrical properties and material characteristics for ECA analysis.

Chapter 7: (Results and Discussion)

The chapter presents and compares the results of the ECA from both CRACKWISE and LINKpipe tools. Also it includes the sensitivity analyses performed by considering the properties of geometrical and material mismatch.

Chapter 8: (Conclusion and Further Work)

The chapter presents the conclusions from the current work and discusses the further work.

2. STATE OF THE ART

2.1 Reeling Installation

2.1.1 General

Reeling is one of the most efficient offshore pipeline installation methods. In this method several miles long of pipeline from spool base is spooled onto a large diameter of a reel located on the vessel. In the installation sites the vessel installs the pipeline by constantly spooling off the pipeline from the reel drum. In case of the reeling installation, all of the pipeline fabrication processes such as assembly, welding, inspection, and coating are completed on shore. This makes possible the reductions in terms of installation time and overall cost due to the continuous laying process.

Main characteristics of the reeling vessel listed in **Table 2.1**.

Table 2.1 Main Characteristics of Reeling Vessels (Ref., Kyriakides, 2007)

Specs	Apache	Chickasaw	Deep Blue	Hercules	Skandi Navica	Seven Ocean
Reel Type	Vertical	Horizontal	Vertical (2)	Horizontal	Vertical	Vertical
Reel Radius (ID, m)	8.23	6.1 (7.2)	9.75	9	7.5	9
Flange Radius (m)	12.5	12.2		17.5	12.5	14
Reel Width (m)	6.5	3.35		7	6.7	10
Ramp Radius (m)	10	*	9	*	-	9
Pipe Capacity (ton)	2,000	2,500	2,500 x 2	6,500	2,500	3,500
Pipe Diameters (in)	4-16	2-12.75	4-18	4-18	4-16	4-16
Tension/Reel (ton)	84-128	-		-	100	100
Tension/Tensioner (ton)	72	82	275 x 2	544	37	400
Date of Operation (ton)	1979	1970	2001	2001	2001	2007

*Pipe reverse bent to approximately the yield curvature.

The mechanism of spooling and unspooling initiates certain bending curvature in pipeline. This causes the pipeline to undergo into plastic deformation. For example, as stated in Kyriakides (2007), in the case of Apache reel with 8.23m radius, a 12-inch pipeline subjected to bending is deformed to maximum strain of 1.93% and 16-inch pipeline to the strain of 2.41%. Hence, to avoid local buckling, wall thickness and mechanical properties of a pipeline shall be chosen properly.

In general, concrete pipeline coating can't be used in the reeling processes. Relatively thick wall thickness is required to avoid the pipe flattening and provide additional weight for pipeline stability (Mousselli, 1981).

According to Mousselli (1981), the advantages and disadvantages for reeling installation method are described below.

The advantages of reeling installation method include:

a. Improved manufacturing control at the spool base;
b. Reduced consequences of bad weather condition due to fast installation speed;
c. Minimum preparation to assemble and spooling various sizes of pipes for continuous installation;
d. It can also be used for pipeline bundles.

Main disadvantages of reeling installation method include:

a. Maximum pipeline size is limited up to 16-inch diameter;
b. Relatively thick wall thickness is required;
c. Limited length of pipeline can be reeled based on the capacity of reel.

Figure 2.1 Typical onshore manufacturing site for reeling installation (spoolbase) (Ref., Pipeline and Riser Lecture notes, UiS, 2012).

A typical onshore manufacturing site or spoolbase can be seen in **Figure 2.1**. Generally it has the assembly workshop which hosts one or two assembly lines. Each of workshops is

equipped with several stations such as beveling station, welding station, Non-Destructive Testing (NDT) and field joint coating stations.

In order to ensure high quality welds and low rejection rates, the assembly operation is carried out in clean and controlled environment. A number of welding techniques can be performed in a several welding stations such as manual or mechanized welding techniques. Furthermore, many NDE (Non Destructive Examination) methods from standard radiography to Automatic Ultrasonic Testing (AUT) can be performed to provide the accurate measurement of defect size (Denniel, 2009).

One of the pipeline design concerns for reeling installation is the girth welds. Inadequate strength in the girth weld could cause failure during reeling operations. The most important measure to avoid this failure is to select the strain tolerant welding material and implement it in welded connections. The common practice is to use the welding material that overmatch the pipeline properties, as stated in the DNV Rules for pipelines subjected to plastic strain. Based on DNV Rules, an Engineering Critical Assessment (ECA) is required for the girth welds that subjected to strain exceeding 0.4% (Sriskandarajah, Jones and Bedrossian, 2003).

2.1.2 Reeling Mechanism

Pipeline is reeled onto a reel drum with certain radius that is placed on the vessel. During laying the pipeline unreeled from the reel drum and passes the delivery ramp with known diameter. **Figure 2.2** shows the typical configuration for pipe reeling. Conversion points means that a point at which the inelastic forward or reverse bend is conducted to the pipeline (Sriskandarajah, Jones and Bedrossian, 2003).

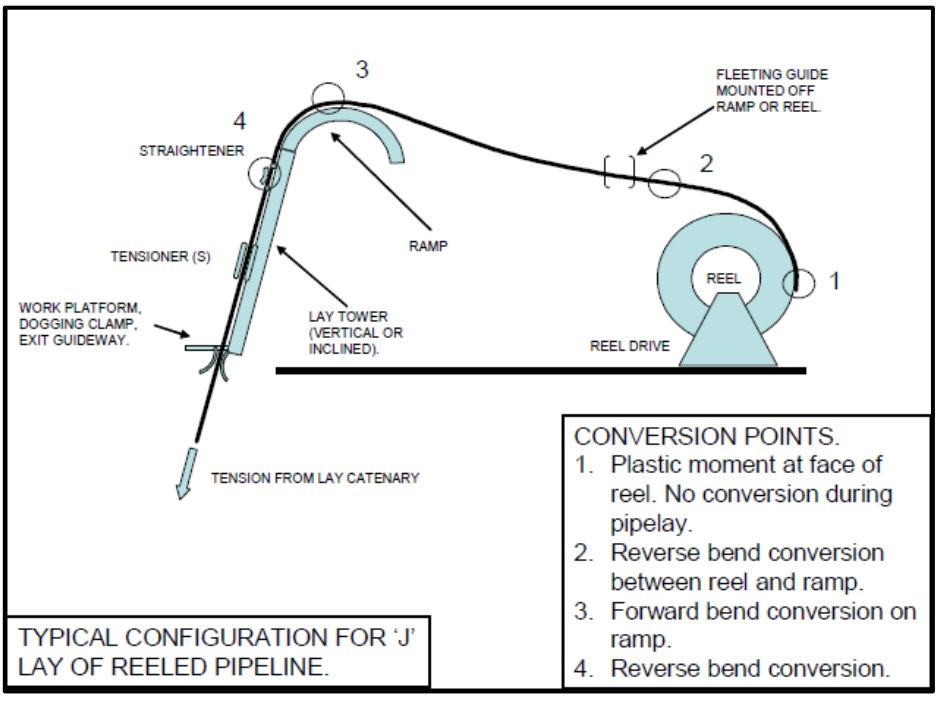

Figure 2.2 Typical configuration of pipeline reeling installation (Ref., Sriskandarajah, Jones and Bedrossian, 2003).

Figure 2.3 describes bending moment and curvature plot of the reeling process as presented in the work of Manouchehri, Howard and Denniel, (2008).

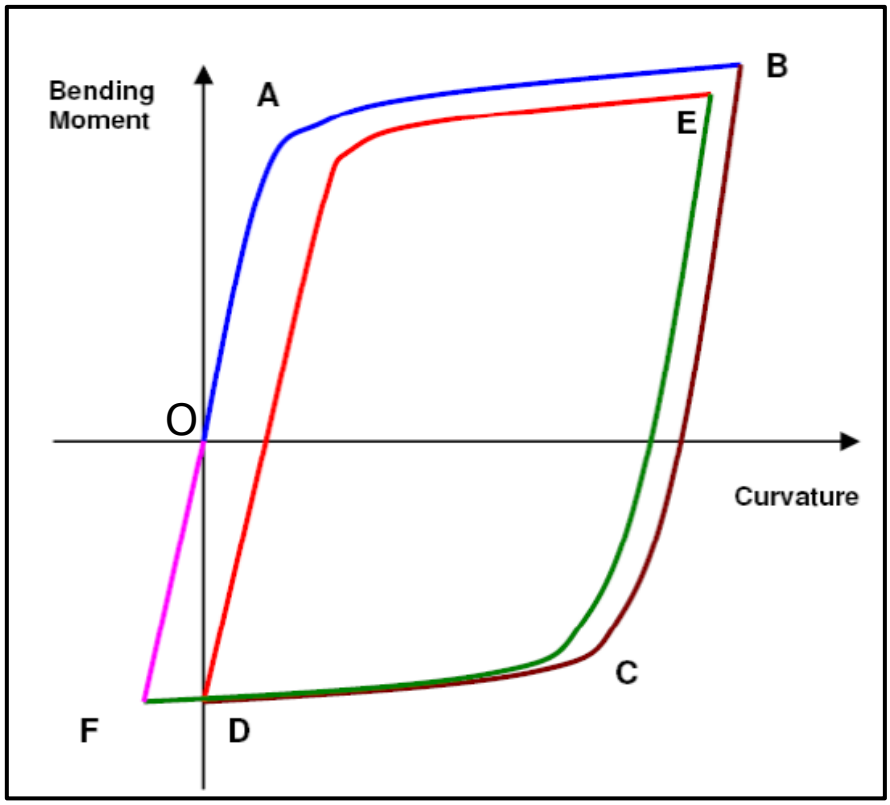

Figure 2.3 Bending moment and curvature curve of the reeling process (Ref., Manouchehri, Howard and Denniel, 2008).

Reeling process in the **Figure 2.3** encompasses five steps:

a. **Step 1**: The pipeline is spooled from the spool base onto the reel drum. Line OAB indicates the pipeline taken beyond the yield point (A) to a maximum curvature (B), equal to the radius of the reel drum. The radius of curvature increases as the reel drum slowly packed with pipeline.

b. **Step 2**: Line BCD shows the unspooling process of the pipeline. Line BCD indicates the pipeline goes into reverse plastic deformation with some residual curvature. Point D represent approximately straight pipeline due to self-weight and back tension, it span from the reel drum to the aligner.

c. **Step 3**: Line DE represent the pipeline is rolled over the aligner in the direction similar as with the first plastic deformation. In the point E, the pipeline curvature equal to the radius of the aligner.

d. **Step 4**: The pipeline is undergoes the reverse plastic bend indicated by Line EFO. It unloads elastically and experiences plastic deformation causing negative curvature

(Point F). The reverse curvature shall carefully select to make sure the pipeline physically straight (Point O).

According to Denniel, (2009) there are some key elements/requirements that establish the reeling is safe and "extremely reliable":

a. Reeling is a displacement controlled process. The pipeline is subjected to plastic bending with tension on the reel drum. However, the reel drum diameter limits the curvature that the pipeline can obtain.

b. The ductile and strain hardening are important properties for pipeline. The ductility is the ability of the pipeline to avoid wall thinning or necking, while strain hardening is defined as increased material strength beyond yield.

   The ductility is an important parameter which enables the pipeline under reeling to plastically deform to the strain level less than that at ultimate limit. Similarly, the strain hardening is also an important factor for providing good level of stability in the reeling operation by assuring uniform distribution of bending strains along pipeline. The strain hardening makes the bending moment needed to raise the curvature of the pipeline continuously increase even after it reaches the yield point.

   Generally, the level of strain hardening is described by the ratio of yield strength (YS) to Ultimate Tensile Strength (UTS). Good material stability under plastic deformation is indicated by having lower value of this ratio as it represents better resistance of the material over the yield.

c. The weld strength shall overmatch the strength of pipeline to assure that larger strain levels will not occur in the welds and that welds are strong points along the line.

According to Manouchehri, Howard and Denniel (2008), the nominal strain, ε_{nom} induced in a pipeline for a given outside diameter (OD), reel drum radius (R_{reel}), and overall coating thickness (t_c):

$$\varepsilon_{nom} = \frac{OD}{2R_{reel} + OD + 2t_c} \quad \text{.....(2.1)}$$

2.1.3 Reeling Installation of Clad and Lined Pipes

Clad and line pipes are being used in subsea applications for carrying corrosive fluids. For the corrosive fluids, mechanically bonded bimetal pipe is considered as a cheaper solution compared to other options such as solid corrosion resistant alloys or metallurgically cladded pipe. The combination of Reeling installation and mechanically lined pipe (Lined Pipe) is further considered as a cost effective solution for the corrosive fluids.

Installation of lined pipe using reeling method needs comprehensive analysis and testing:

- To verify the response of the pipe subjected to global plastic deformation under reeling process;

- To check the interaction between liner pipe and outer pipe and the capacity of the liner against acceptance criteria for local buckling.

There exist some challenges with regard to the reeling of lined pipes. According to Toguyeni and Banse (2012):

a. There is risk of local buckling (wrinkling) of the liner pipe when the mechanically lined pipe is in reeling process or global plastic deformation in bending;
b. In case of no internal pressure applied, the straightening process of the lined pipe lowers the magnitude of wrinkles but it cannot remove them completely;
c. The interfacial contact stress or gripping force between the carbon steel pipe and the CRA liner is reduces the magnitude of wrinkles but it cannot rule out the formation of the wrinkles;
d. Applying of minimum 30 bar of internal pressure in reeling process prevents the development of wrinkles.

2.2 ECA for Pipeline Girth Welds in Reeling Installation

Engineering Critical Assessment (ECA) and workmanship criteria are two acceptance levels for welding flaws. The workmanship acceptance levels for welding flaws in pipeline girth welds can be found in several guidelines such as BS 4515-1, API 1104 and DNV-OS-F101. These acceptance levels are not fitness-for purpose defect limits, but it clarifies what a "good welder" should be able to accomplish. Furthermore, ECA applies the fracture mechanics in order to ensure the weld integrity on a rational basis.

Mostly the ECA procedures were not applied in the older onshore and offshore pipelines. Lately, the ECA has been conducted widely since the latest pipeline designs are introduced higher complexities such as high-temperatures and pressures, plastic strain during installation, deep water installation, and aggressive internal conditions. Other reason is the use of transition technology application from the radiography to the Automatic Ultrasonic Testing (AUT). This is used as the main inspection method during construction and it produces the flaw sizing and information of location in 2-dimension (Macdonald and Cheaitani, 2010).

In the present industry practice, ECA is carried out along the subsea pipeline design work in order to analyze the acceptable flaws size in the girth weld. The ECA is carried out through all the phases of pipeline's life cycle from the installation until the end of the design life. Furthermore, the fracture mechanics based ECA is also used to evaluate the acceptable flaw sizes in structures i.e. "to demonstrate fitness-for-purpose".

Usually defects exist initially in the girth welds during the pipeline fabrication. The main purpose of applying ECA in the reeled rigid pipeline is to determine the largest bounding envelope of initial defect sizes (for depth and length of defect) that could be accepted for the given loading history in pipeline design life.

The basic procedure is to assume the existence of certain defect size in the girth welds and to carry out the ECA in order to ensure these defects are acceptable without resulting in fracture during the loading history of pipeline.

As the basis of ECA, fracture mechanics provides criticality predictions of structures with existing crack like defects, given:

1. Geometry (size, orientation and location of cracks, geometry of structure, etc.);
2. Material properties (tensile yield and strength, stress strain curve, weld metal mismatch, fracture toughness, tearing resistance, etc.);
3. Total loading history (from initial spooling onto vessel to end of design life conditions).

Steel structures that have a particular minimum ductility, such as rigid pipelines with existing defects in the girth welds, could fail by fracture during reeling installation. The failure during reeling installation can be induced by many mechanisms:

1. Extreme tearing during single action of high axial load (spooling/reeling);
2. Cyclic tearing, or so-called 'tear-fatigue', during the repeated actions of high axial load (spooling/reeling/straightening cycles) in plastic range;
3. High cycle fatigue or cyclic growth of cracks during higher frequency smaller amplitude cyclic loading (installation hold periods on vessel) in the elastic range.

In case of seamless rigid pipelines, preventing possible failure due to fracture is mainly concentrated in the girth welds. As was mentioned in the work from Subsea7 (2011), there need to be considered several features such as:

- The basic geometry and material data;
- Misalignment at the girth welds;
- Effect of weld residual stress;
- Evolution of stress-strain curve of parent material under reeling cycles;
- The effect of internal pressure.

2.2.1 Main Loading Condition on Rigid Pipeline in Reeling Installation

Two main load conditions that a rigid pipeline usually experiences during reeling installation are described below. Each of these loadings has large different characteristics with associated pipeline responses (Subsea7, 2011).

1. **Initial spooling onto vessel at spool base, and subsequent offshore reeling off with straightening on vessel, and installation.**

   In the spooling on and reeling off stages, pipeline is subjected to the high curvature associated with plastic deformation of the pipe material. This initiates hoop stresses in the pipe due to small level of ovalisation. Also, during these stages, the cyclic tearing mechanism takes place in the defects. Therefore, prediction and assessment of this cyclic tearing of the defects is the most important objective of the ECA. It should also be noted

that there are significant changes in the material stress-strain behavior and in the weld residual stresses during these stages.

2. **Installation fatigue during hold periods on vessel.**

   Fatigue during hold periods is induced by wave loading on vessel and pipeline. It causes relatively high frequency fluctuations in the pipe axial stresses just below the clamp on the vessel. This situation happen when pipeline is needed to be held on the vessel for certain period of time. Long exposure to this loading condition has to be avoided as it would cause excessive cyclic growth of the defects. The main characteristics of the loading are high cycle, low amplitude, loading in the elastic range.

2.2.2 Engineering Critical Assessment (ECA) Codes

The code, **BS 7910** outlines procedures in detail regarding how to carry out the Engineering Critical Assessment. The procedures are mainly stress based and the codes could not directly be applied to the strain-based situations. As a general standard, BS7910 is also supplemented by additional guidance in pipeline design codes and standards.

The design code, **DNV-RP-F108** was established to provide guidelines for ECAs of girth welds subjected to cyclic plastic strains during installation. It introduced the constraint matched Single Edge Notch Tension (SENT) fracture mechanics specimen design. SENT specimen developed for pipeline girth welds assessment.

The code, **DNV-OS-F101** provides additional guidelines for operation and installation methods, involving plastic strain in the pipeline, such as reeling which introduce several cycles of tensile and compressive plastic deformation.

In accordance with **DNV-OS-F101**, Section 5 D1100 (Fracture and supplementary requirement P), it is stated that pipeline systems shall have adequate resistance to unstable fracture. **Table 2.2** summarizes the requirements of unstable fracture against the safety as described in Table 5-10 from Section 5 D1100, DNV-OS-F101. The parameters $\varepsilon_{1,nom}$ and ε_p in the table are referred as total nominal strain and accumulated plastic strain, respectively.

Supplementary requirement (P) refers to line pipe for plastic deformation (Section 7 I300, DNV-OS-F101). The main objective of supplementary requirement (P) is to ensure that the material has sufficient properties after being subject to plastic deformation, and that the material has sufficient ductility.

Section 10E from DNV-OS-F101 (check) gives additional requirements for pipeline installation methods that involve plastic deformation (e.g. reeling) (Macdonald and Cheaitani, 2010).

Table 2.2 Requirement to Unstable Fracture[1)] (Ref., DNV-OS-F101)

Total nominal strain	*Accumulated plastic strain*	
$\varepsilon_{1,nom} \leq 0.4\%$		*Materials, welding, workmanship and testing are in accordance with the requirements of this standard* *As an alternative girth welds allowable defect sizes may be assessed according to Appendix A.*
$0.4\% < \varepsilon_{1,nom}$		*The integrity of the girth welds shall be assessed in accordance with Appendix A*
$1.0\% < \varepsilon_{1,nom}$[2)] *or*	$2.0\% < \varepsilon_p$	*Supplementary requirement (P) shall be applied*

1) The strain levels refers to after NDT
2) Total nominal strain in any direction from a single event

2.3 ECA for Girth Welds in Clad and Lined Pipes

In the subsea gathering systems, Subsea flowlines that transport highly corrosive hydrocarbons are typically built from carbon manganese (CMn) steel linepipe or Corrosion Resistant Alloy (CRA) material. There are two typical material selection strategies for this type of situation:

a. Carbon steel linepipe designed with thicker wall thickness as a corrosion allowance: The objective of thicker wall thickness is to compensate the thickness loss due to corrosion over the design life of the flowline. It is often combined with mitigating method to reduce the loss of wall thickness.
b. Clad or Lined pipes that are basically CMn steel linepipe with internal layer of CRA material: For both clad and lined pipes, there is no need for additional wall thickness for corrosion allowance. The CRA layer in the clad pipe is metallurgically bonded to the carbon steel substrate; on the other hand the CRA layer in Lined pipes is mechanically bonded in place within the parent pipe.

Clad and Lined pipes carry a big challenge in terms of design and welding. The weld features in these types of pipeline are typically more complex than in rigid C-Mn flowlines. This fact is reflected in the difficulty in conducting ECAs using existing codes and standard (Macdonald and Cheaitani, 2010).

2.3.1 Girth Welding of Clad and Lined Pipes

Girth welds in typical solid carbon steel pipelines with no internal cladding or lining by CRA layer are always made of weld consumables with characteristics of maintaining full

overmatch of yield and tensile strength over the parent pipe. This technique has been considered advantageous to protect the girth weld and the existing small defects that are induced during welding under loading conditions involving high plastic deformation.

The full strength overmatching of weld consumable over the parent pipe will avoid strain localization in the weld and lower the amplitude of loading on local defects in the welds. However, the tearing resistance and fracture toughness of the weld consumable is typically lower than that of parent pipe.

Metallurgically clad or mechanically bonded internal thin layers of CRA are normally butt welded using weld consumables of the same CRA material. The most of CRA materials have lower yield strength but with significantly higher work hardening compared to the carbon steel of parent pipe that can be assumed to be up to X65 grade. The typical ranges of "cross-over" strain level will vary between 2% and 5%. Above this strain level the CRA material overmatches the carbon parent pipe. This situation is called partial overmatching (mismatch) of the parent pipe by the weld consumable (Sriskandarajah, Bedrossian, and Ngai, 2012).

According to DNV-JIP Lined and Clad Pipelines (2013), there are three different types of weld strength mismatches:

1. **Weld Overmatch**

The filler weld is identified as overmatch if all of the criteria below are fulfilled (**Figure 2.4**):

a) The tensile stress-strain curve of the weld filler metal crosses the stress-strain curve of the parent pipe material before 0.5% strain ($Y_{Sw} > Y_{Spp}$);

b) The tensile strength of the weld filler metal is more than 15% higher than the tensile strength of the parent pipe material ($T_{Sw} > 1.15*T_{Spp}$);

c) The strain value at TS (Tensile Strength) is higher for the weld filler metal than the strain value at TS for the parent pipe material (if the stress-strain curves do not show the TS of the weld metal, it is acceptable to estimate the remaining stress-strain curve based on the test machine displacement).

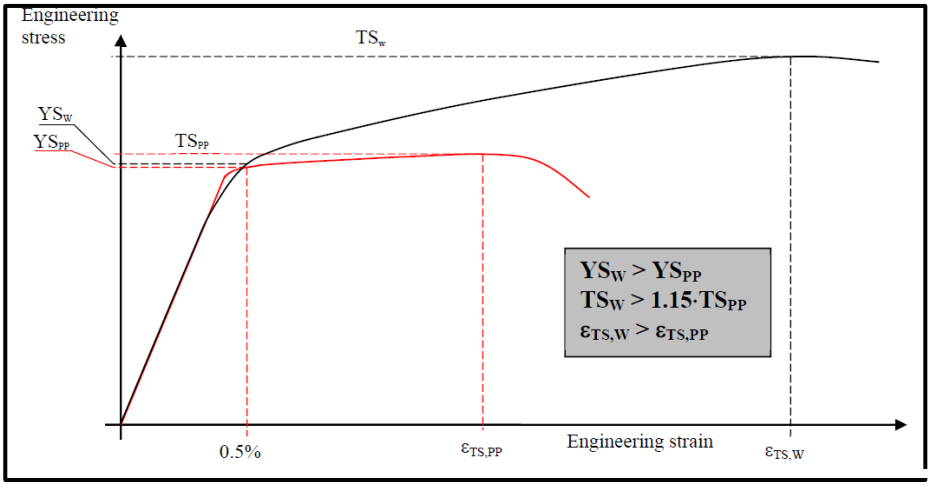

Figure 2.4 Weld over-match definition (Ref., DNV, JIP Lined and Clad Pipelines, Phase 3, 2013).

2. Weld Partially Overmatch

The filler weld is identified as partially overmatch if all of the criteria below are fulfilled (**Figure 2.5**):

a) The yield strength of the CRA girth weld is at least 0.85 times the yield strength of the parent pipe material;

b) The tensile stress-strain curve of the weld filler metal crosses the stress-strain curve of the parent pipe after 0.5% strain but before the TS of the parent pipe is reached and before a strain level of 5%;

c) The tensile strength of the filler weld metal (T_{Sw}) is at least 10% higher than the TS of the parent pipe material (T_{Spp});

d) The strain at TS is higher for the weld filler metal (if the stress-strain curves do not show the TS of the weld metal, it is acceptable to estimate the remaining stress-strain curve based on the test machine displacement);

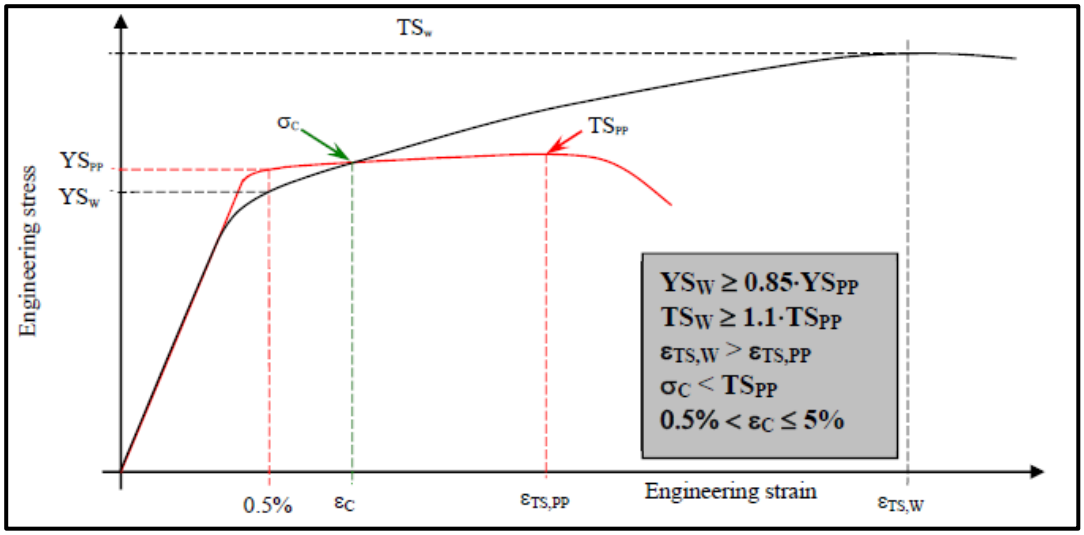

Figure 2.5 Weld partially over-matches definition (Ref., DNV, JIP Lined and Clad Pipelines, Phase 3, 2013).

3. Weld Under-match

The girth weld metal identified as weld under-match when it does not fulfilled either overmatch or partially overmatch.

Where,

Y_{Sw}	=	Yield strength of the weld filler metal,
Y_{Spp}	=	Yield strength of the parent pipe material,
T_{Sw}	=	Tensile strength of the weld filler metal,
T_{Spp}	=	Tensile strength of the parent pipe material,
$\varepsilon_{TS,W}$	=	Strain value at tensile strength of the weld filler metal,
$\varepsilon_{TS,PP}$	=	Strain value at tensile strength of the parent pipe material,
ε_C	=	strain where stress-strain curve of the weld filler metal crosses the stress-strain curve of the parent pipe,

σ_C = Stress where stress-strain curve of the weld filler metal crosses the stress-strain curve of the parent pipe.

Figure 2.6 illustrates the definition of different region of girth weld in clad and lined pipe.

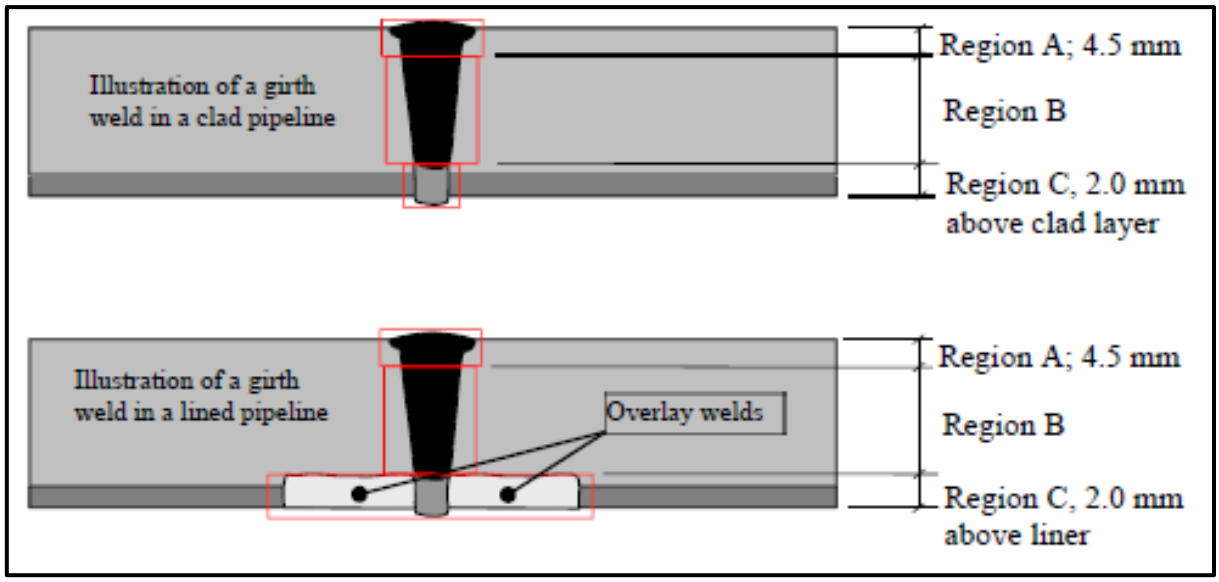

Figure 2.6 Illustration of different region in clad and lined pipe (Ref., DNV, JIP Lined and Clad Pipelines, Phase 3, 2013).

2.3.2 ECA Procedures for Clad and Lined Pipes

According to DNV-JIP Lined and Clad Pipelines (2013), the ECA-analysis for clad and lined pipes can be categorized into:

Category 1 ECA:

The first category is based on the analytical solutions and does not need the FE-based fracture mechanics. The category 1 ECA adopts conservative approach to construct the Failure Assessment Diagram. The conservative approach is based on a lower bound stress-strain curve.

Category 2 ECA:

The second category is based on the conventional ECA procedures which are presented in DNV-OS-F101. However, in this category fracture mechanics based FE analysis is carried out to compare the crack driving force from the new developed stress-strain curve.

The new developed stress-strain curve is addressed as the equivalent stress-strain curve. Typically it is acceptable to adjust the crack driving force with other process such as establishing the appropriate reference stress solution to modify the shape of the FAD curve or assigning the safety factor to determine the conservative crack driving force calculation.

If the procedures above are used it should be verified that it does not give potentially non-conservative results. The traditional ECA approach in accordance with DNV-OS-F101 is

acceptable to carry out when it shown that for given flaw sizes the crack driving force for the models representing the "worst case" stress strain curves for all material are smaller than the models where only the parent pipe tensile properties are defined.

Category 3 ECA:

The 3D FE fracture mechanics analyses are used to represent the maximum allowable flaw sizes in Category 3 ECA. Hence a specific and chosen "worst case" well geometry and misalignment shall be illustrated in the FE model. The summary for requirements and methodology of ECA categories for girth welds in pipes with liner or clad can be seen below in **Table 2.3.**

Table 2.3 Girth Weld Integrity Assessment Procedures during Installation for Pipelines with CRA Cladding/Liner (Ref., DNV, JIP Lined and Clad Pipelines Phase 3, 2013)

Girth Weld Classification	Installation
"Undermatch"	Only category 3 ECA is acceptable
"Overmatch"	Category 1 shall be used to verify the "workmanship" NDT acceptance criteria for the root for strains below 0.4% (tearing shall be evaluated)
	For region A and B: Appendix A of DNV-OS-F101 is applicable. ECA shall be performed if $\varepsilon_{l,nom}$ exceeds 0.4%
	For Region C: Category 1, 2 or 3 ECA shall be performed if $\varepsilon_{l,nom}$ exceeds 0.4%
"Partially overmatch"	Category 1 shall be used to verify the "workmanship" NDT acceptance criteria for the root for strains below 0.4% (tearing shall be evaluated)
	Category 2 or 3 ECA shall be used if $\varepsilon_{l,nom}$ exceeds 0.4%. Tearing analyses shall always be assessed for region C

The first category of ECA is only used to verify that the "workmanship" NDT acceptance criterion is acceptable for load cases where the installation maximum applied strain during installation is less than 0.4%.

a) Stress-strain characteristics used in the FE fracture mechanics analysis

The applied stress-strain characteristics in the FE analysis are important and the characteristics are to be described depending on chosen load case and the location of the defect in the weld joint. The illustration of various materials which are typically involved in lined and clad pipelines can be seen in **Figure 2.7**.

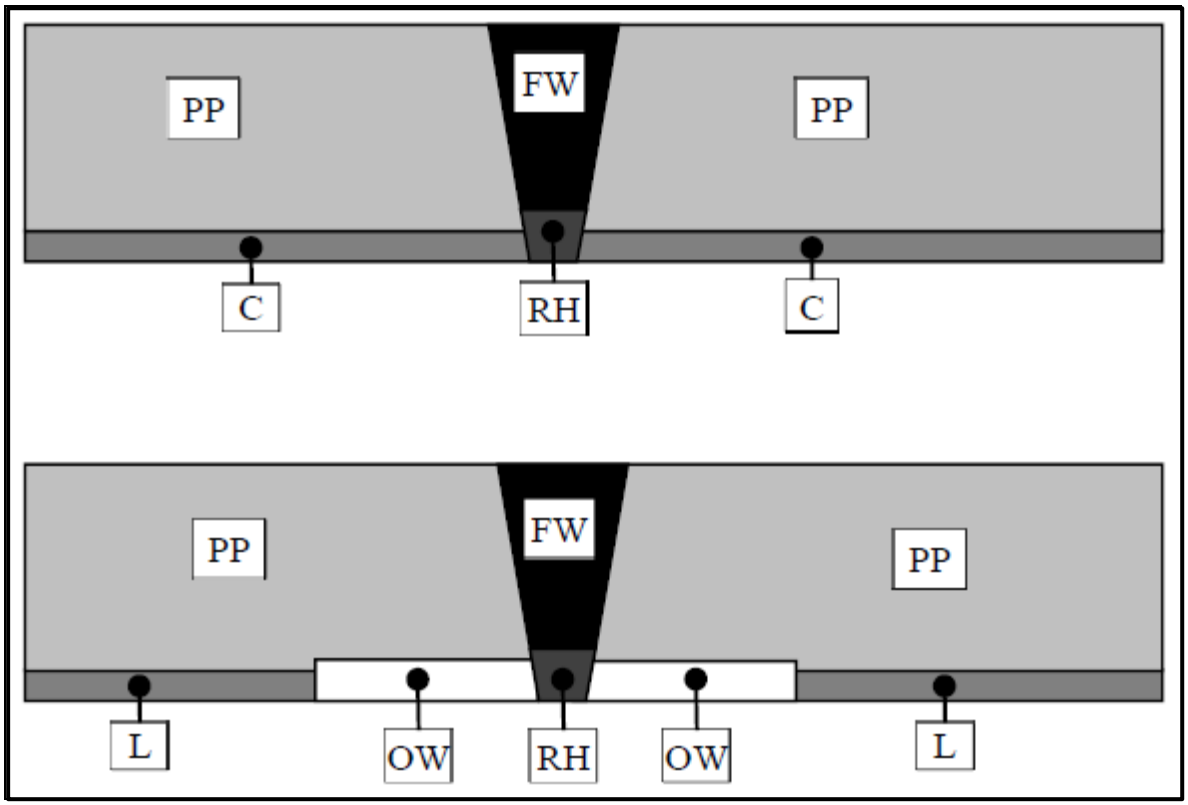

Figure 2.7 Illustration of various materials typically involved in lined and clad pipelines (Ref., DNV, JIP Lined and Clad Pipelines, Phase 3, 2013).

In Clad Pipe:

PP = Parent Pipe

FW = Filler Weld

C = Clad Layer

RH = Root/hot passes

In Lined Pipe:

PP = Parent Pipe

FW = Filler Weld

C = Clad Layer

RH = Root/hot passes

OW = Overlay Weld

The stress-strain characteristics applied in the FE analysis shall be determined according to **Table 2.4** for clad pipelines and according to **Table 2.5** for lined pipelines. The guidance to determine the upper-bound and lower-bound material characteristics are specified below.

Table 2.4 Stress-Strain Curves Used In Category 2 ECA FE, Clad Pipe (Ref., DNV, JIP Lined and Clad Pipelines Phase 3, 2013)

Flaws in weld region A and B		Flaws in weld region C	
Strain<0.25% or stress-based (Optional)	**Strain>0.25% or strain-based**	**Strain<0.25% or stress-based (Optional)**	**Strain>0.25% (strain-based)**
PP: lower-bound[1)]	PP: upper-bound[3)]	PP: lower-bound[3)]	PP: upper-bound[3)]
FW: lower-bound[2),4)]	FW: lower-bound[2),4)]	FW: lower-bound[2),4)]	FW: lower-bound[2)]
C: mean-curve[4)]	C: lower-bound[2),4)]	C: lower-bound[2),4)]	C: upper-bound[5)]
RH: mean curve[2),4)]	RH: lower-bound[2),4)]	RH: lower-bound[2),4)]	RH: lower-bound[2)]

1) *Lower-bound is either a curve fitted through SMSY or SMTS with reasonable shape based on stress-strain curves established from testing or in accordance with DNV-OS-F101.*
2) *Lower-bound is fitted curve through the lower yield stress out of five and the lowest tensile strength out of the same five tests. The shape of the curve shall still represent the material reasonably.*
3) *The upper-bound curve shall be determined in accordance with DNV-OS-F101*
4) *It is acceptable to use the same curve for the filler weld, the clad and the root/hot passes as long as the curve is representing a lower-bound curve*
5) *The upper-bound curve is fitted through the highest yield stress out of five tests and the minimum tensile strength out of the same 5 tests. The shape of the curve shall still represent the material reasonably*

Table 2.5 Stress-Strain Curves Used In Category 2 ECA FE, Lined Pipe (Ref., DNV, JIP Lined and Clad Pipelines Phase 3, 2013)

Flaws in weld region A and B		Flaws in weld region C	
Strain<0.25% or stress-based (Optional)	**Strain>0.25% or strain-based**	**Strain<0.25% or stress-based (Optional)**	**Strain>0.25% (strain-based)**
PP: lower-bound[1)]	PP: upper-bound[3)]	PP: lower-bound[1)]	PP: upper-bound[3)]
FW: lower-bound[2),4)]	FW: lower-bound[2)]	FW: lower-bound[2),4)]	FW: lower-bound[2),6)]
L: mean-curve[4)]	L: lower-bound[2)]	L: lower-bound[2),4)]	L: upper-bound[6)]
RH: mean curve[4)]	RH: lower-bound[2)]	RH: lower-bound[2),4)]	RH: lower-bound[2),6)]
OW: mean curve[4)]	OW: lower-bound[2)]	OW: lower-bound[2),4)]	OW: upper-bound[5)]

1) *Lower-bound is either a curve fitted through SMSY or SMTS with reasonable shape based on stress-strain curves established from testing or in accordance with DNV-OS-F101.*
2) *Lower-bound is fitted curve through the lower yield stress out of five and the lowest tensile strength out of the same five tests. The shape of the curve shall still represent the material reasonably.*
3) *The upper-bound curve shall be determined in accordance with DNV-OS-F101*
4) *It is acceptable to use the same curve for the filler weld, the clad and the root/hot passes as long as the curve is representing a lower-bound curve*
5) *The upper-bound curve is fitted through the highest yield stress out of five tests and the minimum tensile strength out of the same 5 tests. The shape of the curve shall still represent the material reasonably*
6) *It is acceptable to use the same curve for the filler weld, the liner material and the root/hot passes as long as the curve represents a lower-bound curve for the materials*

b) Defect Type

The Category 2 and 3 ECA's shall be conducted for both external and internal surface breaking flaws as a minimum. It is acceptable to evaluate embedded flaws independently and establish the dedicated acceptance criteria for embedded flaws.

Moreover, it is also acceptable to use similar acceptance criteria for embedded flaws as for surface breaking flaws. Hence, the criticality of surface breaking defects and embedded defects are the same except for the embedded flaws which located close to surface with the ligament less than half the defect height.

In such cases the height of defect shall be defined as the combination of ligament height plus measured defect height. The AUT/UT flaw sizing error shall be considered by reducing the maximum allowable flaw sizes.

c) Determination of Equivalent Stress-strain Curves

The equivalent stress-strain is calculated in several steps as follows:

1. The FE analysis is carried out to calculate The Crack Driving Force (CDF) for certain flaws.
2. The Crack Driving Force (CDF) is also calculated based on the BS7910. Both of the calculated results from FE analysis and BS7910 are compared.
3. The CDF is a function of geometry and tensile properties of the materials. Hence, changing the stress-strain curve defined in BS7910 will change the CDF.
4. The equivalent stress-strain curve is generated when the CDF as the result of BS7910 procedure equal to the CDF by FE analysis.

Olsø et al., (2011) proposed a new procedure to develop the equivalent stress-strain curve accounting the weld metal mismatch in clad pipes which are implemented in LINKpipe.

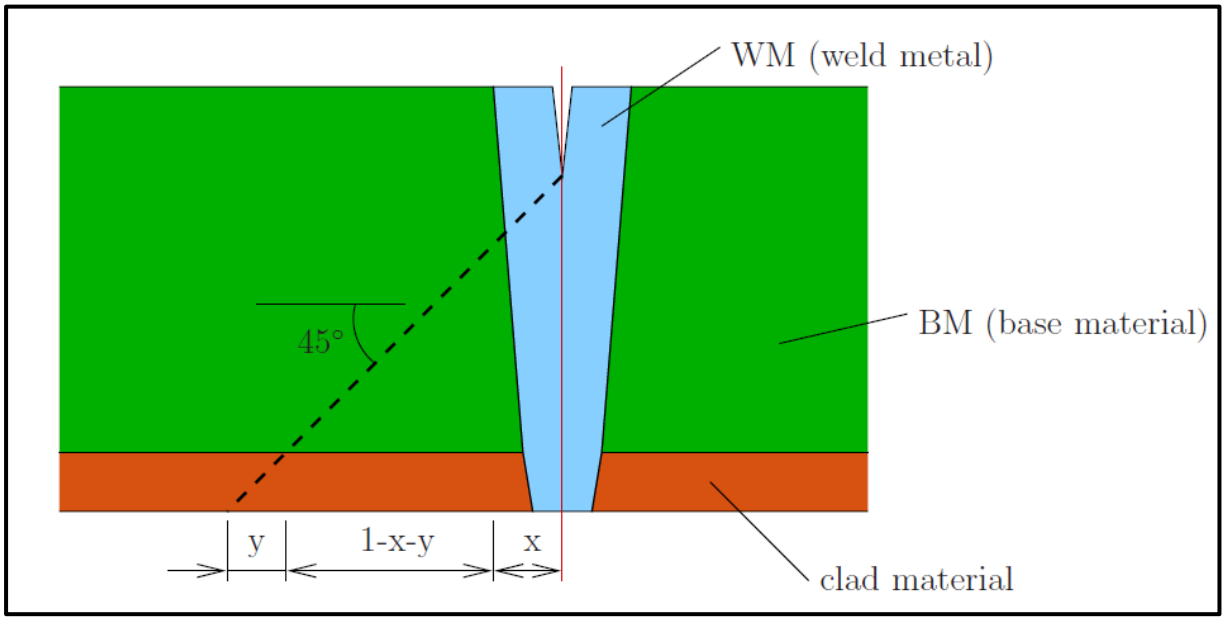

Figure 2.8 Weld geometry and different materials (Ref., LINKpipe theory manual).

A simple alternative procedure for developing an equivalent material curve is the weighting principle. This methodology has been developed as a simple approach, because the equivalent material curve is generated without the FE analysis. In addition to weld metal, there are two materials through the thickness in the base material of a clad pipe; backing steel and clad material.

The description about the basis of the weighting principle is as follow:

> *"The different materials all contribute to the total deformation and opening of the crack as the ligament strain at the crack tip extends into the different material zones."*

The **Figure 2.8** shows the illustration of ligament strain which extending from the crack tip around 45 degrees. It is clearly shown that the deformation will exist for different material region close to the crack tip and the weighted average of the stress-strain curve is approximated by the relative length of line for each material zone line.

Hence, the equivalent stress strain curve can be determined from the **Equation 2.2** as follow:

$$\sigma_{eff}(\varepsilon) = (1 - x - y)\sigma_{BM}(\varepsilon) + x\sigma_{WM}(\varepsilon) + y\sigma_{clad}(\varepsilon) \quad \textbf{..... (2.2)}$$

Where,

$\sigma_{BM}(\varepsilon)$ = The stress strain curve for the base material,

$\sigma_{WM}(\varepsilon)$ = The stress strain curve of the weld material,

$\sigma_{clad}(\varepsilon)$ = The stress-strain curve for the clad material,

x = The fraction of the length of the localized ligament deformation passing through the weld metal,

y = The same for the clad material.

The developed equivalent stress-strain curve can be employed to calculate ECA analysis. It should be noted that the similar analysis steps can be used for the weighting along the weld metal and the base metal layers (only) in the conventional pipes without clad layer.

3. THEORETICAL BACKGROUND

3.1 The Concept of Fracture Mechanics

Fracture mechanics is a technique to describe the fracture behavior of cracked or flawed structural members based on stress analysis in the crack or notch region. Hence, it is not depending on the use of "extensive service experience" to interpret test results into practical design information as long as we can obtain:

1. The fracture toughness of the material, using fracture-mechanics tests;
2. The nominal stress on the structural member;
3. Flaw size and geometry of the structural member.

Cracks or sharp notches are common defects that happen in structures such as bridges, building, ships or even pipeline girth welds. Fracture in the structure can be prevented by applying fracture mechanics and by calculating the allowable stress levels and inspection requirements. Fracture mechanics can also be used to determine the critical size of the crack in the structure under fatigue loading or stress corrosion cracking.

Hence, fracture mechanics analysis and testing have many advantages compared to the traditional toughness test method. The fracture mechanics proposed a method of quantitative design to avoid the fracture in structures. It also can be used to assess the fitness for service, or "life extension", of existing structures (Barsom and Rolfe, 1999).

There are basically two categories of fracture mechanics:

- Linear Elastic Fracture Mechanics (LEFM)
- Elastic-Plastic Fracture Mechanics (EPFM)

Of the above two categories, the LEFM is the most established one and it analyzes the nature of the materials where cracking is assumed to appear primarily in the elastic conditions. It also assumes that the amount of plasticity is limited and the crack tip is sharp.

There are some limitations in using LEFM such as when analyzing ductile materials or lower strength steel, it is difficult to identify plastic behavior by LEFM. Hence, EPFM was developed from LEFM to analyze ductile materials. Compared to LEFM, EPFM considers that the crack tip is not sharp and that there is an amount of crack tip plasticity or blunting. Lower-strength and higher-toughness steels are typical structural materials that are designed using EPFM (Dieter, 1997).

3.1.1 Linear Elastic Fracture Mechanics (LEFM)

The basic theory of linear elastic fracture mechanics (LEFM) is that the stress field around the sharp crack can be described by stress intensity factor, $\mathbf{K_I}$, parameter having unit of $Pa\sqrt{m}$ (Barsom and Rolfe, 1999).

Figure 3.1 shows the three fracture modes of loading, the stress intensity typically given a subscript correspond to the modes of loading i.e., K_I, K_{II}, or K_{III}.

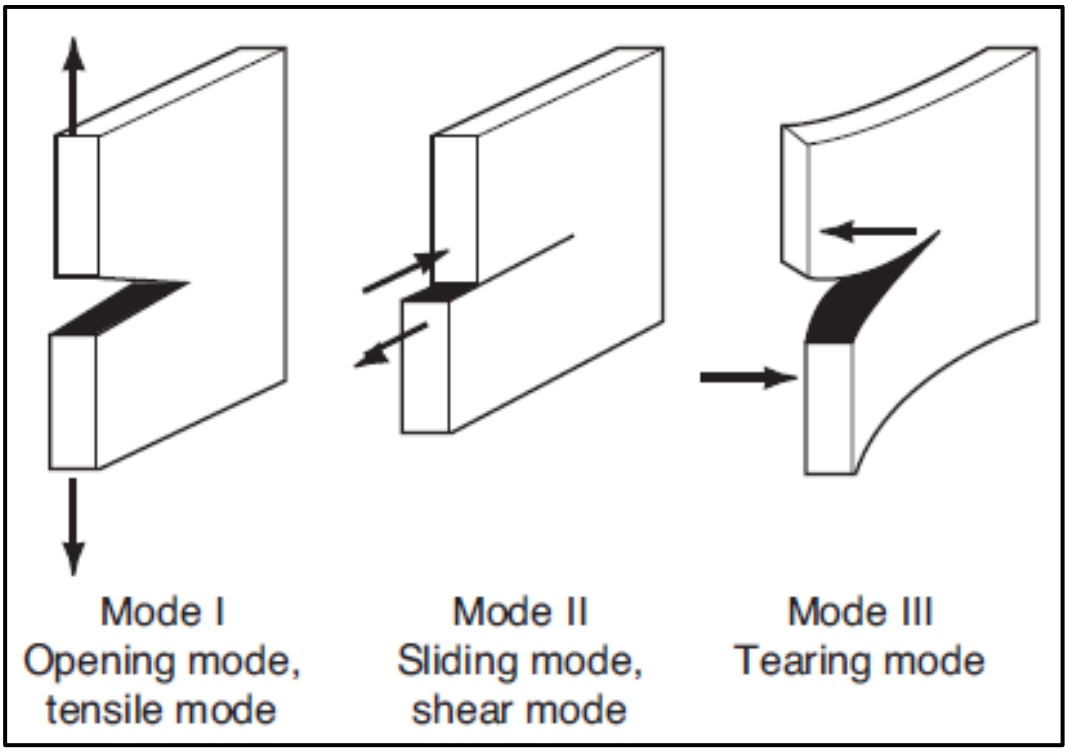

Figure 3.1 Fracture Modes of loading (Ref., Howard and Dana, 2000).

According to Howard and Dana (2000), the stress intensity factor can be associated with the local stress at the crack tip as:

$$\sigma_{yy} = \frac{K_I}{\sqrt{2\pi r}} \quad \text{.....(3.1)}$$

Where,

σ_{yy} = The local stress near the crack tip,

$\mathbf{K_I}$ = The stress intensity factor (Mode I - tensile opening load),

r = The distance in front of the crack tip (with $\theta = 0$) (as indicated in **Figure 3.2**).

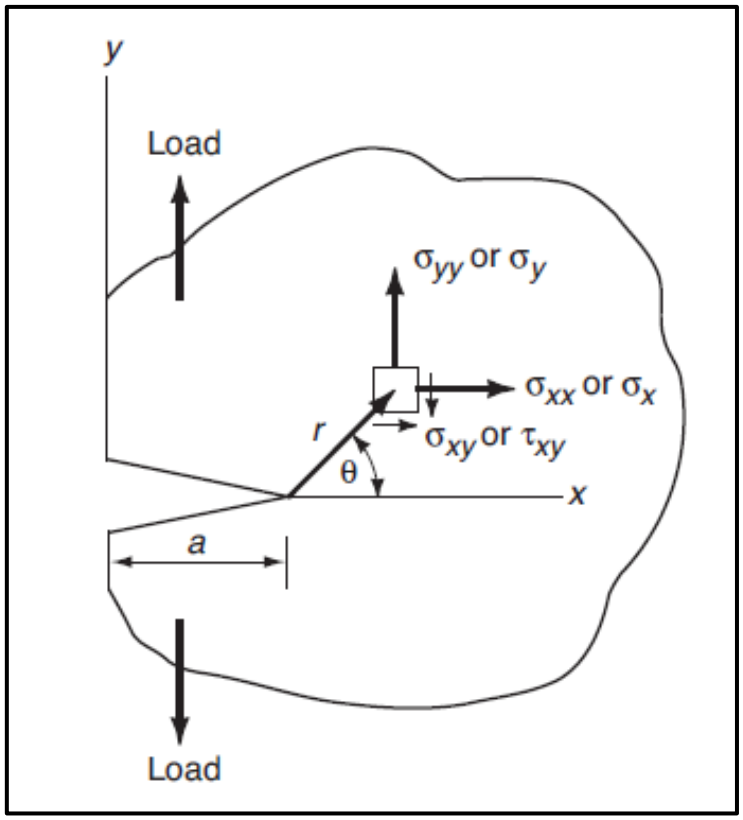

Figure 3.2 Coordinate system for crack tip stresses (mode I loading) (Ref., Howard and Dana, 2000).

Based on the work of Barsom and Rolfe (1999), the single parameter, $\mathbf{K_I}$, is a function of the stress level, σ, and the crack or flaw size, **a**. It is similar with the driving force, σ, in structural design. The fracture that follows unstable crack growth appears when parameter, σ and flaw size, **a**, resulting in critical value of, $\mathbf{K_I}$, called, $\mathbf{K_c}$.

For a body subjected to tensile stresses, **Figure 3.3** presents the equations describing the elastic-stress field around the crack tip for different crack configurations. The equations show, $\mathbf{K_I}$, as a function of, σ, and crack size, **a**.

$\mathbf{K_c}$, or the critical value of stress-intensity factor at failure is a material property. It is similar to the yield strength, σ_{ys}, which resist yielding in structural design. This parameter can be determined for a given material at particular thickness and specific temperature from testing.

The critical value of stress-intensity factor can be used to determine the allowable flaw size in structural member for given stress level, temperature, and loading rate. It can also be used to calculate safe design stress level that can be applied to the existing flaw size in the structure.

The critical stress-intensity factor is greatly influenced by "service conditions" like temperature, loading rate and constraint. For structural materials, it must be determined through testing of actual material until failure at different temperature and loading rates.

The concepts of fracture mechanics can be used in the design to avoid fractures in the structures and also to extend the life of existing structures through fitness-for-service analyses.

The essential basic method to avoid fracture in structural material is to make sure that the calculated stress-intensity factor, $\mathbf{K_I}$ (the driving force), less than the critical stress-intensity factor, $\mathbf{K_c}$ (the resistance force).

A typical design procedure to avoid fracture in structural members is as follows:

1. Calculate the maximum nominal stress, σ, for the structure member being analyzed;
2. Evaluate the typical flaw geometry and initial crack size, $\mathbf{a_0}$;
3. To prevent fracture during the expected lifetime of a structure, calculate the maximum probable crack size during the expected lifetime;
4. Calculate $\mathbf{K_I}$ for the stress, σ, and flaw size, **a**, using the suitable, $\mathbf{K_I}$, relation;
5. Carry out the testing of material from member of structure to be built to determine the critical stress-intensity factor, $\mathbf{K_c}$, which is the function of the appropriate service temperature and loading rate;
6. Make sure that, $\mathbf{K_I}$, will be lower than the critical stress-intensity factor, $\mathbf{K_c}$, throughout the entire life of the structure. This will need the selection of different type of material or reduction of the maximum nominal service stress;

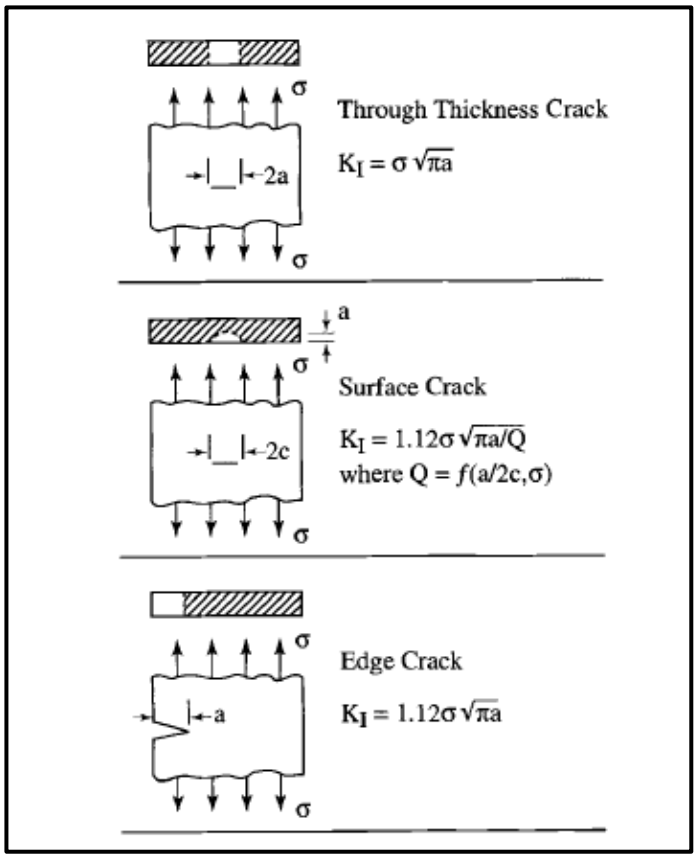

Figure 3.3 $\mathbf{K_I}$, values for different crack geometries (Ref., Barsom and Rolfe, 1999).

Furthermore, Barsom and Rolfe (1999) also explained about schematic relation between material fracture toughness, $\mathbf{K_c}$, to the nominal stress, σ, and crack size, **a**, (see **Figure 3.4**). As mentioned earlier, the stress intensity factor, $\mathbf{K_I}$, will depend on a combination of stress and flaw size while the material fracture toughness represents the ability of a material to resist fracture in the presence of crack.

Hence, the fracture will occur when the stress intensity factor, $\mathbf{K_I}$, coincides with the critical value of, $\mathbf{K_c}$. $\mathbf{K_c}$, value is determined from laboratory testing in particular temperature and loading rate. The combination of stress and flaw size will not cause fracture in structural material as long as it doesn't achieve the critical value of $\mathbf{K_c}$.

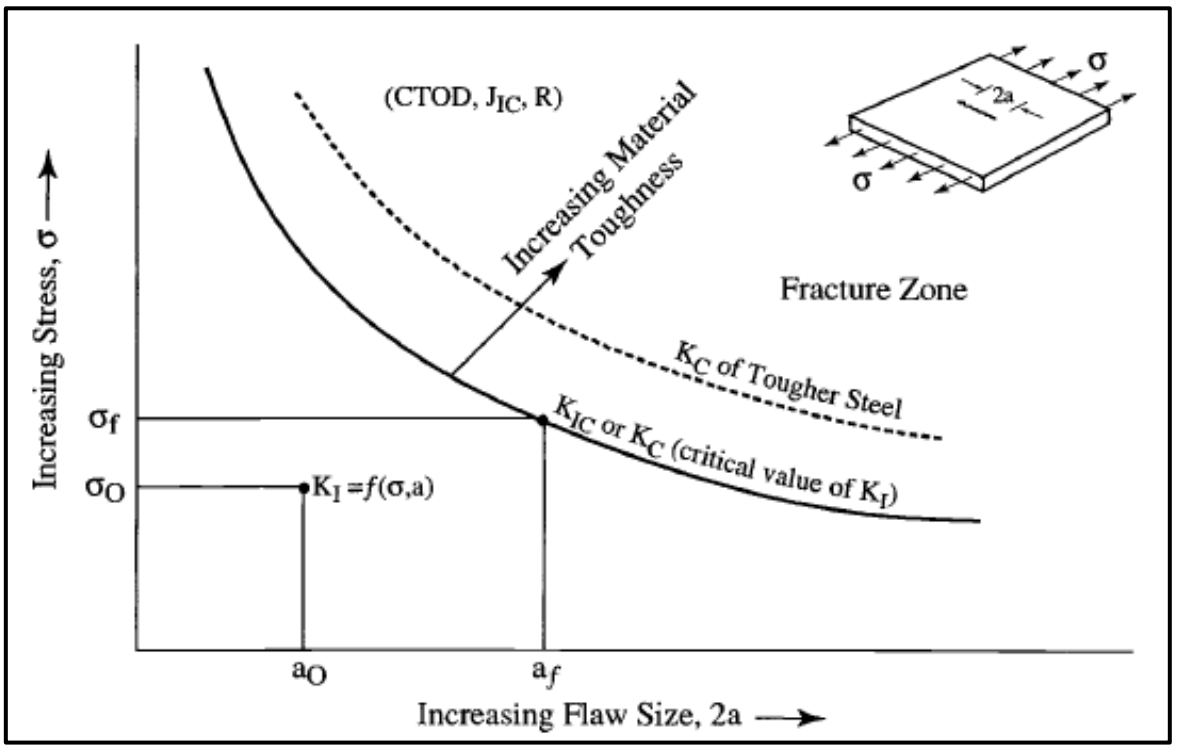

Figure 3.4 Relation between stress, flaw size, and material toughness (Ref., Barsom and Rolfe, 1999).

The **Figure 3.5** shows the analogy to explain the essential points in fracture-mechanics by comparing it to Euler Column instability. In order to prevent buckling occurred to the column, the applied stress and L/r value should be below the critical stress in Euler curve. On the other hand, to prevent fracture the applied stress, σ, for given flaw size, **a**, should be below the material fracture toughness or $\mathbf{K_c}$.

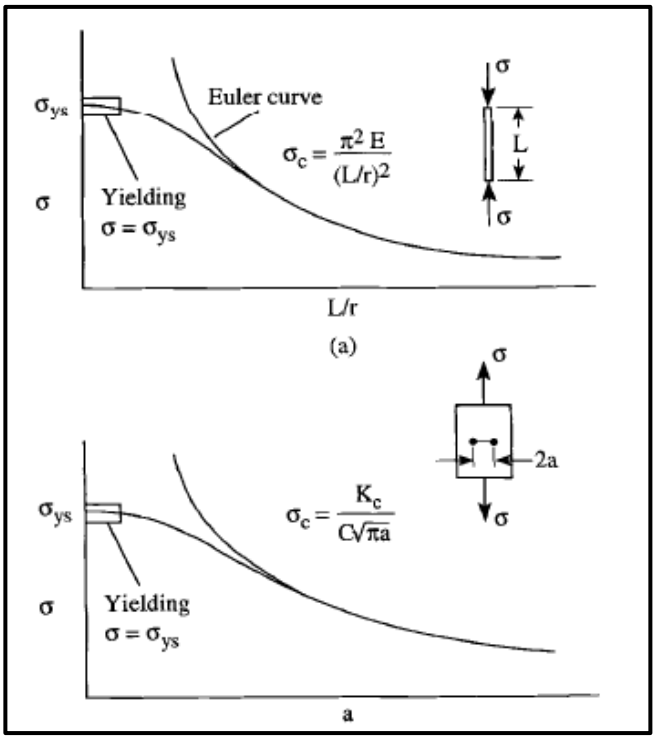

Figure 3.5 Ilustration describing analogy between column instability and crack instability: (a) Column instability (b) Crack Instability (Ref., Barsom and Rolfe, 1999).

The method of linear-elastic fracture mechanics still can be applied to a material with small sizes of plastic zone compared with the size of the crack. For such cases, the stresses in the plastic zone and the development of the process zone are related to the calculated elastic stress intensity factor.

Hence, the beginning of crack extension, that is determined by a critical state in the process zone, is relates to critical intensity factor, $\mathbf{K_c}$.

It should be noted that the assumptions mentioned above are valid if the size of plastic zone is relatively smaller than the crack size **a**, and the rest of cross section, **W - a**, where, **W**, is the plates thickness. The relation of linear elastic fracture mechanics (LEFM) can be used when the **Equations 3.2** and **3.3** below are fulfilled:

$$a > \beta_1 \left(\frac{K_c}{\sigma_{ys}} \right)^2 \quad \text{..... (3.2)}$$

and

$$W - a > \beta_2 \left(\frac{K_c}{\sigma_{ys}} \right)^2 \quad \text{.....(3.3)}$$

Where, $\beta_1 = \beta_2 = 2.5$. The methods of Elastic Plastic Fracture Mechanics (EPFM) have to be used when the above equations above are not fulfilled (Buschow et al., 2001).

3.1.2 Elastic Plastic Fracture Mechanics (EPFM)

For many structural parts which are made from low-strength, tough material, a considerable amount crack tip plastic deformation and stable crack growth (tearing) can present before instability.

In this case, the methods of linear elastic fracture mechanics is not adequate to be applied since this method no longer has ability to identify the crack tip behavior in the occurrence of large yielding and extensive stable crack growth. Hence, another concept is required to analyze the structural integrity for ductile materials.

There are two concepts that can be applied for non-linear fracture mechanics:

1. The path independent J-Integral that is used to quantify the crack tip area, and
2. Crack Tip Opening Displacement (CTOD) that is related to the amount of opening of the two faces of crack at the crack tip.

Both of these concepts can be applied to extend fracture mechanics for the low strength and tough material (Farahmand, 2001).

3.1.3 CTOD (Crack Tip Opening Displacement)

The concept, CTOD (Crack Tip Opening Displacement) concept is addressed for analyzing fracture based on crack trip strain criterion. CTOD is the diameter of the circular arc at the blunted crack tip as shown in **Figure 3.6**. **Figure 3.6** illustrates the concept of CTOD and CMOD (Crack-Mouth Opening Displacement) before and after deformation of a sample specimen with crack. It is clearly shown that the CTOD is analyzed on the crack tip while the CMOD is at center line of the loads.

The design codes, British Standard 7448 - Part 1 and the ASTM E 1290 can be used as the guidelines for analyzing the CTOD. The crack-opening displacement, v, for a crack in an elastic regime can be calculated by using **Equation 3.4**, It is depend on the stress intensity, **K**, and the distance, **r**, from the crack tip.

$$v = \frac{2K}{\pi E}(2\pi r)^{1/2} \quad \textbf{.....(3.4)}$$

Where,

E is the elastic modulus of the material,

K is stress intensity,

v is crack opening displacement,

r is distance of v from the crack tip.

The displacement at the crack tip, δ, in case of small scale yielding can be determined by assuming the effective crack tip is at a distance, $\mathbf{r_y}$, from the actual crack tip $(a_{eff} = a + r_y)$.

$$\delta = 2v = \frac{4K}{\pi E}(2\pi r)^{1/2} = \frac{4K^2}{\pi E \sigma_{yy}} \quad \text{..... (3.5)}$$

Where, σ_{yy}, is the local stress at the crack tip.

Theoretically, fracture occurs if the displacement at the crack tip, δ, reaches the critical value of CTOD. The CTOD method is limited by analytical and experimental uncertainties of the crack tip area as follows:

1. Analytically the definition of, δ, is "*the CTOD at the interface of the elastic-plastic boundary and the crack surface."*
2. Experimentally, δ, is *"calculated from displacement measurements taken remotely from the crack tip because direct physical measurements are not precise."*
3. Other uncertainty is shown by **Equation 3.5**, by the term, σ_y, that may vary by 75%, "*depending on the degree of elastic constraint a crack tip characteristic that cannot be measured directly*."

The CTOD concept presents better quality results over linear-elastic method in the plastic regime (Kuhn and Medlin, 2000).

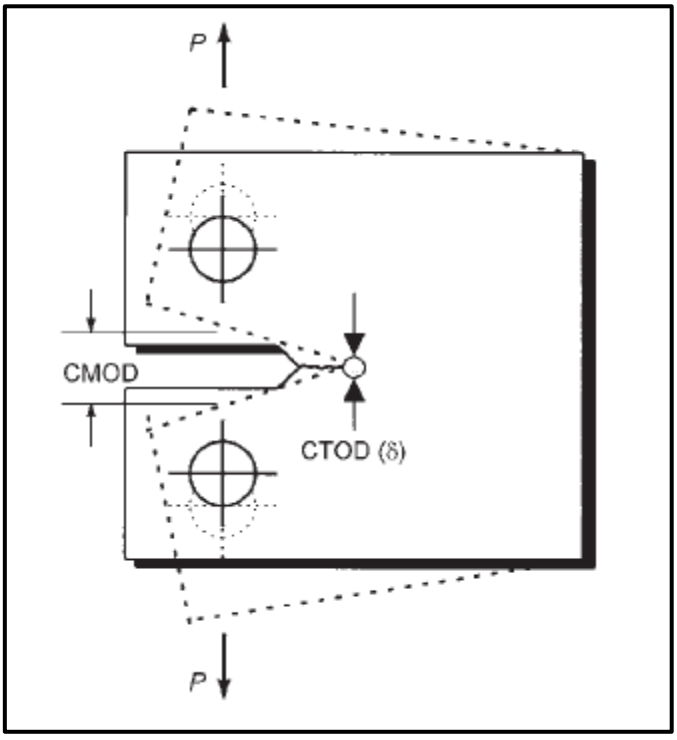

Figure 3.6 An illustration showing the definition of CMOD and CTOD (Ref., Kuhn and Medlin, 2000).

3.1.4 J-Integral

The J-integral describes the elastic-plastic field in the vicinity of at the crack tip. J-integral is defined as the line integral:

$$J = \int_{\Gamma}\left[wdy - \vec{T}\frac{\partial \vec{u}}{\partial x} ds \right] \text{ .....(3.6)}$$

Where,

Γ = Any contour surrounding the crack tip,

w = The strain-energy density,

$\vec{T}$ = The force vector normal to Γ,

$\vec{u}$ = The displacement vector,

s = Arc length along Γ.

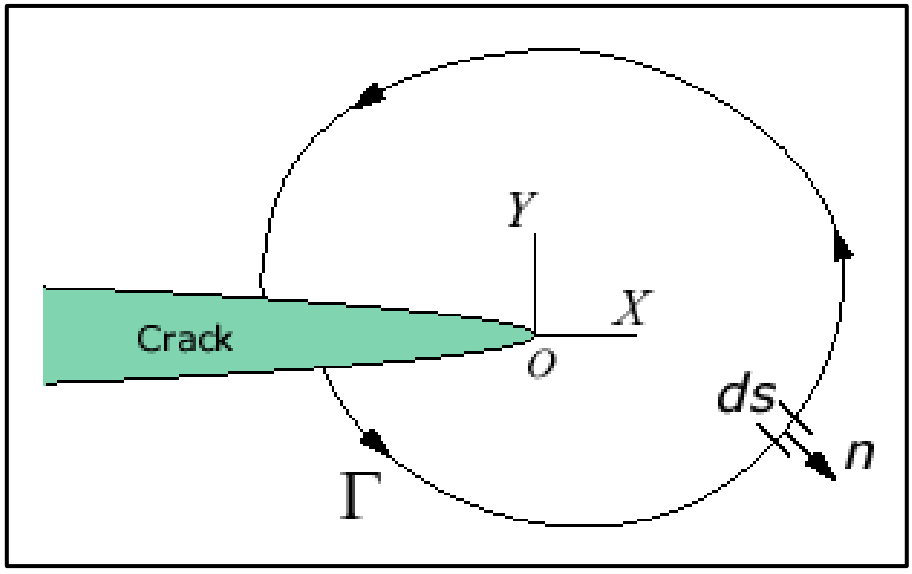

Figure 3.7 An illustration of J-Integral (Ref., http://www.efunda.com/formulae/solid_mechanics/fracture_mechanics/images/JIntegral.gif).

According to Kuhn and Medlin (2000), *"J-Integral is path independent for linear and nonlinear elastic materials and nearly so for most structural materials (elastic-plastic) under monotonic loading condition"*. The J-Integral can be calculated using numerical methods by computing the load and the displacement along a contour away from the crack tip. By using J-Integral, the uncertainties of the crack tip area in the CTOD method can be eliminated.

An equivalent interpretation is that J-Integral is defined as the ratio between *"the change of the pseudopotential energy"* (the area under the curve of load-displacement), **U**, and an increment of crack extension of unit area, **A**, as shown in **Equation 3.7**,

$$J = \frac{dU}{dA} \quad \text{.....(3.7)}$$

Furthermore Kuhn and Medlin (2000) states that *"the strain energy released upon crack extension is the driving fracture force for fracture in cracked material under linear-elastic conditions".* The elastic strain energy, **U**, is the work done by a load, **P**, creating a displacement, **Δ**. The formula for the elastic strain energy can be seen in **Equation 3.8**.

$$U = \frac{P\Delta}{2} = \frac{C_e P^2}{2} \quad \text{.....(3.8)}$$

Where $C_e = \frac{\Delta}{P}$, is the elastic compliance.

The strain-energy release rate, **G**, is defined as the ratio of the loss of elastic potential energy, **U**, over the crack extension of unit area, **A**. The strain-energy release rate, **G**, for a crack extending at constant load or deflection can be determined by the **Equation 3.9** as follows:

$$G = \frac{dU}{dA} = \left(\frac{P^2}{2}\right)\frac{dC_e}{dA} \quad \text{.....(3.9)}$$

In the linear-elastic situation, the potential energy = the strain energy (U=V). Hence, **Equation 3.7** is similar as **Equation 3.9** and J=G. Thus, J appears to be logical extension of LEFM method into elastic-plastic range.

However, the energy interpretation of the J-integral does not apply to the process of crack extension. J is not equal to the energy available for the crack extension in elastic-plastic materials as G is for elastic materials. This is happen because of the irreversibility of plastic deformation. J is simply analytically suitable, a measurable parameter to determine the characteristic of the elastic-plastic area at the crack tip. The $\mathbf{J_{Ic}}$, is a critical value of J when the crack initiation under elastic-plastic conditions occurs.

Moreover, the J-Integral method is also relevant for crack initiation and crack propagation. For most of materials that fail in the elastic-plastic range, significant fracture resistance occurs after the crack initiation. Hence, the J-integral method as a fracture criterion might be overly conservative in some cases.

3.2 Stress-Strain Characteristics

All materials have an elastic limit (yield strength). Brittle materials will subject to sudden fracture when they are loaded beyond the elastic limit. On the other hand, ductile materials will deform plastically beyond its elastic limit which means that the materials will have permanent deformation.

Figure 3.8 shows the linear stress-strain response of elastic material as described by Hooke's law. The stress-strain response is linear for most of solid materials at small strains, "less than

0.001 or 0.1%". The slope of linear response is then defined as Young's modulus i.e. the ratio of the stress over the strain. The shaded area describes the elastic energy stored in solid per unit volume and the energy can be restored when the load is withdrawn (Ashby and Jones, 2012).

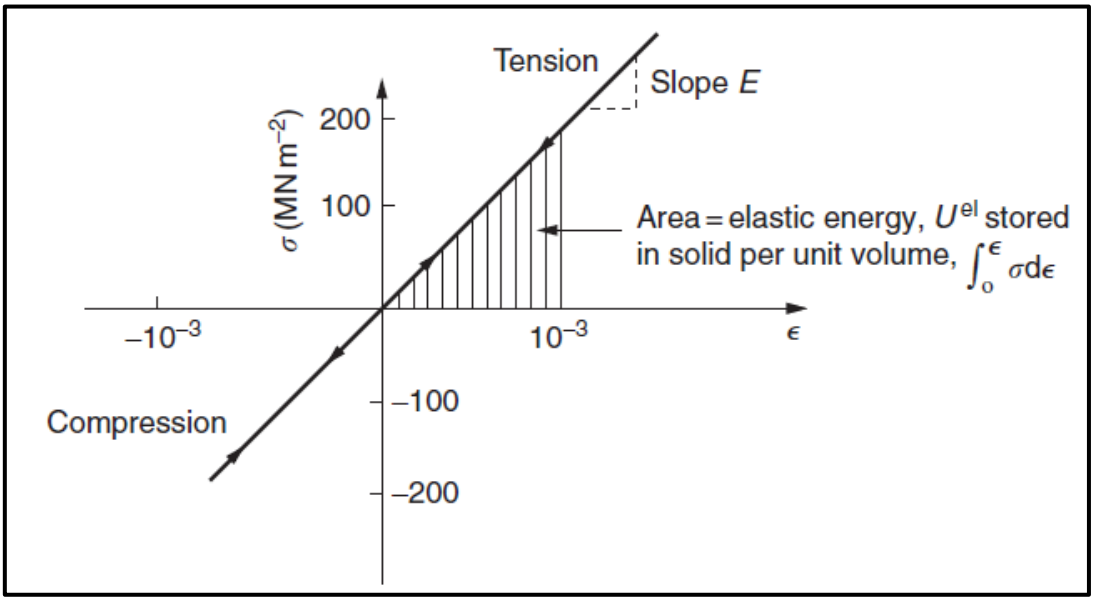

Figure 3.8 The curve of stress–strain for a linear elastic solid (Ref., Ashby and Jones, 2012).

Elastic limit is defined as the maximum stress the material could hold without any permanent deformation when all the loads have been withdrawn. Strains that occur happen before the material reach its elastic limit are small and reversible (Marlow, 2002).

Proportional limit is the highest stress point at which stress is directly proportional to strain. Beyond this point, most of material will deviate from line elastic behavior. This nonlinearity is correlated with "stress-induced, plastic flow" in the material where the new equilibrium of microscopic structure is introduced.

This plasticity depends upon the mechanism of molecular mobility of the materials. If it has lacking mobility, the material will be brittle than ductile. For brittle materials, the stress-strain curves are linear over the strain range and fracture will be occurred without noticeable plastic region (Roylance, 2001).

On the other hand, the ductile material has capability to restrain large strains during loading prior to fracture. A visible elongation or the transformations of cross sectional dimension are found as the result of these large strains. This deformation can be regarded as warning of the failure of the materials. The mild steel, aluminum and some its alloys, copper and polymer are some of examples for this type of materials (Marlow, 2002).

In order to increase the strain and continue to rise beyond the proportional limit, the amount of stress will be needed. The mechanism where the materials need an increasing stress to

continue straining is called strain hardening. Generally the proportional limit is equal to or close to the elastic limit of the material because the microstructure transformation associated with "plastic flow" is not reversed during unloading. A typical stress-strain response of carbon steel can be seen below in **Figure 3.9**. The yield point is the condition which the amount of stress will be needed to induce a specific of permanent strain, "typically 0.2%" (Roylance, 2001).

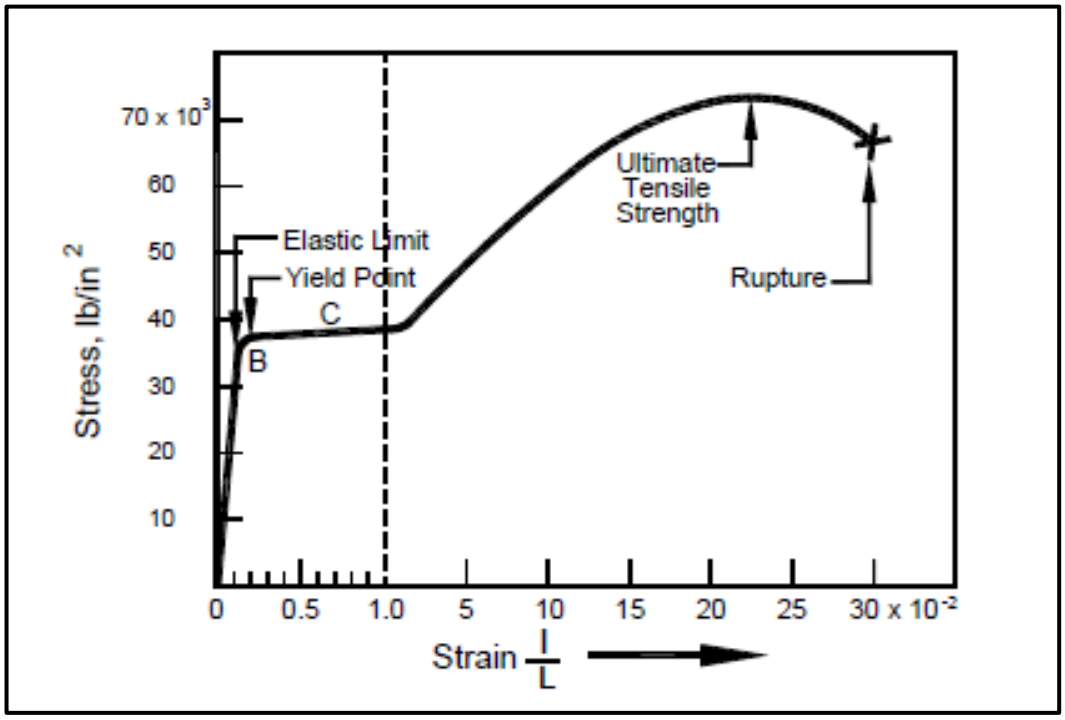

Figure 3.9 The example of typical stress-strain curve for carbon steel (Ref., Marlow, 2002).

From **Figure 3.9**, it can be clearly seen that the rate of strain hardening is faded away closer to UTS point (Ultimate Tensile Strength). Beyond this point, the carbon steel will tend to be "strain softens" and the required stress will therefore be smaller for each increment of additional strain. The rate of strain hardening is the slope of the stress-strain curve (tangent modulus).

A. TRUE STRESS AND TRUE STRAIN

According to Roylance, (2001) a noticeable decrement in the cross sectional area (A) is occurred under tension due to the molecular/microstructure transformation in solid materials. Engineering stress, $\sigma_e = \frac{P}{A_0}$ is calculated based on original cross sectional area of specimen before testing, while true stress, $\sigma_t = \frac{P}{A}$, is calculated based on true (or reduced) cross sectional area of specimen after testing. Hence, true stress-strain response of a ductile material is higher than engineering stress-strain response.

Generally the engineering stress-strain curve and the true stress-strain will be similar until it reaches the elastic limit. Beyond the elastic limit, the engineering stress-strain will be different to the true stress-strain due to the change of original dimension. Hence, the engineering stress-strain must be interpreted with caution beyond the elastic limit. The true stress rather than the engineering stress can give a more direct measure of material's response in the plastic flow range.

B. THE RAMBERG–OSGOOD STRESS–STRAIN FIT

According to the work of Kyriakides (2007), the relation of stress and strain can be defined by using the power law relationship. The most commonly used formula is the three parameter Ramberg–Osgood Equation as follows:

$$\varepsilon = \frac{\sigma}{E}\left[1+\frac{3}{7}\left(\frac{\sigma}{\sigma_y}\right)^{n-1}\right] \quad \textbf{.....(3.10)}$$

Where **E**, σ_y , and, **n**, are fit parameters. These parameters can be determined from a measured stress-strain curve as follows:

a) E is the slope of the linearly elastic part of the curve;
b) σ_y , is the stress at the intersection of the stress-strain curve and a line through the origin with a slope of 0.7E (see **Figure 3.10**);
c) An approximate value of n is determined from the slope of the linear part of plot of log $\left(\varepsilon-\frac{\sigma}{E}\right)$ vs. log (σ);
d) Plot this first estimate of the fit and compare the curve with the curve from the experiment. Change, σ_y , and, **n**, repeatedly until the best fit is achieved.

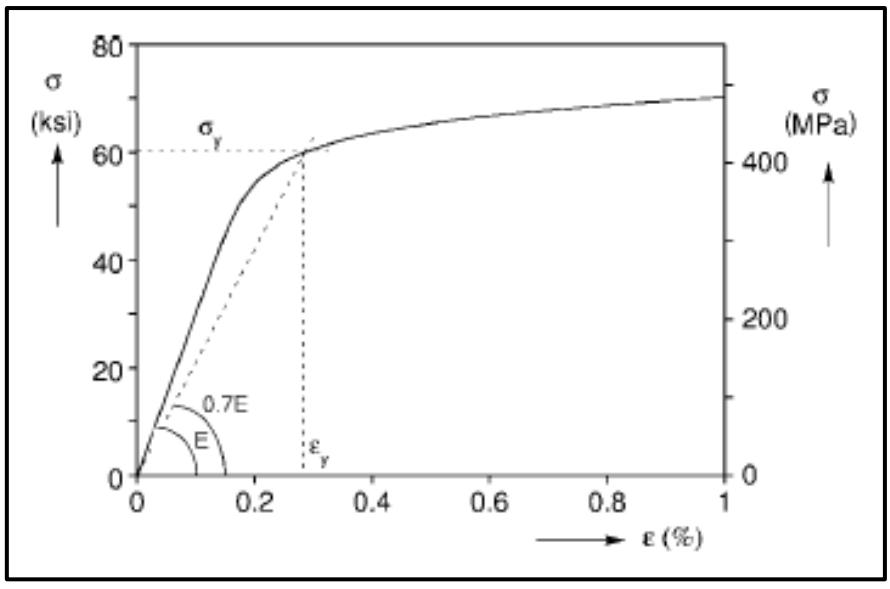

Figure 3.10 The example of Ramberg–Osgood stress-strain curve (Ref., Kyriakides, 2007).

C. DISCONTINUOUS YIELDING ON STRESS STRAIN CURVE

The transition from elastic to plastic deformation of hot-finished low carbon steel is usually characterized by a material instability called *Lüders strain*. The Lüders strain can be defined as the stretch of strain during the yield stress point. The macroscopic effect of the instability is inhomogeneous deformation.

The example of phenomenon for "Lüders strain" and inhomogeneous strain in low-carbon steel can be seen in **Figure 3.11**. It shows the typical stress-strain response in a uniaxial test in X60 line-grade carbon steel.

The **Figure 3.11(a)** shows the zoom of stress-strain response along the Lüders strain band. The figure clearly shows two yield points, σ_U , (upper yield stress) and σ_L , (lower yield stress). The localized plastic deformation begins at the upper yield stress with sudden drop in stress.

During displacement control, *Lüders strain* spreads along the material of steel while the stress is relatively constant. In the end of the Lüders strain band ($\Delta\varepsilon_L \approx 2.67\%$), the material of steel will start hardens and return back to homogenous deformation. From the **Figure 3.11(a)**, it can be determined that the yield stress is, σ_L , (418MPa) as the plateau stress value.

The **Figure 3.11(b)** shows the continuation of stress-strain response of X60 steel containing Lüders strain, until specimen fail. From this figure, the steel hardens during strains range from 2.97% to 15.5% and the material deforms homogeneously (Kyriakides, 2007).

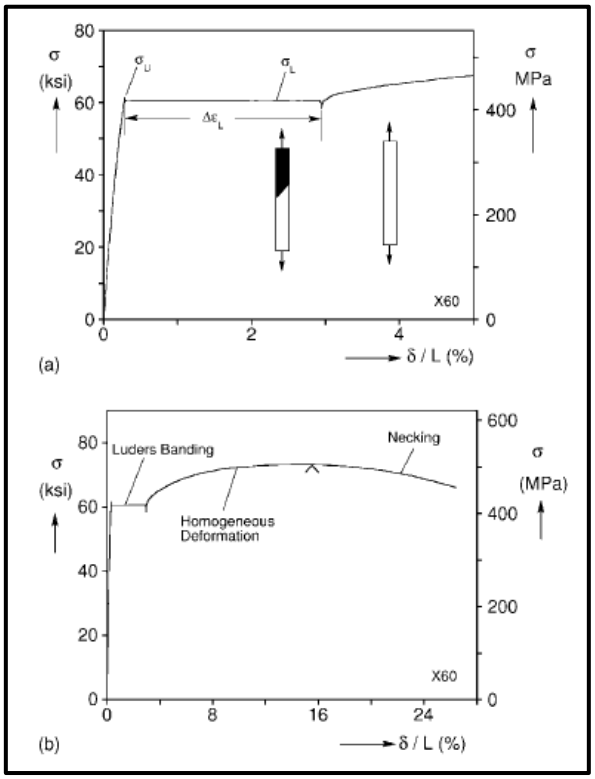

Figure 3.11 Example stress–strain curve of an X60 steel exhibiting Lüders banding: (a) small strain regime and (b) straining to failure (Ref., Kyriakides, 2007).

It is well established that the material instability (Lüder's plateau behavior) can be seen in the stress-strain response of the as-received seamless pipe in tension only. The mechanical cold working during spooling and reeling off process will transform Lüder's plateau behavior into new stress-strain response with more continuously yielding curve.

Figure 3.12 shows an example of comparison results between model test and FE modeling by ABAQUS. It can be observe from **Figure 3.12**:

1. The Lüder's plateau behavior during the first tensile loading with initial peak of yield stress;
2. "The apparent onset of yielding" in compression at relatively low stress;
3. Lower yield stress under subsequent tensile loading.

The description above represents the steel behavior during the loading cycles. It is started by tensile loading continued with compression loading. When the compression is first applied, the plateau behavior is not appearing as shown in **Figure 3.13**. It shows the stress-strain response of X65 steel during the loading cycle in tension and compression.

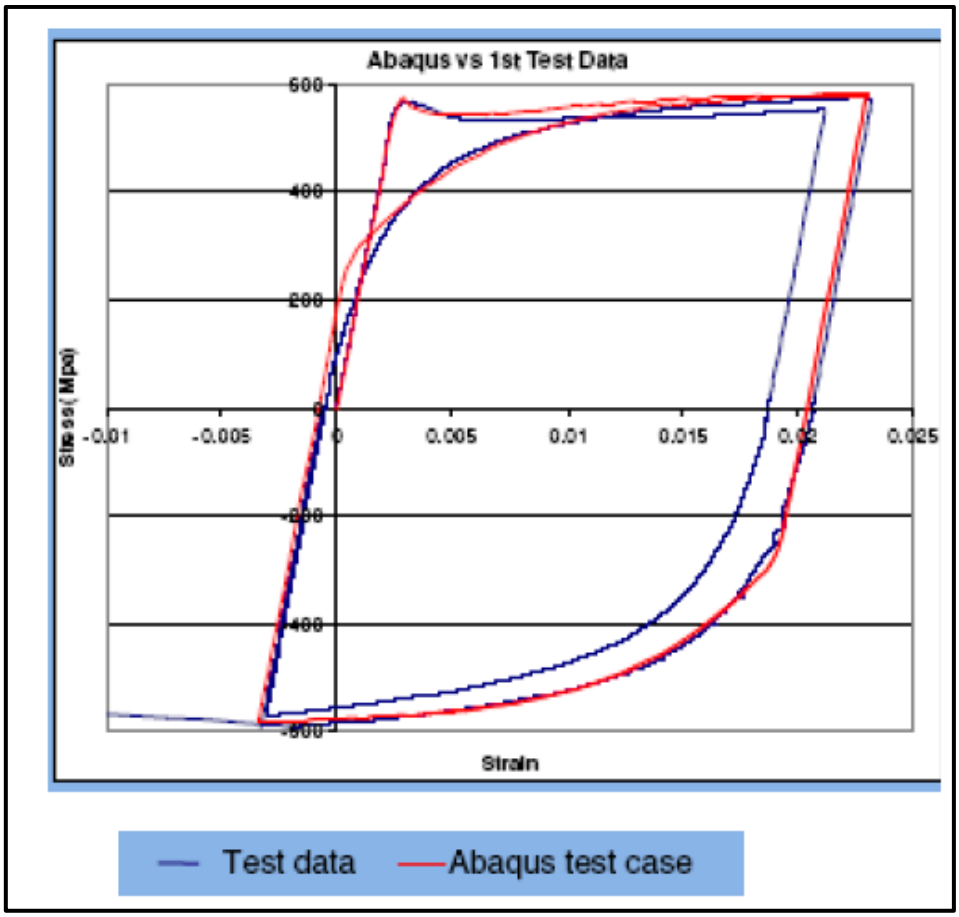

Figure 3.12 Stress–strain behavior of seamless pipe – first and subsequent cycles (Ref., Subsea7 Technical Guideline: ECA of Reeled Rigid Pipelines).

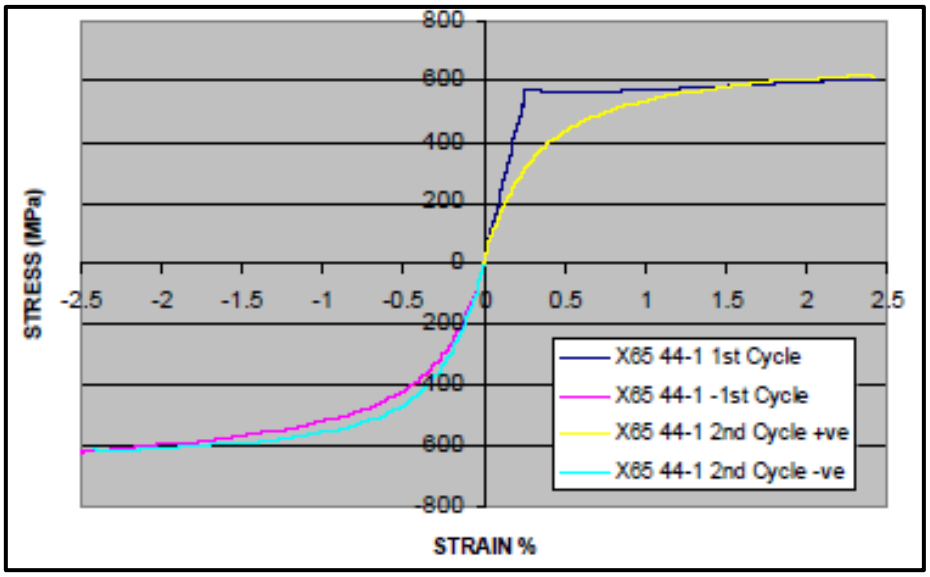

Figure 3.13 Example of stress-strain behavior in tension and compression (Ref., Subsea7 Technical Guideline: ECA of Reeled Rigid Pipelines, 2011).

The **Figure 3.14** shows the steel behavior during the second tension and compression with no plateau behavior. It is shows that the stress strain response between tension and compression in the second cycle is quite similar.

It is now generally accepted that the continuous curve behavior is the result of mechanical straining during reeling. The plateau behavior will reappears after certain period of time, depending on the temperature (Subsea7, 2011).

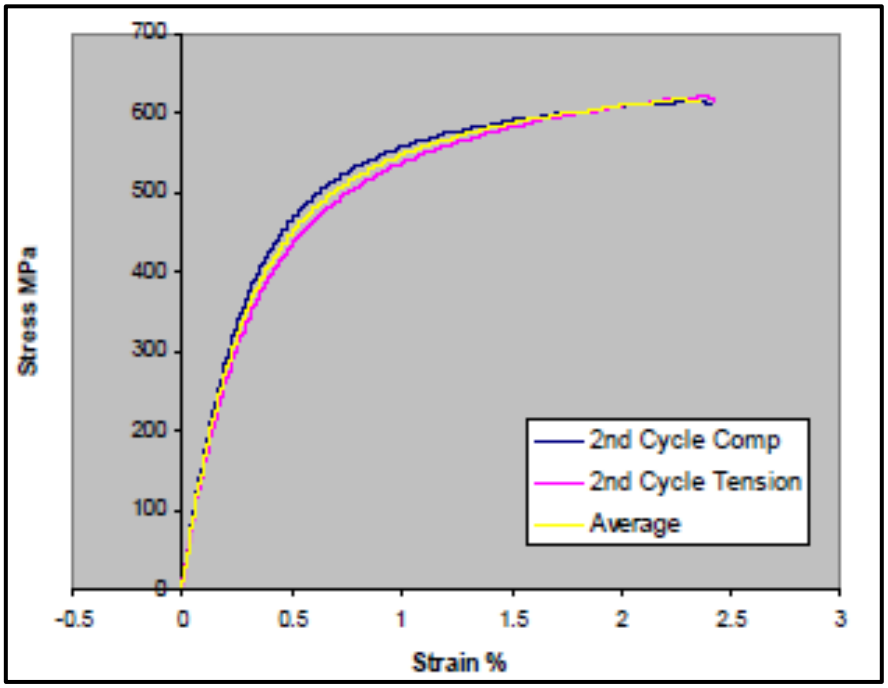

Figure 3.14 Example of second cycle stress-strain behavior in tension and compression (Ref., Subsea7 Technical Guideline: ECA of Reeled Rigid Pipelines, 2011).

3.3 Small Scale Testing for ECA

3.3.1 Tensile Test

The tensile test can be done for base and weld metal by using conventional round bar dumbbell shaped tensile test specimens. The samples of base metal are taken along the pipe longitudinal direction while the samples of the weld metal are taken along the direction transverse to the pipe axis. Usually, the yield strength on the weld is higher than the yield strength of the base metal as referred to over match girt weld condition (Subsea7, 2011).

The tensile test is conducted to generate a stress-strain response. In this test, the engineering stress is calculated based on the basis of the original cross-sectional area of the sample instead of the true stress that is based on the actual area of cross section. The significant reductions in cross-sectional area are presented between yield and fracture at the latter stage of the tensile test for ductile materials. Furthermore, the ultimate stress, the yield stress and Young's modulus, **E**, can be determined from the stress–strain curve (Megson, 2005).

3.3.2 Fracture Resistance Test

According to DNV-RP-F108, the objective of the fracture resistance test is to determine the fracture resistance for both of the pipe and girth welds to calculate to the acceptable flaw sizes.

Furthermore for the installation phase, DNV-RP-F108 recommended conducting the fracture test by using the SENT (Single Edge Notched Tension) specimen (see **Figure 3.15**).

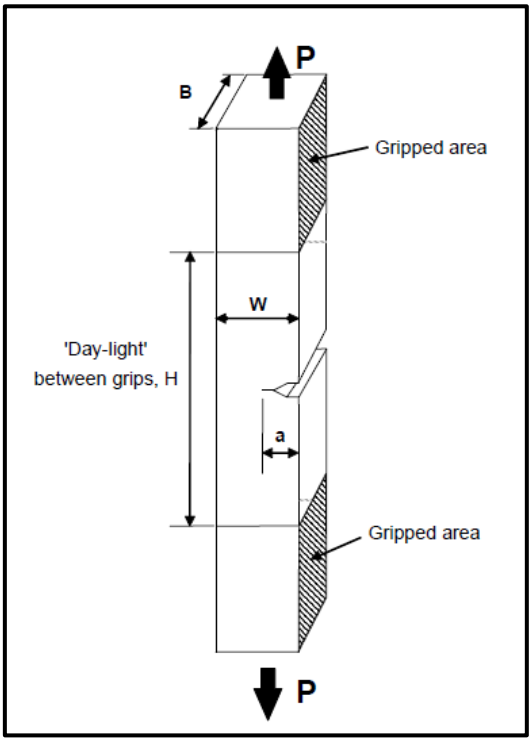

Figure 3.15 The clamped SENT (Single Edge Notched Tension) specimen (Ref., DNV-RP-F108).

The material fracture resistance can be described typically by K (Stress Intensity Factor), CTOD (Crack Tip Opening Displacement) or the J-integral. However, it is well-known that the stress-strain state at a crack tip cannot be fully described only by single parameter alone. The fracture resistance also influences by the crack tip constraint i.e., the degree of crack tip stress tri-axiality.

In addition to DNV-RP-F108, the BS 7448 and ASTM E 1820 also define the methodology for fracture resistance testing by using SENB (Single Edge Notched Bend) or CT (Compact Tension) specimen. The difference between SENB and CT with SENT specimen is that both specimen predominantly loaded in bending and has high crack tip constraint. Hence, the fracture resistance test by using SENB and CT will give lower bound estimation of material fracture resistance. Therefore, for conservative fracture assessment, these tests can be selected for a large range application of engineering structure.

During installation, pipeline girth welds are primarily loaded in tension even though the pipeline is globally subjected bending. Furthermore, the flaws size being analyzed is usually governed by the weld pass height, around 2-6mm which is relatively small. Therefore, the crack tip constraint in pipe will be decreased due to these aspects when compared to deeply notch standard specimens, SENB and CT. Hence, it is acceptable to obtain the fracture resistance using the specimen with a crack tip constraint closer to the actual crack tip constraint in the pipe.

The SENT specimen is a specimen that has loading mode and crack tip constraint similar to the actual loading mode and crack tip constraint in the girth weld of a pipe subjected to the bending and axial loading.

High toughness materials are needed in the installation method involving significant plastic strain in order to generate realistic allowable flaw sizes in the girth welds.

1. The J-R (or CTOD-R) curves is typically used to described the fracture resistance;
2. The brittle fracture is not allow to occur before achieving the maximum load plateau or stable crack extension of at least 1.5mm.

A. CRACK ORIENTATION AND LOCATION

Figure 3.16 shows the SENT specimen that shall normally be designed with a Surface Notch (SN), since it is the relevant orientation for flaws in the girth welds.

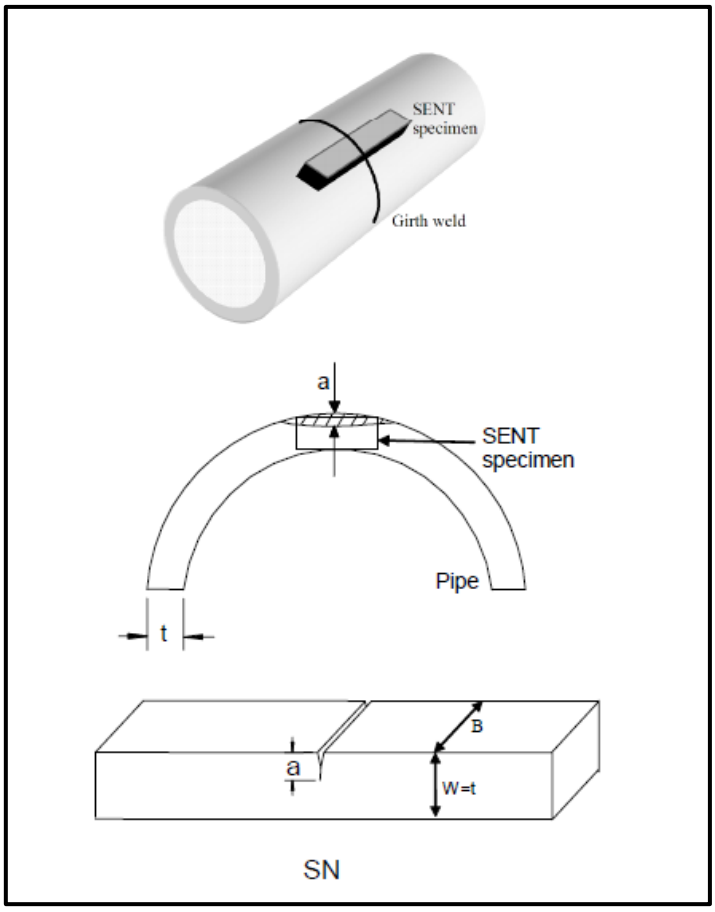

Figure 3.16 Relationship between defect orientation and height in the pipe with the crack orientation and size in the specimen (Ref., DNV RP F108).

B. SPECIMEN DIMENSIONS

The dimensions for the SN specimen are recommended with ratio **B=2W** where **W**, is the wall thickness **t**, of specimen and **B**, is the specimen width. It is also required that the **W**, should be less than the minimum amount of machining necessary in order to acquire a rectangular specimen. The examples of SENT specimen with definition of various dimensions can be seen in **Figure 3.15** and **Figure 3.16** respectively.

If the reductions in wall thickness, because of pipe dimension (**D/t**), will be more than 15% (i.e. $W < 0.85 \times t$). The specimen width, **B**, may be reduced, as long as this reduction not less than $B \geq W$. **Figure 3.16** illustrates the notch orientations and their connection to circumferential defect in the pipe.

The crack tip constraint tends to be insensitive by the pre-crack depth (a/W, machined notch + fatigue pre-cracking) in both the clamped SENT specimen and circumferential cracks of the pipe. Therefore, the actual pre-crack depth in the clamped SENT specimen is not crucial as long as the ratio between the pre-crack depth and the specimen a/W is around $0.2 \leq a/W \leq 0.5$.

During determining pre-crack in the SENT specimen, the actual microstructure sampled by the crack tip and its relation to the subsequent defect assessment shall be considered.

C. LOADING CONDITIONS

The SENT specimen can be clamped (see **Figure 3.15**) or pin-loaded in the test machine. Since both of these loading conditions give acceptable crack tip constraint similar to defects in pipe girth welds.

If the clamped specimen is used, the free length or "day-light" between the grips (H) of the test machine shall be equal to ten times specimen width, **10W**, when using the formula for estimating, **J**. On the other hand, for pin loaded specimen, the clamping distant is not affecting the results.

In pin loaded specimen, the testing machine does not give restraining bending moment on the SENT specimen. It may difficult to achieve ideally pin loaded specimen gripping in practical condition. The formula in **Equation 3.14** will however usable to obtain slightly conservative result, when the specimen is gripped e.g., in an ordinary wedge clamp which is connected to the testing machine by using bolt bearing.

D. TESTING CONDITIONS

The multiple specimens approach with at least 6 specimens or 6 valid results for each crack location shall be used to produce the J-R (or CTOD-R) curves. The specimens shall be loaded to tearing lengths between 0.2 and 3 mm. The majority of data shall be between 0.5 and 1.5 mm. The J-R or CTOD curves shall be generated as a lower bound curve for experimental results.

Generally, the fitting data with the form $J = x \cdot \Delta a^m$ is fits the data well. If the cut off level, $\mathbf{L_{r\ max}}$, is calculated from the SENT test, it shall be determined from at least three specimens that loaded beyond maximum load. The tearing length, **Δa**, for the J-R curve shall include blunting.

For assessment of the installation phase, testing shall be performed for as-welded (un-deformed condition) and at the lowest anticipated temperature for reeling-on and reeling-off.

However, the test at the highest anticipated temperature shall also be considered if the pipe temperature during installation may be higher than 50°C (25°C for Duplex stainless steels) due to field coating application. The stable crack tearing resistance may be lowered at high temperatures.

E. FORMULA TO CALCULATE J FOR SENT SPECIMENS

The crack growth resistance is recommended to be described by J-R curves. The elastic and plastic parts are considered separately when generating the total J-integral.

The **Equation 3.11** can be used to calculate J-integral when the amount of ductile crack growth lower than 10% of the initial remaining ligament ($\mathbf{W - a_0}$).

$$J = J_e + J_p \cong J_e + J_{p0} \quad \textbf{..... (3.11)}$$

Where,

J_e = Elastic part of the J-Integral,

J_p = Plastic part of the J-Integral,

J_{p0} = Plastic part of the J-Integral without crack growth correction.

The relation between the elastic part of the J-integral and the Stress Intensity Factor **K**, can be seen in **Equation 3.12** below:

$$J_e = \frac{K^2}{E'} \quad \text{..... (3.12)}$$

Where,

E' = E for plane stress (E is Young's Modulus)

$$E' = \frac{E}{1-\nu^2} \quad \text{for Plane Strain ..... (3.13)}$$

ν = Poisson's ratio

The plastic part of the J-Integral is calculated through the plastic work applied to the cracked specimen:

$$J_p = \frac{\eta_p \cdot U_p}{B(W-a_0)} \quad \text{..... (3.14)}$$

Where,

η_p = Dimensionless function of the geometry,

U_p = The plastic part of the area under the load vs. Crack Mouth Opening Displacement (CMOD) curve (**Figure 3.17**),

B = The width of the specimen (**Figure 3.15**),

$(W-a_0)$ = The remaining ligament (**Figure 3.15**),

a_0 = The initial crack length.

The CMOD can be determined from two ways; direct measurement from the crack mouth of specimen or double clip gauges approximation. The formula of, η_p, to determine, J_p, can be seen in **Equation 3.15**. It can be used for:

$0.2 \leq a/W \leq 0.5$;

$1 \leq B/W \leq 5$;

H = 10W.

$$\eta_p = 0.88 \times \left\{ \begin{array}{l} \left(209{,}747 \cdot e^{-\left(\frac{B}{W}\right)} - 85{,}668\right) \cdot \left(\frac{a}{W}\right)^5 + \left(-467{,}666 \cdot e^{-\left(\frac{B}{W}\right)} + 195{,}032\right) \cdot \left(\frac{a}{W}\right)^4 \\ + \left(393{,}925 \cdot e^{-\left(\frac{B}{W}\right)} - 163{,}572\right) \cdot \left(\frac{a}{W}\right)^3 + \left(-160{,}931 \cdot e^{-\left(\frac{B}{W}\right)} - 61{,}334\right) \cdot \left(\frac{a}{W}\right)^2 \\ + \left(32{,}319 \cdot e^{-\left(\frac{B}{W}\right)} - 9{,}568\right) \cdot \left(\frac{a}{W}\right) + \left(-1{,}72 \cdot e^{-\left(\frac{B}{W}\right)} + 1{,}333\right) \end{array} \right\} \quad \textbf{(3.15)}$$

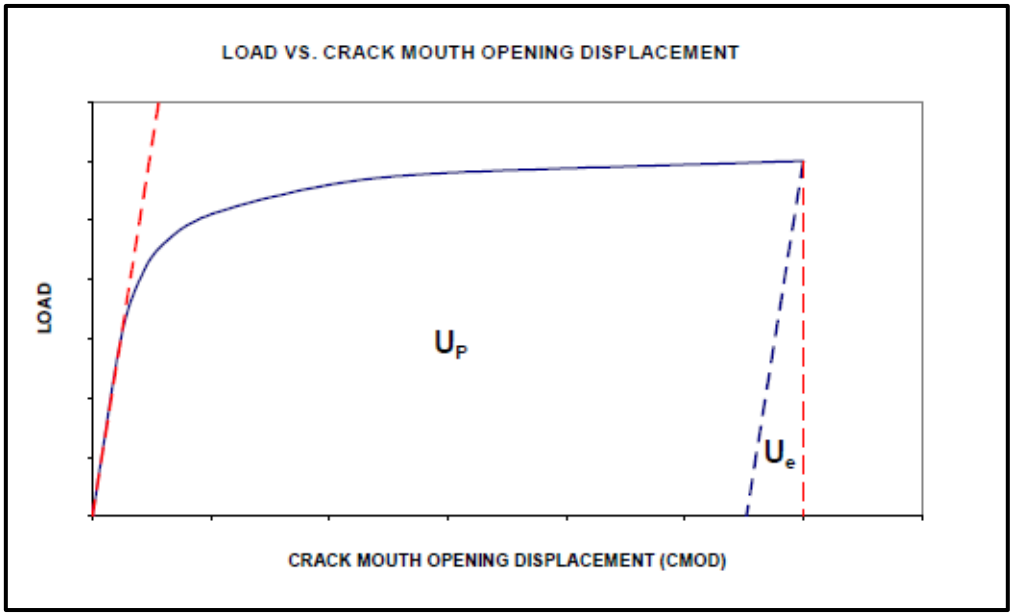

Figure 3.17 Load as a function of Crack Mouth Opening Displacement (Ref., DNV-RP-F108).

3.3.3 CTOD from J Fracture Toughness

Fracture toughness is defined by J-integral in relation to SENT specimen testing. However, majority of works and literatures concerning ECA and circumferential defects in pipeline girth welds at high strain, defined crack driving force in terms of CTOD rather than J-integral. Hence, it will be necessary to convert the J-integral from SENT specimen into an equivalent CTOD (Macdonald, 2011).

According to DNV OS-F101, the **Equation 3.16** can be used to transform the J-integral into CTOD conservatively.

$$\delta = \frac{J}{m\left(\frac{YS + UTS}{2}\right)} \quad \textbf{(3.16)}$$

$$m = 1.221 + 0.793\frac{a}{W} + 2.751n - 1.418n\frac{a}{W} \quad \textbf{.....(3.17)}$$

$$n = 1.724 - 6.098\left(\frac{YS}{UTS}\right) + 8.326\left(\frac{YS}{UTS}\right)^2 - 3.965\left(\frac{YS}{UTS}\right)^3 \quad \textbf{.....(3.18)}$$

Where,

YS = The engineering yield stress at test temperature,

UTS = The tensile strength at the test temperature,

m = Constraint parameter according to ASTM E1290-02,

n = The strain-hardening parameter,

a = The original crack size,

W = The specimen width.

Another way to convert J-integral to CTOD can be seen in the work of Shih (1981) cited in Anderson (2005), **Equation 3.19** can be used as an alternative approach to calculate CTOD which can be applied well beyond the validity limits of LEFM.

$$\delta = \frac{d_n J}{\sigma_o} \quad \textbf{.....(3.19)}$$

Where d_n is a dimensionless constant, which can be selected from **Figure 3.18** which shows that d_n is highly dependence on the strain hardening exponent (n) and a slightly dependence on $\frac{\alpha\sigma_0}{E}$. For $\alpha \neq 1$, the **Equation 3.19** should be multiplied by $\alpha^{1/n}$.

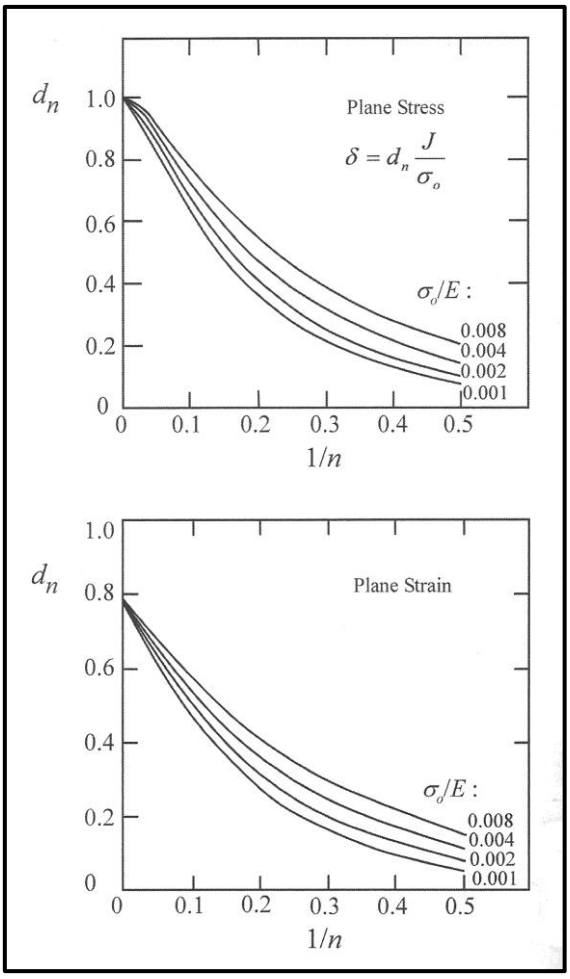

Figure 3.18 Predicted J-CTOD relationship for plane stress and plane strain, assuming $\alpha = 1$ (Ref., Anderson, 2005).

4. MODELING TOOLS

4.1 Modeling Concept by LINKpipe

4.1.1 General

Three dimensional solid finite elements are commonly used in discretizing the shell structure for the crack analysis in traditional approach. An illustration of typical mesh can be seen in **Figure 4.1**. However, this approach needs higher demand of CPU capacity and requires long duration of simulation process. Hence, an alternative approach is introduced by using shell finite elements for solving fracture mechanics related problems and by modeling cracks using line-spring finite elements.

A typical solid finite element mesh requires 30,000 degrees of freedom (utilizing two symmetry planes) while the similar shell model will have around 1,000 degrees of freedom (using symmetry). Hence, the CPU utilization will reduce typically by a factor of 10. The main advantage of using shell/line-spring elements is to reduce the required time during pre and post processing of the FE analyses. An illustration of solid and shell/line-spring modeling of surface cracked shells can be seen in **Figure 4.1**.

Using line-spring finite elements, the crack is modeled as nonlinear springs between the shell elements with varying compliance as a function of crack depth and plastic deformations. The accuracy of predicted fracture mechanics parameters such as crack tip opening displacement (CTOD) and J-integral is important for this approach.

On the other hand, this method still has limitations for short crack and large deformation analysis. Short cracks with respect to practical situations are the cracks with depth less than 25% of the shell thickness. To assess the criticality of the defects, simultaneous use of large displacement and rotations are needed to consider in many applications. These features are well-considered and implemented in a new commercial code, LINK.

LINK is a general nonlinear shell finite element program accounting large rigid body motion and plasticity. The type of the shell element is a rectangular ANDES element in a co-rotated formulation. The local strains assumed to be small. Within this formulation, better line-spring finite element is implemented.

These features made LINK a tool that can consider both cracks and global/local buckling in the same simulation. One of industry practice where this is applicable is in reeling installation with nominal strain around ~2% (LINKftr, 2012).

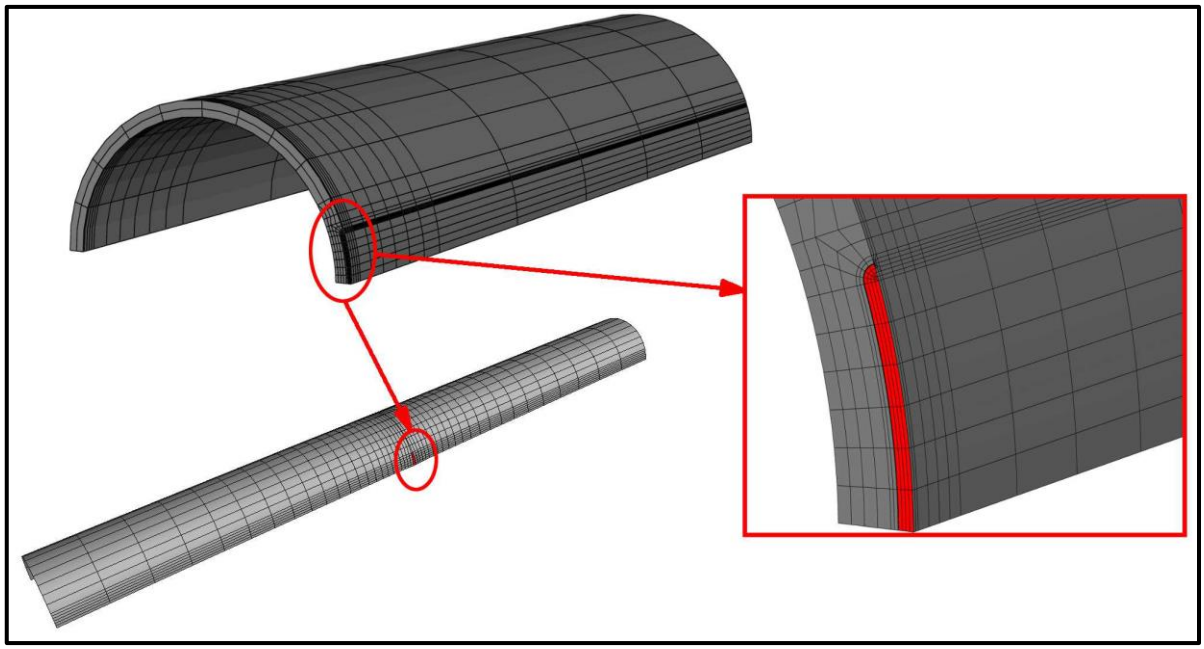

Figure 4.1 Solid and shell/line-spring modeling of surface cracked shells (Ref., LINKpipe theory manual, 2012).

4.1.2 LINKpipe Verification

Comparison using LINKpipe and large scale test for pipeline with surface cracks has been done by Berg et al., (2007). The summary of the work is as follows:

a. The study was to compare the results from large scale experiments of pipe segments with the results predicted by LINKpipe;
b. For the modeling, it is assumed that pipeline was subjected to pure bending load to represent the external applied load;
c. For the case of bending of the pipes having external surface defects, the results from shell-line spring model and large scale testing were compared. The comparison showed that the results are "generally in good agreement quantitatively";
d. The comparison adds support for the implementation of LINKpipe software for fracture analysis of pipeline loaded beyond yielding.

Several verifications of the software by comparing with the predictions from 3D solid finite element analysis are provided by the following literature:

1. The summary from the work of Sandvik et al., (2011) is as follows:

   FE analyses using 3D FE model from Abaqus and Shell-Line spring element model from LINKpipe were performed. The FE models included the ductile tearing and material crack growth resistance characteristics. A comparison has been done by comparing the crack driving forces i.e., plotting the crack tip opening displacement (CTOD) against the global longitudinal tension strain. The work concluded that LINKpipe software results are "*in reasonable accordance with the Abaqus/Explicit Simulations and should be suitable for the pipeline engineering fracture assessment model.*"

2. Thaulow et al., (2006), performed fracture assessment of pipeline using efficient and accurate line-spring model. 3D FE analysis and large scale testing were performed to compare the results. The main conclusions of the study are:

    a) The fracture parameters that calculated from LINKpipe model (line-spring) for surface cracked pipes are in "good agreement" with 3D FE simulation;
    b) Line-spring model is proved to be an efficient and accurate tool to estimate constraint in pipeline with surface cracked;
    c) Also, in case of crack driving force for ECA, LINKpipe give very close result to the 3D calculations.

3. Jayadevan et al., (2006) carried out a study to examine ductile crack growth in surface cracked pipes. They used the line-spring model to simulate ductile tearing surface cracked pipes with a focus on the through-thickness ductile crack growth of the circumferential surface crack. The predictions from the line-spring model were compared against that from 3D FE analyses. The influence of ductile tearing on crack driving force for surface cracked pipes was investigated using line-spring model. The main conclusions are:

    a) The results of ductile crack growth from line-spring were in "good agreement" with detailed continuum simulation;
    b) The study showed that the crack growth line-spring model is an accurate method for ductile crack growth simulation in surface cracked pipes.

4. Jayadevan et al., (2005), conducted a study to determine the constraint in pipelines using efficient and accurate line-spring model, the results are then compared with detailed 3D FE analysis. The main conclusions are:

    a) The results for elastic SIF (Stress Intensity Factor) and T-stress results from the line-spring model are in "good agreement" with the results from 3D FE analysis;
    b) Even under large-scale yielding, the results for T-stress from the elastic-plastic line-spring model correspond well with the constraint results from 3D FE analysis.

5. Skallerud B, Holthe K, and Haugen B., (2005), compared the results from shell and line-spring finite element simulations with the results from detailed solid finite element analyses using Abaqus. The numerical simulation is performed for several cases i.e., Single Edged Notched Tensile (SENT) specimen, cracked cylindrical shell in tension, and cracked cylindrical shell in bending. The study showed that the co-rotated thin shell elements based on assumed natural deviatoric strains and co-rotated line-spring finite elements combination works well.

4.1.3 Line-Spring and Shell Finite Element

A. LINE-SPRING FINITE ELEMENT

According to Berg et al., (2007), a 3D-problem can be represented by a 2D shell structure by using the line-spring technology. A surface crack is then modeled by using line-spring

elements. The compliance in the line-spring elements is calculated based on known solutions of a single edge notch (SEN) specimen.

The local compliance of a spring at a point depends on the depth of the surface crack at that point. Once the local compliance computed, the stress intensity factor, $\mathbf{K_I}$ and the crack tip opening displacement, CTOD, can be calculated along the crack front.

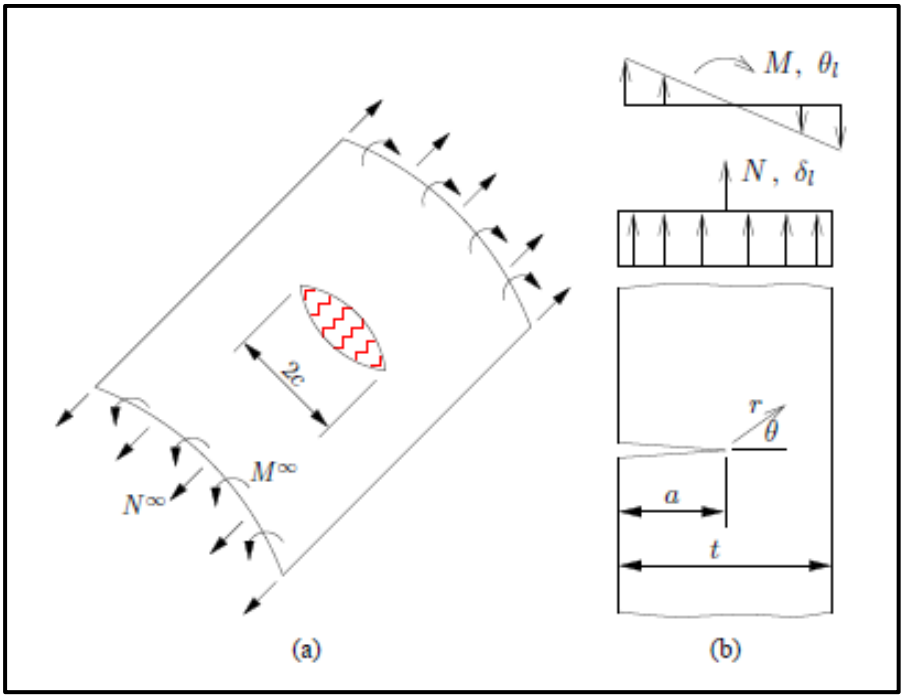

Figure 4.2 (a) 2D shell model with line-springs representing the surface crack. (b) The compliance at any point along the line-spring (Ref., Berg et al., 2007).

B. SHELL FINITE ELEMENT

According to LINKpipe theory manual (2012), the shell finite element used in LINKpipe is an Assumed Natural Deviatoric Strains (ANDES) shell element. The shell and line-spring element in LINKpipe is a high-performance and non-conforming thin shell finite element based on ANDES.

The ANDES element was initially developed by Felippa and Militello (1992) as cited in LINKpipe theory manual (2012). It was further extended by Skallerud and Haugen (1999) as cited in LINKpipe theory manual (2012) to handle large rotations and inelastic behavior. The ANDES shell finite element is derived in a co-rotated formulation that gives a "stringent way" of extracting only the strains and curvatures generating deformations in the element.

The strains at element level are assumed to be small, but the global deformations can still be large. Detailed descriptions for the derivations of the co-rotated ANDES shell finite are published by Skallerud et al. (2005) as cited in LINKpipe theory manual (2012).

4.1.4 Ductile Crack Growth

Ductile crack growth is applied in the line-spring element for fully plastic deformation conditions. Jayadevan et al., (2006) as cited in LINKpipe theory manual (2012) showed the applicability of using the crack growth resistance curve that is in accordance with the established use as defined in BS7910:1999. The crack growth resistance curve used in LINKpipe can be given by **Equation 4.1**.

$$CTOD = CTOD_i + C_1(\Delta a)^{C_2} \quad \textbf{.....(4.1)}$$

Where, $CTOD_i$ is the critical CTOD-value at onset of ductile tearing. C_1 and C_2 are fitting constants. The updated crack depth, **a**, at the end of a load increment is expressed by **Equation 4.2**.

$$a^{(i+1)} = a^{(i)} + da^{(i)} \quad \textbf{.....(4.2)}$$

4.1.5 Fatigue Crack Growth

The high cycle fatigue load station in LINKpipe is based on the analysis methods described in BS7910. The computations are based on the K-solution in BS7910, but not from the finite element calculations. To determine accumulated fatigue crack growth under certain loading cycles, LINKpipe conducts a numerical integration of Paris' equation for crack growth.

4.1.6 Clad and Lined Pipes

According to Olsø et al., (2011), a new bi-metallic shell element was developed in LINKpipe in order to analyze fracture and local buckling on clad pipes.

For fracture assessment in clad pipes, LINKpipe uses through thickness integration of the shell element. The through thickness integration is executed in two steps, one step for each material layer. In the shell element, the strain and stress resultants are calculated in the mid-thickness (reference plane). The strain components in each integration point through the thickness will then be based on the strains in the nodes.

According to LINKpipe theory manual (2012) to account mismatch in weld metal, a simplified approach in the line-spring finite element is implemented. Input data are the stress-strain curves for each of the material. **Figure 4.3** shows an illustration where base material, weld metal and clad material are present. It is assumed that the strain localization in the ligament follows a 45^0 line from the crack tip to the opposite surface.

Based on the assumptions in **Figure 4.3**, a weight function is used to calculate an equivalent stress-strain curve which should be assigned to the line-spring element. The weight function can be seen in **Equation 2.2**.

Furthermore, in the work of Olsø et al., (2011), the procedure can also be applied for the conventional pipeline without clad layer.

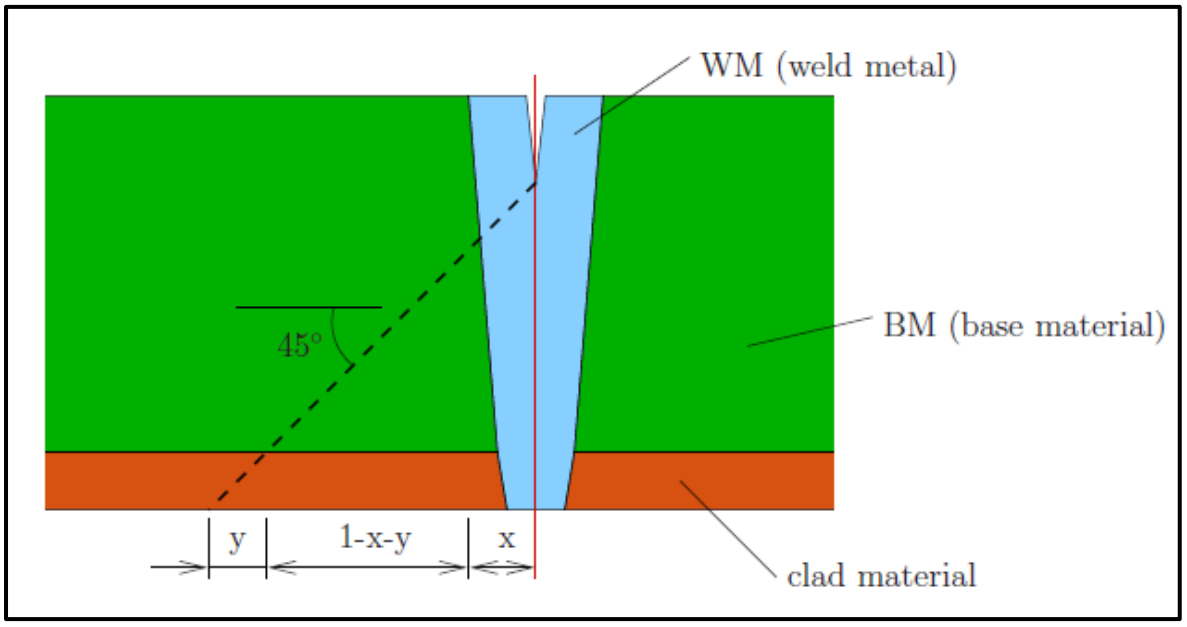

Figure 4.3 Illustration of clad pipes (Ref., LINKpipe theory manual, 2012).

4.2 Modeling Concept by CRACKWISE

According to CRACKWISE help documentation (2009), CRACKWISE automates the procedures of fracture and general fatigue analyses based on BS 7910: 2005 (incorporating Amendment No.1). BS7910 provides guidance on methods for analyzing the consequence of defects in terms of the structural integrity of welded structures. The methods are based on fracture mechanics, and relate to planar, crack-like defects. However, they may be used conservatively for evaluating volumetric flaws.

CRACKWISE complies with BS 7910 and provides additional features that enable it to examine the issues relating to the structural integrity assessment. The software automates the following calculations:

1. Fracture - known parameter, critical, sensitivity and critical sensitivity calculations;
2. Fatigue - crack growth calculations;
3. Fatigue and fracture - crack growth with fracture check (fatigue life).

CRACKWISE has the capability to perform the following type of calculations:

1. Fracture assessments: these (default setting) includes:

    - Performing known parameter assessments for different defect types combine with critical parameter calculations;
    - Assessing the maximum allowable defect dimensions, stresses, minimum required toughness and tensile properties;
    - Performing sensitivity analyses for most of the input parameters;
    - Carrying out critical and sensitivity parameter calculations by using input of geometry, stresses and material.

2. Fatigue assessments: these enable crack growth to be projected for structures subjected to cyclic loading.
3. Combined fatigue and fracture assessment: when both options fatigue and fracture are chosen, CRACKWISE includes a check from fracture at each stage of fatigue crack growth, to enable the fatigue life to be computed.

The BS 7910 fracture assessment methods are based on the concept of the Failure Assessment Diagram (FAD). The vertical axis of the FAD denotes the likelihood of fracture, whereas the horizontal axis denotes the likelihood of plastic collapse. The interaction between these two failure modes is taken into account in the analyses and shown by plotting a failure line on the FAD.

The analysis of a specific defect generates a single point on the FAD for assessment **Levels 1 and 2**, and an assessment line for **Level 3**. If the assessment point or assessment line is within or on the failure line then the defect is acceptable. If the point or line lies entirely outside the failure line then there is a possibility of structural failure, and the defect is not acceptable. For **Level 3**, if the assessment locus lies partially within the failure locus then the defect is acceptable, but with some tearing possible.

BS 7910 includes three levels of fracture assessments. Each assessment is based on the concept of a failure assessment diagram (FAD), which accounts for both fracture and plastic collapse modes:

Level 1 is a simplified method, and has an objective as preliminary assessments, or when input data are uncertain. Level 1 largely complies with PD6493:1980 and includes the CTOD design curve. Level 1 incorporates in-built safety factors of about 2 on defect size in terms of fracture, and 1.25 on stress in terms of plastic collapse. Level 1 procedure is based on simplified assumptions regarding stress distributions and FAD, and worst-case input data should be used.

Level 2 is the normal assessment method. Level 2 does not include in-built safety factors. However, guidance is provided to set certain partial safety factors on stress, flaw dimensions, toughness and yield strength. A various types of failure assessment diagrams are available, depending on material type and available data.

Level 3 is the most advanced method, and is capable of modeling ductile tearing, based on toughness expressed in terms of an R-curve. Furthermore, the Level 3 FAD is based on the specific stress-strain curve for the material to be assessed. However, a default option is given if the stress-strain curve is unknown. Also for this level, a various types of failure assessment diagrams are available, depending on material type and available data.

According to BS9710:2005, there are three types of level 3 assessment methods: Levels 3A, 3B and 3C. Each method applies a ductile tearing analysis and uses a different assessment line. The analysis results from the assessment are either a single assessment point or a locus of assessment points. If either the point or any part of the locus lies within the area bounded

by the axes and the assessment line, the flaw is acceptable; if it lays outsides the area then the flaw is not acceptable.

The ECA for the spooling on and reeling off are performed using Level 3B of the BS 7910 methods. This is based on permitting some tearing of the defect to take place and the FAL (The Failure Assessment Line) is produced from the specific material stress-strain curve (Subsea 7, 2011).

Figure 4.4 shows level 3 – ductile tearing instability assessment flowchart taken from BS9710.

4.2.1 Defining Stresses

According to BS7910:2005, the stresses that will be considered in the analysis are those that would be calculated by a stress analysis of the unflawed structure. The actual stress distributions may be used or the stresses may be linearized, as shown in **Figure 4.5**. The linearized method will usually overestimate the stress but it has the advantage that it does not need to be repeated with crack growth.

It is important that the effect of local or gross discontinuities or by misalignment is taken into account in the primary membrane and bending stresses, the secondary stresses and the magnification of the primary stresses.

A. PRIMARY STRESS (P)

The primary stress is stresses that could (if sufficiently high) contribute to plastic collapse. It is different from secondary stresses, which do not contribute to the plastic collapse. However, both stresses can contribute to failure by fracture, fatigue, creep or stress corrosion cracking.

They include all stresses arising from internal pressure and external loads. The primary stresses are separated into primary membrane, $\mathbf{P_m}$, and primary bending, $\mathbf{P_b}$, components as follows:

a. **Primary membrane stress (P_m)** is *"the mean stress through the section thickness that is necessary to ensure the equilibrium of the component or structure."*
b. **Primary bending stress (P_b)** is *"the component of stress due to imposed loading that varies linearly across the section thickness. The bending stresses are in equilibrium with the local bending moment applied to the component."*

B. SECONDARY STRESS (Q)

The secondary stresses, Q, are *"self-equilibrating stresses necessary to satisfy compatibility in the structure."* It can be relieved by local yielding, heat treatment, etc. Thermal and residual stresses are normally categorized as secondary stresses, but fluctuating thermal stresses are treated as primary in a fatigue assessment. A significant characteristic of secondary stresses is that they do not, contribute to plastic collapse, since they arise from strain/displacement limited phenomena.

The secondary stresses may be distributed into **secondary membrane, Q_m,** and **secondary bending, Q_b,** components similar to primary stresses. For level 3 assessment the residual stresses may in general be assumed to be uniform, as for Level 1, or non-uniform.

If the residual stresses are assumed to be uniform, the residual stress component, Q_m, may be assumed to be equal to the lower of the following values:

$$Q_m = \sigma'_Y \quad \textbf{..... (4.3)}$$

or

$$Q_m = \left(1.4 - \frac{\sigma_{ref}}{\sigma'_f}\right)\sigma'_Y \quad \textbf{.....(4.4)}$$

Where,

σ'_Y = The appropriate material yield strength at the given temperature for analysis. Except for temperatures below ambient, the room temperature value of σ'_Y is used in **Equation 4.3**.

σ'_f = The appropriate flow strength (assumed to be the average of the yield and the tensile strengths) at given temperature for the analysis. *(For the purposes of determining the residual stress, the flow stress is not restricted to a maximum of 1.2 times the yield strength).*

σ_{ref} = Reference stress.

Table 4.1 Symbols Definition in **Figure 4.4** and **Figure 4.5**

Symbols	***Description***
K_{mat}	Material toughness measured by stress intensity factor
δ_{mat}	Material toughness measured by CTOD method
Δa	Increment in a
a_0	Initial flaw size
a_j	Intermediate value of tearing flaw extension
a_g	Limit tearing flaw extension
L_r	Ratio of applied load to yield load
K_r	Fracture ratio of applied elastic K value to K_{mat}
δ_r	Fracture ratio using CTOD parameters
$\Delta\sigma_b$	Bending component of stress range
$\Delta\sigma_m$	Membrane component of stress range

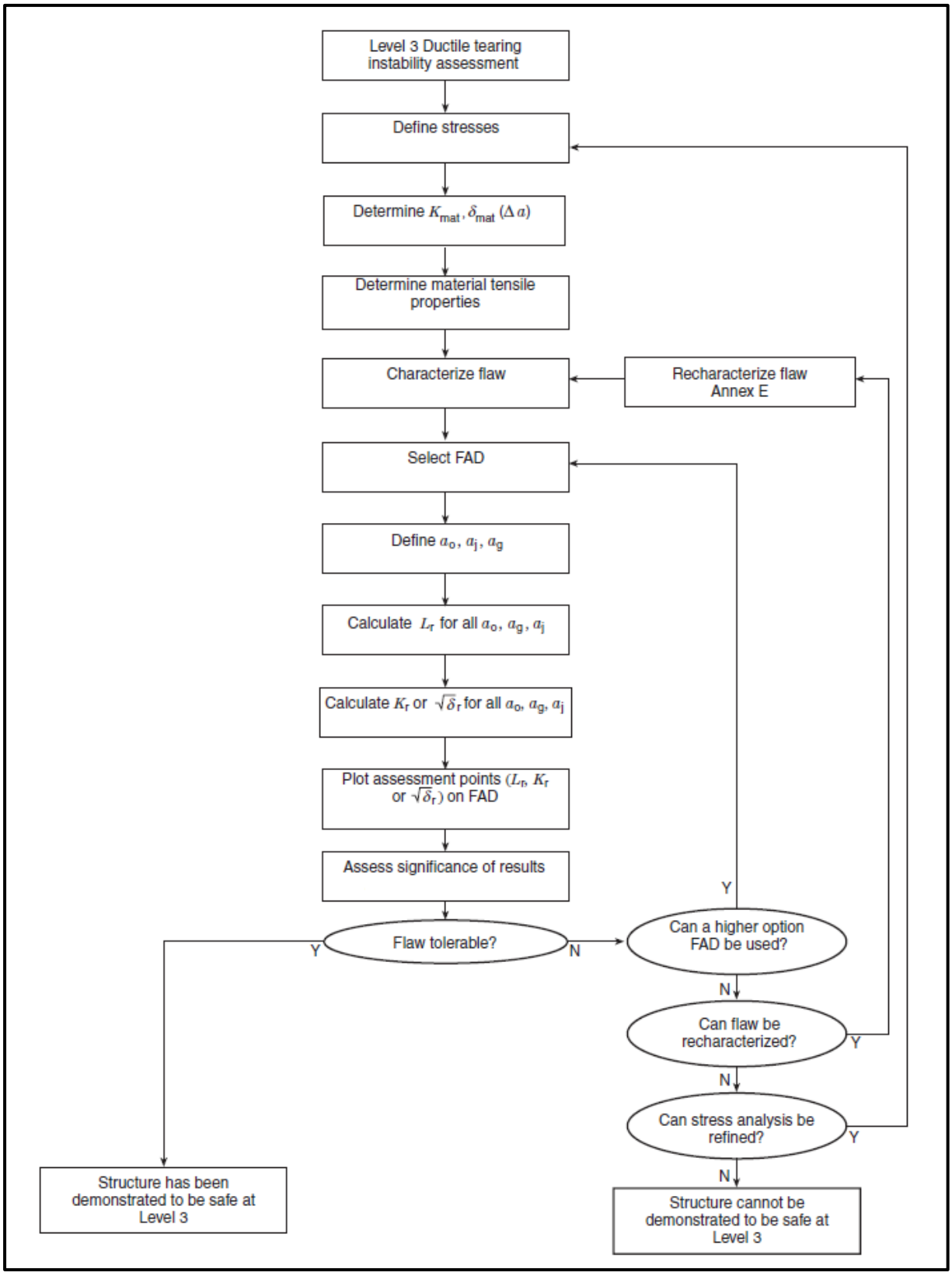

Figure 4.4 Level 3 – ductile tearing instability assessment flowchart (Ref., BS7910: 2005).

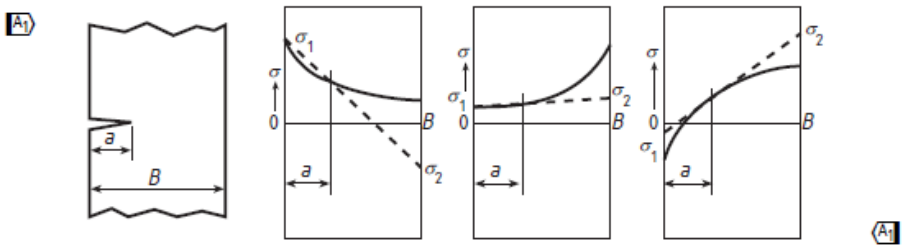

i) Examples of linearization of primary or secondary stress distributions for surface flaws

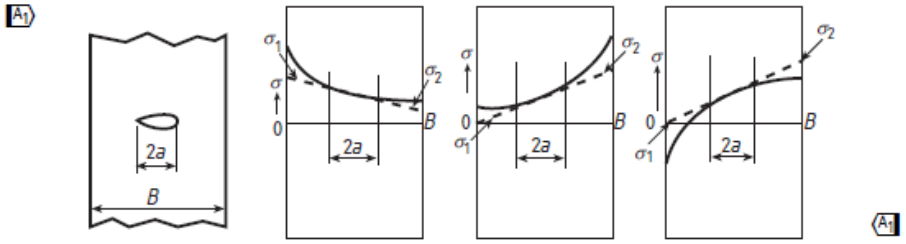

ii) Examples of linearization of primary or secondary stress distributions for embedded flaws

P_m, Q_m and P_b, Q_b can be determined from the distributions in i) and ii) using the following equations:

$$P_m, Q_m = \frac{\sigma_1 + \sigma_2}{2} \qquad P_b, Q_b = \frac{\sigma_1 - \sigma_2}{2}$$

NOTE Any linearized distribution of stress is acceptable provided that it is greater than or equal to the magnitude of the real distribution over the flaw surface.

a) Linearization of stress distributions in fracture assessments

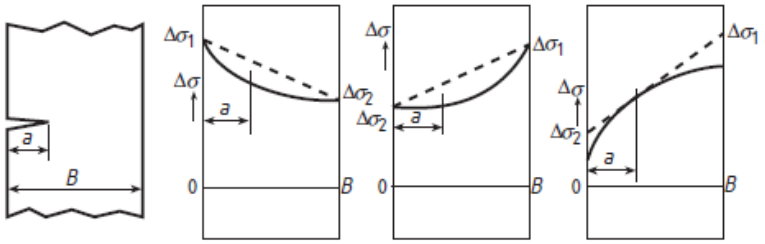

i) Examples of linearization of stress range distributions for surface flaws

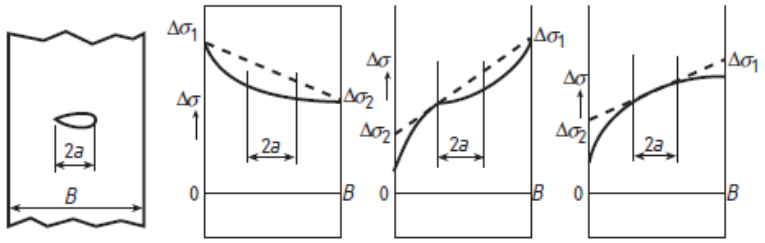

ii) Examples of linearization of stress range distributions for embedded flaws

$\Delta\sigma_m$ and $\Delta\sigma_b$ can be determined from the distributions in i) and ii) using the following equations:

$$\Delta\sigma_m = \frac{\Delta\sigma_1 + \Delta\sigma_2}{2} \qquad \Delta\sigma_b = \frac{\Delta\sigma_1 - \Delta\sigma_2}{2}$$

b) Linearization of stress range distributions in fatigue assessments

Figure 4.5 Linearization of stress distributions (Ref., BS7910: 2005).

4.2.2 Selecting FAD (Failure Assessment Diagram)

The procedure for selecting FAD is taken (quotes) directly from BS9710:2005 as follows:

A. FAD for Level 3A: Generalized FAD of Level 2A (not requiring stress-strain data)

The FAD is the same as that for Level 2A (p.45 BS9710):

The equations describing the assessment line are the following (p.39 BS9710):

For $L_r \le L_{rmax}$:

$$\sqrt{\delta_r} \text{ or } K_r = \left(1 - 0.14L_r^2\right)\left\{0.3 + 0.7\exp\left(-0.65L_r^6\right)\right\} \quad \textbf{(4.5)}$$

For $L_r > L_{rmax}$:

$$\sqrt{\delta_r} \text{ or } K_r = 0 \quad \textbf{(4.6)}$$

The FAD is shown in ***Figure 4.6*** *with different cut-offs for different materials.*

For materials which exhibit a yield discontinuity (often referred to as Lüders plateau) in the stress-strain curve (i.e. any curve which is not monotonically increasing), or for which it cannot be assumed with confidence that no discontinuities exist, either a cut-off value for L_r of 1.0 should be applied or Level 2B should be used.

This FAD provides a reasonable underestimate of the flaw tolerance of a structure but the underestimate may be excessive in cases where the initial rate of hardening in the stress-strain curve is high (such as materials operating in the strain ageing régime). In those cases, Level 3B should be considered (p.45 BS9710).

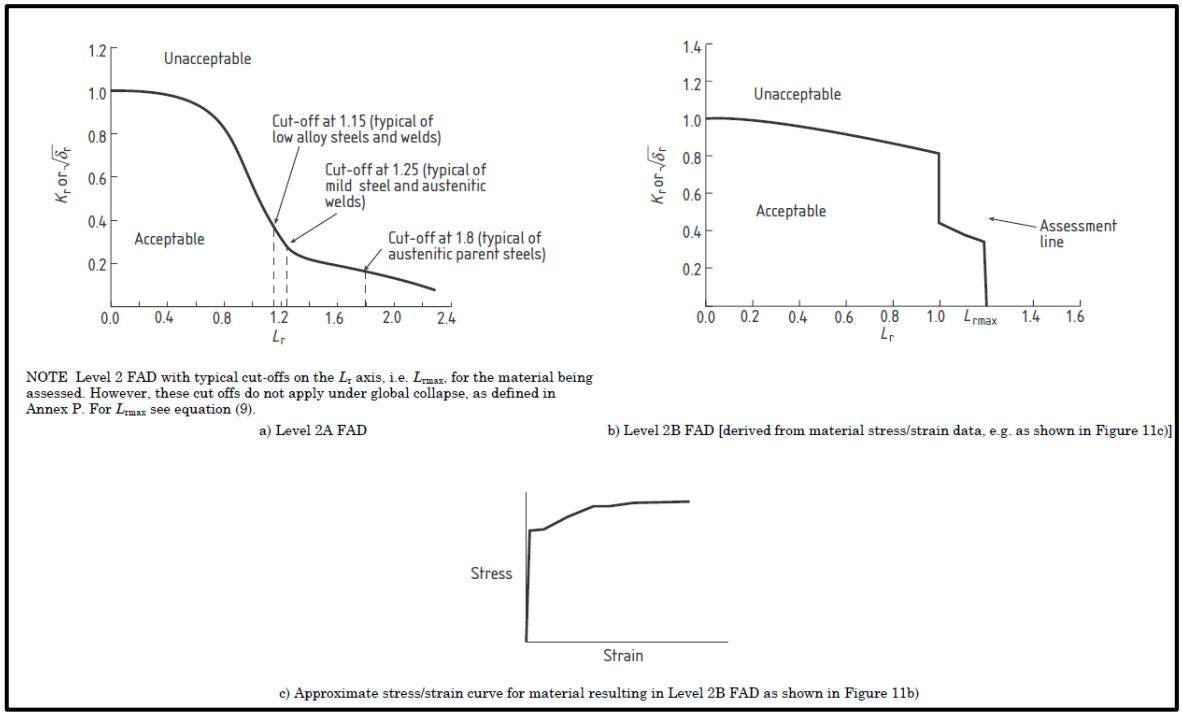

Figure 4.6 Level 2 FADs (Ref., BS7910: 2005).

B. FAD for Level 3B: Material –specific curve

The material-specific FAD is derived as for Level 2B. Stress-strain data for the material are needed, especially at strains below 1%. This diagram is suitable for all metals, regardless of their stress-strain behavior (p.45 BS9710).

This method is suitable for parent material and weld metal of all types. It will generally give more accurate results than Level 2A but requires significantly more data. It requires a specific stress-strain curve; Stress-strain data are required at the appropriate temperature for parent material and/or weld metal (p.41 BS9710).

The lower yield or 0.2% proof strength, tensile strength, and modulus of elasticity should be determined together with sufficient co-ordinate stress/strain points to define the curve. Particular attention should be paid in defining the shape of the stress/strain curve for strains below 1%.

C. Estimation of Lr

The cut-off is to prevent localized plastic collapse and it is set at the point at which $L_r = L_{rmax}$ where (p.38 BS9710):

$$L_{r\,\max} = \frac{\sigma_{ys} + \sigma_{uts}}{2\sigma_{ys}} \quad \textbf{..... (4.7)}$$

For level 2 and 3, the load ratio L_r is calculated from the following equation (p.44 BS9710):

$$L_r = \frac{\sigma_{ref}}{\sigma_{ys}} \quad \textbf{..... (4.8)}$$

Where,

σ_{ref} *is obtained from an appropriate reference stress solution as outlined in* ***Equation 4.9****.*

For Internal surface flaws in cylinders oriented circumferentially, the reference stress is calculated from the following equation (p.245 BS9710):

$$\sigma_{ref} = \frac{P_m\left\{\pi\left(1-\frac{a}{B}\right)+2\left(\frac{a}{B}\right)\sin\left(\frac{c}{r}\right)\right\}}{\left(1-\frac{a}{B}\right)\left\{\pi-\left(\frac{c}{r}\right)\left(\frac{a}{B}\right)\right\}} + \frac{2Pb}{3(1-a'')^2} \quad \textbf{..... (4.9)}$$

Where,

$$a'' = \frac{\frac{a}{B}}{\left\{1+\left(\frac{B}{c}\right)\right\}} \qquad \text{for } \pi r \geq c + B \quad \textbf{.....(4.10)}$$

$$a'' = \left(\frac{a}{B}\right)\left(\frac{c}{\pi r}\right) \qquad \textit{for } \pi r_c \geq c + B \quad \textbf{.....(4.11)}$$

Where,

P_m = *The total membrane stress due to external bending, axial loads and pressure,*

P_b = *The total through-wall bending stress due to external bending and/or local misalignment,*

a = *Crack height,*

c = *Half of crack length,*

B = *The section thickness,*

r_c = *Radius of the cylinder.*

D. Fracture Ratio (Kr)

K_r is calculated from the following equation (p.42-43 BS9710):

$$K_r = \frac{K_I}{K_{mat}} \quad \textbf{.....(4.12)}$$

Where secondary stresses are present, a plasticity correction factor, ρ, is necessary to allow for interaction of the primary $(Y\sigma)_p$ and secondary $(Y\sigma)_s$ stress contributions, such that:

$$K_r = \frac{K_I}{K_{mat}} + \rho \quad \textbf{.....(4.13)}$$

*For Level 2 and 3, the applied stress intensity factor, **K_I**, has the following general form (p.37, 42 BS9710):*

$$K_I = (Y\sigma)\sqrt{(\pi a)} \quad \textbf{.....(4.14)}$$

$$(Y\sigma) = (Y\sigma)_p + (Y\sigma)_s \quad \textbf{.....(4.15)}$$

Where $(Y\sigma)_p$ and $(Y\sigma)_s$ represent contributions from primary and secondary stresses, respectively.

$$(Y\sigma)_p = Mf_w\left[k_{tm}M_{km}M_mP_m + k_{tb}M_{kb}M_b\{P_b + (k_m - 1)P_m\}\right] \text{ ..... } \textbf{(4.16)}$$

$$(Y\sigma)_s = M_mQ_m + M_bQ_b \text{ ..... } \textbf{(4.17)}$$

Where,

F_w = *Finite width correction factor,*

$K_{tm/tb}$ = *Membrane/bending stress SCF,*

$M_{m/b}$ = *Membrane/bending stress intensity magnification factors,*

Km = *Misalignment,*

$M_{km/kb}$ = *Membrane/bending stress intensity magnification factors for weld toe.*

In the above equations, expressions for $\boldsymbol{M}$, $\boldsymbol{f_w}$, $\boldsymbol{M_m}$ *and* $\boldsymbol{M_b}$ *are given in* ***BS9710 Appendix M*** *for different types of flaw in different configurations.*

$\boldsymbol{M_{km}}$ *and* $\boldsymbol{M_{kb}}$ *apply when the flaw or crack is in a region of local stress concentration.*

For $\boldsymbol{k_{tm}}$, $\boldsymbol{k_{tb}}$ *and* $\boldsymbol{k_m}$, *reference should be made to BS9710 part 6.4 and Annex D.*

5. ANALYSIS METHODOLOGY

5.1 ECA of Pipeline Girth Welds

Based on DNV-OS-F101 Appendix A, the analysis procedure and necessary testing rely upon the level of monotonic and cyclic deformations. DNV-OS-F101 divides the ECA into three different analysis categories. The analysis procedure for reeled pipeline is categorized as "*ECA static – high"* which means the pipeline undergoes maximum longitudinal strain equal to or larger than 0.4% with maximum number of strain cycle limited to 10.

The Engineering Critical Assessment of pipeline girth welds is performed on rigid pipeline during reeling installation particularly in spooling on and reeling off stages. During these stages the pipeline is in high curvature condition and is subjected to large plastic deformation. The analysis of ECA does not include the installation fatigue during hold period on vessel. In this assessment, the base pipe tensile properties and the weld metal tensile properties are assumed to be even-matching.

The analysis only considers surface defect as it is conservative assumption. According to DNV-RP-F108, p.12 (Guidance note 10):

> *"It is normally acceptable to only analyze surface breaking defects and use the same acceptance criteria also for embedded defects (note that the defect height, 2a, of an embedded defect is then the same as the defect height, a, of a surface defect). If the embedded defect is located close to the surface (ligament less than half the defect height) the ligament between the defect and the surface shall be included in the defect height."*

5.1.1 ECA using LINKpipe

LINKpipe analyzes fracture and crack growth based on shell and line-spring finite elements. The shell element used in LINKpipe is a rectangular ANDES (Assumed Natural Deviatoric Strain) element in a co-rotated formulation. The crack is modeled by line-spring element as nonlinear springs between the shell elements.

LINKpipe has the capability to run an ECA-analysis using non-linear direct calculation. To perform the ECA analysis using LINKpipe, it needs to model the minimum and the maximum defect sizes (crack depth and length). LINKpipe performs ECA on iterative process in a loop. The loop of ECA-analysis will start with the maximum crack length and then the iteration begins to find the critical crack depth that satisfies the acceptance criteria for the given crack length.

Input data for ECA-analysis using LINKpipe is as follows:

1. **Material Data**

   The input for material data include basic material properties (Young's Modulus, Poisson's Ratio, True stress-strain curve) and parameters of ductile crack growth based on **Equation 4.1** (CTOD as a function of crack growth). LINKpipe uses power law hardening model as a default option for the input of stress and strain curve.

2. **Geometry**

   The input data for geometry includes: Pipe Geometry (Outer diameter, wall thickness, pipe length), Defect Geometry (Crack Depth, Crack Length, Orientation, Type, Shape), Misalignment, Shell Thickness Properties (base metal wall thickness, CRA wall thickness for clad pipes), and Weld Geometry.

3. **Load Condition and Residual Stress**

   There are four types of load stations in LINKpipe such as load controlled, reeling, displacement and rotation controlled.

4. **Fracture Stop Criteria for ECA-Analysis**

   LINKpipe requires the fracture stop criteria during the ECA-analysis. There are three fracture stop criteria used in LINKpipe, such as Maximum CTOD, Maximum Crack Growth, and Maximum Crack Depth.

The flowchart of ECA analysis using LINKpipe describes the work steps consist of input data, calculation and modeling sequences as seen in **Figure 5.1**.

5.1.2 ECA using CRACKWISE

CRACKWISE is windows based software that automates fracture analysis procedures based on BS9710:2005. The ECA for pipeline girth welds in reeling installation are carried out using level 3B analysis procedure according to BS9710. A level 3 analysis procedure enables ductile tearing to be analyzed. The FAD in the level 3B analysis is based on the specific stress-strain curve of the material being assessed.

The List of required input data used for ECA of pipeline girth welds using CRACKWISE is as follows:

1. **Geometry:**

   The input data for geometry includes type of geometry, type of flaw, weld profile, weld cap width, maximum misalignment, wall thickness **B**, width or length **W**, radius $\mathbf{r_m}$, flaw height **a**, and flaw length **2c**. **Figure 5.2** illustrates the pipe geometry in CRACKWISE. Stress Intensity Factor (SIF) and reference stress solution depend on the type of flaw and geometry.

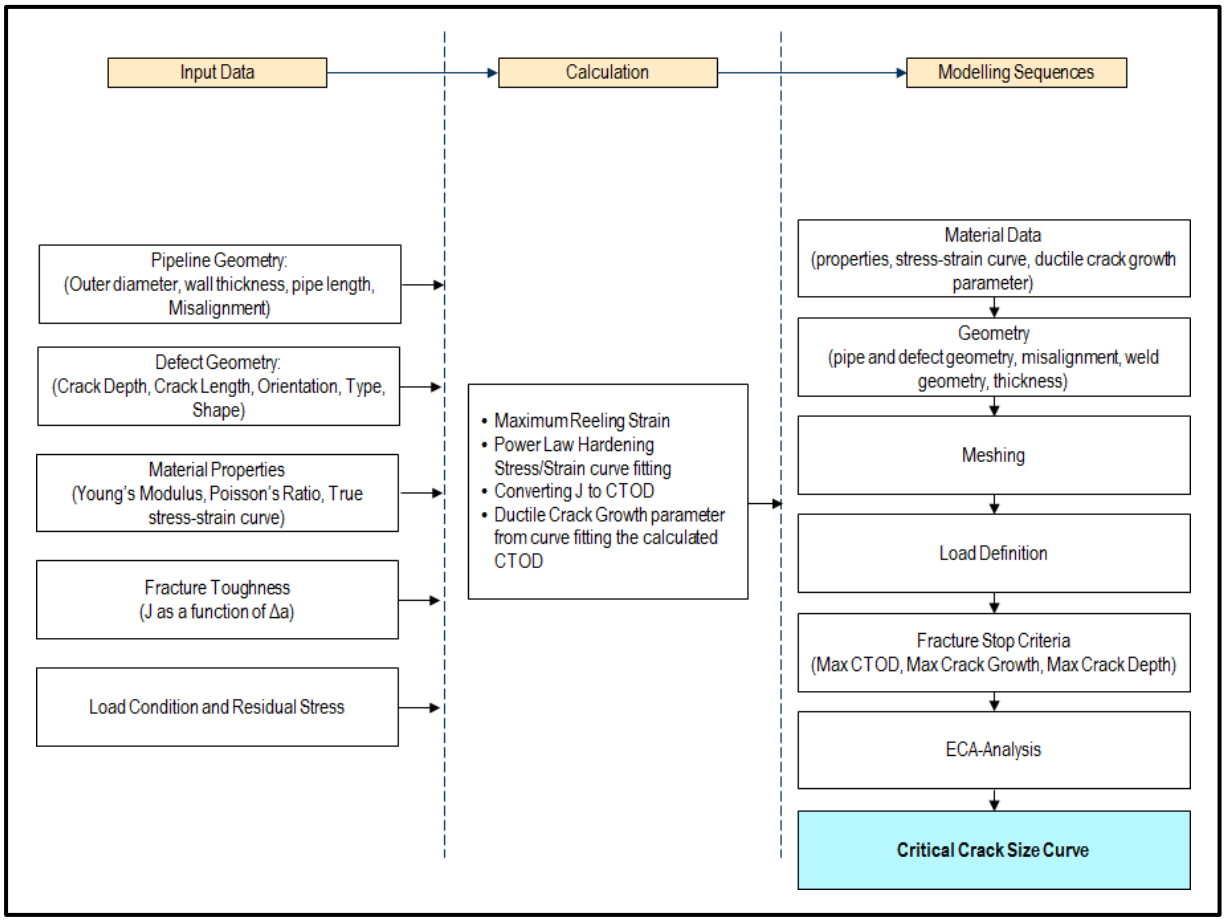

Figure 5.1 The analysis flowchart using LINKpipe (input data, calculation and modeling sequences).

2. **Fracture Toughness:**

   The data regarding fracture toughness in level 3 analysis include fracture resistance curve in the form of J-integral or CTOD as a function of Δa.

3. **Primary Stress:**

   The stress value for primary stress is the stress derived from material's stress-strain curve corresponding to the nominal strain of the pipeline during reeling installation. This stress value is the input as parameter $\mathbf{P_m}$ (primary membrane stress) in CRACKWISE. Bending stress component $\mathbf{P_b}$ (primary bending stress), that is induced by misalignment in the pipeline is calculated using SCF (Stress Concentration Factor) in association with Neuber's rule.

4. **Secondary Stress**

   The input secondary stress is welding residual stress which is given as a parameter $\mathbf{Q_m}$, (secondary membrane stress) in CRACKWISE.

5. Critical Parameter

Main result of ECA is the generic curve of critical crack size or allowable defect size. The generic curve can be generated by CRACKWISE by selecting flaw height as critical analysis parameter and flaw length as sensitivity analysis parameter.

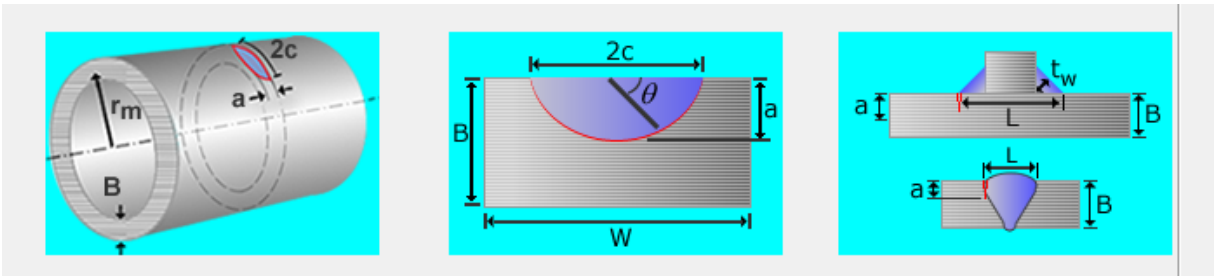

Figure 5.2 An illustration of pipe geometry on CRACKWISE (Ref., CRACKWISE software, 2009).

The flowchart describing the analysis steps using CRACKWISE can be seen in **Figure 5.3**.

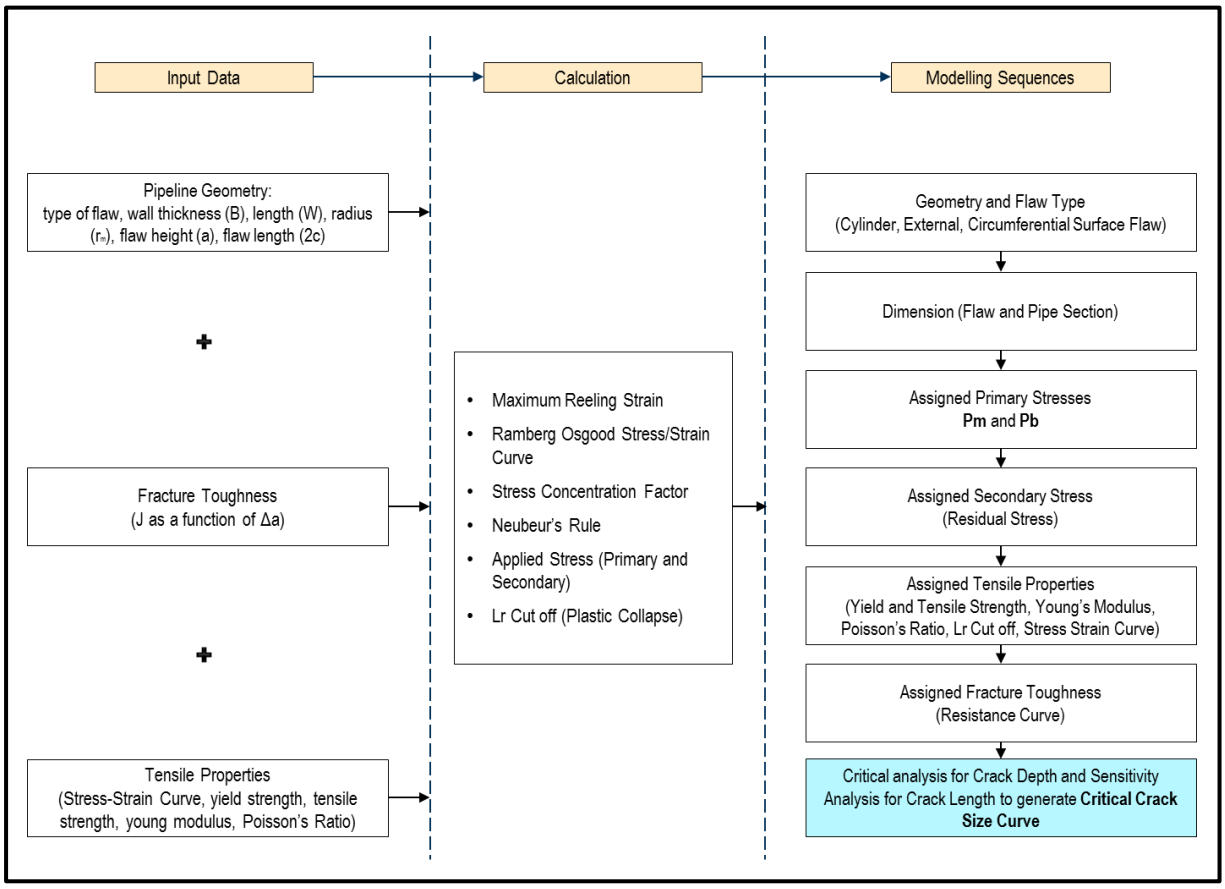

Figure 5.3 The analysis flowchart using CRACKWISE (input data, calculation and modeling sequences).

5.2 ECA of Clad Pipes using LINKpipe

Engineering Critical Assessment for girth weld in clad pipes is analyzed using LINKpipe. LINKpipe has the capability to assess the integrity of Clad Pipe through the implementation of bimetallic shell element combined with line-spring elements.

According to Olsø et al., (2011), the application of the bi-metallic shell element in LINKpipe is assumed no relative sliding or full bonding between the CRA layer and the base metal. This assumption is applicable for clad pipes. But in case of lined pipes the CRA layer is mechanically bonded by friction force between the layer and the base metal. The bond makes the layer in lined pipes more likely to slide from the base metal and there is also the possibility of liner wrinkling the pipe when subjected to large bending moments.

However, the main objective of ECA is the fracture integrity of the girth welds. Furthermore, at the ends of each lined pipe the CRA layer usually welded to the base metal so that the pipes can be assumed locally behave like clad pipe. Hence, it can be concluded that the application of bi-metallic shell element can also be used to analyze the ECA of lined pipes.

To handle the strength mismatch in the clad pipes, LINKpipe has similar approach with DNV that is to develop an equivalent material stress-strain curve. The difference is that DNV method requires performing FE analysis to build a single equivalent curve, whereas LINKpipe uses weighting principle (see **Figure 2.8**) that has been described in the **Section 2.3.2**.

For the present thesis work, the fracture assessment for clad pipes has been performed for two stages of ECA analysis i.e., the spooling on and reeling off stages and installation fatigue during hold periods on vessel.

For Clad Pipes, the flowchart describing the analysis steps using LINKpipe can be seen in **Figure 5.4**.

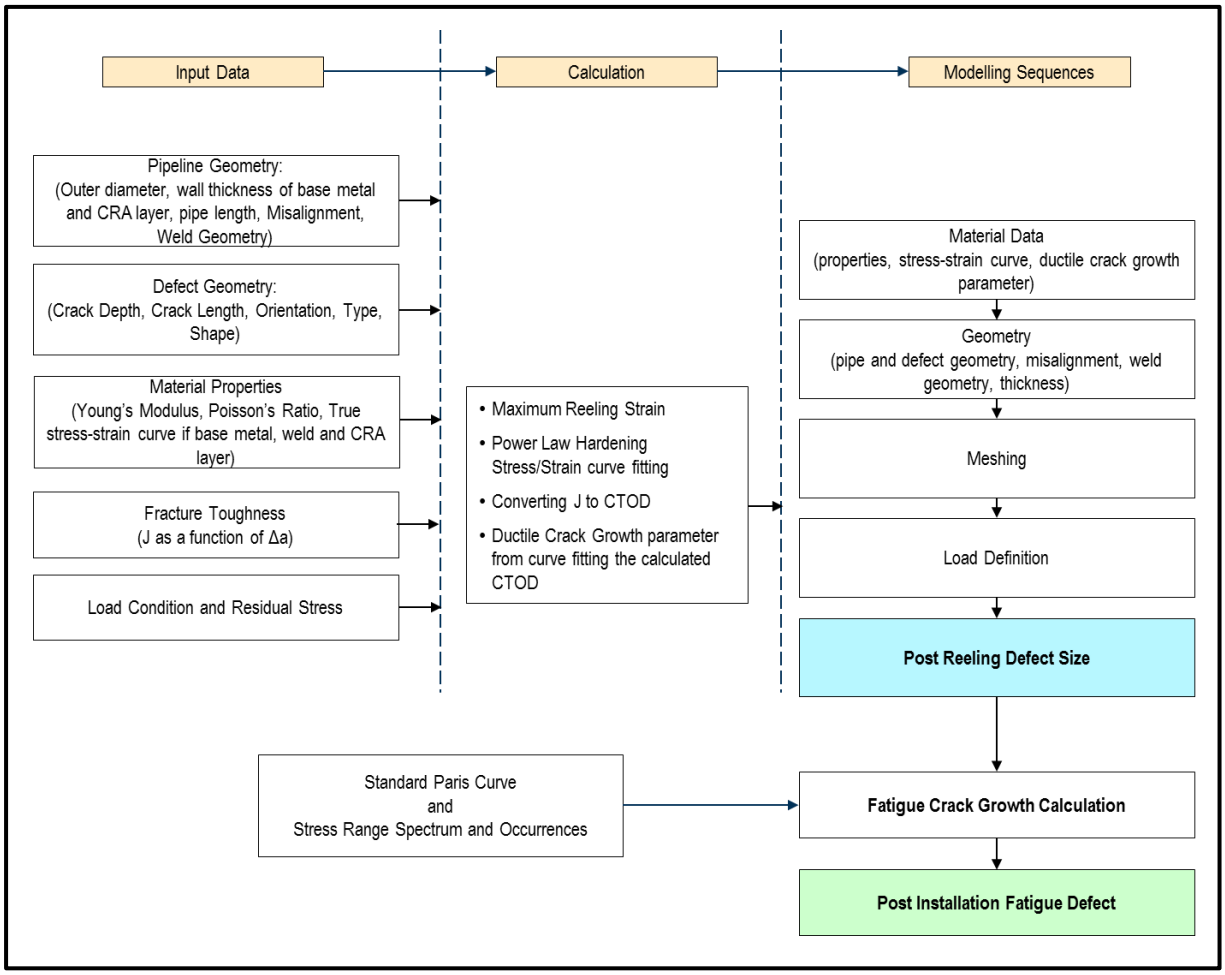

Figure 5.4 The analysis flowchart using LINKpipe for Clad pipes.

6. CASE STUDY

There are two sets of different input data used in the analysis. The first set of data is for ECA of martensitic stainless steels pipeline and the second set of data is for ECA of clad pipe.

6.1 ECA of Pipeline Girth Weld

This section presents all of the input data required for Engineering Critical Assessment of pipeline girth weld during reeling installation.

6.1.1 Pipeline Geometries

The 10" pipeline made of 13Cr martensitic stainless steel is used for the current study. **Table 6.1** presents geometric and material data for the pipeline.

Table 6.1 Pipeline Geometries and Material (Ref., Subsea7, 2006)

Pipeline	WPQ	OD (mm)	WT (mm)	WT tolerance	Coating Thickness (mm)	Pipeline Material
10"	ES0063-WPQ-01&01a	273.1	15.6	±12.5%	70	13%Cr, 2.5%Mo (SML 13Cr I PDF)

The possible minimum wall thickness has been used in the analysis. The minimum wall thickness is nominal wall thickness minus the wall thickness tolerance. During reeling installation the pipe experiences the load cycles of bending over the reel drum and straightening. The diameter of the reel drum used for the current assessment is 15m.

6.1.2 Stress Concentration Factor (SCF)

The bending component of applied stress is the input CRACKWISE and it is calculated using elastic Stress Concentration Factor (SCF) which induced by eccentricities from wall thickness differences and misalignment. SCF can be calculated using **Equation 6.1** in accordance to DNV RP F108:

$$SCF = 1 + \frac{6(\delta_t + \delta_m)}{t} \cdot \frac{1}{\left(1 + \left(\frac{T}{t}\right)^{2.5}\right)} \cdot e^{-a} \quad \text{..... (6.1)}$$

Where,

$$\alpha = \frac{1.82L}{\sqrt{OD \cdot t}} \cdot \frac{1}{\left(1+\left(\frac{T}{t}\right)^{2.5}\right)} \quad \text{..... (6.2)}$$

Where,

T and t = Wall thickness of the pipes on each side of the girth weld, T > t,

$\delta_t + \delta_m$ = Eccentricities from wall thickness differences and misalignment (including out-of-roundness, center eccentricity, different diameters etc.),

L = Width of girth weld cap,

OD = Outside diameter of pipe (nominal value is acceptable).

It is assumed that maximum misalignment is **1.95mm** and the corresponding SCF value is **1.242**.

6.1.3 Pipeline Tensile Properties

For ECA analyses using CRACKWISE with level 3B assessment, it is required to define the pipeline material characteristics in the form of engineering stress-strain curve. The curve can be described either by means of the Ramberg–Osgood equation or by entering the actual strain–strain data manually.

CRACKWISE uses the following Ramberg–Osgood equation:

$$\frac{\varepsilon}{e_{yo}} = \frac{\sigma}{s_{yo}} + \alpha\left(\frac{\sigma}{s_{yo}}\right)^n \quad \text{..... (6.3)}$$

Where,

s_{yo} = Reference Stress,

e_{yo} = Reference Strain,

n = Strain Hardening Exponent.

On the other hand, for ECA analyses using LINKpipe, it is required to model true stress-strain curve either by using the default option power hardening law (see **Equation 6.4**) as a default input or by entering the actual stress–strain data manually.

$$\sigma = \sigma_0\left(\frac{\varepsilon_{pl} \cdot E}{\sigma_0} + 1\right)^n \quad \text{..... (6.4)}$$

Where,

σ_0 = Initial yield stress,

ε_{pl} = True Plastic strain,

E = Young's Modulus,

n = Strain Hardening Exponent.

The ECA analyses have been performed with the assumption that the weld metal strength is evenly matches with the strength of the base metal (parent pipe). The stress-strain curve used in the assessment is based on Ramberg-Osgood hardening law. **Figure 6.1** presents the stress-strain curve based on the material parameters summarized in **Table 6.2**.

Table 6.2 Ramberg - Osgood Stress/Strain Curves Parameter (Ref., Subsea7, 2006)

Parameter	R-O Base Metal
Yield stress, $R_{p0.5}$	691 MPa
Ultimate Tensile Strength, (UTS)	899 MPa
Young's Modulus, E	205,000 N/mm^2
Poisson's Ratio	0.3
Elastic Parameter, α	0.593
Hardening parameter, n	14.276

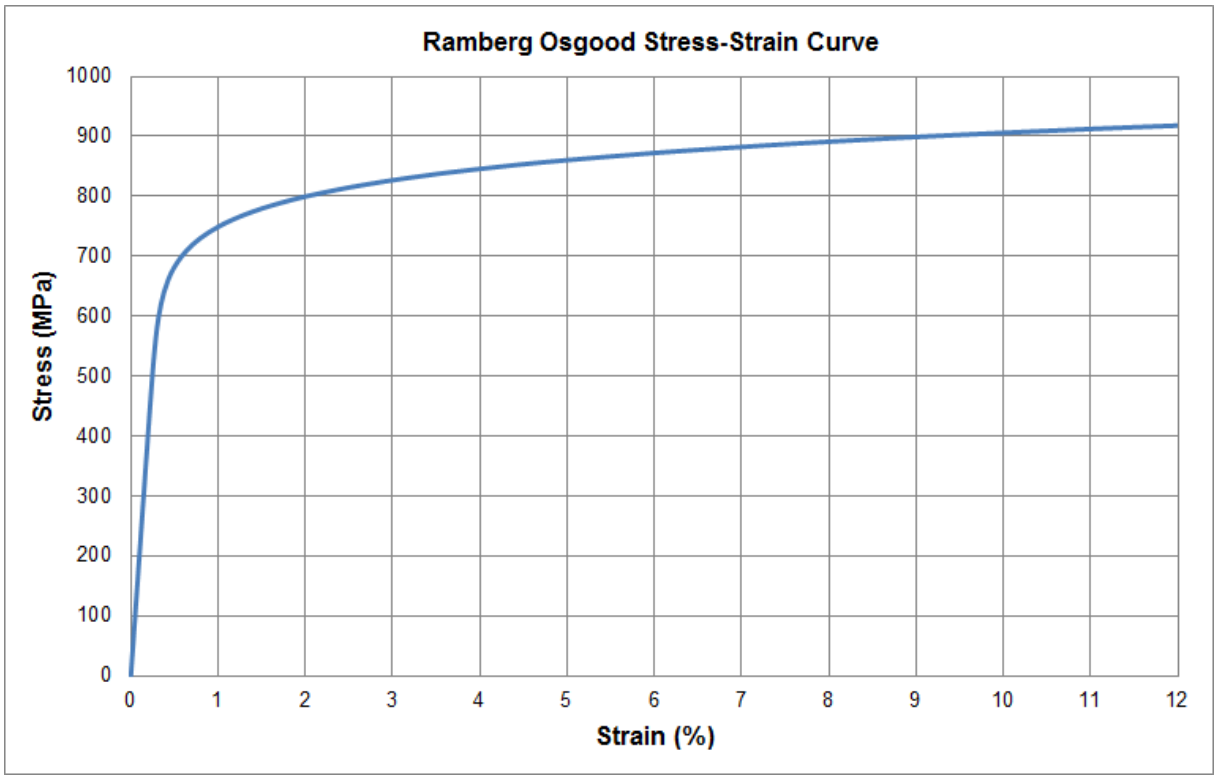

Figure 6.1 Ramberg-Osgood stress and strain curve (Ref., Subsea7, 2006).

6.1.4 Fracture Toughness

The material's fracture resistance is described by the J-integral and determined by testing of the SENT (Single Edge Notched Tension) specimen. The specimen is designed to have a loading mode and crack tip constraint similar to the loading mode and constraint for a crack in the pipeline girth weld. The fracture resistance is defined by The J-integral value as a function of measured ductile crack extension (Δa). The test results are then described as J-Δa curve fitted with lower bound experimental values.

The test results for SENT specimen can be found in **Table 6.3**, whereas the corresponding lower bound J-Δa curve can be seen in the **Figure 6.2**.

Based on DNV-RP-108, *"The J-R curves shall be established as a lower bound curve for the experimental results. Often a curve of the form $J=x*\Delta a^m$ fits the data well."*

The representative lower bound curve used in the analyses is as follows: $J = 1{,}410 \cdot \Delta a^{0.68}$

Table 6.3 SENT Specimen Test Results (Ref., Subsea7, 2006)

Weld Procedure/ Pipeline	Notch Location	Specimen Width, B (mm)	a_0/W	J (N/mm)	Δa (mm)
10" Main Line & Tie-in Procedure	WM	25.71	0.33	1,860.10	1.36
		25.49	0.42	1,194.70	0.64
		25.70	0.41	540.80	0.13
		26.04	0.42	1,836.40	1.31
		26.05	0.38	1,408.90	0.70
		26.05	0.43	535.00	0.16
10" Main Line & Tie-in Procedure	FL/HAZ	25.99	0.41	1,734.41	1.32
		26.00	0.38	1,087.00	0.73
		26.00	0.38	507.10	0.12
		25.98	0.37	1,857.10	1.53
		26.00	0.35	1,152.50	0.67
		26.01	0.37	516.60	0.15

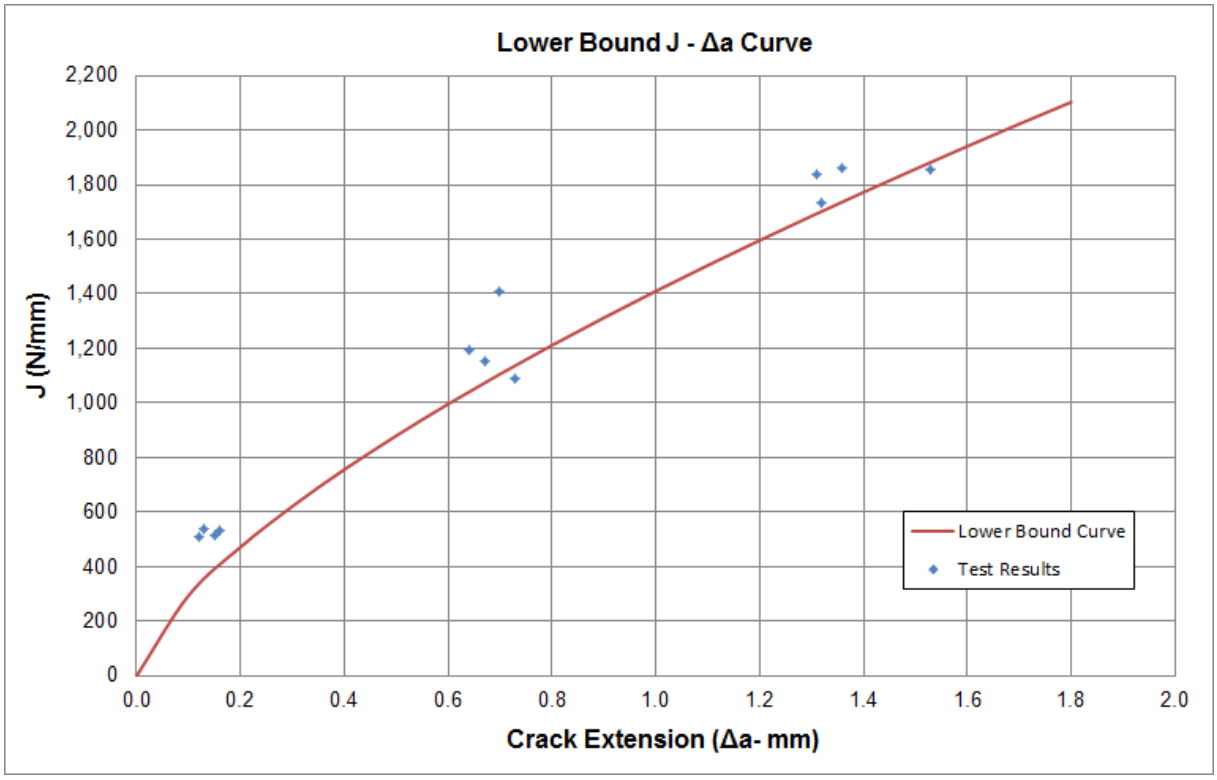

Figure 6.2 Fracture resistance curve (Ref., Subsea7, 2006).

6.2 ECA of Clad Pipes Girth Weld

This section presents the input data required for Engineering Critical Assessment of clad pipes girth welds. The assessment considers the reeling installation including fatigue due to hold periods on vessel. It is assumed that ECA analysis for clad pipes is also applicable for lined pipes as described in the **Section 5.2**.

6.2.1 Reeling Strain

The reeling installation phases used in the ECA of clad pipes consisted of:

1. Reeling on;
2. Reeling off – assumed pulled straight;
3. Bending over the aligner;
4. Through straightener;
5. Back onto aligner;
6. Back through straightener.

The installation phases mentioned above are with addition of half cycle of "adjustment of the ramp". Hence, a total of three tensile strain cycles are used in the analysis. **Table 6.4** presents the reeling strain for all cycles.

Table 6.4 The Reeling Strain for All Cycles (Ref., Subsea7, 2010)

Cycle	Reeling Strain
Cycle 1	1.77%
Cycle 2	1.42%
Cycle 3	1.62%

6.2.2 Clad Pipes Geometry and Material

The current work of ECA analysis for clad pipes considers the pipeline with pipe diameter and wall thickness: 273.1mm OD x 15mm WT (+3.0 mm Clad). **Table 6.5** presents the details of clad pipe geometry and material used in the analyses.

Table 6.5 Pipeline Geometries and Material of Clad Pipes (Ref., Subsea7, 2010)

Parameter	273.1 x 18 mm - Clad Production Line
Min WT	17.7 mm
Max WT	19.4 mm
Coating Thickness Start of Life	82 mm
Boat Reel Hub Diameter	15 m
Parent Pipe Material	SAWL 415 I SFPDU
Clad Material	UNS S31603 CRA

6.2.3 Clad Pipes Tensile Properties

There are three different materials in a clad pipe i.e. parent pipe material, clad layer material, and weld metal material. To determine the type of strength mismatch, all of the three materials stress-strain curve shall be compared. The true stress-strain curve from the tensile testing is used for ECA using LINKpipe.

For the present analysis, the following stress-strain curves were applied:

a. Upper bound stress-strain curve for parent pipe material;
b. Lower bound stress-strain curve for girth weld;
c. Lower bound stress-strain curve for clad material.

The young's modulus used for the analysis can be seen in **Table 6.6**. The as-received and strained-aged true stress-strain curve for parent pipe, weld, and clad materials can be seen in **Figure 6.3** and **Figure 6.4,** respectively. For the as-received condition the girth welds is identified as partially overmatch, whereas for the strained & aged condition the girth welds is considered as fully overmatch.

Table 6.6 Young's Modulus of Materials (Ref., Subsea7, 2010)

Material	Young's Modulus (Mpa)
Parent material – As Received	200,000
Parent material – Strained & Aged	200,000
Mainline weld – As Received	170,000
Mainline weld – Strained & Aged	200,000
CRA Clad	200,000

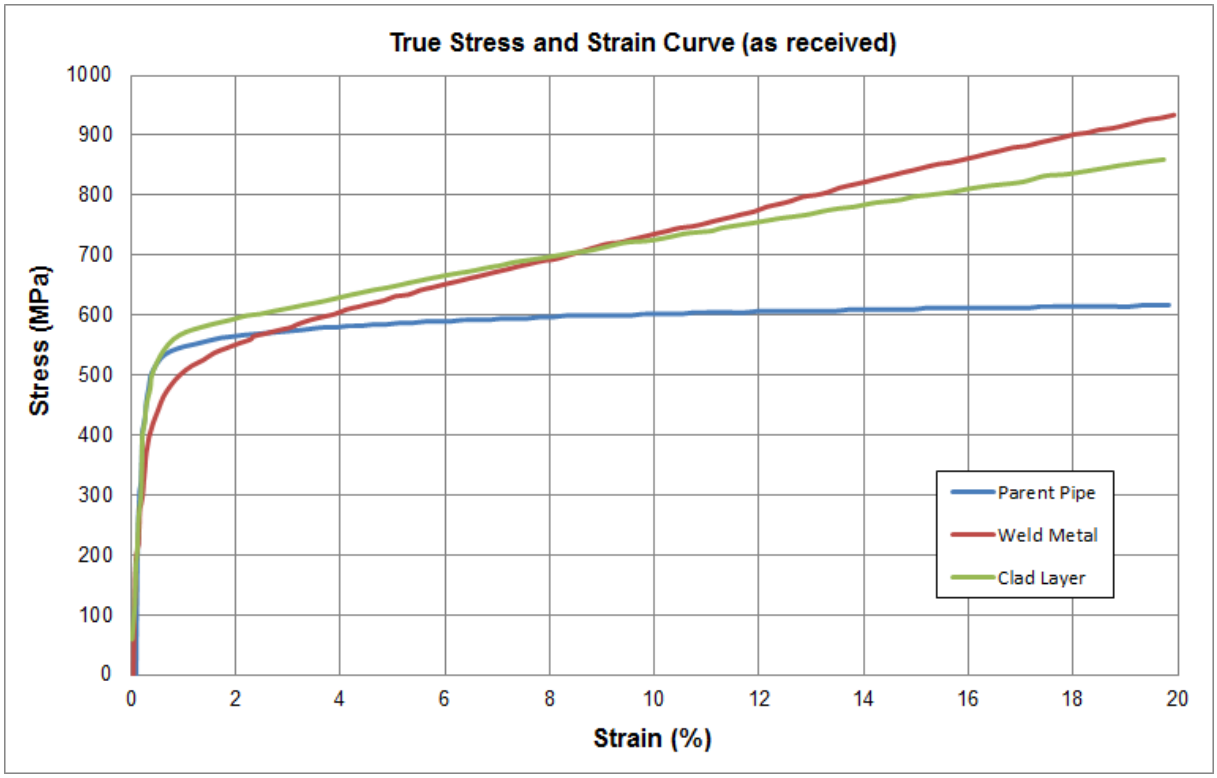

Figure 6.3 As received true stress and strain curve used in the analysis (Ref., Subsea7, 2010).

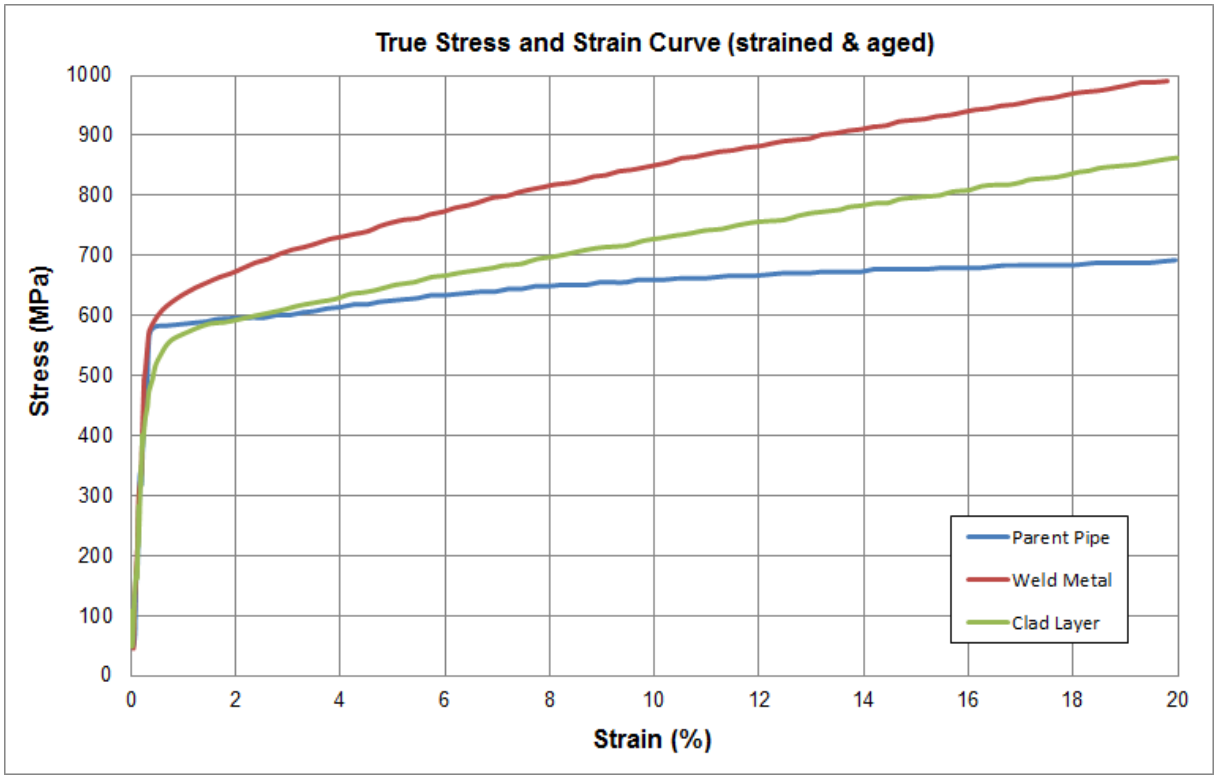

Figure 6.4 Strained & Aged true stress and strain curve (Ref., Subsea7, 2010).

6.2.4 Fracture Toughness

Table 6.7 summarizes SENT specimen test results for material fracture resistance. **Figure 6.5** presents lower bound fracture resistance curve (J-Δa curve).

The representative equation of the lower bound curve is: $J = 920 \cdot \Delta a^{0.8}$

Table 6.7 SENT Specimen Test Results (Ref., Subsea7, 2010)

Location	B (mm)	W (mm)	a_0 (mm)	Δa (mm)	J (N/m)
WCL	39.86	20.33	7.96	2.01	1,622
WCL	39.93	20.08	6.30	1.30	1,265
WCL	39.99	20.04	7.03	0.60	760
WCL	39.90	20.04	6.40	1.33	1,506
WCL	39.97	20.02	6.68	0.52	565
WCL	39.95	20.13	6.61	0.61	671
HAZ	40.06	20.15	5.95	1.56	1,803
HAZ	39.99	20.06	6.82	0.31	661
HAZ	40.04	20.05	6.73	0.78	1,113
HAZ	40.10	20.14	5.51	0.86	1,223
HAZ	40.00	20.06	6.28	0.56	986
HAZ	40.04	20.10	5.86	1.29	1,643

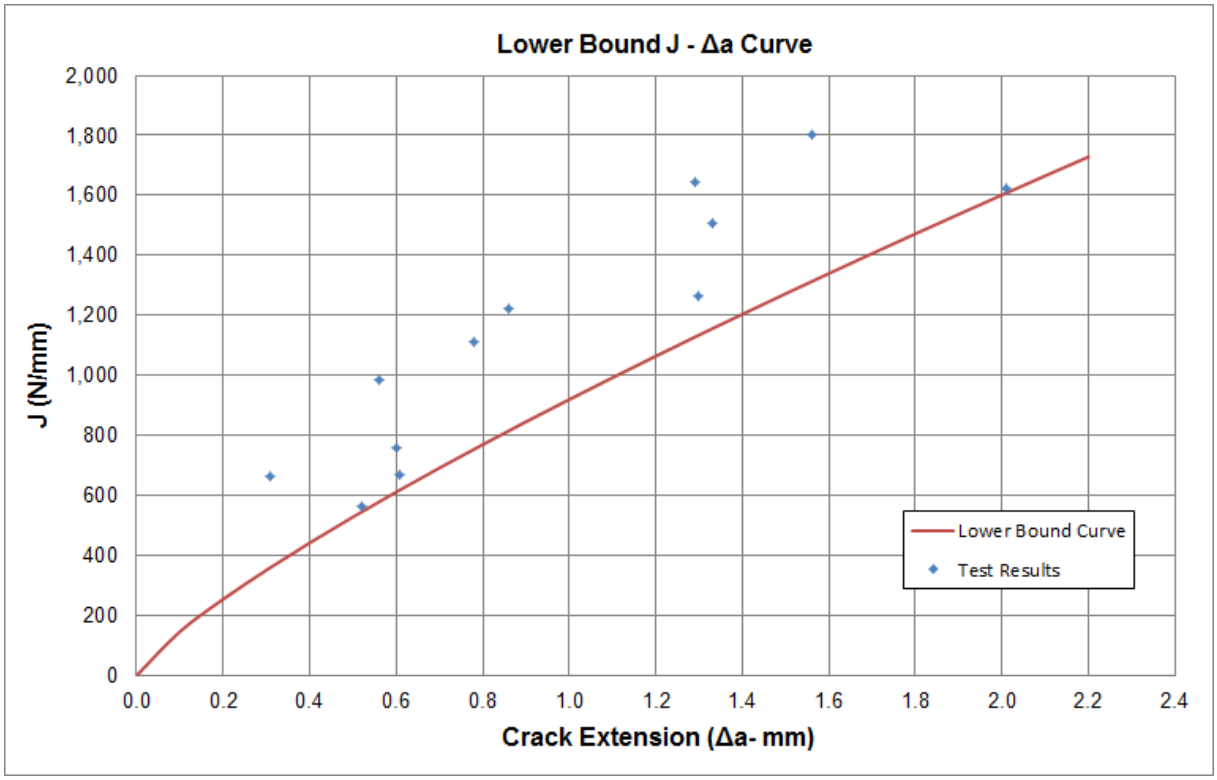

Figure 6.5 Fracture resistance curve (Ref., Subsea7, 2010).

6.2.5 Installation Fatigue Data

The cyclic loading is used as input for the ECA analysis of high cycle fatigue condition. The loading is normally generated from the simulation of the dynamic wave and current loadings during installation under specified sea state and vessel motions. The simulation itself is usually performed over a minimum duration of time. Pipeline response from this loading is then recorded in the form of a stress range spectrum and occurrences.

The blocks data of stress range in the analysis are based on an infinite stiff clamp. However, the infinite stiff clamp assumptions gives over conservative analysis results. Therefore, the input stress ranges given in **Table 6.8** shall be multiplied by a factor of 0.9 for the ECA analysis for fatigue crack growth during hold on period.

Additional stress multiplication factor is also applied to accommodate different clamp positions (distance between clamp and the weld). **Table 6.9** shows the multiplication factor for different clamp positions.

Table 6.8 Installation Stress Range (Ref., Subsea7, 2010)

10" pipeline – 18 hours clamping time Water Depth: 383m Hs: 3.0m Condition: Empty – No current	
Stress Upper Limit (MPa)	**Number of Cycles (pr. 18h)**
35	510
69	845
104	995
138	941
173	708
207	623
242	426
276	390
311	234
346	251
380	132
415	126
449	24
484	36
518	30
553	12
587	0
622	12
657	12
691	6

Table 6.9 Multiplication Factor for Different Clamp Position (Ref., Subsea7, 2010)

Distance from Clamp (m)	**Reduction Factor**
2	0.85
4	0.65
6	0.52

7. RESULTS AND DISCUSSION

7.1 Results for ECA of Pipeline Girth Welds

7.1.1 Reeling Strain

During reeling installation pipeline experiences large plastic strains during bending into reel drum and bending over the aligner. The reeling installation phase can be described as follow:

1. Reeling on (Bending over reel);
2. Reeling off (The pipeline span from the reel drum to the aligner);
3. Bending over the Aligner;
4. Bending through straightener;
5. Out of the straightener.

The maximum strain is induced in pipeline during the phase of reeling on (bending over the reel). For the given input data from **Section 6.1.1**, the maximum strain obtained from **Equation 2.1** is **1.772%**.

7.1.2 CRACKWISE Simulation

A. APPLIED STRESS CALCULATION

The input value of applied stress (Primary Stress) for CRACKWISE is determined from the stress-strain curve of the base metal based on the nominal strain induced in the pipeline during reeling installation. The calculated nominal strain is **1.772%**. The stress value corresponding to the nominal strain in the stress-strain curve is used as the value of parameter $\mathbf{P_m}$ (primary membrane stress) in CRACKWISE. The estimated value of P_m is **791.4 MPa**.

The bending component of this stress is calculated using elastic Stress Concentration Factor (SCF). For the assumed maximum misalignment of **1.95mm**, the value of SCF used for the analysis is **1.242** based on the expression given in **Section 6.1.2**.

The value of SCF is then used in the Neuber rule to determine the actual stress.

According to DNV RP F108, *The Neuber method was originally developed to assess strains at notches it has been found useful for reeling analyses and there have not been any failures reported that can be attributed to non-conservatism due to the use of this method.*

The Neuber method is defined by the following equation:

$$\sigma_1 \times \varepsilon_1 = S \times \varepsilon_{nom} \times K_t^2 \quad \text{.....(7.1)}$$

Where,

K_t = Elastic stress concentration factor (SCF),

S = Nominal stress (excluding SCF),

ε_{nom} = Nominal strain (excluding SCF),

ε_1 = Actual strain (including SCF),

σ_1 = Actual stress (including SCF).

The intersection between the Neuber curve and the stress-strain curve of the material determines the actual stress and strain as a result of the elastic SCF. The additional stress from eccentricities calculated by the Neuber method is applied as a primary bending stress, **Pb**.

Neuber Curve is defined by:

$$\frac{S \times \varepsilon_{nom} \times K_t^2}{\sigma} \quad plotted\ \ against \quad S$$

The intersection between the Neuber curve and the stress-strain curve of the material can be seen in **Figure 7.1**. The intersection point from the figure is (2.64, 818.6).

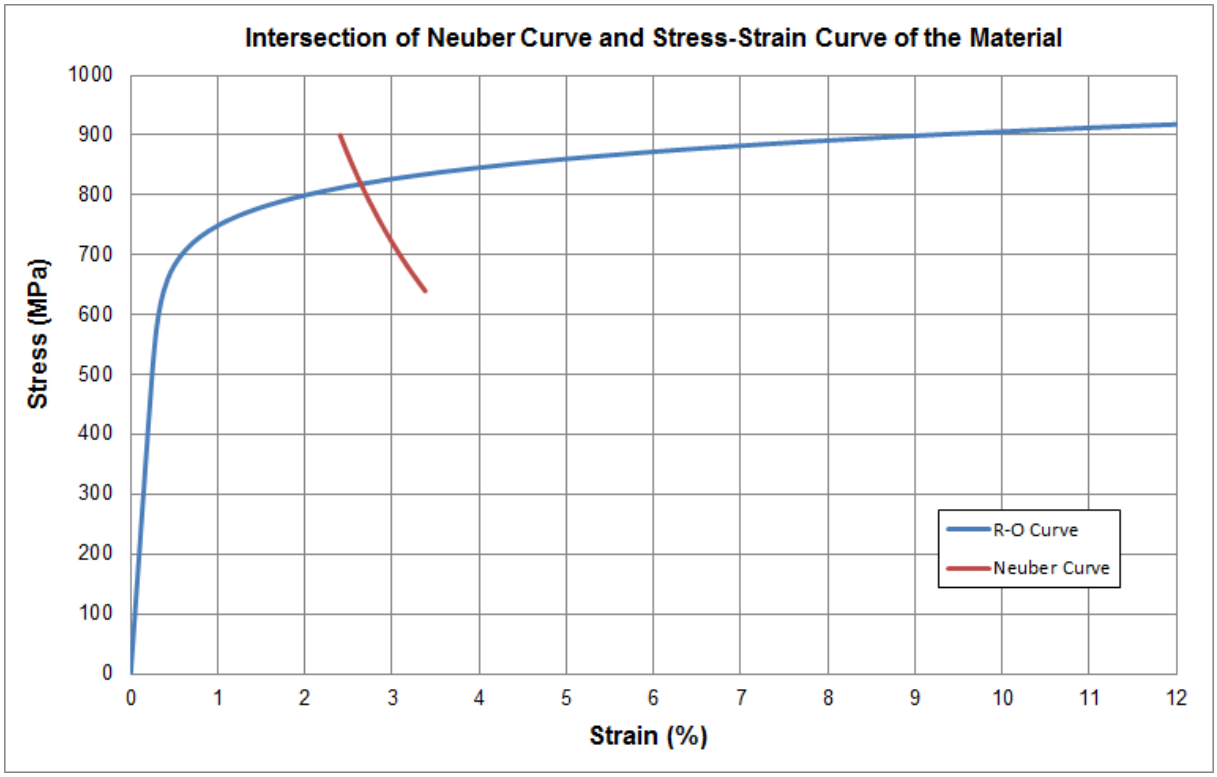

Figure 7.1 Intersection between Neuber curve and the stress-strain curve of the material.

The value of $\mathbf{P_b}$ is equal to **27.2 MPa** obtained by subtracting the primary stress from the stress at the intersection point. The summary of the applied primary membrane and bending stresses **($\mathbf{P_m}$** and **$\mathbf{P_b}$)** for 10" pipeline can be seen in the **Table 7.1**.

Table 7.1 Applied Stress Summary for CRACKWISE Analysis

Pipeline	Max Reeling Strain	SCF	Pm (Mpa)	Pb (Mpa)
10"	1.772%	1.242	791.4	27.2

B. Lr CUT OFF CALCULATION

According to DNV-RP-F108, the FAD (Failure Assessment Diagram) cannot be extended to arbitrarily large plastic deformation and a cut off limit for L_r ($L_r = \frac{\sigma_{ref}}{\sigma_Y}$) must be defined. For displacement controlled situations such as the situation in reeling installation, it is acceptable to increase the cut off level ($L_{r\ max}$) in the FAD, (from $L_r = \frac{\sigma_{flow}}{\sigma_Y}$ as suggested in BS 7910:2005) provided there is experimental support for such an extension.

The support can be provided by SENT specimen that has constraint similar to the constraint of pipeline. If the test results are available, the following procedure for determining $L_{r\ max}$ is acceptable:

- *The maximum load shall be determined from at least three tests. The location of the cracks in the specimens must correspond to the location considered in the pipe.*
- $L_{r\ max} = \frac{\sigma_{ref}}{\sigma_Y}$ *Corresponding to the recorded maximum loads shall be calculated and used to define* $L_{r\ max}$.
- *The actual value of* $L_{r\ max}$ *to be used in the analyses shall be chosen taking scatter in the results into consideration.*

The L_r cut off value calculation can be seen in the **Table 7.2**.

Table 7.2 L_r Cut off Value Calculation (Ref., Subsea7, 2006)

Specimen	Max Load (kN)	Width, B (mm)	Thickness, W (mm)	a_0 (mm)	Ligament, p (mm)	σ_{ref} (MPa)	Lr cut-off σ_{ys} = 650Mpa
6-1	215.86	25.71	12.85	4.30	8.55	981.98	1.511
6-2	196.38	25.49	12.65	5.28	7.37	1,045.35	1.608
6-4	195.76	26.04	12.99	5.52	7.47	1,006.38	1.548
6-5	206.94	26.05	13.11	5	8.11	979.53	1.507
6-7	187.28	25.99	13.15	5.42	7.73	932.19	1.434
6-8	196.14	26.00	13.17	5.06	8.11	930.19	1.431
6-10	203.4	25.98	13.01	4.86	8.15	960.63	1.478
6-11	213.4	26.00	13.17	4.57	8.60	954.38	1.468
						Mean	**1.498**
	Notch in weld					**Min**	**1.431**
	Notced to FL/HAZ					**Max**	**1.608**

According to DNV-OS-F101- 2007, Appendix A (E208):

$$\sigma_{ref} = \frac{Max\ load}{B(W - a_0)} \quad \text{..... (7.2)}$$

$$L_r\ cut - off = \frac{\sigma_{ref}}{\sigma_{ys}} \quad \text{..... (7.3)}$$

C. ENGINEERING CRITICAL ASSESSMENT BY CRACKWISE

DNV-OS-F101 states that the maximum tearing permitted during the whole installation phase should not exceed 1 mm. The loading history of reeling installation is indicated for two cycles of tensile plastic strain: reel on and bending over the aligner. Accordingly, one tensile occurrence permits only 0.5mm allowable tearing.

In the analysis, the DNV requirement of 1 mm allowable ductile tearing for the whole reeling installation is assumed to be satisfied by applying only one cycle of plastic strain (1.772%) but with maximum tearing of 0.3 mm. This assumption is considered to be more conservative than that according to DNV requirement. The summary of parameters for calculating the maximum allowable crack size curves using CRACKWISE is as follow:

1. The wall thickness used in the analysis is the minimum wall thickness determined by nominal wall thickness minus wall thickness tolerance;
2. The weld residual stress is set to equal to the yield stress with enabled relaxation;
3. Lower bound J-R curve ($J = 1{,}410 \cdot \Delta a^{0.68}$);
4. Maximum allowable tearing of 0.3mm;
5. Upper bound stress and strain curve (Ramberg-Osgood Fitted);

6. Maximum applied strain of 1.772%.

The maximum allowable crack size curve given the parameter above is defined as a base case for comparison. In the simulation, the Kastner solution was used to calculate the reference stress. As stated in the DNF-RP-F108, reference stress determined by Kastner solution is recommended for the assessment of surface cracks.

Using the input parameters mentioned above, CRACKWISE analyses were performed to predict the critical crack sizes. The critical crack size curve predicted from CRACKWISE analyses is shown in the **Figure 7.2**.

The curve in **Figure 7.2** shows relatively smaller critical crack depth for crack length in the range of 100-200mm. For crack length in the range of 25-100, the critical depth increases rapidly and the maximum critical depth is at the crack length of 25mm.

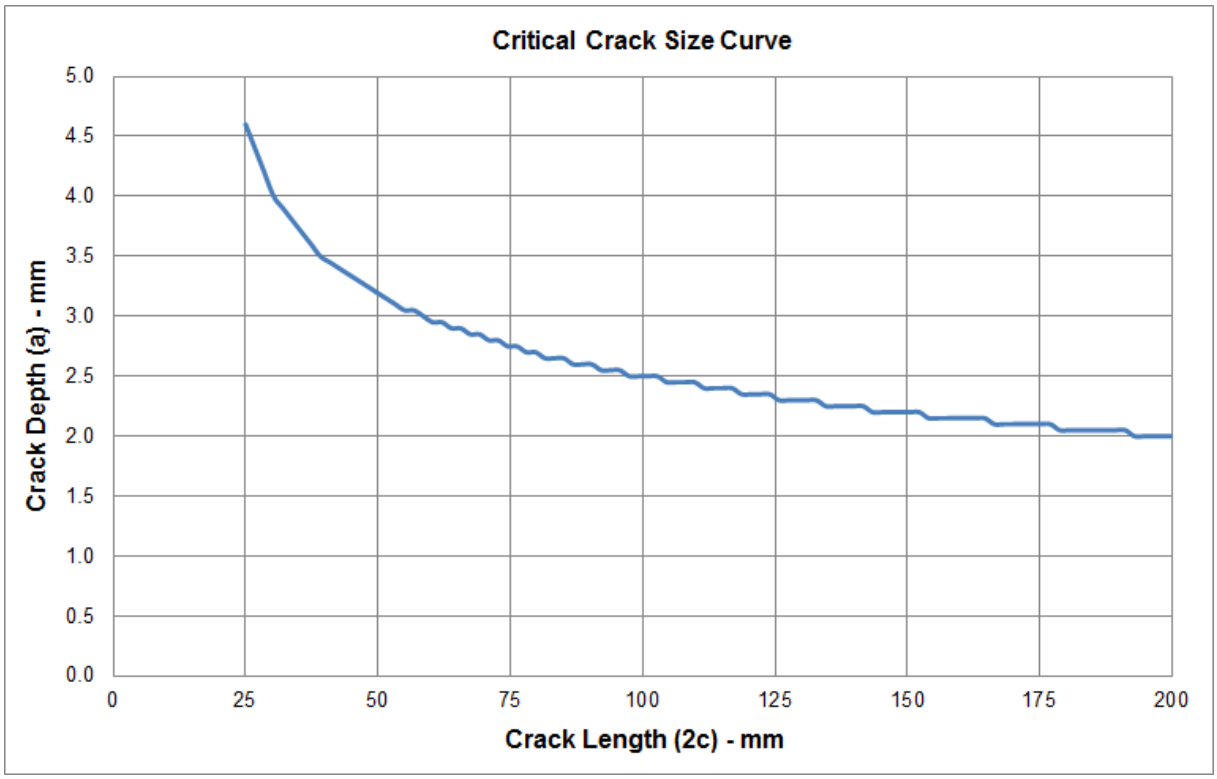

Figure 7.2 Critical Crack Size curve from CRACKWISE analysis (Base Case).

1. EFFECT OF RESIDUAL STRESS

Welding residual stress is included in the analysis as the secondary membrane stress. The critical crack size curve in the **Figure 7.2** shows the results where the residual stress is set to equal to yield stress with enabled relaxation. **Figure 7.3** shows the results from sensitivity analyses when the residual stress input ($\mathbf{Q_m}$) on CRACKWISE was introduced.

It is seen that the introduction of residual stress yields lower critical crack sizes compared to the sizes predicted from the analyses without residual stress. The difference between

the predictions from the analyses with and without considering residual stress is significant. From the results, it can be concluded that the critical crack size predicted by CRACKWISE is greatly influenced by residual stress.

For the case where residual stress is considered to be equal to yield stress, the critical crack size reduces very significantly especially for short crack length (<50mm). The results show that assigning residual stress equal to yield stress yields more conservative results compared to the cases of without and relaxed residual stress. In other words, neglecting residual stress predicts less conservative results of critical crack size curve.

The results from analyses are in agreement with those from the work of Lei (2005) cited in Tkaczyk, et.al. (2007). It has been concluded that the BS7910 procedure is handling the residual stress in a conservative manner.

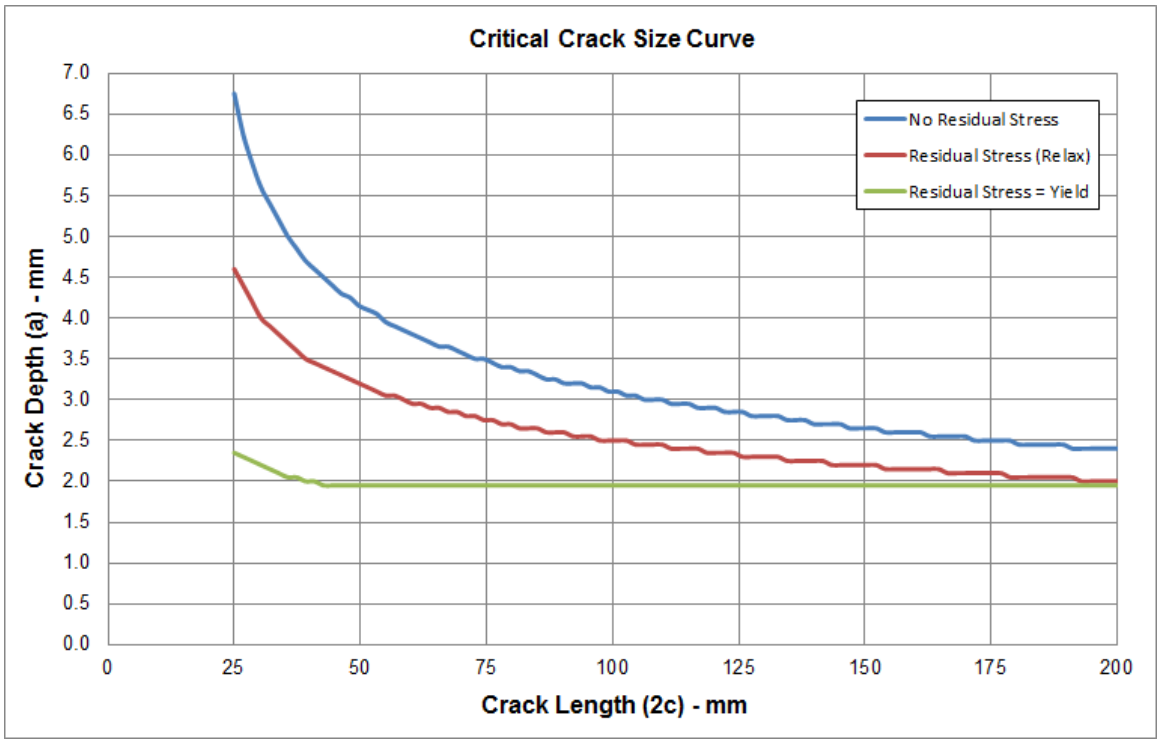

Figure 7.3 Critical Crack Size curve from CRACKWISE analysis with various residual stresses.

2. EFFECT OF MISALIGNMENT

In CRACKWISE ECA simulations, pipeline misalignment is incorporated into primary bending stress (P_b). This bending component is calculated using Stress Concentration Factor and Neuber rule. The maximum misalignment assumed in this analysis is 1.95mm as mentioned in the **Section 6.1.2**. **Figure 7.4** shows the comparison between the base case curve with maximum misalignment and the critical crack size curve without misalignment.

The result shows that the critical crack size is smaller for the case of pipeline with maximum misalignment. The difference between the pipeline with maximum

misalignment and without misalignment is not significant although the considered misalignment of 1.95mm is relatively high.

From the analyses of CRACKWISE simulations, it can be concluded that the influence of misalignment for the critical crack size curve is less significant compared to the effect of residual stress.

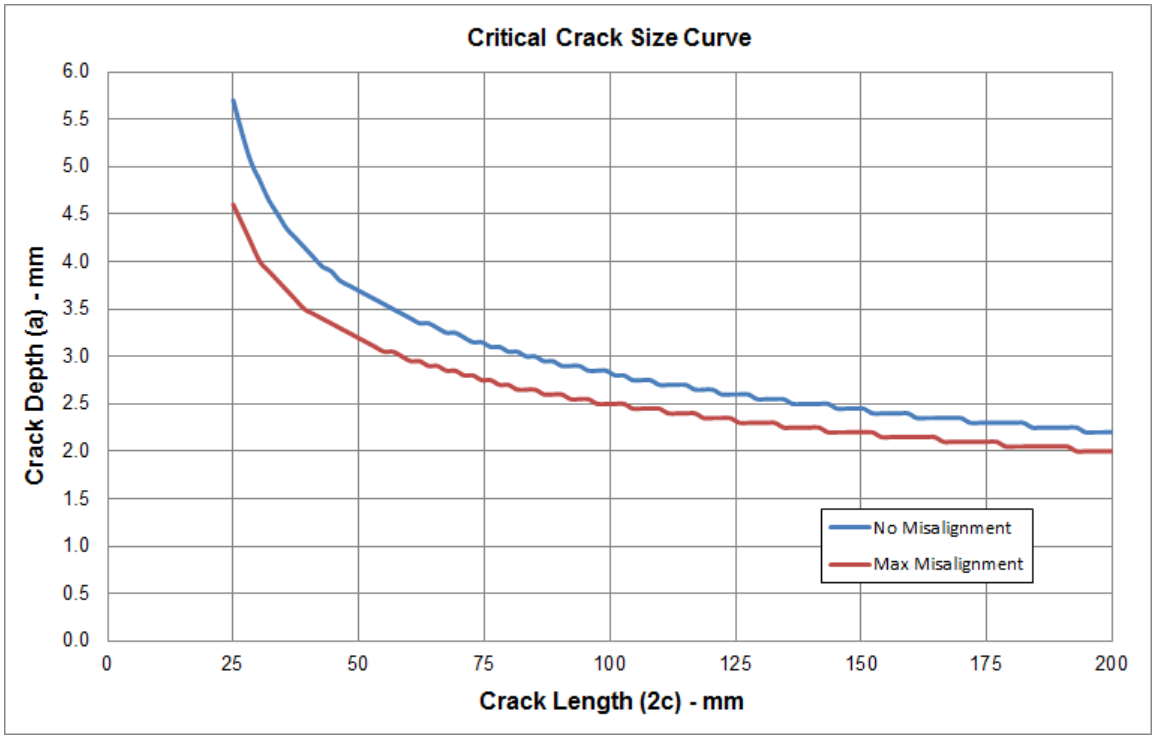

Figure 7.4 Critical Crack Size curve from CRACKWISE analysis with different misalignment.

7.1.3 LINKpipe Simulation

A. MATERIAL PROPERTIES INPUT

As mentioned, LINKpipe simulation uses true stress-strain curves in the form power hardening law as default input option. **Figure 7.5** shows the true stress-strain curve used in the analyses.

The form of power hardening equation can be seen in the **Equation 6.4.**

The parameters for power law hardening are determined by fitting the curve with the true stress-strain curve. The fitted curve can be seen in **Figure 7.6** and the identified parameters used in LINKpipe simulation are as follow:

Table 7.3 Parameters for Power Law Hardening

σ_0	**n**	**E**
630 MPa	0.136	205,000 MPa

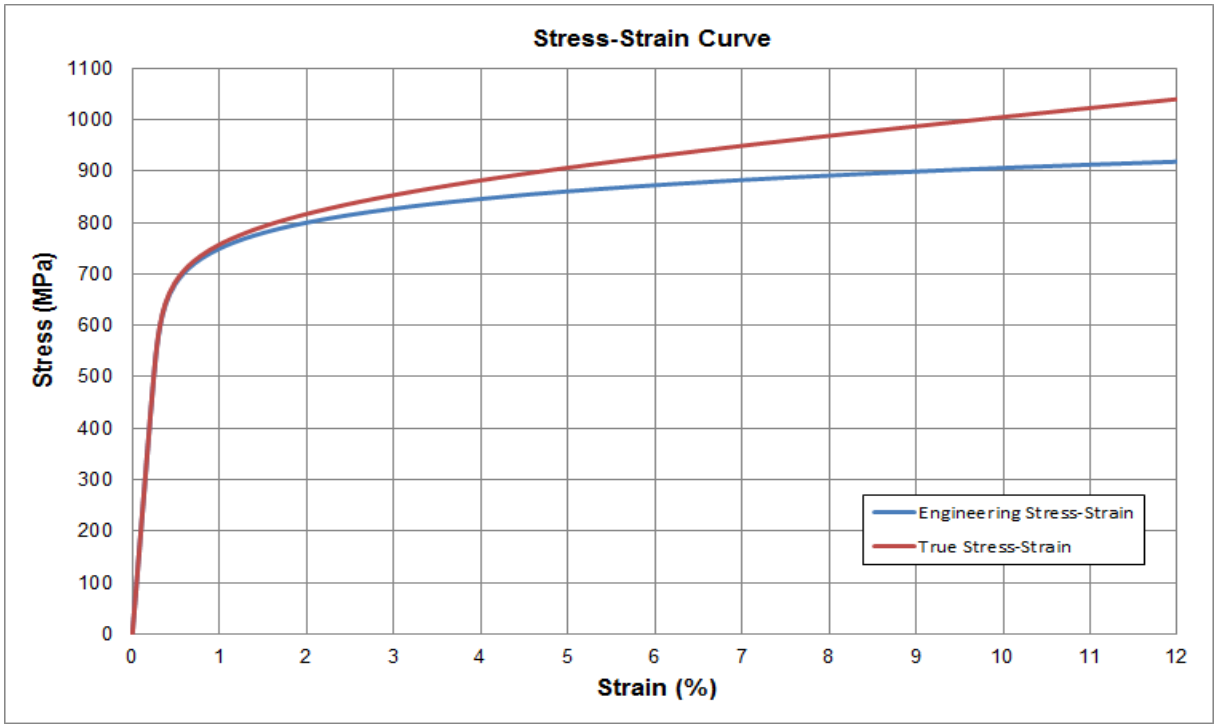

Figure 7.5 True stress-strain curve used in LINKpipe simulation.

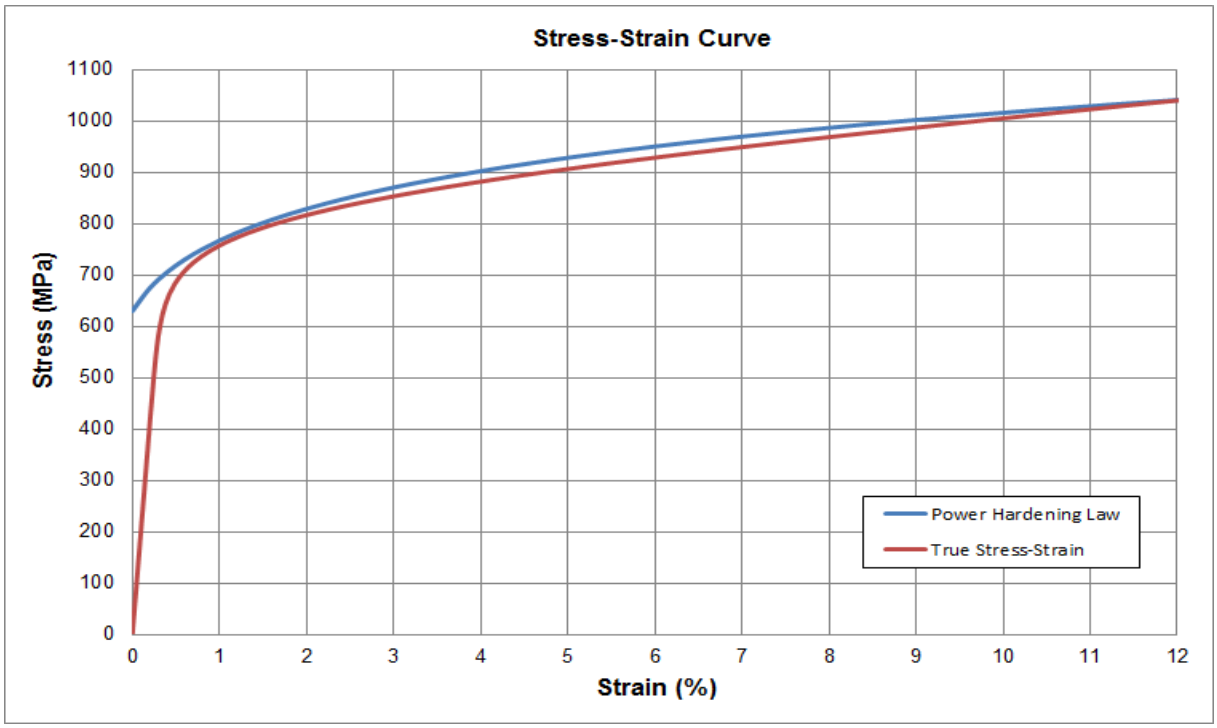

Figure 7.6 Power law hardening curve fitted to the true stress-strain curve.

B. FRACTURE TOUGHNESS ANALYSIS

The crack driving force in LINKpipe is measured by CTOD. To simulate the crack propagation LINKpipe uses the ductile crack growth formulation in the form of CTOD as a function of ductile crack extension (Δa) (See **Section 4.1.4**).

$$CTOD = CTOD_i + C_1(\Delta a)^{C_2} \quad \text{..... (7.4)}$$

The fracture resistance curve determined by the results of SENT specimen testing is in the form of J-Δa. When CTOD test data is not available, the values of CTOD need to be calculated from J-integral values. DNV-OS-F101 provides the conservative method to estimate CTOD from J-integral. The equation that used in this analysis is explained in **Section 3.3.3**.

The calculated CTOD values are summarized in **Table 7.5**. For performing FE analyses using LINKpipe, the fracture resistance parameters expressed in **Equation 7.4** need to be defined. These fracture parameters can be identified by fitting the expression in **Equation 7.4** against with test results of CTOD. It should be noted that in the present study, CTOD values are computed from test data of J-integral. The parameters identified from the curve fitting are as follows:

Table 7.4 Fracture Resistance Parameters

CTODi	C_1	C_2
0.06	0.95	0.58

Figure 7.7 shows the curve fitted with CTOD computed values.

Table 7.5 Summary of CTOD Calculation from J

a/W	J (N/mm)	n	m	CTOD - mm (Computed)	Δa (mm)
0.38	507.1	0.1553	1.866	0.34	0.12
0.41	540.8	0.1553	1.883	0.36	0.13
0.37	516.6	0.1553	1.860	0.35	0.15
0.43	535	0.1553	1.895	0.36	0.16
0.42	1194.7	0.1553	1.889	0.80	0.64
0.35	1152.5	0.1553	1.849	0.78	0.67
0.38	1408.9	0.1553	1.866	0.95	0.7
0.38	1087	0.1553	1.866	0.73	0.73
0.42	1836.4	0.1553	1.889	1.22	1.31
0.41	1734.41	0.1553	1.883	1.16	1.32
0.33	1860.1	0.1553	1.837	1.27	1.36
0.37	1857.1	0.1553	1.860	1.26	1.53

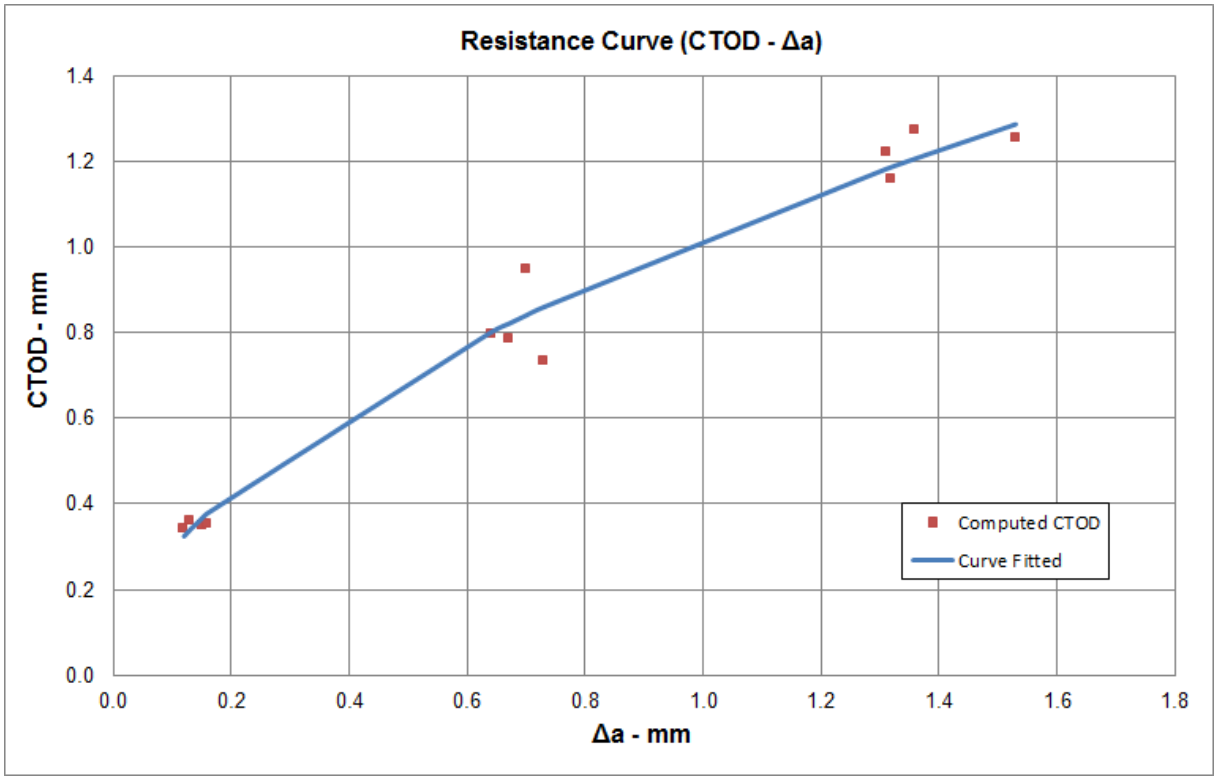

Figure 7.7 Curve fitted of computed CTOD values.

C. ENGINEERING CRITICAL ASSESSMENT BY LINKPIPE

The summary of parameters for calculating the critical crack size curve using LINKpipe is as follows:

1. The pipeline wall thickness is the minimum wall thickness determined by nominal wall thickness minus wall thickness tolerance;
2. CTOD-Δa curve obtained through conversion of lower bound J-R curve by adopting a conservative approach stated in the DNV-OS-F101 Appendix A;
3. Maximum allowable tearing 0.3mm;
4. Upper bound stress and strain curve (Power law hardening);
5. Maximum applied strain of 1.772%.

Based on the input of above mentioned parameters, the analyses using LINKpipe were performed to identify the critical crack sizes. The predicted critical crack size curve obtained from the analyses is shown in the **Figure 7.8** the curve is referred as a base case for the comparison of the results from the sensitivity analysis.

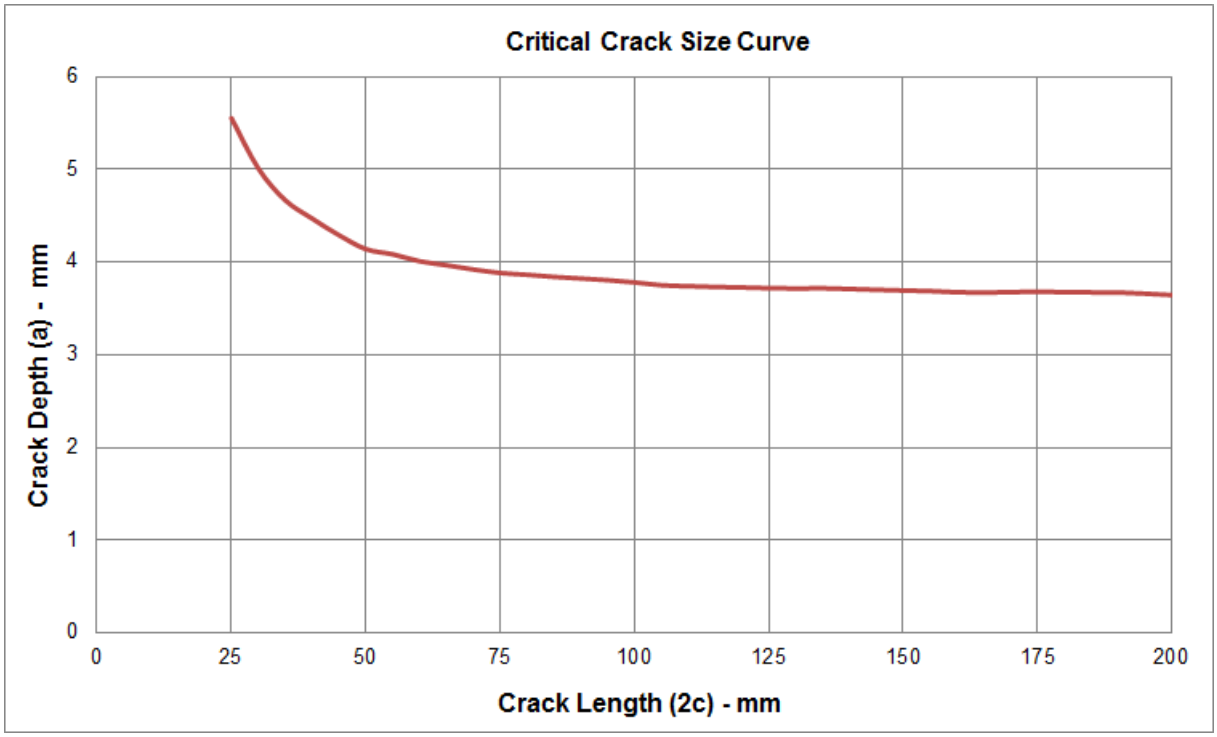

Figure 7.8 Critical Crack Size curve from LINKpipe analysis.

The Crack Driving Force (CDF) in the form of CTOD as a function of nominal strain can be seen in the **Figure 7.9. Figure 7.9** describes the difference of CTOD and Nominal Strain curves for four various crack lengths with the same crack depth (2mm).

The curves can be divided into two categories: the first one is the CDF in the short cracks with length range of 35-50mm and the second one is long cracks with length range of 75-100mm. The reason for distinction is that the CDF in the short crack category has relatively similar quantity for both cases, whereas the CDF in the long crack category is also has similar quantity for both cases.

The difference of CDF between short crack and long crack in LINKpipe can be distinguished for nominal strain larger than 0.5%. For relatively short crack length, LINKpipe predicted slightly higher crack driving force compared to long crack length.

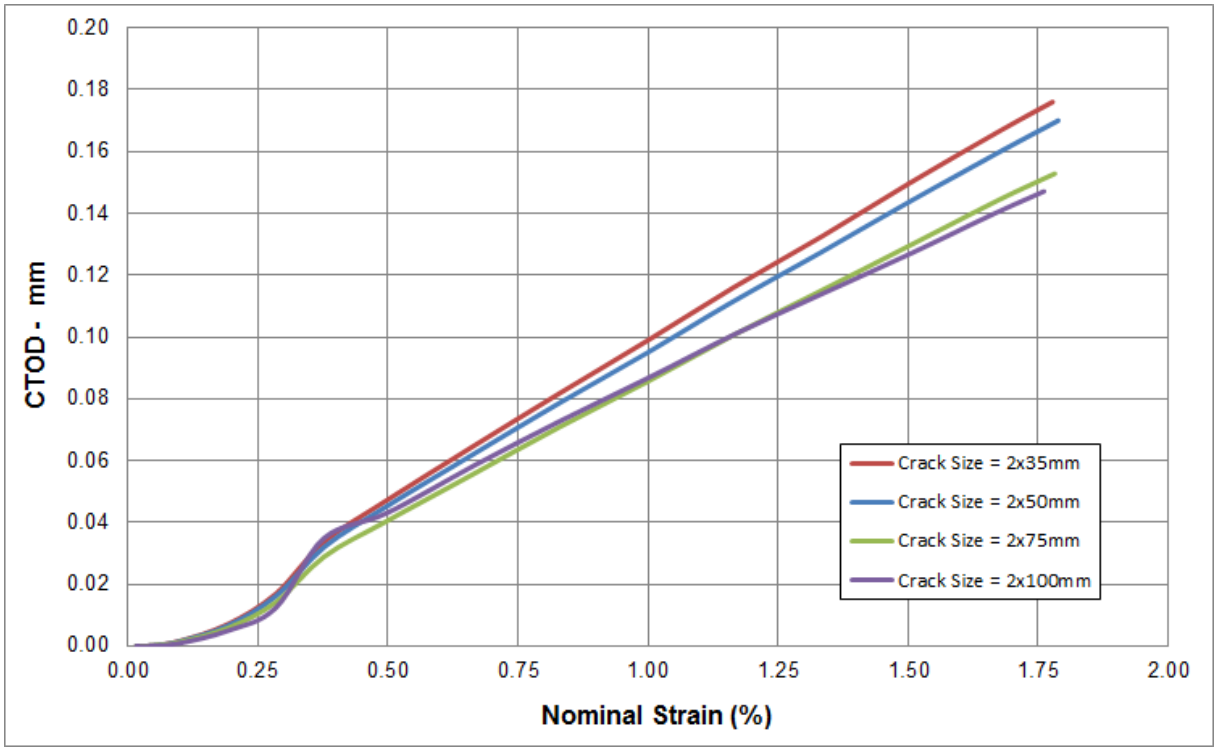

Figure 7.9 CTOD as a function of nominal strain for different crack size.

7.1.4 Sensitivity Analysis of LINKpipe Simulation

The sensitivity analyses were performed to evaluate the influence of several parameters in predicting critical crack sizes. The critical size curve generated from the sensitivity analyses is compared to the curve from base case. The cases that have been analyzed are as follows:

1. Case 1: Meshing Sensitivity
2. Case 2: Pipe Misalignment
3. Case 3: Residual Stress
4. Case 4: Strength Mismatch

A. CASE 1: MESHING SENSITIVITY

LINKpipe uses meshing arrangement as shown in **Figure 7.10**. For the present case, several analyses were performed using different mesh densities to evaluate the effect of mesh in predicting the Crack Driving Force (CDF) and Ductile Crack Growth (DCG). In FE modeling using LINKpipe, different mesh density is achieved by changing the following mesh related parameters:

1. The values of dx1 and dx2 describe element size in x-direction at the different locations from the crack as seen (**Figure 7.10)**;
2. The values dy, dy2, and dy1 similarly describe element size in circumferential direction at the different locations from the crack as seen (**Figure 7.10)**.

The analyses have been carried out for the following three different mesh configurations:

1. The first configuration (Mesh1 in **Figure 7.11**): The configuration has the same mesh as the base case, but differs from the mesh along circumferential crack length. The mesh is more dense along circumferential crack length (see **Table 7.6**);
2. The second configuration (Mesh2 in **Figure 7.11**): This configuration differs from the base case mesh with respect to the parameter dx2 (see **Table 7.6**). Compared to the based case, the configuration has more dense mesh in longitudinal direction at the vicinity of the crack;
3. The third configuration (Mesh3 in **Figure 7.11**): This configuration differs from the base case mesh with respect to the parameter dx2, dy2, and dy (see **Table 7.6**). It is seen in this configuration that all these parameters are halved compared to the base case configuration. Further, **Figure 7.11** shows that this configuration comprises more dense mesh at the vicinity of crack with respect to both longitudinal and circumferential direction.

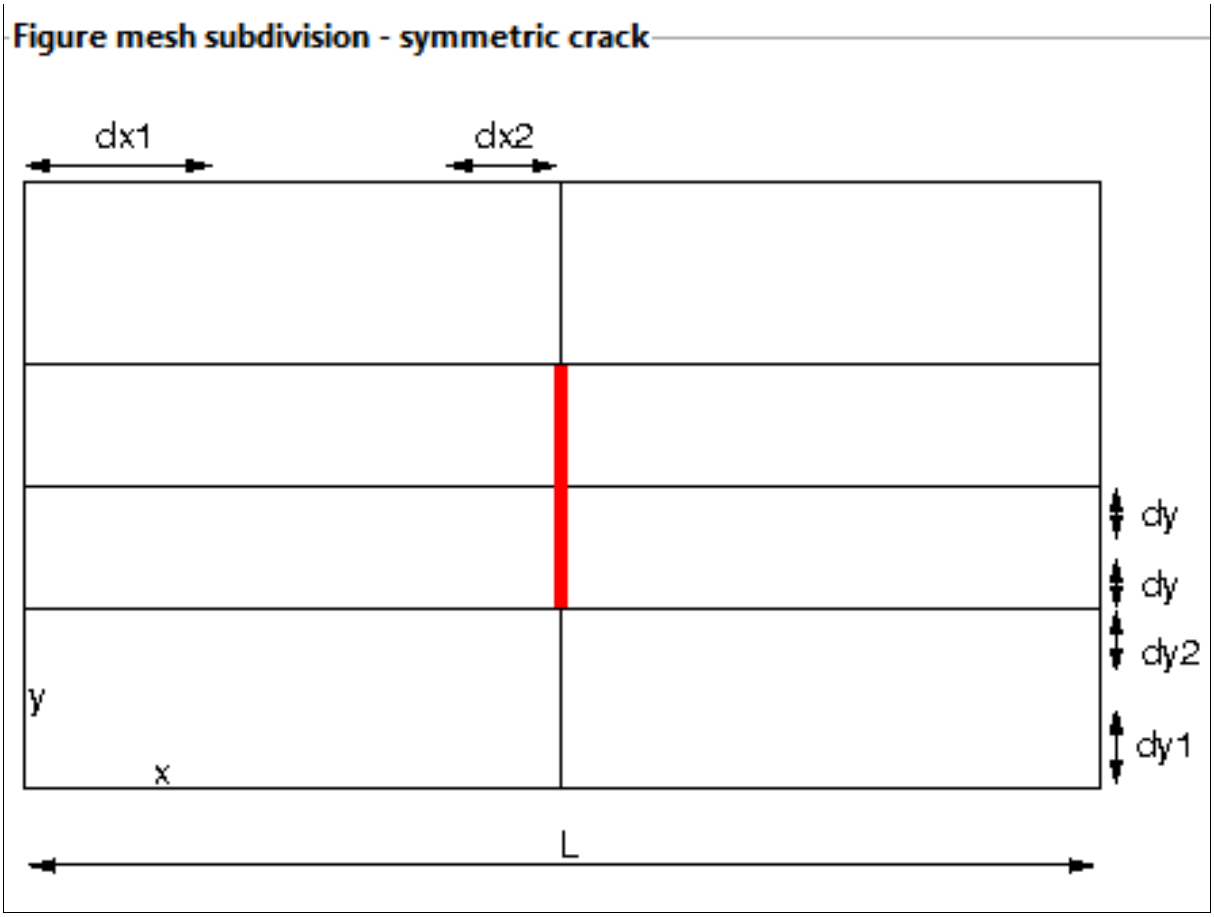

Figure 7.10 Meshing arrangement in LINKpipe (Ref., LINKpipe software).

Table 7.6 Mesh Configurations for The Analysis

Parameter	Base Case	Mesh 1	Mesh 2	Mesh 3
dx1	100	100	100	100
dx2	10	10	5	5
dy1	20	20	20	20
dy2	6	6	6	3
dy	3	1.5	3	1.5

The predicted CDF and DCG from different mesh configurations is then compared against the CDF and DCG from base case mesh configuration as can be seen in **Figure 7.12**, and **Figure 7.13** respectively. It is seen in **Figure 7.11** that the base configuration has coarse mesh which obviously takes less computational time compared to the other mesh patterns.

However, the accuracy of the model predictions is more important. The three different configurations yield approximately similar predictions as seen in the **Figure 7.11**, and **Figure 7.13**. It can be said that the chosen mesh patterns do not show much influence on the model predictions in terms of accuracy. Hence, the base case mesh configuration is therefore used for the subsequent sensitivity analyses.

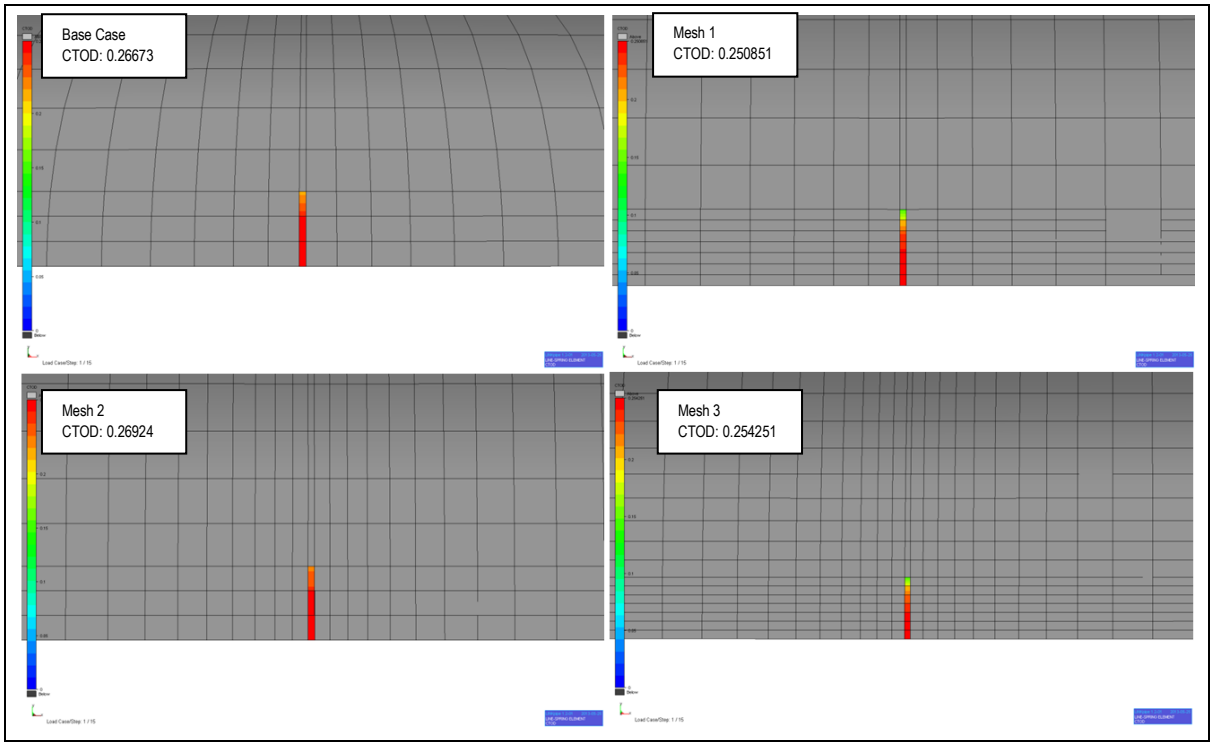

Figure 7.11 Four different types of mesh configurations and the CTOD value.

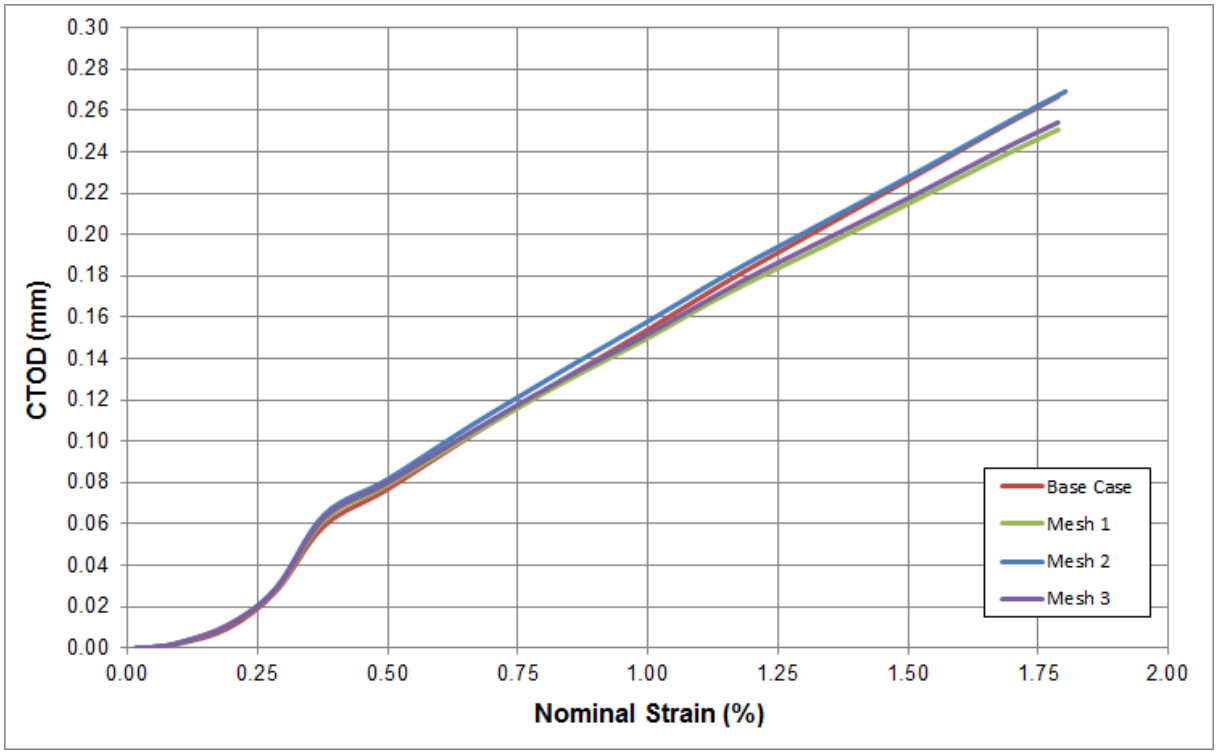

Figure 7.12 CTOD as a function of nominal strain for different mesh configurations.

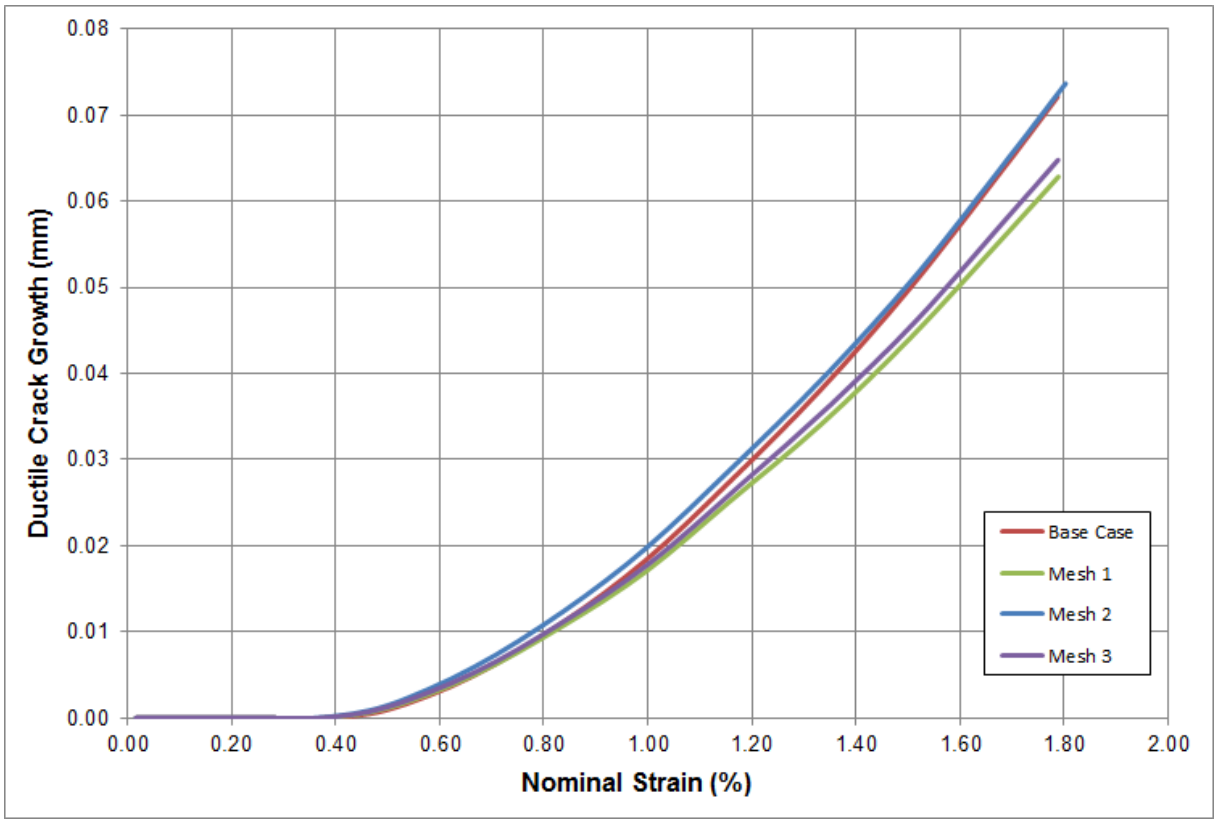

Figure 7.13 Four different types of mesh configurations and the CTOD value.

B. CASE 2: PIPE MISALIGNMENT

As stated in the theory and user manual (2012), LINKpipe used linear dependencies between the nodes from the left and the right pipe segment to handle the geometrical discontinuities such as misalignment. Pipe misalignment in the model will give additional bending moment to the crack.

The influence of misalignment to determine the critical crack size curve is analyzed using three different amounts of misalignment i.e., 0.5mm, 1.5mm and 2.5mm. All the critical crack size curves obtained from different amounts of misalignment were then compared against base case curve.

Figure 7.14 shows critical crack size curve from LINKpipe analysis for three different cases of misalignment and compares against the base case curve. It can be seen from the **Figure 7.14** that misalignment greatly influences the critical crack size. When the amount of misalignment increases, the allowable defect size is decreasing which means that the curve tends to be more conservative.

The small quantity of critical crack size because of misalignment concludes that the crack driving force is increases as the misalignment in the pipeline increases. **Figure 7.15** shows the CTOD value as a function of nominal strain for crack size of 2x50 mm. It can be seen that misalignment in the pipeline shows the significant effect in increasing the crack driving force, which make the allowable crack size became smaller. It can be concluded that LINKpipe covers misalignment in a conservative way.

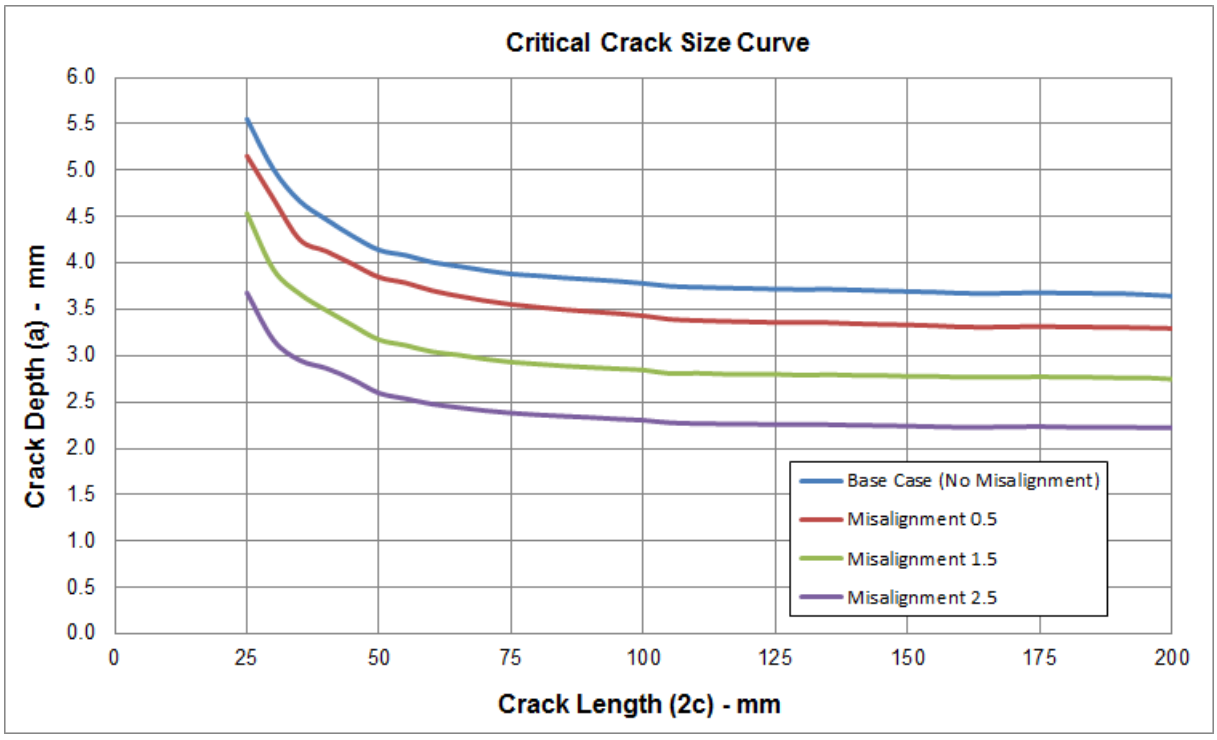

Figure 7.14 Critical crack size curve from LINKpipe analysis for three different cases of misalignment compare to base case curve.

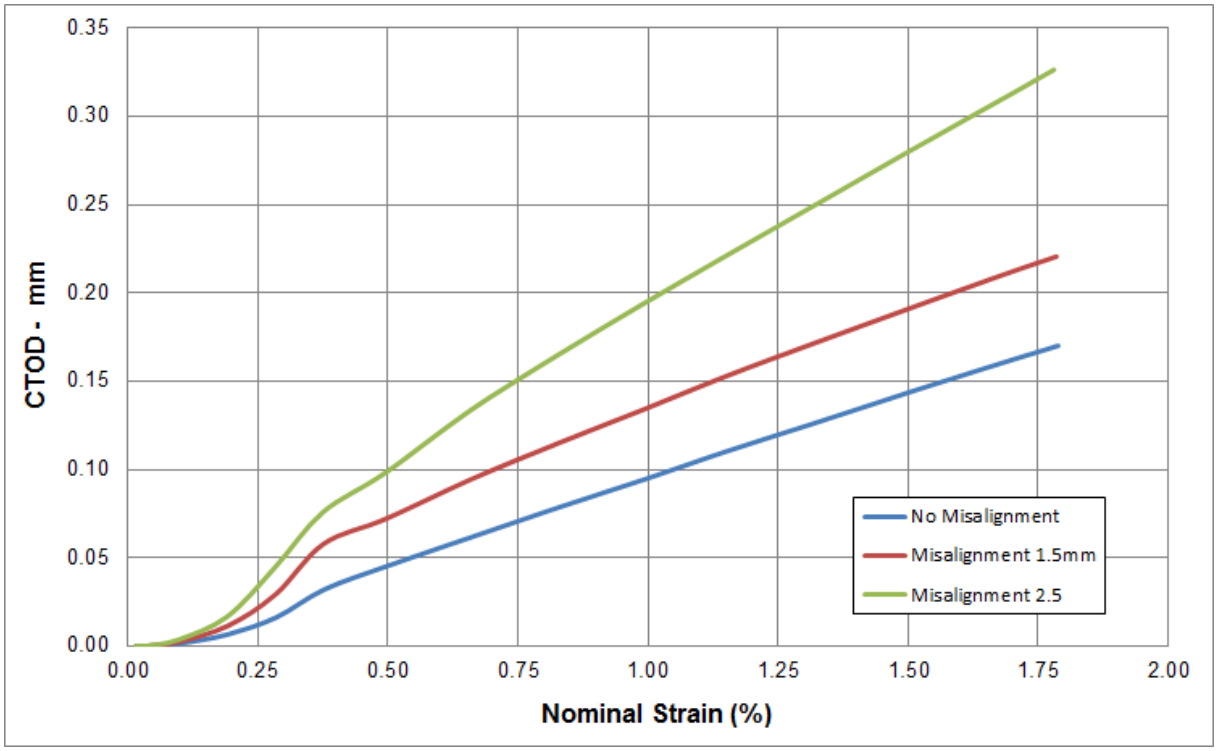

Figure 7.15 CTOD as a function of nominal strain for different quantity of misalignment.

C. CASE 3: RESIDUAL STRESS

In this case, the effect of residual stress to determine the critical crack size using LINKpipe is investigated. **Figure 7.16** shows the comparison of critical crack size curve for the three different situations i.e., no welding residual stress, welding residual stress with relaxation enable, and welding residual stress equal to yield stress.

When the relaxation is applied in LINKpipe, the reduction in the residual stress is similar to the procedure in the BS7910 2005 Section 7.3.4.2.

Compared to the effect of misalignment, the residual stress shows very slightly influence over the critical crack size. The effect of the residual stress can also be seen in **Figure 7.17** in terms of CTOD as a function of nominal strain. From the analyses using LINKpipe, it is seen that the influence of residual stress on the predictions of critical crack sizes and CTOD is insignificant and it only caused slightly increase in the crack driving force.

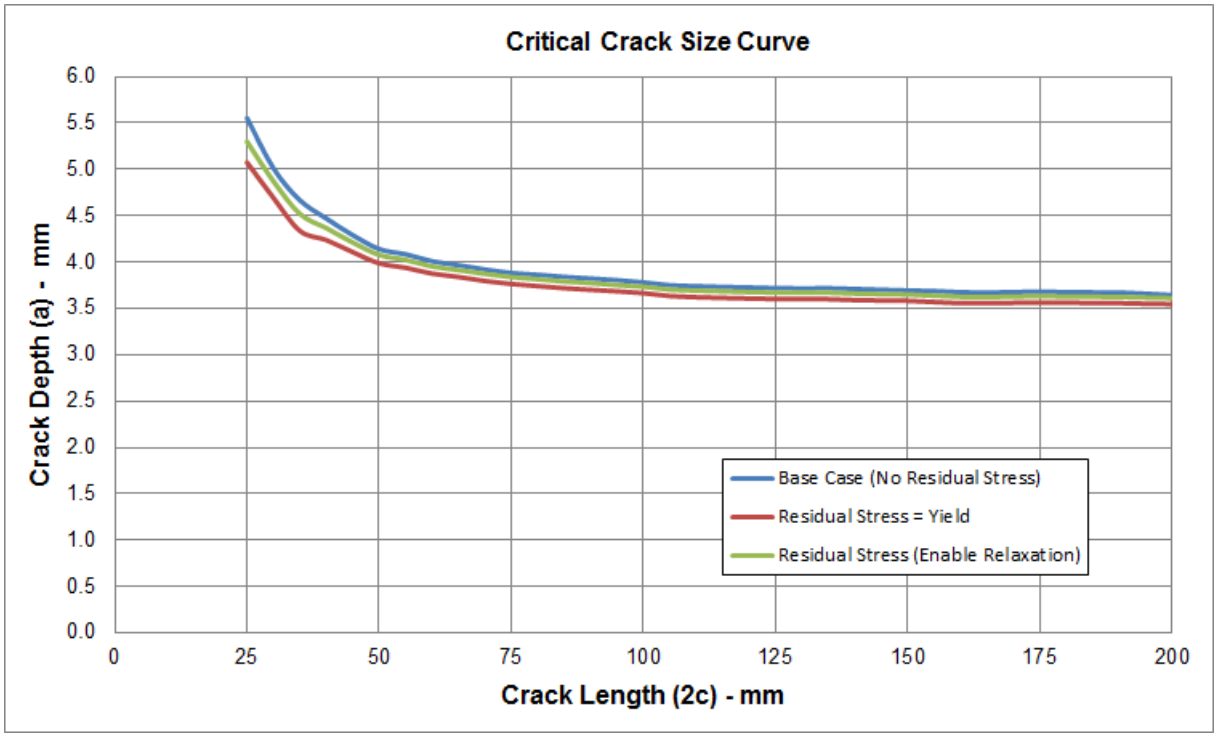

Figure 7.16 Critical crack size curve from LINKpipe analysis for different situations of residual stress.

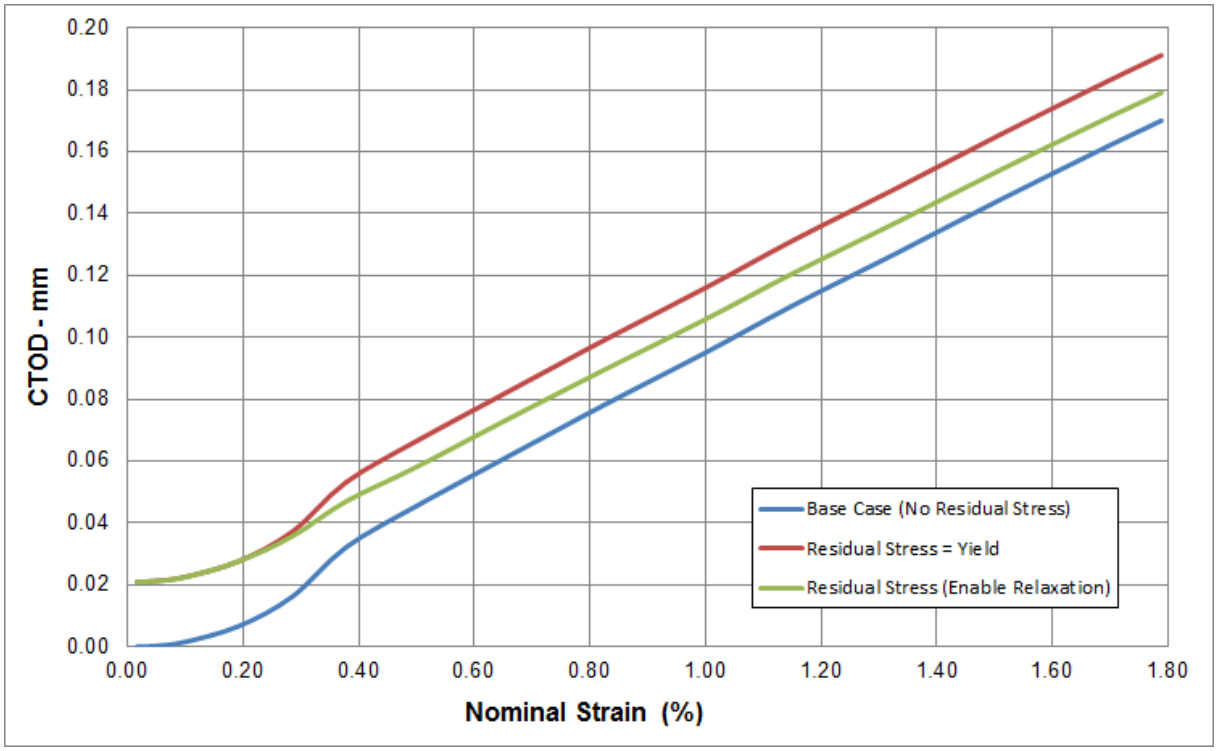

Figure 7.17 CTOD as a function of nominal strain for different conditions of residual stress.

D. CASE 4: STRENGTH MISMATCH

Regarding the welding consumable for the girth welds, the previous work shows that the case of weld strength overmatch with the strength of the base pipe is beneficial. Hence, it is important to assess the effect of weld strength under-match in the prediction of critical crack size.

The present work considers weld strength even-match as a base case and assesses the effect of weld under-match by comparing the predicted results for the critical crack size against with the results from the base case.

The properties of the weld metal used for the analysis are summarized in the **Table 7.7**. **Figure 7.18** shows the engineering stress-strain curves of base metal and weld metal. The figure presents the strength of weld that under matches with the strength of base metal.

Table 7.7 Summary of Weld Metal Properties (Ramberg-Osgood)

Parameter	Weld Metal
Yield stress, $R_{p0.5}$	650 MPa
Ultimate Tensile Strength, (UTS)	840 MPa
Young's Modulus, E	190,000 N/mm^2
Poisson's Ratio	0.3
Elastic Parameter, α	0.585
Hardening parameter, n	17.872

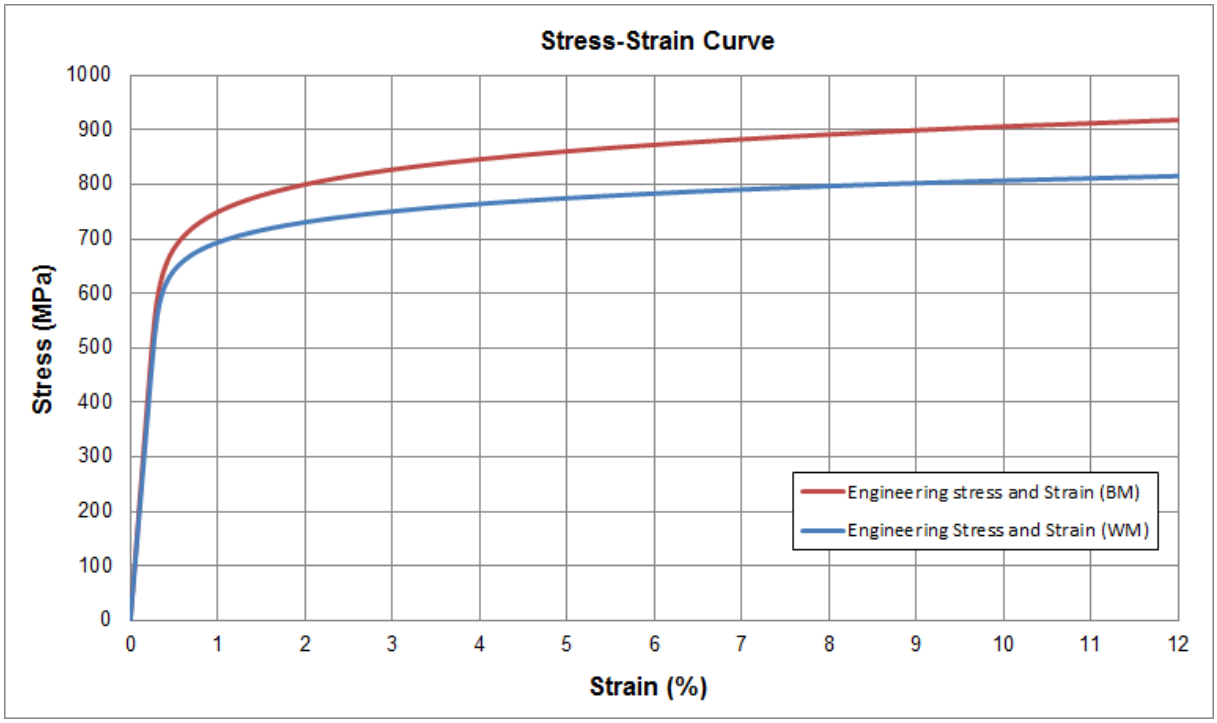

Figure 7.18 Engineering stress-strain curves of Base Metal (BM) and Weld Metal (WM).

As mentioned is the **Section 4.1.6**, to account for material mismatch LINKpipe uses a weight function to generate the equivalent stress-strain curve for weld metal and base metal.

The results from ECA analyses using LINKpipe can be seen in the **Figure 7.19** for the case where strength of the weld metal under-matches with that of the base metal. The critical crack size curve for weld under-match case is compared against the base case curve. It can be seen from **Figure 7.19** that the weld strength under-match condition gives smaller critical crack size compared to the even-match condition.

Further, **Figure 7.20** shows that the case of strength under-match significantly increases the Crack Driving Force that made the critical crack size curve become smaller.

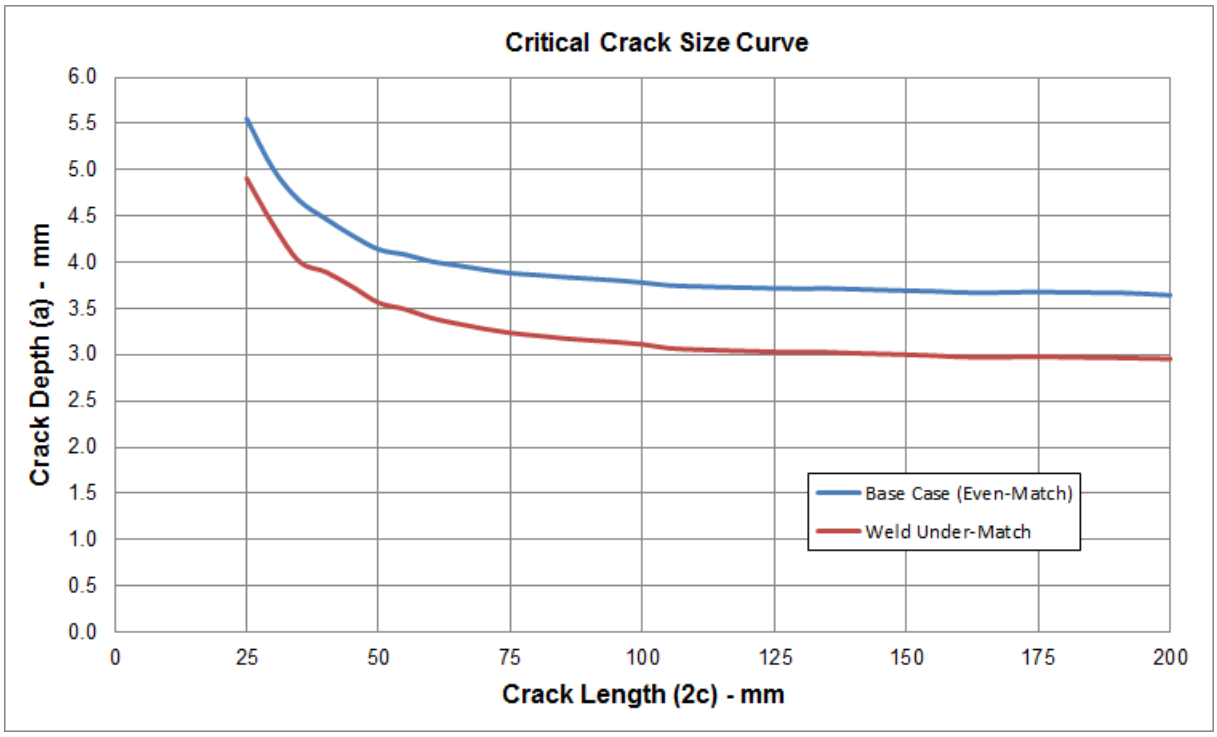

Figure 7.19 Critical crack size curve comparison between weld under-match and even-match conditions.

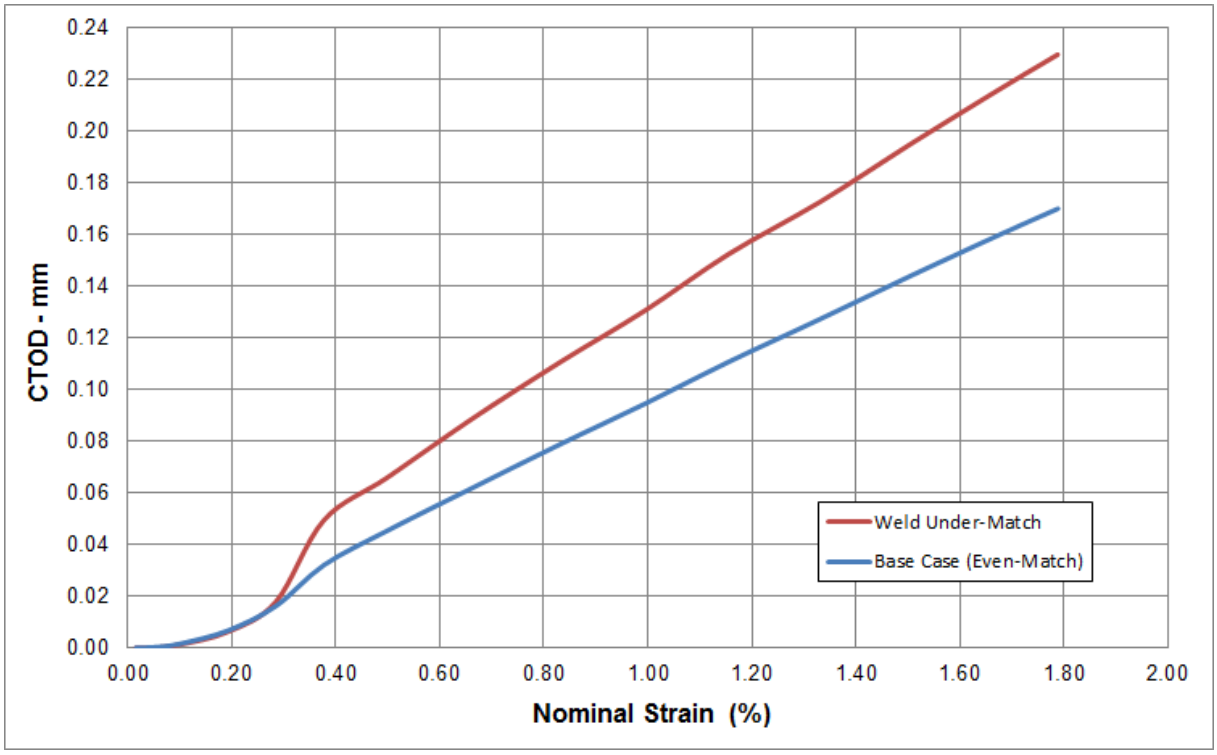

Figure 7.20 CTOD as a function of nominal strain for weld even-match and under-match conditions.

7.2 ECA Results Comparison (LINKpipe and CRACKWISE)

The software tools CRACKWISE and LINKpipe obviously have different approach to do the Engineering Critical Assessment. In addition, these tools also have several differences in terms of input parameters for ECA. These input parameters have to be taken into account to get the accurate comparison of the results from both tools. The differences in terms of input parameters used in the current are as follows:

1. The stress-strain curve used in CRACKWISE modeling is in the form of Ramberg-Osgood curve. On the other hand, the stress-strain curve used in LINKpipe is in the form of power hardening law;
2. J-integral data was used as fracture toughness parameter in CRACKWISE analyses, whereas CTOD data was used as fracture toughness parameter in LINKpipe analyses.

The comparison of ECA results from CRACKWISE and LINKpipe has been done using the same input parameters as listed below:

1. The wall thickness used in the analysis is the minimum wall thickness determined by nominal wall thickness minus wall thickness tolerance;
2. The weld residual stress is set to equal the yield stress with enabled relaxation;
3. Maximum applied strain is 1.772%;
4. Maximum allowable tearing is 0.3mm;
5. No misalignment;

6. Upper bound stress and strain curve;
7. Lower bound fracture resistance curve.

Figure 7.21 shows the critical size curve comparison obtained from CRACKWISE and LINKpipe. The figure presents the results for critical depth predicted by both the software for given crack length range from 25-200mm.

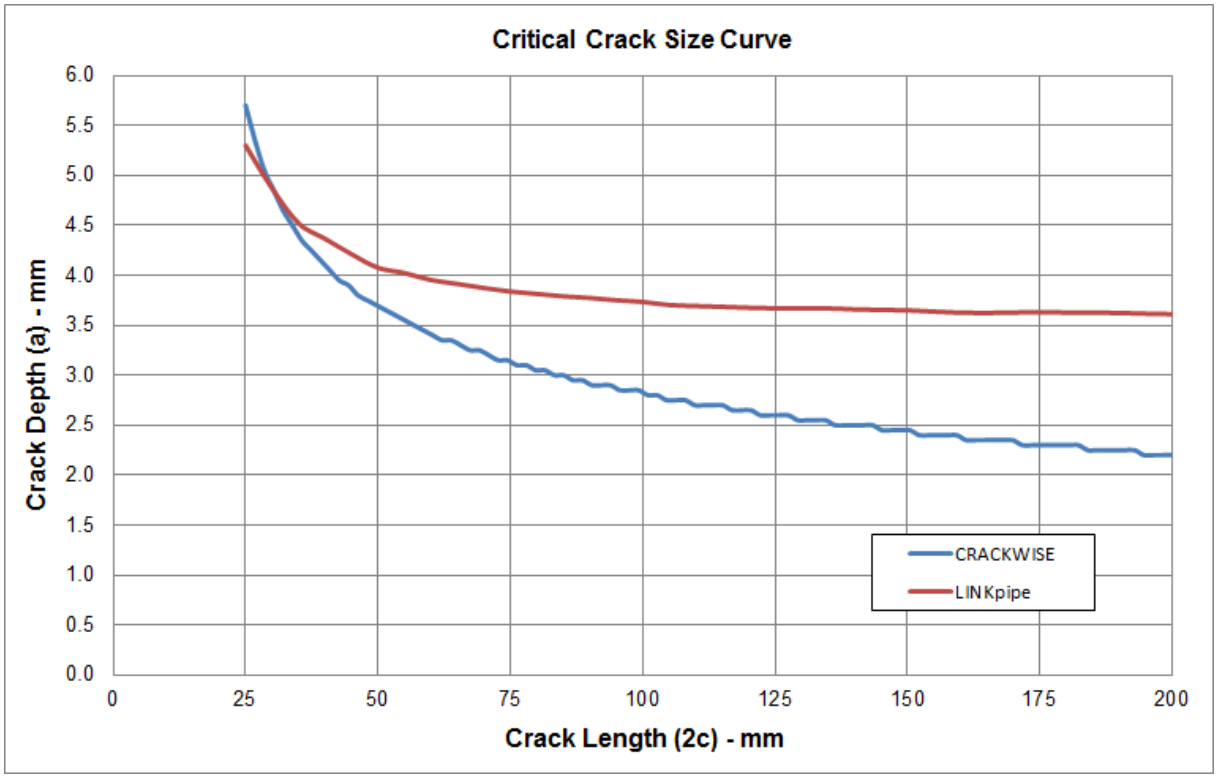

Figure 7.21 Comparison of Critical Crack Size curves from LINKpipe and CRACKWISE.

It can be seen that CRACKWISE gave more conservative results almost for every crack length except for short crack lengths in the range of about 25 to 30mm. For the crack lengths in the range of 30 to 200mm, CRACKWISE underestimated the results compared to the results from LINKpipe. The maximum difference is in the order of about 39% for crack length of 200mm.

The above comparison is made with the assumptions of accounting residual stress and neglecting the pipe misalignment. Also combined effect of residual stress and misalignment was investigated using the same other input mentioned above. Maximum possible misalignment which is 1.95mm as mentioned previously is used for the analyses and comparison.

With respect to the prediction of Crack Driving Force (CDF), the influence of misalignment on the predictions from CRACKWISE is less compared to that from LINKpipe. On the other hand, from **Figure 7.3** and **Figure 7.16** residual stress showed greater influence on the prediction of the CDF from CRACKWISE rather than that from LINKpipe.

Figure 7.22 compares the results obtained from CRACKWISE and LINKpipe and shows the influence of considered misalignment and residual stress (with relaxation). With both variables (residual stress and misalignment) accounted on in the analyses, the critical crack size curve resulted from both tools is relatively close to each other. However, the results from CRACKWISE still tend to be conservative for long crack lengths (>90mm) compared to the results from LINKpipe, whereas for short crack lengths (<90mm) CRACKWISE yields less conservative results of cracks size.

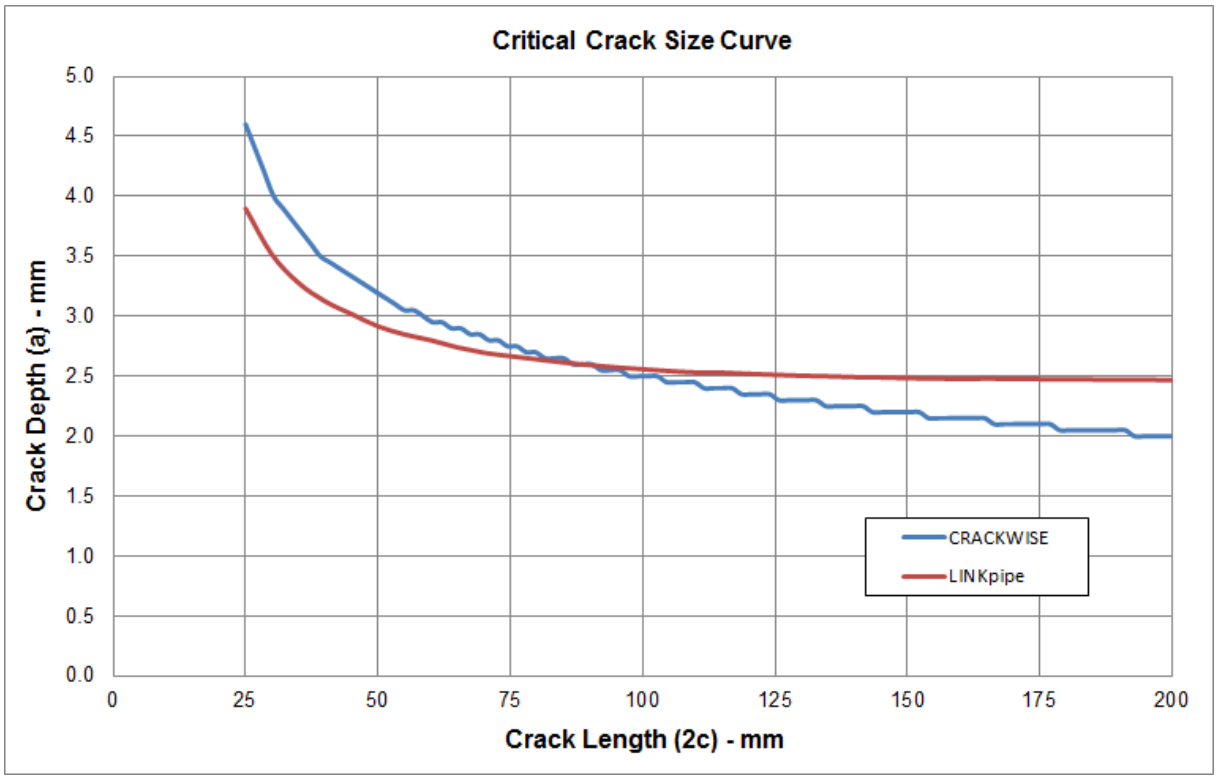

Figure 7.22 Comparison of Critical Crack Size curves obtained from LINKpipe and CRACKWISE for the case with maximum possible misalignment.

7.3 Results for ECA of Clad Pipes with Girth Welds

The two stages of Engineering Critical Assessment of clad pipes with girth welds have been carried out using LINKpipe. The input data for the analysis is adopted from the **Section 6.2**.

A. INPUT DATA FOR MATERIAL PROPERTIES

The as-received true stress-strain data given in the **Section 6.2.3** is used by fitting by power hardening law (see **Equation 6.4**). The parameters for power hardening law for modeling the true stress-strain curve are shown in **Table 7.8** for the materials: parent pipe, CRA layer and weld metal. The resultant true stress-strain curves for the three materials can be seen in **Figure 7.23**.

Table 7.8 Identified Material Parameters of Power Hardening Law

Parameter	Parent Pipe	CRA Layer	Weld Metal
Yield Stress (σ_0) - MPa	500	415	310
Strain Hardening Exponent (n)	0.051	0.16	0.232
Young's Modulus (E) - MPa	200,000	200,000	170,000

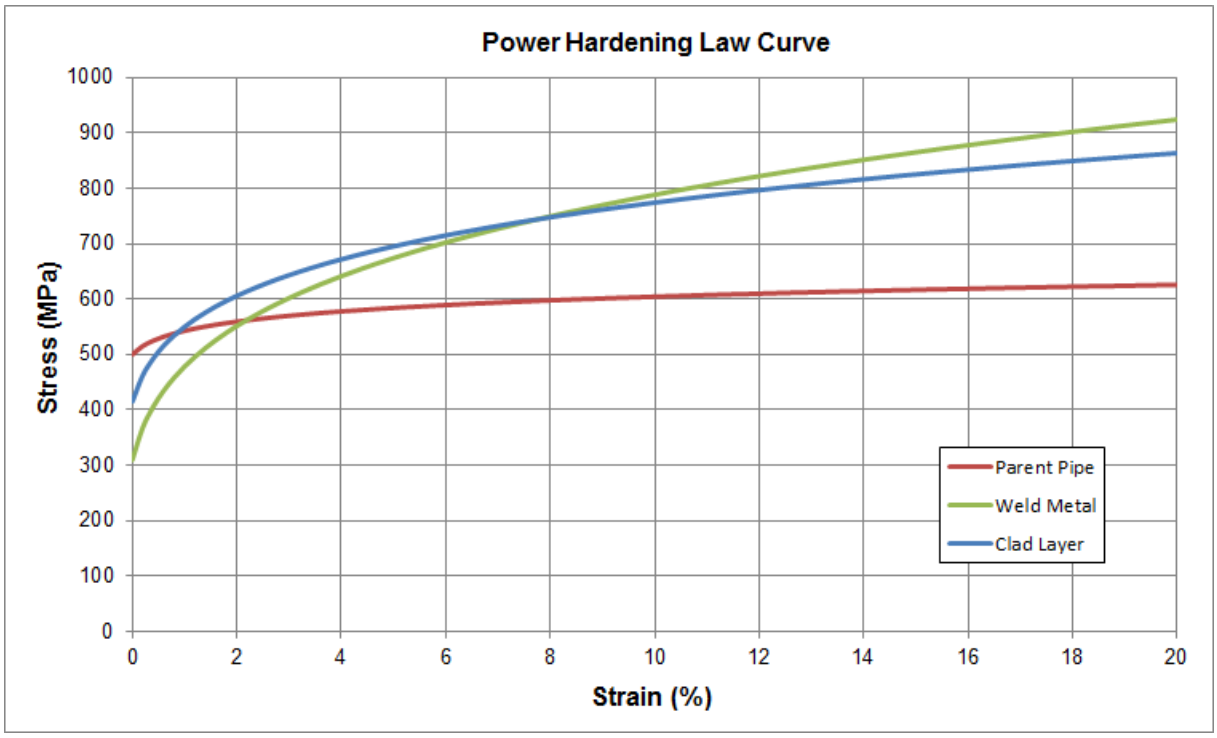

Figure 7.23 True stress-strain curves of the materials (as-received).

B. FRACTURE TOUGHNESS ANALYSIS

As mentioned previously, the crack driving force from LINKpipe analyses is measured by CTOD. To analyze the crack propagation, LINKpipe uses the ductile crack growth formulation in the form of CTOD as a function of ductile crack extension (Δa) (See **Section 4.1.4**). The methodology of computing the fracture resistance parameter CTOD for ECA analyses is explained in detail in **Section 3.3.3**.

The summary of computed CTOD values can be seen in **Table 7.9**.

Table 7.9 Summary of CTOD Values Computed from J-Integral Values

a/W	J (N/mm)	n	m	CTOD (mm)	Δa (mm)
0.392	1,622	0.2231	2.021	1.26	2.01
0.314	1,265	0.2231	1.984	1.00	1.30
0.351	760	0.2231	2.002	0.60	0.60
0.319	1,506	0.2231	1.987	1.19	1.33
0.334	565	0.2231	1.994	0.45	0.52
0.328	671	0.2231	1.991	0.53	0.61

It is known that LINKpipe uses the ductile crack growth formulation in the form of CTOD as a function of ductile crack extension (Δa). The parameters of the crack growth formulation are determined by fitting the CTOD curve with the computed CTOD values. The identified parameters are as listed below in **Table 7.10**.

Table 7.10 Fracture Resistance Parameters

CTODi	C_1	C_2
0.01	0.752	0.786

Figure 7.24 shows the curve fitted of CTOD computed values.

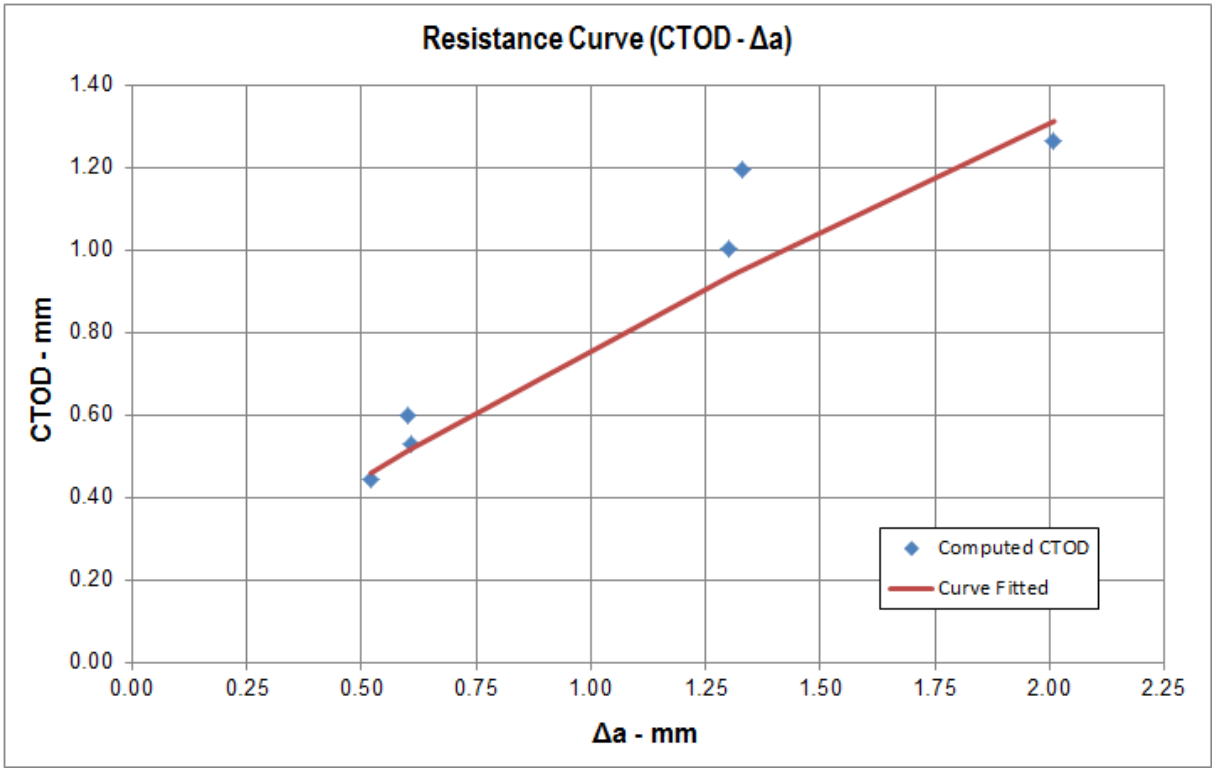

Figure 7.24 Curve fitted of computed CTOD values.

C. ENGINEERING CRITICAL ASSESSMENT BY LINKPIPE

The ECA for clad pipes was carried out for two stages of reeling installation:

1. Reeling tensile strain cycle.
2. Installation fatigue during hold periods on vessel.

As mentioned in **Section 6.2.1**, three tensile strain cycles are used in the analysis. The following two cases of analyses have been carried out:

1. Case 1: Critical Crack Size for Reeling Tensile Strain Cycles Without Misalignment and Residual Stress

The critical crack depths were determined by LINKpipe for different selected crack lengths. Five different cracks length were selected for the analysis. In this case the residual stress and misalignment are neglected. The summary of parameters to generate the trend of maximum allowable crack size for clad pipes using LINKpipe is as follows:

1. The pipeline wall thickness used in the analysis is the possible minimum wall thickness;
2. CTOD-Δa curve obtained through conversion of lower bound J-R curve by adopting a conservative approach stated in the DNV-OS-F101 Appendix A;
3. Maximum allowable tearing of 1.27mm for three tensile strain cycles;
4. True stress-strain curves of parent pipe material, girth weld and clad layer;
5. Three strain cycles was applied i.e., 1.77%, 1.42% and 1.62%;
6. No residual stress applied is assumed;
7. No misalignment is assumed.

The critical cracks size predicted based on given the parameters above are summarized in **Table 7.11**.

Table 7.11 Critical Crack Size for Reeling Installation (First Case)

Critical Crack Size (Pre-Installation)		Crack Size after Reeling	
Crack Depth (a) - mm	Crack Length (2C) - mm	Crack Depth (a) - mm	Crack Length (2C) - mm
2.75	110	3.75	110
2.80	90	3.81	90
2.85	65	3.87	65
2.90	45	3.88	45
3.05	30	4.04	30

2. Case 2: Critical Crack Size for Reeling Tensile Strain Cycles With Misalignment and Residual Stress)

The data of input parameters used in this analysis is the same as the data used for the first case except for the data of misalignment and residual stress which are included in the present analyses. The possible maximum misalignment used in the analysis is 1.4mm and the residual stress is set to equal yield strength. For the second case, the predicted critical cracks sizes obtained from the analyses are listed below in **Table 7.12**.

The predicted critical crack sizes for the second case are smaller than that for the first case, which is due to the effect of misalignment and residual stress. As discussed in the **Section 7.1.4**, the results from analyses using LINKpipe conclude that the use of misalignment in the pipeline highly reduces the critical cracks size.

Table 7.12 Critical Crack Size for Reeling Installation (Second Case)

Critical Crack Size (Pre-Installation)		Crack Size after Reeling	
Crack Depth (a) - mm	Crack Length (2C) - mm	Crack Depth (a) - mm	Crack Length (2C) - mm
1.25	110	2.87	110
1.35	90	2.76	90
1.40	65	2.75	65
1.42	45	2.66	45
1.50	30	2.49	30

3. Fatigue Crack Growth due to Installation Fatigue

The objective of this present analysis is to assess post installation fatigue crack size. Fatigue crack growth during hold periods on vessel was estimated by using LINKpipe considering high cycle fatigue load stations based on the assessment procedures described in BS9710. The size of the cracks at the start of this ECA stage is the crack size obtained at the end of previous stage, which is the end of reeling installation (refer to **Table 7.11** and **Table 7.12** - Crack size after reeling).

For clad pipes, the summary of assumptions to generate post installation fatigue crack sizes using LINKpipe is as follows:

1. Installation fatigue spectrum input is taken from **Table 6.8**, with hold period of 18 hours and 2 m distance from clamp to weld.
2. Several multiplication factors were applied such as:
    - A factor of 0.9 to reduce the conservatism of infinite stiff clamp assumption;
    - A factor of 0.85 for 2m clamp distance assumption.

Paris law of fatigue crack growth for steels in air as recommended by BS7910 was used in the analysis. **Table 7.13** and **Table 7.14** show the critical cracks size and post installation crack due to reeling and fatigue for the first and second cases respectively.

Table 7.13 Crack Growth due to Reeling and Installation Fatigue (First Case)

Critical Crack Size (Pre-Installation)		Crack Size after Reeling		Post Installation Fatigue Defect	
Crack Depth (a) - mm	Crack Length (2C) - mm	Crack Depth (a) - mm	Crack Length (2C) - mm	Crack Depth (a) - mm	Crack Length (2C) - mm
2.75	110	3.75	110	9.21	110.89
2.80	90	3.81	90	8.56	90.94
2.85	65	3.87	65	7.65	66.04
2.90	45	3.88	45	6.75	46.15
3.05	30	4.04	30	6.22	31.44

Table 7.14 Crack Growth due to Reeling and Installation Fatigue (Second Case)

Critical Crack Size (Pre-Installation)		Crack Size after Reeling		Post Installation Fatigue Defect	
Crack Depth (a) - mm	Crack Length (2C) - mm	Crack Depth (a) - mm	Crack Length (2C) - mm	Crack Depth (a) - mm	Crack Length (2C) - mm
1.25	110	2.87	110	5.45	110.19
1.35	90	2.76	90	4.97	90.19
1.40	65	2.75	65	4.72	65.26
1.42	45	2.66	45	4.28	45.32
1.50	30	2.49	30	3.47	30.37

D. ENGINEERING CRITICAL ASSESSMENT BY CRACKWISE

For clad pipes, the section compares the ECA results from LINKpipe analyses against the results from CRACKWISE. The results from CRACKWISE were adopted from the work of Subsea7, 2010. The stress-strain curve used in the analyses is the equivalent stress-strain curve generated by FE analysis as described in **Section 2.3.2**. The equivalent stress-strain curve can be seen in **Figure 7.25**.

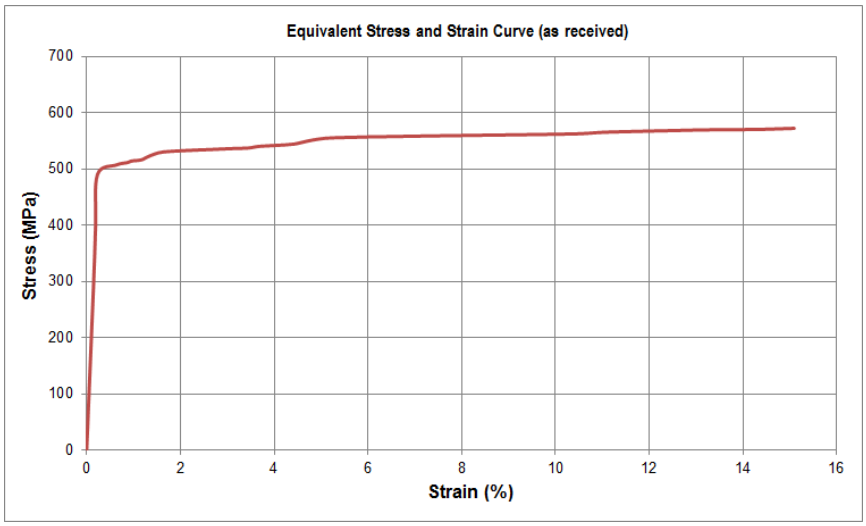

Figure 7.25 Equivalent stress-strain curve generated from FE analysis (Subsea 7, 2010)

In the work of Subsea7, 2010, the summary of the parameters used in the CRACKWISE simulations are as follows:

1. The possible minimum wall thickness;
2. Lower bound J-R curve;
3. Three strain cycles were applied i.e., 1.77%, 1.42% and 1.62%;
4. Assumed pipe misalignment was of 1.4mm and corresponding applied stress was treated as bending stress (Pb);
5. The residual stress was treated as welding strain (welding stress divided by young's modulus), with no relaxation;
6. Maximum allowable tearing was assumed to be 1.27mm for three tensile strain cycles.

The critical crack sizes predicted using CRACKWISE can be seen in the **Table 7.15**.

Table 7.15 Critical Defects Sizes for Reeling Installation (Ref., Subsea 7, 2010)

Crack Depth (mm)	Crack Length (mm)
1.5	110
2.0	90
2.5	65
3.0	45
3.5	35
4.0	30

E. ECA OF CLAD PIPE RESULTS COMPARISON (LINKPIPE vs. CRACKWISE)

The critical crack size predicted using CRACKWISE is compared with the critical crack size predicted using LINKpipe. The critical crack size predictions from LINKpipe listed in the **Table 7.12** (Case 2) are used for the comparison.

The ECA of clad pipe results comparison between CRACKWISE and LINKpipe has been carried out for the same input parameters as listed follow:

1. The pipeline wall thickness used in the analysis is the possible minimum wall thickness;
2. Maximum allowable tearing of 1.27mm for three tensile strain cycles;
3. Three strain cycles was applied i.e., 1.77%, 1.42% and 1.62%;

However, there are some input parameters which show difference between LINKpipe and CRACKWISE are:

1. FRACTURE RESISTANCE CURVE

   LINKpipe: CTOD-Δa curve obtained through conversion of lower bound J-R curve by adopting a conservative approach stated in the DNV-OS-F101 Appendix A.

   CRACKWISE: Lower bound J-R curve.

2. STRESS-STRAIN CURVE

   LINKpipe: Equivalent stress-strain curve generated by LINKpipe using weight principle described in **Section 4.1.6**.

   CRACKWISE: Equivalent stress-strain curve generated using FE analysis described in **Section 2.3.2**.

3. RESIDUAL STRESS

   LINKpipe: Residual stress equal to yield with no relaxation.

   CRACKWISE: The residual stress is treated as welding strain (welding stress divided by young's modulus), with no relaxation.

4. MISALIGNMENT

   LINKpipe: Maximum misalignment of 1.4mm is applied.

   CRACKWISE: Maximum misalignment was of 1.4mm and corresponding applied stress was treated as bending stress (Pb).

Figure 7.26 compares the results from LINKpipe and CRACKWISE using the same input data. The figure shows that the results from LINKpipe are more conservative than CRACKWISE. This behavior can be explained as follows:

1. The effect of misalignment over the predictions of critical crack sizes from LINKpipe is more significant than the influence of misalignment over the predictions from CRACKWISE.
2. The residual stress in CRACKWISE analyses is treated as welding strain in addition to the nominal strain and incorporated into primary stress. Hence, the effect of residual stress is no longer significant to the predictions of critical crack size curve.

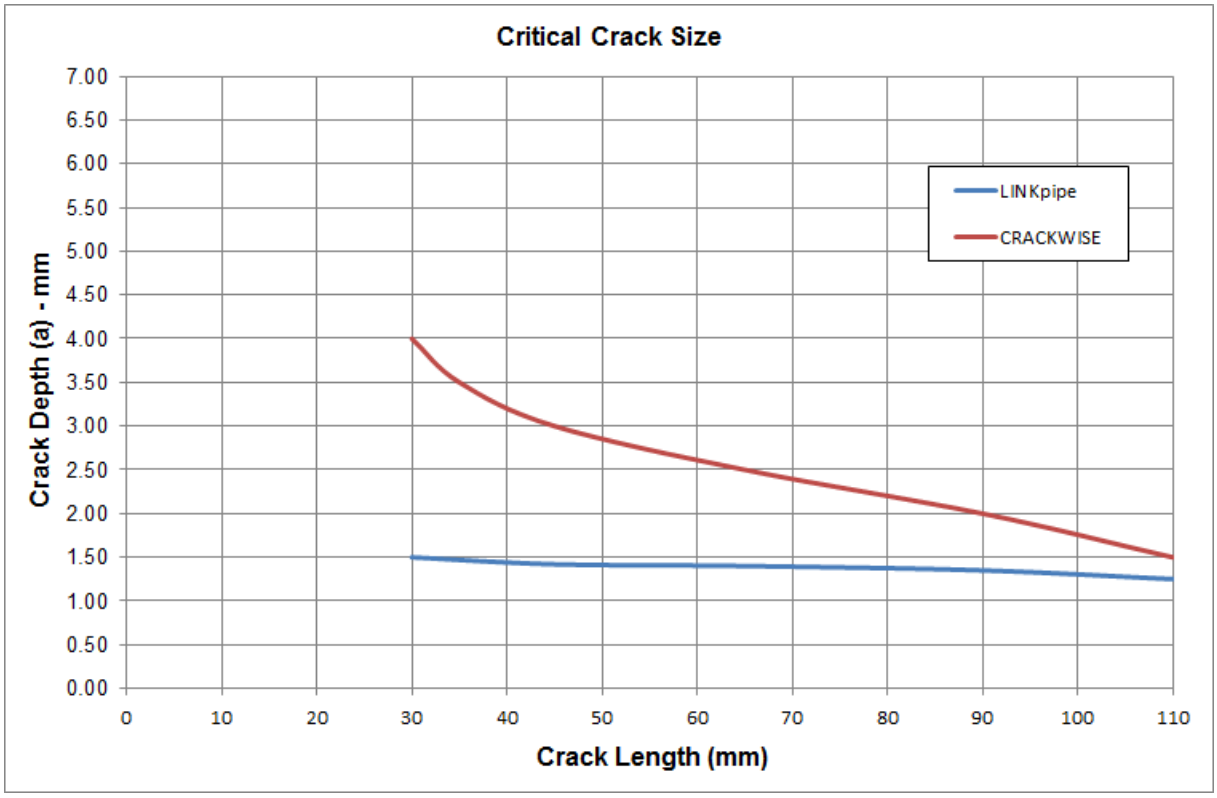

Figure 7.26 Comparison of Critical Crack Size curves from LINKpipe – Case 2 and CRACKWISE for clad pipe.

8. CONCLUSIONS AND FURTHER WORK

8.1 Conclusions

Reeling installation method causes large plastic deformation in the pipeline girth welds. Due to the existing cracks commonly found during fabrication phase in the girth welds, the plastic strain can cause possible crack growth. The ECA analyses have been carried out for reeling installation using the software tools CRACKWISE and LINKpipe. The purpose ECA is to generate the generic trend of critical crack sizes in the girth welds.

The present thesis work includes Engineering Critical Assessment for 10" pipeline made of 13 Cr martensitic stainless steel using CRACKWISE and LINKpipe. For the selected pipeline, the analyses that have been performed are as follow:

1. Analyses considering the influence of misalignment and residual stress to predict the critical crack sizes using CRACKWISE.
2. The sensitivity analyses for ECA using LINKpipe to evaluate the influence of the important parameters in predicting the critical crack size. The parameters such as misalignment, residual stress, strength mismatch, and meshing configuration are considered for the analyses.
3. Analyses for comparison of critical crack sizes predicted from CRACKWISE and LINKpipe simulations.

In addition, ECA analyses were also performed for clad pipe with 273.1mm OD and 15mm WT (+3.0 mm Clad) using LINKpipe. The results from these analyses are compared against those from previous work based on CRACKWISE.

The following conclusions are made based on the above mentioned analyses performed for the work:

1. The critical crack size predicted by CRACKWISE can be greatly influenced by residual stress. For the case where the residual stress is considered to be equal to the yield stress, the critical crack size reduces very significantly especially for short crack length (<50mm). The results from **Figure 7.3** show that assigning residual stress equal to yield stress gives more conservative results compared to the cases of zero residual stress and relaxed residual stress. In other words, neglecting residual stress predicts less conservative results for critical crack sizes.
2. The results from CRACKWISE simulations in **Figure 7.4** show that the critical crack size is smaller for the case of pipeline with maximum misalignment. However, the influence of misalignment for the critical crack size curve is less significant compared to the effect of residual stress.

3. Based on the sensitivity analyses for ECA using LINKpipe in **Section 7.1.4**, pipe misalignment and strength mismatch can show high influence on the prediction of Crack Driving Force. Pipe misalignment in LINKpipe ECA simulations can show the effect in increasing the Crack Driving Force very significantly, which makes the critical crack size became smaller. It can be concluded that LINKpipe treats the pipe misalignment conservatively.
4. Weld under-match condition from analyses using LINKpipe can significantly increase the Crack Driving Force (see **Figure 7.20**) that made the critical crack sizes became smaller.
5. The residual stress showed little influence in the prediction of the critical crack size using LINKpipe (see **Figure 7.16**). Furthermore, the influence of residual stress on the predictions of CTOD can be insignificant and it only caused very small increase in the crack driving force (see **Figure 7.17**).
6. The comparison of predicted critical crack size from CRACKWISE and LINKpipe has been carried out. The comparison is made based on neglecting misalignment and applying the weld residual stress equal the yield stress with enabled relaxation. CRACKWISE gave more conservative results almost for every crack length except for short crack lengths in the range of about 25 to 30mm. For the crack lengths in the range of 30 to 200mm, CRACKWISE underestimated the results compared to the results from LINKpipe. The maximum discrepancy in the results is in the order of about 39% for crack length of 200mm (see **Figure 7.21**).
7. When the maximum possible misalignment (which is 1.95mm) along with the residual stress is applied, the critical crack size curves resulted from CRACKWISE and LINKpipe, are relatively close to each other. However, CRACKWISE tends to be conservative for long crack lengths (>90mm) compared to LINKpipe, whereas for short crack lengths (<90mm) CRACKWISE yields less conservative critical crack sizes (see **Figure 7.22**).
8. Comparison has also been made between the predictions from LINKpipe and CRACKWISE for the clad pipes with girth welds. For the same given input data, LINKpipe predicts the critical crack size conservatively compared to the results from CRACKWISE.

8.2 Further Work

Further works that can be carried out to improve the conclusion of the thesis are as follows:

1. Comparison of ECA with various pipeline geometries (diameter and wall thickness) and using experimental CTOD values;
2. Three Dimension Finite Element Analysis to verify the results from LINKpipe and CRACKWISE, especially for ECA analysis of clad pipe.

REFERENCE

Anderson, T.L., 2005. Fracture Mechanics Fundamentals and Applications, 3rd Edition. Taylor and Francis Group: Boca Raton.

Ashby, Michael F., Jones, David R. H., 2012. Engineering Materials 1 - An Introduction to Properties, Applications, and Design. 4th Ed. Elsevier.

Barsom, John M. and Rolfe, Stanley T., 1999. Fracture and Fatigue Control in Structures - Applications of Fracture Mechanics: (MNL 41).ASTM International.

Berg, Espen, et al., 2007. Ductile Fracture of Pipelines-Effects of Constraint Correction and Circumferential Crack Growth. Proceedings of the Seventeenth (2007) International Offshore and Polar Engineering Conference Lisbon, Portugal, July 1-6, 2007.

Berg, Espen., et al., 2007. Ultimate fracture capacity of pressurised pipes with defects – Comparisons of large scale testing and numerical simulations. Engineering Fracture Mechanics 75 (2008) 2352–2366

British Standard. BS7910: 2005, 2007. Guide to methods for assessing the acceptability of flaws in metallic structures.

Buschow, K.H. Jürgen; Cahn, Robert W.; Flemings, Merton C.; Ilschner, Bernhard; Kramer, Edward J.; Mahajan, Subhash., 2001. Encyclopedia of Materials - Science and Technology, Volumes 1-11.. Elsevier.

Cosham, Andrew and Macdonald, Kenneth. A, 2008. Fracture Control in Pipelines Under High Plastic Strains – A Critique of DNV-RP-F108. Proceedings of the 7th International Pipeline Conference IPC September 30 - October 03, 2008, Calgary, Alberta, Canada.

Denniel, S., 2009. Optimising Reeled Pipe Design Through Improved Knowledge of Reeling Mechanics. The 2009 Offshore Technology Conference held in Houston, Texas, USA, 4-7 May 2009.

Det Norske Veritas, 2013. Guideline for Design and Construction of Lined and Clad Pipelines, JIP Lined and Clad Pipelines, Phase 3.

Det Norske Veritas. 2006. DNV-RP-F108: Fracture Control for Pipeline Installation Methods Introducing Cyclic Plastic Strain.

Det Norske Veritas. 2007. DNV-OS-F101: Submarine Pipeline Systems.

Dieter, George E. (1997). ASM Handbook, Volume 20 - Materials Selection and Design. ASM International.

Farahmand, Bahram., 2001. Fracture Mechanics of Metals, Composites, Welds, and Bolted Joints - Application of LEFM, EPFM, and FMDM Theory. Springer - Verlag.

Jayadevan, K.R., et al., 2006. Numerical investigation of ductile tearing in surface cracked pipes using linespring. International Journal of Solids and Structures 43 (2006) 2378–2397

Jayadevan, K.R., et al., 2005. Structural integrity of pipelines: T-stress by linespring. Fatigue Fract Engng Mater Struct 28,467-488. Blackwell Publishing Inc.

Kuhn, Howard and Medlin, Dana., 2000. ASM Handbook, Volume 08 - Mechanical Testing and Evaluation. ASM International.

Kyriakides, Stelios, 2007. Mechanics of Offshore Pipelines Vol. I Buckling and Collapse. 1ST Ed. Burlington: Elsevier.

Linkftr. 2012. LINKpipe Theory Manual.

Macdonald, Kenneth A., 2011. Fracture and Fatigue of Welded Joints and Structures. Woodhead Publishing.

Macdonald, Kenneth. A and Cheaitani, Mohamad., 2010. Engineering Critical Assessment In The Complex Girth Welds of Clad and Lined Linepipe Materials. Proceedings of the 8th International Pipeline Conference September 27-October 1, 2010, Calgary, Alberta, Canada.

Manouchehri, S., Howard, B., and Denniel, S., 2008. A Discussion of the Effect of the Reeled Installation Process on Pipeline Limit States. Proceedings of the Eighteenth (2008) International Offshore and Polar Engineering Conference Vancouver, BC, Canada, July 6-11, 2008.

Marlow, Frank M., 2002. Welding Fabrication and Repair - Questions and Answers. Industrial Press.

Megson, T.H.G., 2005. Structural and Stress Analysis (2nd Edition). Elsevier.

Mousselli, A.H., 1981. Offshore Pipeline Design, Analysis, and Methods. Oklahoma: Pennwell Publishing Company.

Olsø, Erlend, et.al., 2011. A New Assessment Approach for ECA of Clad and Lined Pipes Based on Shell and Line-spring Finite Elements. Proceedings of the Twenty-first (2011) International Offshore and Polar Engineering Conference Maui, Hawaii, USA, June 19-24, 2011.

Olsø, Erlend, et al., 2008. Effect of embedded defects in pipelines subjected to plastic strains during operation. Proceedings of the Eighteenth (2008) International Offshore and Polar Engineering Conference Vancouver, BC, Canada, July 6-11, 2008.

Roylance, David, 2001. Stress-strain curves. [pdf] Department of Materials Science and Engineering Massachusetts Institute of Technology Cambridge. Available at: <http://web.mit.edu/course/3/3.11/www/modules/ss.pdf> [Accessed 12 February 2013].

Sandvik, A., et al., 2011. An Efficient FE-based Probabilistic Model for Ductile Fracture Assessment of Pipelines with Surface Defects. Proceedings of the Twenty-first (2011) International Offshore and Polar Engineering Conference

Skallerud, B., Holthe, K., and Haugen, B., 2005. Thin shell and surface crack finite elements for simulation of combined failure modes. Comput. Methods Appl. Mech. Engrg. 194 (2005) 2619–2640

Skallerud, B., Berg, E., Jayadevan, K.R., 2006. Two-parameter fracture assessment of surface cracked cylindrical shells during collapse. Engineering Fracture Mechanics 73 (2006) 264–282

Sriskandarajah, T., Bedrossian, A., and Ngai, T., 2012. Reeling of Offshore Pipes with Partially Overmatching Girth Welds.

Sriskandarajah, T., Jones, AL Howard., and Bedrossian, AN., 2003. Extending the Strain Limits for Reeling Small Diameter Flowlines. Proceedings of the Thirteenth (2003) International Offshore and Polar Engineering Conference Honolulu, Hawaii, USA, May 25–30, 2003.

Subsea 7, Technical Guideline for ECA of Reeled Rigid Pipelines, Doc. No. GD-GL-PD-COE-010, February 2011.

Subsea 7, Development of Methodology for Reeling Analysis and ECA using LINKpipe, Doc. No. ES0021-R-ST-001, July 2006.

Subsea 7, ECA Report 10" OD CRA, Doc. No. SKA-SSN-M-RA-0018, February 2010.

Thaulow, C., et al., 2006. Fracture control of pipelines using linkpipe: from rule based design to direct calculations. In: Proceedings of HSLP-IA2006: international seminar on application of high strength line pipe and integrity assessment of pipeline, 2006, Xian, People's Republic of China, 2006.

Tkaczyk, T., O'Dowd, N.P., and Howard, B.P., 2007. Comparison of Crack Driving Force Estimation Schemes for Weld Defects in Reeled Pipelines. Proceedings of the Sixteenth (2007) International Offshore and Polar Engineering Conference Lisbon, Portugal, July 1-6, 2007.

Toguyeni, Gregory A., and Banse, Joachim., 2012. Mechanically Lined Pipe: Installation by Reel-lay. Offshore Technology Conference held in Houston, Texas, USA, 30 April-3 May 2012.

TWI Software. 2009. CRACKWISE 4 help content version 4.1.6795.0 Final.

Appendix A

CRACKWISE ECA Simulation Results Summary

CRACKWISE ECA Simulation Results Summary

(Used in Figure 7.2, 7.3, 7.4 and 7.22 – Base Case)

Project Information

Current input file	C:\Users\SS7N1346\Documents\Master Thesis\21 Crackwise Simulation Files\Projek_Data_Modify_BaseCaseThesis.cw4
Calculation type	Fracture
Assessment level	Level 3

Geometry

Geometry type	Cylinder, external, circumferential flaw
Flaw type	Surface

Stress intensity solution

Surface flaw in plate M.3.2

Reference stress solution

Surface flaw in cylinder oriented circumferentially P.4.3.2

Wall thickness, B	13,65	mm
Width/length, W	815	mm
Radius, rm	129	mm

Flaw Dimensions

Flaw height, a	2	mm
Flaw length, 2c	100	mm
Parametric angle	Max	

Primary Stresses

Membrane stress, Pm	791,4	MPa	**Stress concentration factor, ktm**	1
Bending stress, Pb	27,2	MPa	**Stress concentration factor, ktb**	1

Secondary Stresses

Type As Welded - Relaxation is Enabled

Thermal membrane stress, Qtm	0	MPa
Thermal bending stress, Qtb	0	MPa
Appropriate σy (Room temp)	691	MPa

Tensile Properties

Yield strength (Assess. temp) σy	691	MPa	**Young's modulus**	2,05E+05	MPa
Yield strength (Room temp) σy	691	MPa	**Poisson's ratio**	0,3	
Tensile strength (Assess. temp) σu	899	MPa	**FAD cut off point**	1,431	

FAD type	Ramberg-Osgood Stress-Strain		
Unit type	Engineering stress strain		
Hardening	14,276	**Resolution**	100
Constant	0,593		
Reference strain	0,0033707		

Toughness (J)

RCurve	BS7448 offset power law	**Tearing direction**	Length and height	
m	0	**Minimum tearing**	0,05	mm
l	1410	**Maximum**	0,3	mm
x	0,68	**Increments**	200	

Criticality/Sensitivity solver settings

Critical Parameter	Flaw height
Iterations	500
Base value	2
Initial step size	0,05
Minimum step size	0,025
Sensitivity Parameter	Flaw length
Minimum	25
Maximum	200
Points	100

Sensitivity results

Flaw length	Flaw height	Results	Errors
25	4,6	Unacceptable	Note, Qm < 0.4 *
26,768	4,4	Unacceptable	Note, Qm < 0.4 *
28,535	4,2	Unacceptable	Note, Qm < 0.4 *
30,303	4	Unacceptable	Note, Qm < 0.4 *
32,071	3,9	Unacceptable	Note, Qm < 0.4 *
33,838	3,8	Unacceptable	Note, Qm < 0.4 *
35,606	3,7	Unacceptable	Note, Qm < 0.4 *
37,374	3,6	Unacceptable	Note, Qm < 0.4 *
39,141	3,5	Unacceptable	Note, Qm < 0.4 *
40,909	3,45	Unacceptable	Note, Qm < 0.4 *
42,677	3,4	Unacceptable	Note, Qm < 0.4 *
44,444	3,35	Unacceptable	Note, Qm < 0.4 *
46,212	3,3	Unacceptable	Note, Qm < 0.4 *
47,98	3,25	Unacceptable	Note, Qm < 0.4 *
49,747	3,2	Unacceptable	Note, Qm < 0.4 *
51,515	3,15	Unacceptable	Note, Qm < 0.4 *
53,283	3,1	Unacceptable	Note, Qm < 0.4 *
55,051	3,05	Unacceptable	Note, Qm < 0.4 *

56,818	3,05	Unacceptable	Note, Qm < 0.4 *
58,586	3	Unacceptable	Note, Qm < 0.4 *
60,354	2,95	Unacceptable	Note, Qm < 0.4 *
62,121	2,95	Unacceptable	Note, Qm < 0.4 *
63,889	2,9	Unacceptable	Note, Qm < 0.4 *
65,657	2,9	Unacceptable	Note, Qm < 0.4 *
67,424	2,85	Unacceptable	Note, Qm < 0.4 *
69,192	2,85	Unacceptable	Note, Qm < 0.4 *
70,96	2,8	Unacceptable	Note, Qm < 0.4 *
72,727	2,8	Unacceptable	Note, Qm < 0.4 *
74,495	2,75	Unacceptable	Note, Qm < 0.4 *
76,263	2,75	Unacceptable	Note, Qm < 0.4 *
78,03	2,7	Unacceptable	Note, Qm < 0.4 *
79,798	2,7	Unacceptable	Note, Qm < 0.4 *
81,566	2,65	Unacceptable	Note, Qm < 0.4 *
83,333	2,65	Unacceptable	Note, Qm < 0.4 *
85,101	2,65	Unacceptable	Note, Qm < 0.4 *
86,869	2,6	Unacceptable	Note, Qm < 0.4 *
88,636	2,6	Unacceptable	Note, Qm < 0.4 *
90,404	2,6	Unacceptable	Note, Qm < 0.4 *
92,172	2,55	Unacceptable	Note, Qm < 0.4 *
93,939	2,55	Unacceptable	Note, Qm < 0.4 *
95,707	2,55	Unacceptable	Note, Qm < 0.4 *
97,475	2,5	Unacceptable	Note, Qm < 0.4 *
99,242	2,5	Unacceptable	Note, Qm < 0.4 *
101,01	2,5	Unacceptable	Note, Qm < 0.4 *
102,78	2,5	Unacceptable	Note, Qm < 0.4 *
104,55	2,45	Unacceptable	Note, Qm < 0.4 *
106,31	2,45	Unacceptable	Note, Qm < 0.4 *
108,08	2,45	Unacceptable	Note, Qm < 0.4 *
109,85	2,45	Unacceptable	Note, Qm < 0.4 *
111,62	2,4	Unacceptable	Note, Qm < 0.4 *
113,38	2,4	Unacceptable	Note, Qm < 0.4 *
115,15	2,4	Unacceptable	Note, Qm < 0.4 *
116,92	2,4	Unacceptable	Note, Qm < 0.4 *
118,69	2,35	Unacceptable	Note, Qm < 0.4 *
120,45	2,35	Unacceptable	Note, Qm < 0.4 *
122,22	2,35	Unacceptable	Note, Qm < 0.4 *
123,99	2,35	Unacceptable	Note, Qm < 0.4 *
125,76	2,3	Unacceptable	Note, Qm < 0.4 *
127,53	2,3	Unacceptable	Note, Qm < 0.4 *

129,29	2,3	Unacceptable	Note, Qm < 0.4 *
131,06	2,3	Unacceptable	Note, Qm < 0.4 *
132,83	2,3	Unacceptable	Note, Qm < 0.4 *
134,6	2,25	Unacceptable	Note, Qm < 0.4 *
136,36	2,25	Unacceptable	Note, Qm < 0.4 *
138,13	2,25	Unacceptable	Note, Qm < 0.4 *
139,9	2,25	Unacceptable	Note, Qm < 0.4 *
141,67	2,25	Unacceptable	Note, Qm < 0.4 *
143,43	2,2	Unacceptable	Note, Qm < 0.4 *
145,2	2,2	Unacceptable	Note, Qm < 0.4 *
146,97	2,2	Unacceptable	Note, Qm < 0.4 *
148,74	2,2	Unacceptable	Note, Qm < 0.4 *
150,51	2,2	Unacceptable	Note, Qm < 0.4 *
152,27	2,2	Unacceptable	Note, Qm < 0.4 *
154,04	2,15	Unacceptable	Note, Qm < 0.4 *
155,81	2,15	Unacceptable	Note, Qm < 0.4 *
157,58	2,15	Unacceptable	Note, Qm < 0.4 *
159,34	2,15	Unacceptable	Note, Qm < 0.4 *
161,11	2,15	Unacceptable	Note, Qm < 0.4 *
162,88	2,15	Unacceptable	Note, Qm < 0.4 *
164,65	2,15	Unacceptable	Note, Qm < 0.4 *
166,41	2,1	Unacceptable	Note, Qm < 0.4 *
168,18	2,1	Unacceptable	Note, Qm < 0.4 *
169,95	2,1	Unacceptable	Note, Qm < 0.4 *
171,72	2,1	Unacceptable	Note, Qm < 0.4 *
173,48	2,1	Unacceptable	Note, Qm < 0.4 *
175,25	2,1	Unacceptable	Note, Qm < 0.4 *
177,02	2,1	Unacceptable	Note, Qm < 0.4 *
178,79	2,05	Unacceptable	Note, Qm < 0.4 *
180,56	2,05	Unacceptable	Note, Qm < 0.4 *
182,32	2,05	Unacceptable	Note, Qm < 0.4 *
184,09	2,05	Unacceptable	Note, Qm < 0.4 *
185,86	2,05	Unacceptable	Note, Qm < 0.4 *
187,63	2,05	Unacceptable	Note, Qm < 0.4 *
189,39	2,05	Unacceptable	Note, Qm < 0.4 *
191,16	2,05	Unacceptable	Note, Qm < 0.4 *
192,93	2	Unacceptable	Note, Qm < 0.4 *
194,7	2	Unacceptable	Note, Qm < 0.4 *
196,46	2	Unacceptable	Note, Qm < 0.4 *
198,23	2	Unacceptable	Note, Qm < 0.4 *
200	2	Unacceptable	Note, Qm < 0.4 *

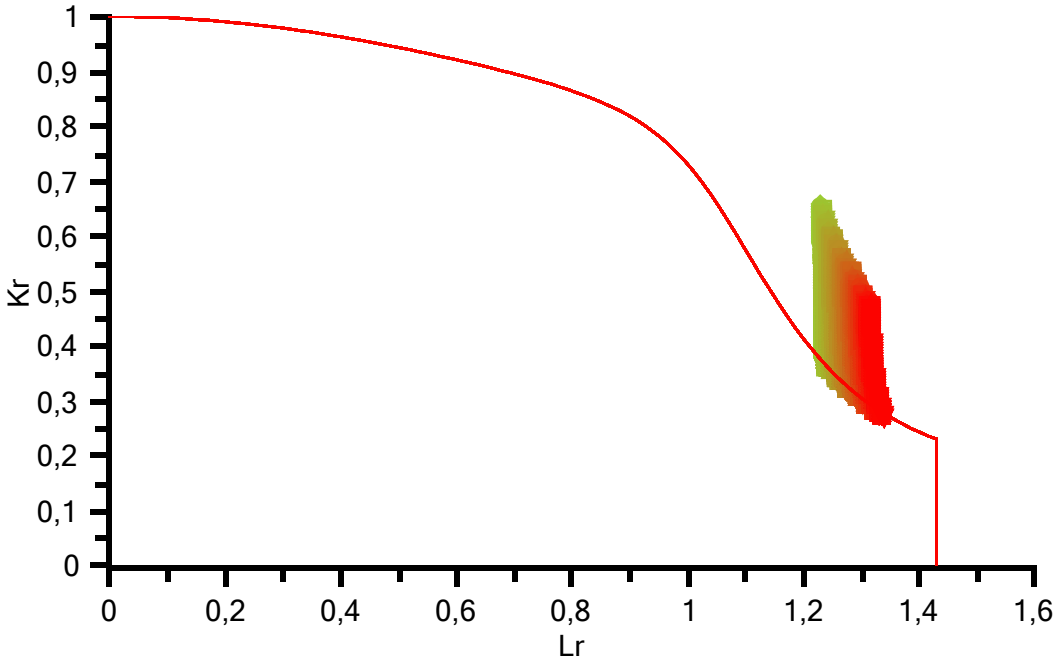

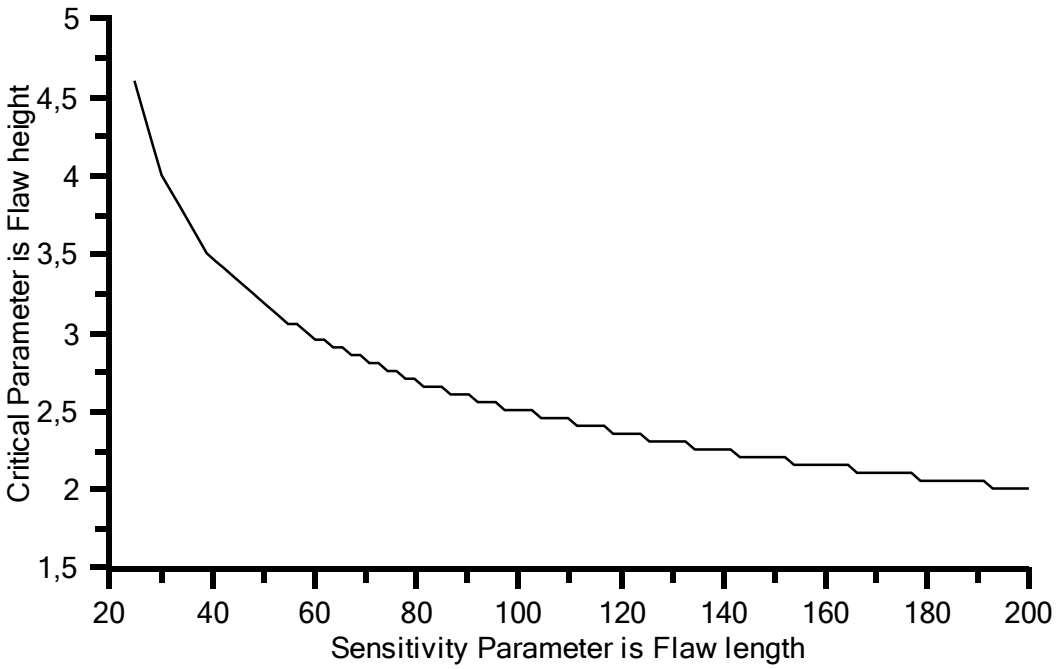

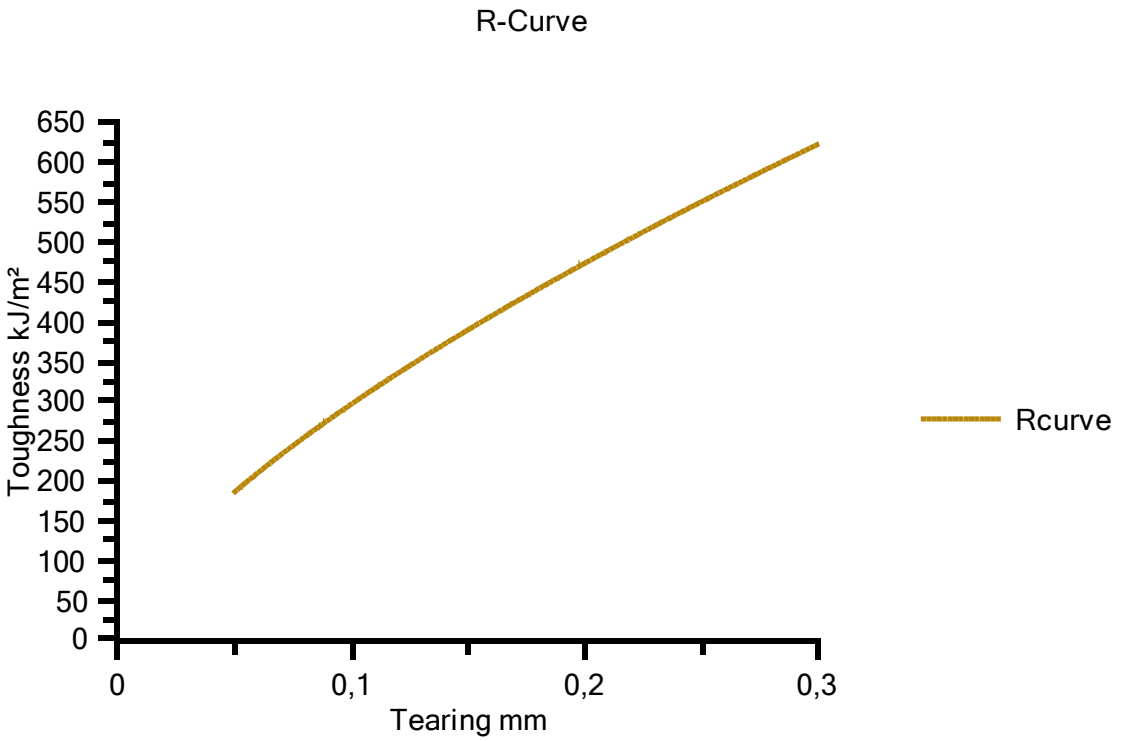

CRACKWISE ECA Simulation Results Summary

(Used in Figure 7.3 – No Residual Stress)

Project Information

Current input file	C:\Users\SS7N1346\Documents\Master Thesis\21 Crackwise Simulation Files\Projek_Data_Modify_BaseCaseThesis.cw4
Calculation type	Fracture
Assessment level	Level 3

Geometry

Geometry type	Cylinder, external, circumferential flaw
Flaw type	Surface

Stress intensity solution

Surface flaw in plate M.3.2

Reference stress solution

Surface flaw in cylinder oriented circumferentially P.4.3.2

Wall thickness, B	13,65	mm
Width/length, W	815	mm
Radius, rm	129	mm

Flaw Dimensions

Flaw height, a	2	mm
Flaw length, 2c	100	mm
Parametric angle	Max	

Primary Stresses

Membrane stress, Pm	791,4	MPa	**Stress concentration factor, ktm**	1	
Bending stress, Pb	27,2	MPa	**Stress concentration factor, ktb**	1	

Secondary Stresses

Type Known Residual Stresses

Thermal membrane stress, Qtm	0	MPa	**Known membrane stress, Qm**	0	MPa
Thermal bending stress, Qtb	0	MPa	**Known bending stress, Qb**	0	MPa

Tensile Properties

Yield strength (Assess. temp) σy	691	MPa	**Young's modulus**	2,05E+05	MPa
Yield strength (Room temp) σy	691	MPa	**Poisson's ratio**	0,3	
Tensile strength (Assess. temp) σu	899	MPa	**FAD cut off point**	1,431	

FAD type	Ramberg-Osgood Stress-Strain		
Unit type	Engineering stress strain		
Hardening	14,276	**Resolution**	100
Constant	0,593		
Reference strain	0,0033707		

Toughness (J)

RCurve	BS7448 offset power law	**Tearing direction**	Length and height	
m	0	**Minimum tearing**	0,05	mm
l	1410	**Maximum**	0,3	mm
x	0,68	**Increments**	200	

Criticality/Sensitivity solver settings

Critical Parameter	Flaw height
Iterations	500
Base value	2
Initial step size	0,05
Minimum step size	0,025
Sensitivity Parameter	Flaw length
Minimum	25
Maximum	200
Points	100

Sensitivity results

Flaw length	Flaw height	Results	Errors
25	6,75	Unacceptable	
26,768	6,25	Unacceptable	
28,535	5,9	Unacceptable	
30,303	5,6	Unacceptable	
32,071	5,4	Unacceptable	
33,838	5,2	Unacceptable	
35,606	5	Unacceptable	
37,374	4,85	Unacceptable	
39,141	4,7	Unacceptable	
40,909	4,6	Unacceptable	
42,677	4,5	Unacceptable	
44,444	4,4	Unacceptable	
46,212	4,3	Unacceptable	
47,98	4,25	Unacceptable	
49,747	4,15	Unacceptable	
51,515	4,1	Unacceptable	
53,283	4,05	Unacceptable	
55,051	3,95	Unacceptable	

56,818	3,9	Unacceptable
58,586	3,85	Unacceptable
60,354	3,8	Unacceptable
62,121	3,75	Unacceptable
63,889	3,7	Unacceptable
65,657	3,65	Unacceptable
67,424	3,65	Unacceptable
69,192	3,6	Unacceptable
70,96	3,55	Unacceptable
72,727	3,5	Unacceptable
74,495	3,5	Unacceptable
76,263	3,45	Unacceptable
78,03	3,4	Unacceptable
79,798	3,4	Unacceptable
81,566	3,35	Unacceptable
83,333	3,35	Unacceptable
85,101	3,3	Unacceptable
86,869	3,25	Unacceptable
88,636	3,25	Unacceptable
90,404	3,2	Unacceptable
92,172	3,2	Unacceptable
93,939	3,2	Unacceptable
95,707	3,15	Unacceptable
97,475	3,15	Unacceptable
99,242	3,1	Unacceptable
101,01	3,1	Unacceptable
102,78	3,05	Unacceptable
104,55	3,05	Unacceptable
106,31	3	Unacceptable
108,08	3	Unacceptable
109,85	3	Unacceptable
111,62	2,95	Unacceptable
113,38	2,95	Unacceptable
115,15	2,95	Unacceptable
116,92	2,9	Unacceptable
118,69	2,9	Unacceptable
120,45	2,9	Unacceptable
122,22	2,85	Unacceptable
123,99	2,85	Unacceptable
125,76	2,85	Unacceptable
127,53	2,8	Unacceptable

129,29	2,8	Unacceptable
131,06	2,8	Unacceptable
132,83	2,8	Unacceptable
134,6	2,75	Unacceptable
136,36	2,75	Unacceptable
138,13	2,75	Unacceptable
139,9	2,7	Unacceptable
141,67	2,7	Unacceptable
143,43	2,7	Unacceptable
145,2	2,7	Unacceptable
146,97	2,65	Unacceptable
148,74	2,65	Unacceptable
150,51	2,65	Unacceptable
152,27	2,65	Unacceptable
154,04	2,6	Unacceptable
155,81	2,6	Unacceptable
157,58	2,6	Unacceptable
159,34	2,6	Unacceptable
161,11	2,6	Unacceptable
162,88	2,55	Unacceptable
164,65	2,55	Unacceptable
166,41	2,55	Unacceptable
168,18	2,55	Unacceptable
169,95	2,55	Unacceptable
171,72	2,5	Unacceptable
173,48	2,5	Unacceptable
175,25	2,5	Unacceptable
177,02	2,5	Unacceptable
178,79	2,5	Unacceptable
180,56	2,45	Unacceptable
182,32	2,45	Unacceptable
184,09	2,45	Unacceptable
185,86	2,45	Unacceptable
187,63	2,45	Unacceptable
189,39	2,45	Unacceptable
191,16	2,4	Unacceptable
192,93	2,4	Unacceptable
194,7	2,4	Unacceptable
196,46	2,4	Unacceptable
198,23	2,4	Unacceptable
200	2,4	Unacceptable

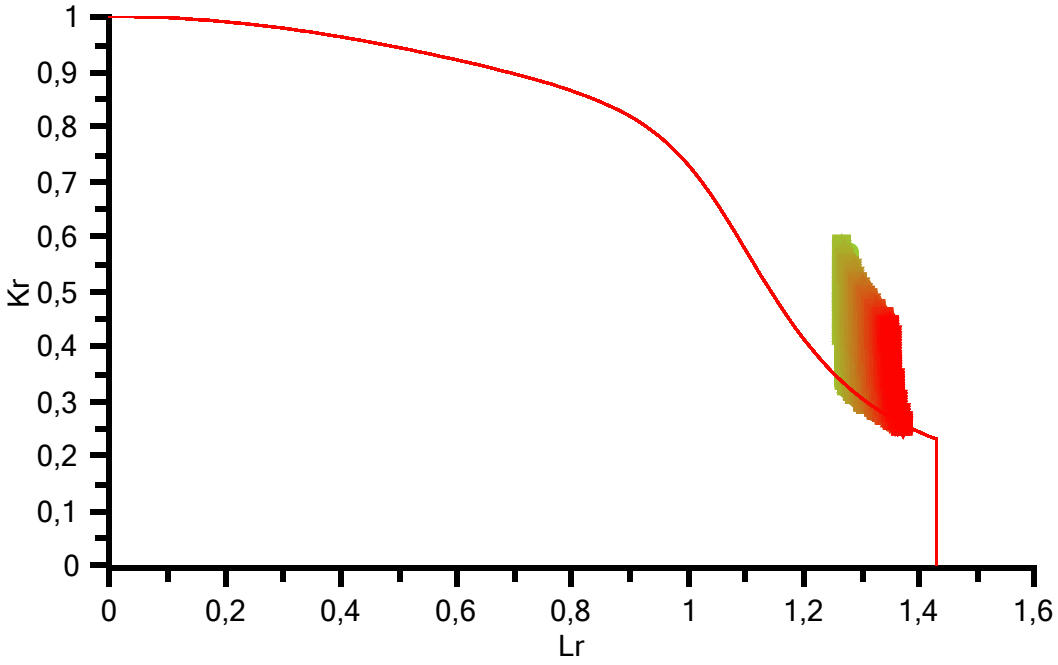

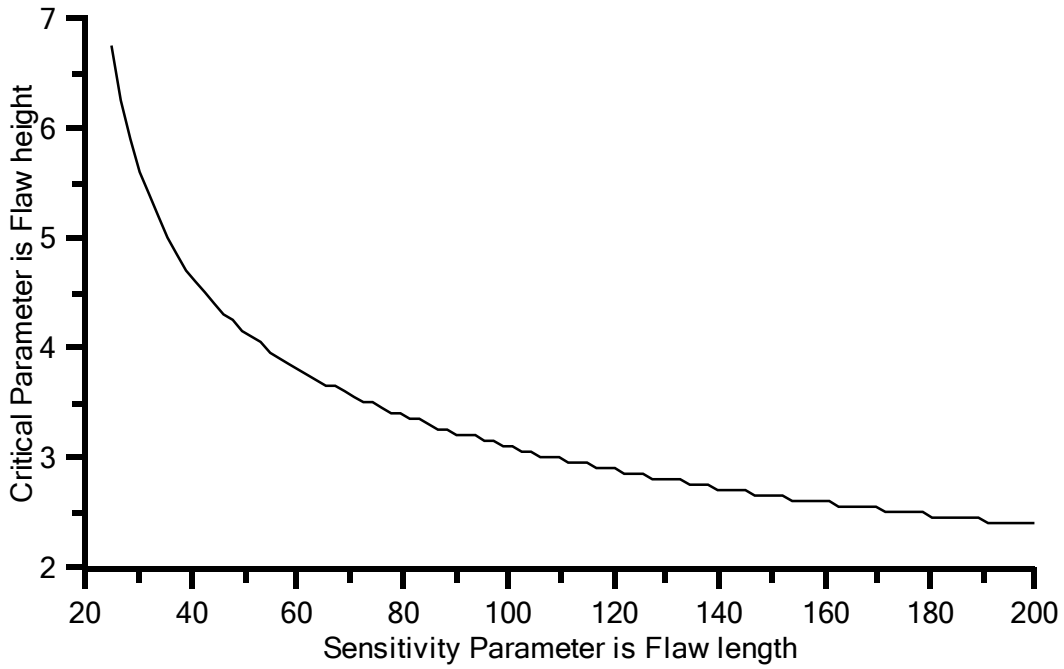

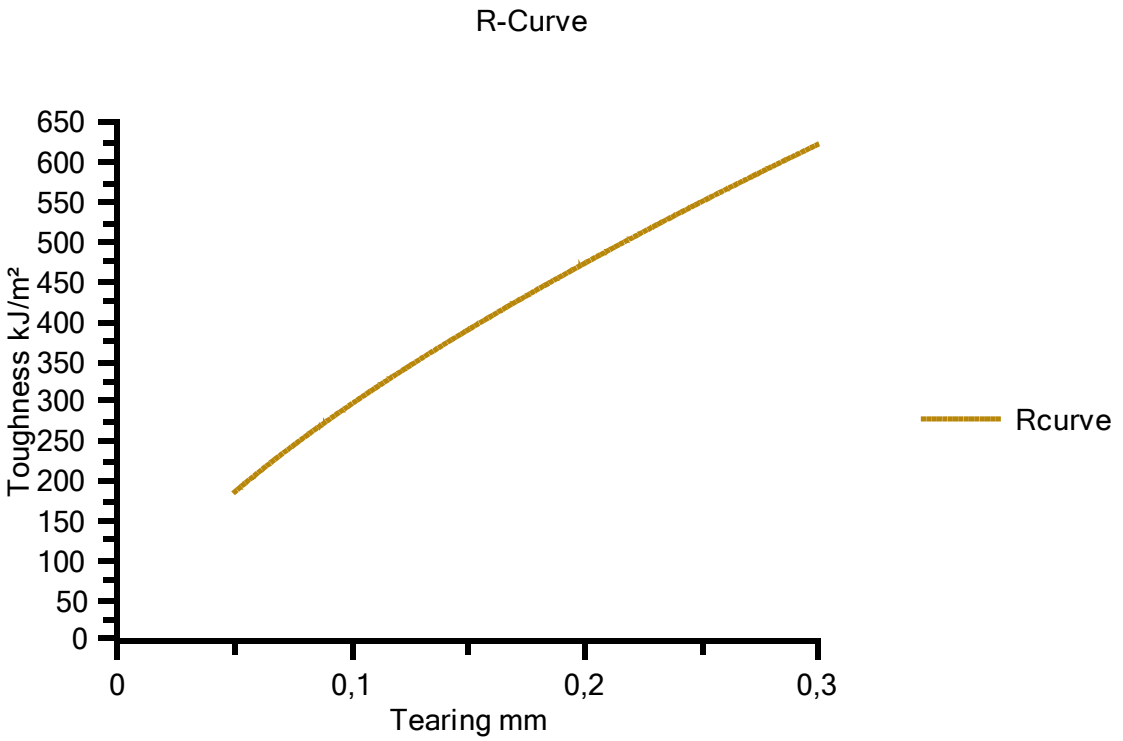

This software is licensed to Acergy Group

CRACKWISE ECA Simulation Results Summary

(Used in Figure 7.3 – Residual Stress Equal Yield)

Project Information

Current input file	C:\Users\SS7N1346\Documents\Master Thesis\21 Crackwise Simulation Files\Projek_Data_Modify_BaseCaseThesis.cw4
Calculation type	Fracture
Assessment level	Level 3

Geometry

Geometry type	Cylinder, external, circumferential flaw
Flaw type	Surface

Stress intensity solution

Surface flaw in plate M.3.2

Reference stress solution

Surface flaw in cylinder oriented circumferentially P.4.3.2

Wall thickness, B	13,65	mm
Width/length, W	815	mm
Radius, rm	129	mm

Flaw Dimensions

Flaw height, a	2	mm
Flaw length, 2c	100	mm
Parametric angle	Max	

Primary Stresses

Membrane stress, Pm	791,4	MPa	**Stress concentration factor, ktm**	1
Bending stress, Pb	27,2	MPa	**Stress concentration factor, ktb**	1

Secondary Stresses

Type As Welded

Thermal membrane stress, Qtm	0	MPa
Thermal bending stress, Qtb	0	MPa
Appropriate σy (Room temp)	691	MPa

Tensile Properties

Yield strength (Assess. temp) σy	691	MPa	**Young's modulus**	2,05E+05	MPa
Yield strength (Room temp) σy	691	MPa	**Poisson's ratio**	0,3	
Tensile strength (Assess. temp) σu	899	MPa	**FAD cut off point**	1,431	

This software is licensed to Acergy Group

FAD type	Ramberg-Osgood Stress-Strain		
Unit type	Engineering stress strain		
Hardening	14,276	**Resolution**	100
Constant	0,593		
Reference strain	0,0033707		

Toughness (J)

RCurve	BS7448 offset power law	**Tearing direction**	Length and height	
m	0	**Minimum tearing**	0,05	mm
l	1410	**Maximum**	0,3	mm
x	0,68	**Increments**	200	

Criticality/Sensitivity solver settings

Critical Parameter	Flaw height
Iterations	500
Base value	2
Initial step size	0,05
Minimum step size	0,025
Sensitivity Parameter	Flaw length
Minimum	25
Maximum	200
Points	100

Sensitivity results

Flaw length	Flaw height	Results	Errors
25	2,35	Unacceptable	
26,768	2,3	Unacceptable	
28,535	2,25	Unacceptable	
30,303	2,2	Unacceptable	
32,071	2,15	Unacceptable	
33,838	2,1	Unacceptable	
35,606	2,05	Unacceptable	
37,374	2,05	Unacceptable	
39,141	2	Unacceptable	
40,909	2	Unacceptable	
42,677	1,95	Unacceptable	First point is unsafe
44,444	1,95	Unacceptable	First point is unsafe
46,212	1,95	Unacceptable	First point is unsafe
47,98	1,95	Unacceptable	First point is unsafe
49,747	1,95	Unacceptable	First point is unsafe
51,515	1,95	Unacceptable	First point is unsafe
53,283	1,95	Unacceptable	First point is unsafe
55,051	1,95	Unacceptable	First point is unsafe

56,818	1,95	Unacceptable	First point is unsafe
58,586	1,95	Unacceptable	First point is unsafe
60,354	1,95	Unacceptable	First point is unsafe
62,121	1,95	Unacceptable	First point is unsafe
63,889	1,95	Unacceptable	First point is unsafe
65,657	1,95	Unacceptable	First point is unsafe
67,424	1,95	Unacceptable	First point is unsafe
69,192	1,95	Unacceptable	First point is unsafe
70,96	1,95	Unacceptable	First point is unsafe
72,727	1,95	Unacceptable	First point is unsafe
74,495	1,95	Unacceptable	First point is unsafe
76,263	1,95	Unacceptable	First point is unsafe
78,03	1,95	Unacceptable	First point is unsafe
79,798	1,95	Unacceptable	First point is unsafe
81,566	1,95	Unacceptable	First point is unsafe
83,333	1,95	Unacceptable	First point is unsafe
85,101	1,95	Unacceptable	First point is unsafe
86,869	1,95	Unacceptable	First point is unsafe
88,636	1,95	Unacceptable	First point is unsafe
90,404	1,95	Unacceptable	First point is unsafe
92,172	1,95	Unacceptable	First point is unsafe
93,939	1,95	Unacceptable	First point is unsafe
95,707	1,95	Unacceptable	First point is unsafe
97,475	1,95	Unacceptable	First point is unsafe
99,242	1,95	Unacceptable	First point is unsafe
101,01	1,95	Unacceptable	First point is unsafe
102,78	1,95	Unacceptable	First point is unsafe
104,55	1,95	Unacceptable	First point is unsafe
106,31	1,95	Unacceptable	First point is unsafe
108,08	1,95	Unacceptable	First point is unsafe
109,85	1,95	Unacceptable	First point is unsafe
111,62	1,95	Unacceptable	First point is unsafe
113,38	1,95	Unacceptable	First point is unsafe
115,15	1,95	Unacceptable	First point is unsafe
116,92	1,95	Unacceptable	First point is unsafe
118,69	1,95	Unacceptable	First point is unsafe
120,45	1,95	Unacceptable	First point is unsafe
122,22	1,95	Unacceptable	First point is unsafe
123,99	1,95	Unacceptable	First point is unsafe
125,76	1,95	Unacceptable	First point is unsafe
127,53	1,95	Unacceptable	First point is unsafe

129,29	1,95	Unacceptable	First point is unsafe
131,06	1,95	Unacceptable	First point is unsafe
132,83	1,95	Unacceptable	First point is unsafe
134,6	1,95	Unacceptable	First point is unsafe
136,36	1,95	Unacceptable	First point is unsafe
138,13	1,95	Unacceptable	First point is unsafe
139,9	1,95	Unacceptable	First point is unsafe
141,67	1,95	Unacceptable	First point is unsafe
143,43	1,95	Unacceptable	First point is unsafe
145,2	1,95	Unacceptable	First point is unsafe
146,97	1,95	Unacceptable	First point is unsafe
148,74	1,95	Unacceptable	First point is unsafe
150,51	1,95	Unacceptable	First point is unsafe
152,27	1,95	Unacceptable	First point is unsafe
154,04	1,95	Unacceptable	First point is unsafe
155,81	1,95	Unacceptable	First point is unsafe
157,58	1,95	Unacceptable	First point is unsafe
159,34	1,95	Unacceptable	First point is unsafe
161,11	1,95	Unacceptable	First point is unsafe
162,88	1,95	Unacceptable	First point is unsafe
164,65	1,95	Unacceptable	First point is unsafe
166,41	1,95	Unacceptable	First point is unsafe
168,18	1,95	Unacceptable	First point is unsafe
169,95	1,95	Unacceptable	First point is unsafe
171,72	1,95	Unacceptable	First point is unsafe
173,48	1,95	Unacceptable	First point is unsafe
175,25	1,95	Unacceptable	First point is unsafe
177,02	1,95	Unacceptable	First point is unsafe
178,79	1,95	Unacceptable	First point is unsafe
180,56	1,95	Unacceptable	First point is unsafe
182,32	1,95	Unacceptable	First point is unsafe
184,09	1,95	Unacceptable	First point is unsafe
185,86	1,95	Unacceptable	First point is unsafe
187,63	1,95	Unacceptable	First point is unsafe
189,39	1,95	Unacceptable	First point is unsafe
191,16	1,95	Unacceptable	First point is unsafe
192,93	1,95	Unacceptable	First point is unsafe
194,7	1,95	Unacceptable	First point is unsafe
196,46	1,95	Unacceptable	First point is unsafe
198,23	1,95	Unacceptable	First point is unsafe
200	1,95	Unacceptable	First point is unsafe

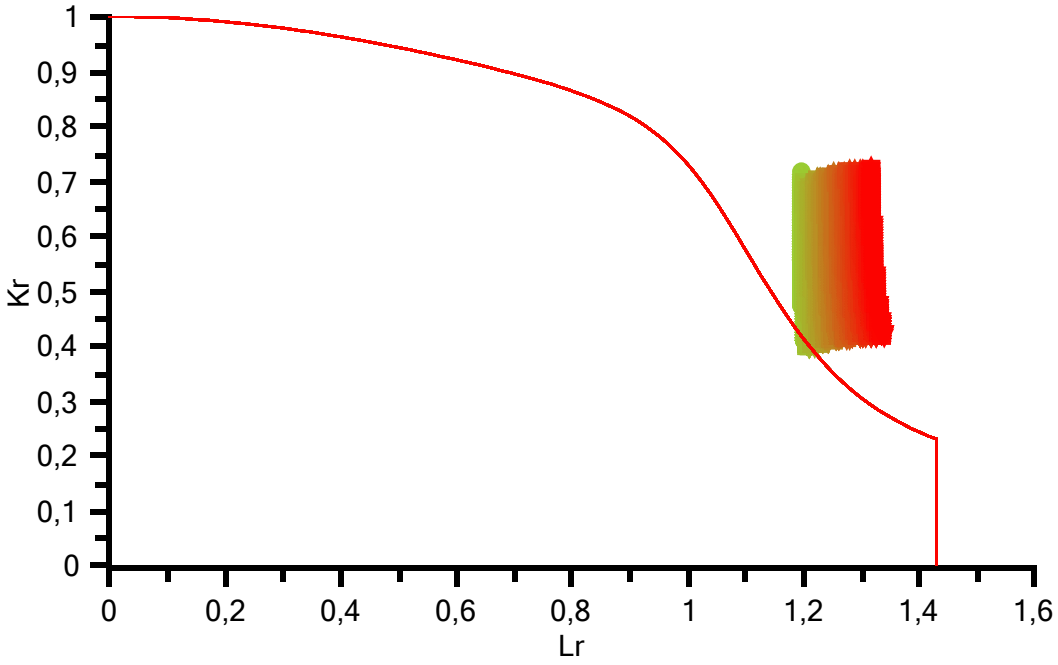

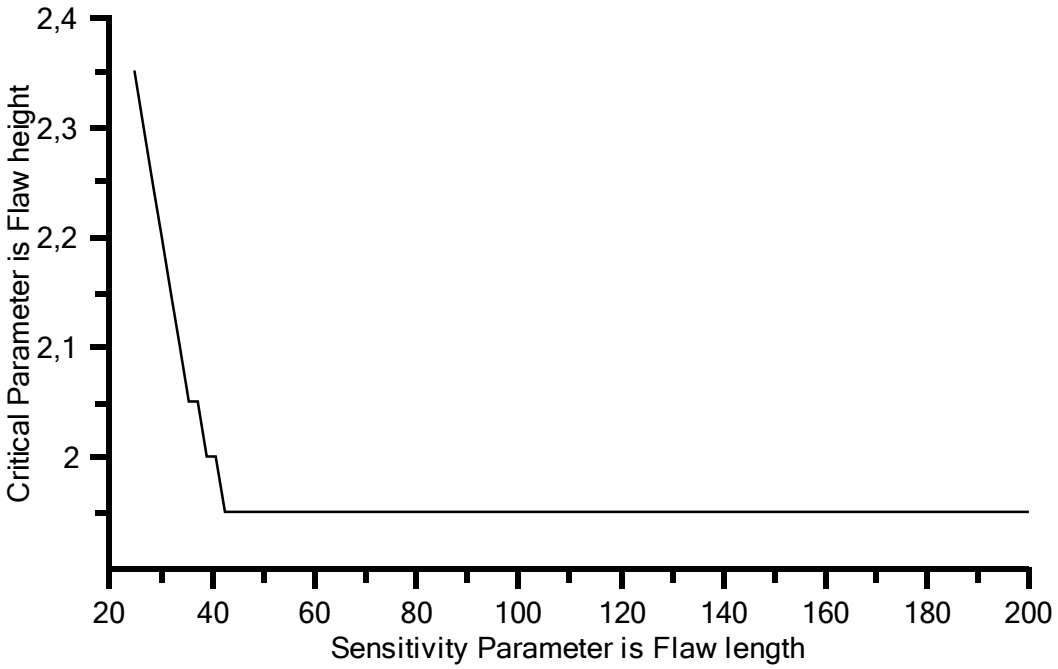

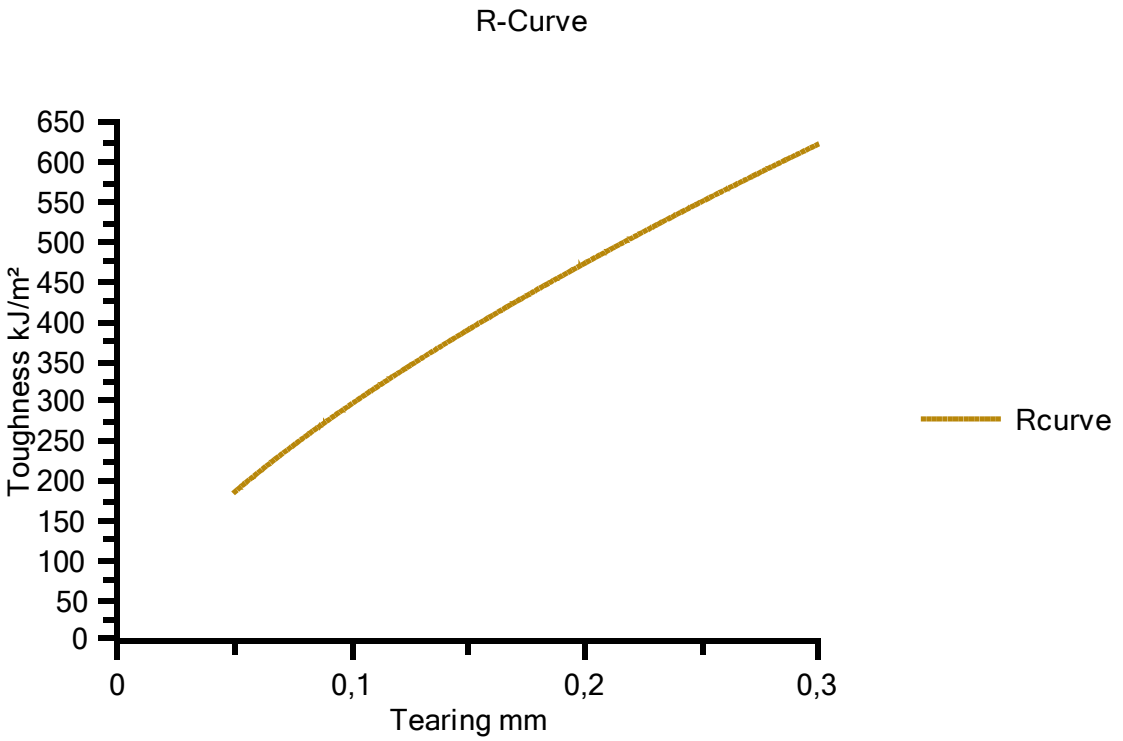

CRACKWISE ECA Simulation Results Summary

(Used in Figure 7.4 and 7.21 – Residual Stress Equal Yield Strength with Relaxation and No Misalignment)

Project Information

Current input file	C:\Users\SS7N1346\Documents\Master Thesis\21 Crackwise Simulation Files\Projek_Data_Modify_BaseCaseThesis.cw4
Calculation type	Fracture
Assessment level	Level 3

Geometry

Geometry type	Cylinder, external, circumferential flaw
Flaw type	Surface

Stress intensity solution

Surface flaw in plate M.3.2

Reference stress solution

Surface flaw in cylinder oriented circumferentially P.4.3.2

Wall thickness, B	13,65	mm
Width/length, W	815	mm
Radius, rm	129	mm

Flaw Dimensions

Flaw height, a	2	mm
Flaw length, 2c	100	mm
Parametric angle	Max	

Primary Stresses

Membrane stress, Pm	791,4	MPa	**Stress concentration factor, ktm**	1
Bending stress, Pb	0	MPa	**Stress concentration factor, ktb**	1

Secondary Stresses

Type As Welded - Relaxation is Enabled

Thermal membrane stress, Qtm	0	MPa
Thermal bending stress, Qtb	0	MPa
Appropriate σy (Room temp)	691	MPa

Tensile Properties

Yield strength (Assess. temp) σy	691	MPa	**Young's modulus**	2,05E+05	MPa
Yield strength (Room temp) σy	691	MPa	**Poisson's ratio**	0,3	
Tensile strength (Assess. temp) σu	899	MPa	**FAD cut off point**	1,431	

FAD type	Ramberg-Osgood Stress-Strain		
Unit type	Engineering stress strain		
Hardening	14,276	**Resolution**	100
Constant	0,593		
Reference strain	0,0033707		

Toughness (J)

RCurve	BS7448 offset power law	**Tearing direction**	Length and height	
m	0	**Minimum tearing**	0,05	mm
l	1410	**Maximum**	0,3	mm
x	0,68	**Increments**	200	

Criticality/Sensitivity solver settings

Critical Parameter	Flaw height
Iterations	500
Base value	2
Initial step size	0,05
Minimum step size	0,025
Sensitivity Parameter	Flaw length
Minimum	25
Maximum	200
Points	100

Sensitivity results

Flaw length	Flaw height	Results	Errors
25	5,7	Unacceptable	Note, Qm < 0.4 *
26,768	5,35	Unacceptable	Note, Qm < 0.4 *
28,535	5,05	Unacceptable	Note, Qm < 0.4 *
30,303	4,85	Unacceptable	Note, Qm < 0.4 *
32,071	4,65	Unacceptable	Note, Qm < 0.4 *
33,838	4,5	Unacceptable	Note, Qm < 0.4 *
35,606	4,35	Unacceptable	Note, Qm < 0.4 *
37,374	4,25	Unacceptable	Note, Qm < 0.4 *
39,141	4,15	Unacceptable	Note, Qm < 0.4 *
40,909	4,05	Unacceptable	Note, Qm < 0.4 *
42,677	3,95	Unacceptable	Note, Qm < 0.4 *
44,444	3,9	Unacceptable	Note, Qm < 0.4 *
46,212	3,8	Unacceptable	Note, Qm < 0.4 *
47,98	3,75	Unacceptable	Note, Qm < 0.4 *
49,747	3,7	Unacceptable	Note, Qm < 0.4 *
51,515	3,65	Unacceptable	Note, Qm < 0.4 *
53,283	3,6	Unacceptable	Note, Qm < 0.4 *
55,051	3,55	Unacceptable	Note, Qm < 0.4 *

56,818	3,5	Unacceptable	Note, Qm < 0.4 *
58,586	3,45	Unacceptable	Note, Qm < 0.4 *
60,354	3,4	Unacceptable	Note, Qm < 0.4 *
62,121	3,35	Unacceptable	Note, Qm < 0.4 *
63,889	3,35	Unacceptable	Note, Qm < 0.4 *
65,657	3,3	Unacceptable	Note, Qm < 0.4 *
67,424	3,25	Unacceptable	Note, Qm < 0.4 *
69,192	3,25	Unacceptable	Note, Qm < 0.4 *
70,96	3,2	Unacceptable	Note, Qm < 0.4 *
72,727	3,15	Unacceptable	Note, Qm < 0.4 *
74,495	3,15	Unacceptable	Note, Qm < 0.4 *
76,263	3,1	Unacceptable	Note, Qm < 0.4 *
78,03	3,1	Unacceptable	Note, Qm < 0.4 *
79,798	3,05	Unacceptable	Note, Qm < 0.4 *
81,566	3,05	Unacceptable	Note, Qm < 0.4 *
83,333	3	Unacceptable	Note, Qm < 0.4 *
85,101	3	Unacceptable	Note, Qm < 0.4 *
86,869	2,95	Unacceptable	Note, Qm < 0.4 *
88,636	2,95	Unacceptable	Note, Qm < 0.4 *
90,404	2,9	Unacceptable	Note, Qm < 0.4 *
92,172	2,9	Unacceptable	Note, Qm < 0.4 *
93,939	2,9	Unacceptable	Note, Qm < 0.4 *
95,707	2,85	Unacceptable	Note, Qm < 0.4 *
97,475	2,85	Unacceptable	Note, Qm < 0.4 *
99,242	2,85	Unacceptable	Note, Qm < 0.4 *
101,01	2,8	Unacceptable	Note, Qm < 0.4 *
102,78	2,8	Unacceptable	Note, Qm < 0.4 *
104,55	2,75	Unacceptable	Note, Qm < 0.4 *
106,31	2,75	Unacceptable	Note, Qm < 0.4 *
108,08	2,75	Unacceptable	Note, Qm < 0.4 *
109,85	2,7	Unacceptable	Note, Qm < 0.4 *
111,62	2,7	Unacceptable	Note, Qm < 0.4 *
113,38	2,7	Unacceptable	Note, Qm < 0.4 *
115,15	2,7	Unacceptable	Note, Qm < 0.4 *
116,92	2,65	Unacceptable	Note, Qm < 0.4 *
118,69	2,65	Unacceptable	Note, Qm < 0.4 *
120,45	2,65	Unacceptable	Note, Qm < 0.4 *
122,22	2,6	Unacceptable	Note, Qm < 0.4 *
123,99	2,6	Unacceptable	Note, Qm < 0.4 *
125,76	2,6	Unacceptable	Note, Qm < 0.4 *
127,53	2,6	Unacceptable	Note, Qm < 0.4 *

129,29	2,55	Unacceptable	Note, Qm < 0.4 *
131,06	2,55	Unacceptable	Note, Qm < 0.4 *
132,83	2,55	Unacceptable	Note, Qm < 0.4 *
134,6	2,55	Unacceptable	Note, Qm < 0.4 *
136,36	2,5	Unacceptable	Note, Qm < 0.4 *
138,13	2,5	Unacceptable	Note, Qm < 0.4 *
139,9	2,5	Unacceptable	Note, Qm < 0.4 *
141,67	2,5	Unacceptable	Note, Qm < 0.4 *
143,43	2,5	Unacceptable	Note, Qm < 0.4 *
145,2	2,45	Unacceptable	Note, Qm < 0.4 *
146,97	2,45	Unacceptable	Note, Qm < 0.4 *
148,74	2,45	Unacceptable	Note, Qm < 0.4 *
150,51	2,45	Unacceptable	Note, Qm < 0.4 *
152,27	2,4	Unacceptable	Note, Qm < 0.4 *
154,04	2,4	Unacceptable	Note, Qm < 0.4 *
155,81	2,4	Unacceptable	Note, Qm < 0.4 *
157,58	2,4	Unacceptable	Note, Qm < 0.4 *
159,34	2,4	Unacceptable	Note, Qm < 0.4 *
161,11	2,35	Unacceptable	Note, Qm < 0.4 *
162,88	2,35	Unacceptable	Note, Qm < 0.4 *
164,65	2,35	Unacceptable	Note, Qm < 0.4 *
166,41	2,35	Unacceptable	Note, Qm < 0.4 *
168,18	2,35	Unacceptable	Note, Qm < 0.4 *
169,95	2,35	Unacceptable	Note, Qm < 0.4 *
171,72	2,3	Unacceptable	Note, Qm < 0.4 *
173,48	2,3	Unacceptable	Note, Qm < 0.4 *
175,25	2,3	Unacceptable	Note, Qm < 0.4 *
177,02	2,3	Unacceptable	Note, Qm < 0.4 *
178,79	2,3	Unacceptable	Note, Qm < 0.4 *
180,56	2,3	Unacceptable	Note, Qm < 0.4 *
182,32	2,3	Unacceptable	Note, Qm < 0.4 *
184,09	2,25	Unacceptable	Note, Qm < 0.4 *
185,86	2,25	Unacceptable	Note, Qm < 0.4 *
187,63	2,25	Unacceptable	Note, Qm < 0.4 *
189,39	2,25	Unacceptable	Note, Qm < 0.4 *
191,16	2,25	Unacceptable	Note, Qm < 0.4 *
192,93	2,25	Unacceptable	Note, Qm < 0.4 *
194,7	2,2	Unacceptable	Note, Qm < 0.4 *
196,46	2,2	Unacceptable	Note, Qm < 0.4 *
198,23	2,2	Unacceptable	Note, Qm < 0.4 *
200	2,2	Unacceptable	Note, Qm < 0.4 *

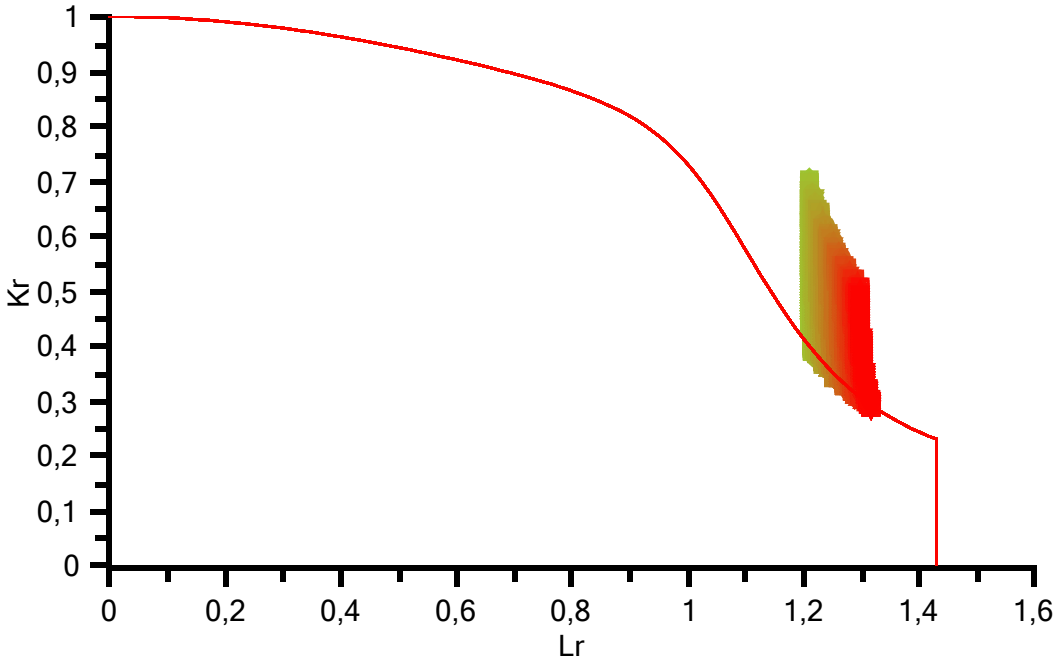

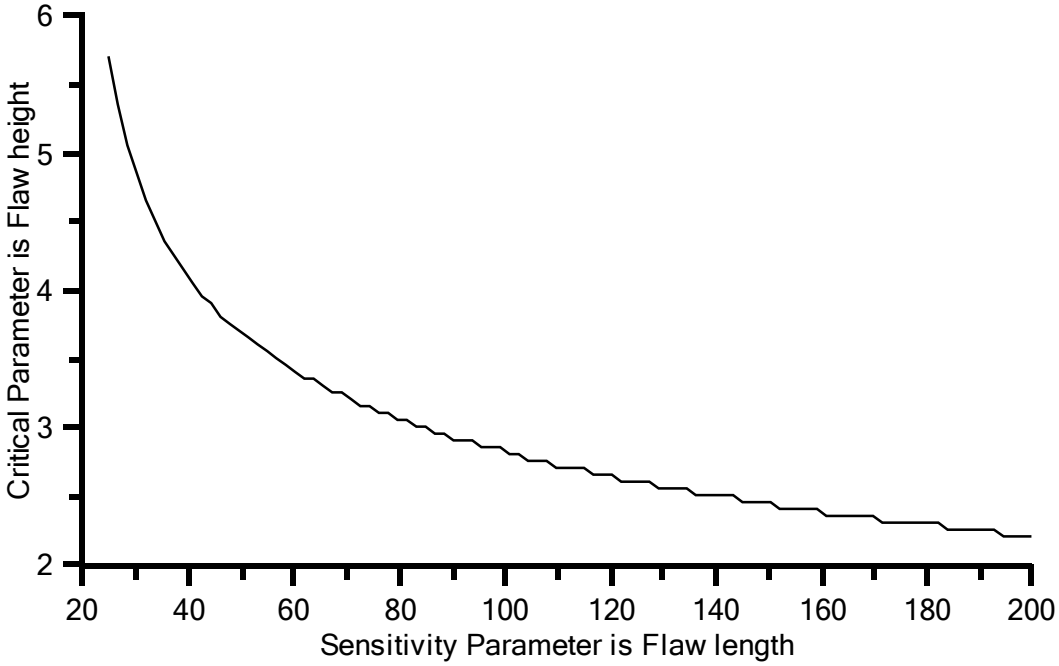

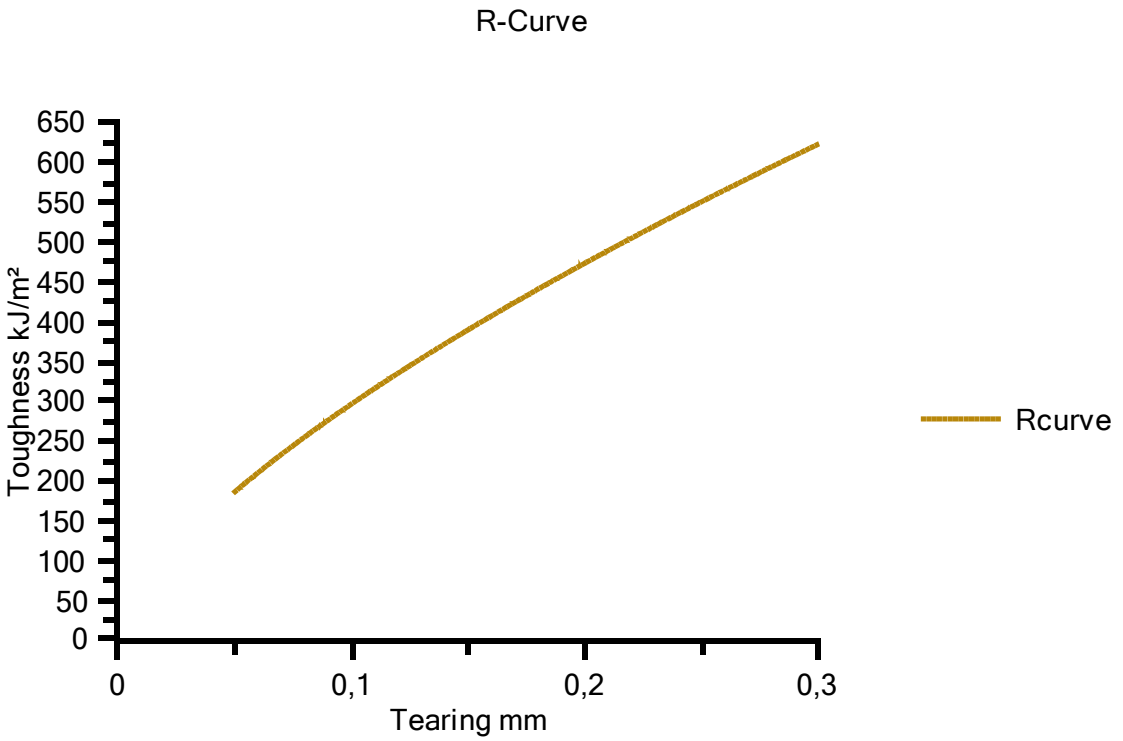

Stress strain curve

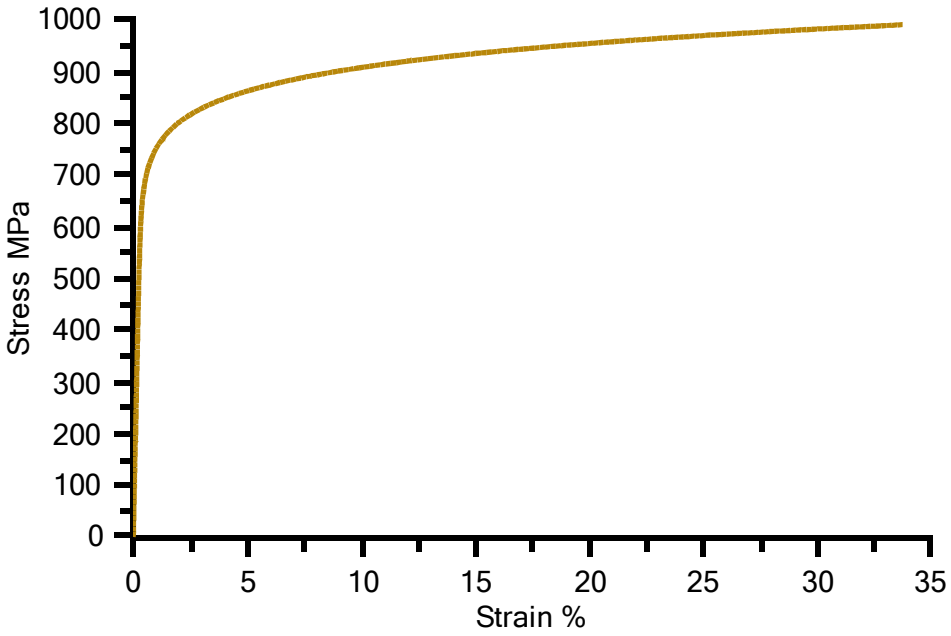

Appendix B

LINKpipe ECA Simulation Results Log

Table B.1 ECA Simulation Results Log (for **Figure 7.8** – Base Case)

Analysis ID	2c	a	Directory	Status	Stop Criteria	Crackgrowth	CrackDepth	CTOD
1	200	2	model0001	Ok		0.013	2.176	0.135
2	200	2.2	model0002	Ok		0.02	2.405	0.157
3	200	2.4	model0003	Ok		0.031	2.641	0.187
4	200	2.6	model0004	Ok		0.049	2.886	0.225
5	200	2.8	model0005	Ok		0.069	3.119	0.261
6	200	3	model0006	Ok		0.092	3.354	0.298
7	200	3.2	model0007	Ok		0.131	3.588	0.352
8	200	3.4	model0008	Ok		0.19	3.84	0.422
9	200	3.6	model0009	Ok		0.267	4.07	0.502
10	200	3.8	model0010	Failure	(CTOD)	0.414	4.399	0.63
11	195	3.644	model0011	Ok		0.285	4.101	0.519
12	195	3.844	model0012	Failure	(CTOD)	0.463	4.497	0.668
13	190	3.674	model0013	Failure	(CTOD)	0.299	4.147	0.531
14	190	3.474	model0014	Ok		0.214	3.921	0.449
15	185	3.682	model0015	Failure	(CTOD)	0.302	4.16	0.534
16	185	3.482	model0016	Ok		0.216	3.902	0.451
17	180	3.666	model0017	Ok		0.29	4.131	0.524
18	180	3.866	model0018	Failure	(CTOD)	0.474	4.531	0.676
19	175	3.678	model0019	Ok		0.295	4.147	0.528
20	175	3.878	model0020	Failure	(CTOD)	0.482	4.553	0.682
21	170	3.69	model0021	Failure	(CTOD)	0.304	4.17	0.536
22	170	3.49	model0022	Ok		0.219	3.874	0.454
23	165	3.662	model0023	Ok		0.291	4.127	0.524
24	165	3.862	model0024	Failure	(CTOD)	0.465	4.519	0.67
25	160	3.667	model0025	Ok		0.292	4.133	0.525
26	160	3.867	model0026	Failure	(CTOD)	0.465	4.523	0.669
27	155	3.68	model0027	Ok		0.291	4.147	0.525
28	155	3.88	model0028	Failure	(CTOD)	0.465	4.538	0.67
29	150	3.707	model0029	Failure	(CTOD)	0.303	4.187	0.536
30	150	3.507	model0030	Ok		0.219	3.886	0.453
31	145	3.695	model0031	Ok		0.292	4.164	0.526
32	145	3.895	model0032	Failure	(CTOD)	0.465	4.554	0.669
33	140	3.71	model0033	Failure	(CTOD)	0.298	4.186	0.531
34	140	3.51	model0034	Ok		0.217	3.889	0.451
35	135	3.716	model0035	Ok		0.297	4.191	0.53
36	135	3.916	model0036	Failure	(CTOD)	0.467	4.579	0.671
37	130	3.725	model0037	Failure	(CTOD)	0.302	4.206	0.534
38	130	3.525	model0038	Ok		0.219	3.907	0.454
39	125	3.709	model0039	Ok		0.291	4.177	0.524
40	125	3.909	model0040	Failure	(CTOD)	0.446	4.55	0.655
41	120	3.722	model0041	Ok		0.295	4.194	0.528
42	120	3.922	model0042	Failure	(CTOD)	0.453	4.569	0.66
43	115	3.735	model0043	Failure	(CTOD)	0.299	4.212	0.532
44	115	3.535	model0044	Ok		0.219	3.916	0.454
45	110	3.736	model0045	Ok		0.295	4.209	0.528
46	110	3.936	model0046	Failure	(CTOD)	0.445	4.576	0.654
47	105	3.748	model0047	Ok		0.296	4.222	0.529
48	105	3.948	model0048	Failure	(CTOD)	0.441	4.584	0.651
49	100	3.762	model0049	Ok		0.286	4.226	0.519
50	100	3.962	model0050	Failure	(CTOD)	0.419	4.576	0.633

Analysis ID	2c	a	Directory	Status	Stop Criteria	Crackgrowth	CrackDepth	CTOD
51	95	3.822	model0051	Failure	(CTOD)	0.305	4.31	0.537
52	95	3.622	model0052	Ok		0.224	4.012	0.458
53	90	3.822	model0053	Ok		0.297	4.299	0.529
54	90	4.022	model0054	Failure	(CTOD)	0.43	4.649	0.642
55	85	3.841	model0055	Failure	(CTOD)	0.298	4.319	0.53
56	85	3.641	model0056	Ok		0.22	4.026	0.454
57	80	3.856	model0057	Ok		0.294	4.329	0.527
58	80	4.056	model0058	Failure	(CTOD)	0.413	4.665	0.629
59	75	3.888	model0059	Failure	(CTOD)	0.3	4.366	0.532
60	75	3.688	model0060	Ok		0.22	4.072	0.455
61	70	3.901	model0061	Ok		0.288	4.366	0.521
62	70	4.101	model0062	Failure	(CTOD)	0.394	4.686	0.613
63	65	3.967	model0063	Failure	(CTOD)	0.298	4.443	0.53
64	65	3.767	model0064	Ok		0.218	4.151	0.453
65	60	4.016	model0065	Failure	(CTOD)	0.3	4.492	0.532
66	60	3.816	model0066	Ok		0.221	4.201	0.456
67	55	4.051	model0067	Ok		0.284	4.509	0.518
68	55	4.251	model0068	Failure	(CTOD)	0.368	4.805	0.592
69	50	4.174	model0069	Failure	(CTOD)	0.31	4.658	0.542
70	50	3.974	model0070	Ok		0.238	4.375	0.473
71	45	4.187	model0071	Ok		0.266	4.62	0.501
72	45	4.387	model0072	Failure	(CTOD)	0.327	4.89	0.557
73	40	4.49	model0073	Failure	(CTOD)	0.302	4.961	0.535
74	40	4.29	model0074	Ok		0.255	4.706	0.49
75	35	4.661	model0075	Ok		0.296	5.119	0.529
76	35	4.861	model0076	Failure	(CTOD)	0.34	5.369	0.568
77	30	4.873	model0077	Ok		0.273	5.293	0.507
78	30	5.073	model0078	Failure	(CTOD)	0.309	5.534	0.54
79	25	5.428	model0079	Ok		0.291	5.854	0.524
80	25	5.628	model0080	Failure	(CTOD)	0.301	6.068	0.533

Table B.2 ECA Simulation Results Log (for **Figure 7.14** – 0.5 Misalignment)

Analysis ID	2c	a	Directory	Status	Stop Criteria	Crackgrowth	CrackDepth	CTOD
1	200	2	model0001	Ok		0.021	2.303	0.161
2	200	2.2	model0002	Ok		0.036	2.555	0.199
3	200	2.4	model0003	Ok		0.057	2.816	0.24
4	200	2.6	model0004	Ok		0.078	3.061	0.276
5	200	2.8	model0005	Ok		0.107	3.315	0.321
6	200	3	model0006	Ok		0.165	3.566	0.394
7	200	3.2	model0007	Ok		0.248	3.8	0.483
8	200	3.4	model0008	Failure	(CTOD)	0.355	4.075	0.581
9	195	3.295	model0009	Ok		0.294	3.916	0.527
10	195	3.495	model0010	Failure	(CTOD)	0.419	4.248	0.633
11	190	3.306	model0011	Ok		0.297	3.925	0.53
12	190	3.506	model0012	Failure	(CTOD)	0.422	4.263	0.636
13	185	3.313	model0013	Failure	(CTOD)	0.3	3.922	0.532
14	185	3.113	model0014	Ok		0.205	3.673	0.439
15	180	3.308	model0015	Ok		0.296	3.913	0.529
16	180	3.508	model0016	Failure	(CTOD)	0.42	4.264	0.634
17	175	3.313	model0017	Ok		0.295	3.917	0.528
18	175	3.513	model0018	Failure	(CTOD)	0.419	4.267	0.633
19	170	3.324	model0019	Failure	(CTOD)	0.303	3.938	0.535
20	170	3.124	model0020	Ok		0.209	3.661	0.443
21	165	3.303	model0021	Ok		0.294	3.906	0.527
22	165	3.503	model0022	Failure	(CTOD)	0.417	4.255	0.632
23	160	3.304	model0023	Ok		0.294	3.906	0.527
24	160	3.504	model0024	Failure	(CTOD)	0.415	4.254	0.63
25	155	3.315	model0025	Ok		0.292	3.917	0.526
26	155	3.515	model0026	Failure	(CTOD)	0.412	4.263	0.628
27	150	3.343	model0027	Failure	(CTOD)	0.302	3.959	0.535
28	150	3.143	model0028	Ok		0.211	3.665	0.445
29	145	3.339	model0029	Failure	(CTOD)	0.298	3.95	0.531
30	145	3.139	model0030	Ok		0.208	3.664	0.442
31	140	3.341	model0031	Ok		0.295	3.95	0.528
32	140	3.541	model0032	Failure	(CTOD)	0.413	4.294	0.629
33	135	3.352	model0033	Ok		0.295	3.961	0.528
34	135	3.552	model0034	Failure	(CTOD)	0.412	4.305	0.628
35	130	3.369	model0035	Failure	(CTOD)	0.303	3.988	0.535
36	130	3.169	model0036	Ok		0.214	3.691	0.449
37	125	3.353	model0037	Ok		0.295	3.962	0.528
38	125	3.553	model0038	Failure	(CTOD)	0.408	4.302	0.625
39	120	3.359	model0039	Ok		0.294	3.967	0.527
40	120	3.559	model0040	Failure	(CTOD)	0.406	4.305	0.623
41	115	3.374	model0041	Failure	(CTOD)	0.298	3.989	0.531
42	115	3.174	model0042	Ok		0.213	3.678	0.447
43	110	3.378	model0043	Ok		0.296	3.991	0.529
44	110	3.578	model0044	Failure	(CTOD)	0.405	4.325	0.622
45	105	3.389	model0045	Ok		0.295	3.999	0.528
46	105	3.589	model0046	Failure	(CTOD)	0.4	4.33	0.618
47	100	3.409	model0047	Ok		0.287	4.014	0.52
48	100	3.609	model0048	Failure	(CTOD)	0.386	4.339	0.607
49	95	3.482	model0049	Failure	(CTOD)	0.308	4.117	0.54
50	95	3.282	model0050	Ok		0.23	3.814	0.465

Analysis ID	2c	a	Directory	Status	Stop Criteria	Crackgrowth	CrackDepth	CTOD
51	90	3.473	model0051	Ok		0.296	4.091	0.528
52	90	3.673	model0052	Failure	(CTOD)	0.393	4.414	0.613
53	85	3.495	model0053	Ok		0.296	4.116	0.529
54	85	3.695	model0054	Failure	(CTOD)	0.392	4.437	0.612
55	80	3.518	model0055	Ok		0.295	4.139	0.528
56	80	3.718	model0056	Failure	(CTOD)	0.388	4.456	0.608
57	75	3.553	model0057	Ok		0.297	4.176	0.53
58	75	3.753	model0058	Failure	(CTOD)	0.39	4.493	0.61
59	70	3.583	model0059	Ok		0.293	4.204	0.526
60	70	3.783	model0060	Failure	(CTOD)	0.382	4.516	0.603
61	65	3.638	model0061	Ok		0.295	4.264	0.528
62	65	3.838	model0062	Failure	(CTOD)	0.383	4.575	0.605
63	60	3.7	model0063	Ok		0.296	4.328	0.529
64	60	3.9	model0064	Failure	(CTOD)	0.387	4.642	0.608
65	55	3.766	model0065	Ok		0.289	4.388	0.522
66	55	3.966	model0066	Failure	(CTOD)	0.378	4.699	0.601
67	50	3.881	model0067	Failure	(CTOD)	0.309	4.528	0.541
68	50	3.681	model0068	Ok		0.243	4.242	0.478
69	45	3.897	model0069	Ok		0.265	4.493	0.5
70	45	4.097	model0070	Failure	(CTOD)	0.338	4.784	0.566
71	40	4.169	model0071	Failure	(CTOD)	0.311	4.821	0.542
72	40	3.969	model0072	Ok		0.249	4.543	0.484
73	35	4.264	model0073	Failure	(CTOD)	0.3	4.9	0.533
74	35	4.064	model0074	Ok		0.256	4.64	0.491
75	30	4.367	model0075	Ok		0.253	4.941	0.488
76	30	4.567	model0076	Ok		0.277	5.178	0.511
77	30	4.767	model0077	Failure	(CTOD)	0.31	5.423	0.541
78	25	5.291	model0078	Failure	(CTOD)	0.32	5.961	0.551
79	25	5.091	model0079	Ok		0.287	5.717	0.521

Table B.3 ECA Simulation Results Log (for **Figure 7.14** – 1.5 Misalignment)

Analysis ID	2c	a	Directory	Status	Stop Criteria	Crackgrowth	CrackDepth	CTOD
1	200	2	model0001	Ok		0.063	2.614	0.251
2	200	2.2	model0002	Ok		0.087	2.879	0.29
3	200	2.4	model0003	Ok		0.137	3.148	0.36
4	200	2.6	model0004	Ok		0.209	3.408	0.444
5	200	2.8	model0005	Failure	(CTOD)	0.331	3.69	0.56
6	195	2.748	model0006	Ok		0.286	3.592	0.52
7	195	2.948	model0007	Failure	(CTOD)	0.469	4.013	0.673
8	190	2.775	model0008	Failure	(CTOD)	0.305	3.634	0.537
9	190	2.575	model0009	Ok		0.198	3.369	0.432
10	185	2.756	model0010	Ok		0.288	3.599	0.522
11	185	2.956	model0011	Failure	(CTOD)	0.468	4.022	0.672
12	180	2.774	model0012	Failure	(CTOD)	0.301	3.649	0.533
13	180	2.574	model0013	Ok		0.197	3.352	0.431
14	175	2.766	model0014	Ok		0.291	3.608	0.524
15	175	2.966	model0015	Failure	(CTOD)	0.47	4.036	0.673
16	170	2.783	model0016	Failure	(CTOD)	0.306	3.645	0.538
17	170	2.583	model0017	Ok		0.201	3.364	0.434
18	165	2.755	model0018	Ok		0.287	3.592	0.521
19	165	2.955	model0019	Failure	(CTOD)	0.462	4.015	0.667
20	160	2.77	model0020	Failure	(CTOD)	0.299	3.621	0.531
21	160	2.57	model0021	Ok		0.198	3.343	0.431
22	155	2.769	model0022	Ok		0.29	3.611	0.523
23	155	2.969	model0023	Failure	(CTOD)	0.462	4.032	0.667
24	150	2.793	model0024	Failure	(CTOD)	0.306	3.657	0.538
25	150	2.593	model0025	Ok		0.201	3.37	0.434
26	145	2.772	model0026	Ok		0.286	3.611	0.52
27	145	2.972	model0027	Failure	(CTOD)	0.451	4.025	0.659
28	140	2.8	model0028	Failure	(CTOD)	0.304	3.664	0.536
29	140	2.6	model0029	Ok		0.202	3.337	0.435
30	135	2.786	model0030	Ok		0.29	3.633	0.523
31	135	2.986	model0031	Failure	(CTOD)	0.448	4.039	0.657
32	130	2.807	model0032	Failure	(CTOD)	0.307	3.676	0.539
33	130	2.607	model0033	Ok		0.201	3.389	0.435
34	125	2.777	model0034	Ok		0.282	3.613	0.515
35	125	2.977	model0035	Failure	(CTOD)	0.431	4.01	0.643
36	120	2.818	model0036	Failure	(CTOD)	0.308	3.688	0.54
37	120	2.618	model0037	Ok		0.204	3.338	0.438
38	115	2.791	model0038	Ok		0.29	3.637	0.523
39	115	2.991	model0039	Failure	(CTOD)	0.432	4.027	0.644
40	110	2.809	model0040	Ok		0.295	3.664	0.528
41	110	3.009	model0041	Failure	(CTOD)	0.438	4.055	0.649
42	105	2.825	model0042	Failure	(CTOD)	0.307	3.695	0.539
43	105	2.625	model0043	Ok		0.203	3.344	0.436
44	100	2.798	model0044	Ok		0.269	3.622	0.504
45	100	2.998	model0045	Failure	(CTOD)	0.389	3.99	0.61
46	95	2.907	model0046	Failure	(CTOD)	0.325	3.812	0.555
47	95	2.707	model0047	Ok		0.216	3.458	0.451
48	90	2.859	model0048	Ok		0.289	3.715	0.523
49	90	3.059	model0049	Failure	(CTOD)	0.404	4.076	0.621
50	85	2.889	model0050	Ok		0.297	3.758	0.53

Analysis ID	2c	a	Directory	Status	Stop Criteria	Crackgrowth	CrackDepth	CTOD
51	85	3.089	model0051	Failure	(CTOD)	0.41	4.118	0.627
52	80	2.906	model0052	Ok		0.295	3.776	0.528
53	80	3.106	model0053	Failure	(CTOD)	0.404	4.13	0.621
54	75	2.933	model0054	Failure	(CTOD)	0.298	3.81	0.531
55	75	2.733	model0055	Ok		0.213	3.48	0.448
56	70	2.952	model0056	Ok		0.291	3.823	0.524
57	70	3.152	model0057	Failure	(CTOD)	0.389	4.165	0.609
58	65	3.006	model0058	Ok		0.296	3.891	0.529
59	65	3.206	model0059	Failure	(CTOD)	0.389	4.228	0.61
60	60	3.056	model0060	Failure	(CTOD)	0.302	3.952	0.534
61	60	2.856	model0061	Ok		0.228	3.636	0.464
62	55	3.074	model0062	Ok		0.283	3.95	0.517
63	55	3.274	model0063	Failure	(CTOD)	0.359	4.266	0.584
64	50	3.199	model0064	Failure	(CTOD)	0.306	4.115	0.538
65	50	2.999	model0065	Ok		0.242	3.811	0.477
66	45	3.225	model0066	Ok		0.271	4.102	0.505
67	45	3.425	model0067	Failure	(CTOD)	0.324	4.392	0.554
68	40	3.531	model0068	Failure	(CTOD)	0.307	4.487	0.539
69	40	3.331	model0069	Ok		0.26	4.204	0.495
70	35	3.657	model0070	Ok		0.294	4.605	0.527
71	35	3.857	model0071	Failure	(CTOD)	0.352	4.896	0.579
72	30	3.852	model0072	Ok		0.278	4.79	0.512
73	30	4.052	model0073	Failure	(CTOD)	0.328	5.07	0.558
74	25	4.235	model0074	Ok		0.27	5.192	0.505
75	25	4.435	model0075	Ok		0.286	5.434	0.519
76	25	4.635	model0076	Failure	(CTOD)	0.309	5.684	0.541

Table B.4 ECA Simulation Results Log (for **Figure 7.14** – 2.5 Misalignment)

Analysis ID	2c	a	Directory	Status	Stop Criteria	Crackgrowth	CrackDepth	CTOD
1	200	2	model0001	Ok		0.168	2.909	0.398
2	200	2.2	model0002	Ok		0.28	3.232	0.514
3	200	2.4	model0003	Failure	(CTOD)	0.444	3.636	0.653
4	195	2.223	model0004	Ok		0.296	3.249	0.528
5	195	2.423	model0005	Failure	(CTOD)	0.465	3.688	0.669
6	190	2.227	model0006	Ok		0.296	3.251	0.529
7	190	2.427	model0007	Failure	(CTOD)	0.465	3.694	0.669
8	185	2.234	model0008	Failure	(CTOD)	0.3	3.265	0.533
9	185	2.034	model0009	Ok		0.182	2.954	0.414
10	180	2.228	model0010	Ok		0.295	3.252	0.528
11	180	2.428	model0011	Failure	(CTOD)	0.462	3.693	0.667
12	175	2.233	model0012	Ok		0.295	3.259	0.528
13	175	2.433	model0013	Failure	(CTOD)	0.461	3.699	0.667
14	170	2.242	model0014	Failure	(CTOD)	0.302	3.279	0.535
15	170	2.042	model0015	Ok		0.184	2.94	0.416
16	165	2.23	model0016	Ok		0.297	3.257	0.53
17	165	2.43	model0017	Failure	(CTOD)	0.464	3.698	0.669
18	160	2.223	model0018	Ok		0.293	3.244	0.527
19	160	2.423	model0019	Failure	(CTOD)	0.458	3.683	0.664
20	155	2.229	model0020	Ok		0.293	3.251	0.526
21	155	2.429	model0021	Failure	(CTOD)	0.453	3.686	0.66
22	150	2.246	model0022	Failure	(CTOD)	0.3	3.292	0.533
23	150	2.046	model0023	Ok		0.184	2.929	0.416
24	145	2.248	model0024	Failure	(CTOD)	0.298	3.283	0.531
25	145	2.048	model0025	Ok		0.184	2.948	0.416
26	140	2.25	model0026	Ok		0.297	3.284	0.53
27	140	2.45	model0027	Failure	(CTOD)	0.455	3.716	0.662
28	135	2.253	model0028	Ok		0.295	3.286	0.528
29	135	2.453	model0029	Failure	(CTOD)	0.449	3.713	0.657
30	130	2.265	model0030	Failure	(CTOD)	0.301	3.307	0.533
31	130	2.065	model0031	Ok		0.187	2.921	0.419
32	125	2.26	model0032	Failure	(CTOD)	0.298	3.298	0.531
33	125	2.06	model0033	Ok		0.185	2.913	0.417
34	120	2.257	model0034	Ok		0.294	3.288	0.527
35	120	2.457	model0035	Failure	(CTOD)	0.441	3.709	0.651
36	115	2.267	model0036	Failure	(CTOD)	0.299	3.308	0.532
37	115	2.067	model0037	Ok		0.188	2.924	0.42
38	110	2.266	model0038	Ok		0.296	3.302	0.528
39	110	2.466	model0039	Failure	(CTOD)	0.438	3.718	0.649
40	105	2.273	model0040	Ok		0.295	3.31	0.528
41	105	2.473	model0041	Failure	(CTOD)	0.434	3.722	0.645
42	100	2.288	model0042	Ok		0.288	3.323	0.521
43	100	2.488	model0043	Failure	(CTOD)	0.419	3.727	0.633
44	95	2.339	model0044	Failure	(CTOD)	0.31	3.414	0.542
45	95	2.139	model0045	Ok		0.204	3.036	0.438
46	90	2.323	model0046	Ok		0.291	3.371	0.524
47	90	2.523	model0047	Failure	(CTOD)	0.413	3.766	0.629
48	85	2.356	model0048	Failure	(CTOD)	0.302	3.425	0.534
49	85	2.156	model0049	Ok		0.202	3.055	0.436
50	80	2.357	model0050	Ok		0.294	3.418	0.527

Analysis ID	2c	a	Directory	Status	Stop Criteria	Crackgrowth	CrackDepth	CTOD
51	80	2.557	model0051	Failure	(CTOD)	0.408	3.803	0.625
52	75	2.379	model0052	Ok		0.296	3.446	0.528
53	75	2.579	model0053	Failure	(CTOD)	0.403	3.824	0.621
54	70	2.404	model0054	Ok		0.295	3.476	0.528
55	70	2.604	model0055	Failure	(CTOD)	0.396	3.847	0.615
56	65	2.438	model0056	Ok		0.295	3.519	0.528
57	65	2.638	model0057	Failure	(CTOD)	0.388	3.881	0.609
58	60	2.48	model0058	Failure	(CTOD)	0.298	3.573	0.53
59	60	2.28	model0059	Ok		0.218	3.227	0.453
60	55	2.517	model0060	Ok		0.29	3.609	0.523
61	55	2.717	model0061	Failure	(CTOD)	0.365	3.95	0.589
62	50	2.607	model0062	Failure	(CTOD)	0.301	3.731	0.533
63	50	2.407	model0063	Ok		0.234	3.401	0.469
64	45	2.657	model0064	Ok		0.274	3.763	0.509
65	45	2.857	model0065	Failure	(CTOD)	0.328	4.078	0.558
66	40	2.935	model0066	Failure	(CTOD)	0.317	4.153	0.548
67	40	2.735	model0067	Ok		0.263	3.841	0.498
68	35	2.972	model0068	Failure	(CTOD)	0.303	4.17	0.535
69	35	2.772	model0069	Ok		0.25	3.861	0.485
70	30	3.021	model0070	Ok		0.262	4.167	0.496
71	30	3.221	model0071	Failure	(CTOD)	0.31	4.466	0.542
72	25	3.452	model0072	Ok		0.273	4.684	0.507
73	25	3.652	model0073	Ok		0.292	4.95	0.525
74	25	3.852	model0074	Failure	(CTOD)	0.334	5.238	0.563

Table B.5 ECA Simulation Results Log (for **Figure 7.16** – Residual Stress = Yield)

Analysis ID	2c	a	Directory	Status	Stop Criteria	Crackgrowth	CrackDepth	CTOD
1	200	2	model0001	Ok		0.019	2.182	0.156
2	200	2.2	model0002	Ok		0.028	2.413	0.18
3	200	2.4	model0003	Ok		0.043	2.653	0.213
4	200	2.6	model0004	Ok		0.065	2.902	0.255
5	200	2.8	model0005	Ok		0.09	3.139	0.295
6	200	3	model0006	Ok		0.118	3.38	0.335
7	200	3.2	model0007	Ok		0.164	3.62	0.393
8	200	3.4	model0008	Ok		0.233	3.877	0.468
9	200	3.6	model0009	Failure	(CTOD)	0.323	4.113	0.553
10	195	3.546	model0010	Ok		0.294	4.036	0.527
11	195	3.746	model0011	Failure	(CTOD)	0.444	4.371	0.653
12	190	3.555	model0012	Ok		0.296	4.038	0.529
13	190	3.755	model0013	Failure	(CTOD)	0.45	4.386	0.658
14	185	3.564	model0014	Failure	(CTOD)	0.299	4.029	0.532
15	185	3.364	model0015	Ok		0.217	3.8	0.452
16	180	3.56	model0016	Ok		0.297	4.022	0.53
17	180	3.76	model0017	Failure	(CTOD)	0.45	4.392	0.657
18	175	3.561	model0018	Ok		0.295	4.022	0.528
19	175	3.761	model0019	Failure	(CTOD)	0.447	4.391	0.656
20	170	3.569	model0020	Failure	(CTOD)	0.301	4.036	0.533
21	170	3.369	model0021	Ok		0.219	3.816	0.454
22	165	3.552	model0022	Ok		0.295	4.013	0.528
23	165	3.752	model0023	Failure	(CTOD)	0.437	4.371	0.648
24	160	3.549	model0024	Ok		0.293	4.007	0.527
25	160	3.749	model0025	Failure	(CTOD)	0.433	4.364	0.645
26	155	3.558	model0026	Ok		0.291	4.015	0.524
27	155	3.758	model0027	Failure	(CTOD)	0.429	4.37	0.642
28	150	3.587	model0028	Failure	(CTOD)	0.3	4.055	0.533
29	150	3.387	model0029	Ok		0.22	3.782	0.455
30	145	3.593	model0030	Failure	(CTOD)	0.3	4.062	0.533
31	145	3.393	model0031	Ok		0.221	3.793	0.456
32	140	3.586	model0032	Ok		0.295	4.048	0.528
33	140	3.786	model0033	Failure	(CTOD)	0.438	4.408	0.648
34	135	3.594	model0034	Ok		0.294	4.055	0.527
35	135	3.794	model0035	Failure	(CTOD)	0.437	4.415	0.647
36	130	3.611	model0036	Failure	(CTOD)	0.301	4.082	0.534
37	130	3.411	model0037	Ok		0.223	3.788	0.458
38	125	3.6	model0038	Ok		0.296	4.065	0.529
39	125	3.8	model0039	Failure	(CTOD)	0.435	4.42	0.646
40	120	3.6	model0040	Ok		0.294	4.061	0.527
41	120	3.8	model0041	Failure	(CTOD)	0.428	4.411	0.641
42	115	3.612	model0042	Ok		0.296	4.077	0.529
43	115	3.812	model0043	Failure	(CTOD)	0.432	4.429	0.644
44	110	3.623	model0044	Failure	(CTOD)	0.298	4.09	0.531
45	110	3.423	model0045	Ok		0.223	3.8	0.458
46	105	3.63	model0046	Ok		0.295	4.093	0.528
47	105	3.83	model0047	Failure	(CTOD)	0.424	4.438	0.638
48	100	3.646	model0048	Ok		0.286	4.102	0.52
49	100	3.846	model0049	Failure	(CTOD)	0.41	4.441	0.626
50	95	3.708	model0050	Failure	(CTOD)	0.307	4.188	0.539

Analysis ID	2c	a	Directory	Status	Stop Criteria	Crackgrowth	CrackDepth	CTOD
51	95	3.508	model0051	Ok		0.232	3.898	0.467
52	90	3.695	model0052	Ok		0.294	4.159	0.527
53	90	3.895	model0053	Failure	(CTOD)	0.416	4.497	0.631
54	85	3.717	model0054	Ok		0.297	4.185	0.53
55	85	3.917	model0055	Failure	(CTOD)	0.417	4.52	0.632
56	80	3.736	model0056	Ok		0.294	4.201	0.528
57	80	3.936	model0057	Failure	(CTOD)	0.41	4.531	0.627
58	75	3.766	model0058	Failure	(CTOD)	0.298	4.234	0.531
59	75	3.566	model0059	Ok		0.231	3.953	0.466
60	70	3.786	model0060	Ok		0.292	4.247	0.525
61	70	3.986	model0061	Failure	(CTOD)	0.4	4.569	0.619
62	65	3.834	model0062	Ok		0.294	4.298	0.527
63	65	4.034	model0063	Failure	(CTOD)	0.4	4.617	0.618
64	60	3.888	model0064	Failure	(CTOD)	0.302	4.358	0.534
65	60	3.688	model0065	Ok		0.232	4.076	0.467
66	55	3.909	model0066	Ok		0.284	4.359	0.518
67	55	4.109	model0067	Failure	(CTOD)	0.374	4.66	0.597
68	50	4.016	model0068	Failure	(CTOD)	0.308	4.489	0.54
69	50	3.816	model0069	Ok		0.237	4.207	0.472
70	45	4.025	model0070	Ok		0.269	4.453	0.504
71	45	4.225	model0071	Failure	(CTOD)	0.339	4.732	0.567
72	40	4.267	model0072	Failure	(CTOD)	0.306	4.732	0.538
73	40	4.067	model0073	Ok		0.249	4.467	0.484
74	35	4.371	model0074	Failure	(CTOD)	0.304	4.827	0.536
75	35	4.171	model0075	Ok		0.263	4.578	0.498
76	30	4.423	model0076	Ok		0.256	4.815	0.491
77	30	4.623	model0077	Ok		0.284	5.048	0.518
78	30	4.823	model0078	Failure	(CTOD)	0.323	5.292	0.553
79	25	5.174	model0079	Failure	(CTOD)	0.316	5.621	0.547
80	25	4.974	model0080	Ok		0.279	5.38	0.513

Table B.6 ECA Simulation Results Log (for **Figure 7.16** – Residual Stress = Yield With Enabled Relaxation)

Analysis ID	2c	a	Directory	Status	Stop Criteria	Crackgrowth	CrackDepth	CTOD
1	200	2	model0001	Ok		0.015	2.178	0.144
2	200	2.2	model0002	Ok		0.023	2.408	0.167
3	200	2.4	model0003	Ok		0.036	2.645	0.197
4	200	2.6	model0004	Ok		0.056	2.892	0.238
5	200	2.8	model0005	Ok		0.078	3.127	0.276
6	200	3	model0006	Ok		0.103	3.365	0.314
7	200	3.2	model0007	Ok		0.144	3.601	0.369
8	200	3.4	model0008	Ok		0.207	3.855	0.441
9	200	3.6	model0009	Ok		0.288	4.088	0.522
10	200	3.8	model0010	Failure	(CTOD)	0.458	4.443	0.664
11	195	3.611	model0011	Ok		0.293	4.074	0.527
12	195	3.811	model0012	Failure	(CTOD)	0.47	4.468	0.673
13	190	3.621	model0013	Ok		0.296	4.086	0.528
14	190	3.821	model0014	Failure	(CTOD)	0.475	4.483	0.677
15	185	3.631	model0015	Failure	(CTOD)	0.3	4.101	0.532
16	185	3.431	model0016	Ok		0.215	3.88	0.45
17	180	3.626	model0017	Ok		0.296	4.094	0.529
18	180	3.826	model0018	Failure	(CTOD)	0.473	4.488	0.676
19	175	3.629	model0019	Ok		0.295	4.095	0.528
20	175	3.829	model0020	Failure	(CTOD)	0.471	4.488	0.674
21	170	3.637	model0021	Failure	(CTOD)	0.301	4.111	0.534
22	170	3.437	model0022	Ok		0.218	3.857	0.452
23	165	3.619	model0023	Ok		0.294	4.084	0.527
24	165	3.819	model0024	Failure	(CTOD)	0.462	4.469	0.667
25	160	3.619	model0025	Ok		0.293	4.083	0.526
26	160	3.819	model0026	Failure	(CTOD)	0.458	4.465	0.664
27	155	3.63	model0027	Ok		0.291	4.092	0.525
28	155	3.83	model0028	Failure	(CTOD)	0.455	4.473	0.662
29	150	3.655	model0029	Failure	(CTOD)	0.3	4.128	0.532
30	150	3.455	model0030	Ok		0.218	3.83	0.453
31	145	3.662	model0031	Failure	(CTOD)	0.3	4.136	0.533
32	145	3.462	model0032	Ok		0.219	3.838	0.454
33	140	3.655	model0033	Ok		0.294	4.123	0.527
34	140	3.855	model0034	Failure	(CTOD)	0.454	4.5	0.661
35	135	3.665	model0035	Ok		0.294	4.133	0.527
36	135	3.865	model0036	Failure	(CTOD)	0.456	4.511	0.663
37	130	3.68	model0037	Failure	(CTOD)	0.302	4.157	0.534
38	130	3.48	model0038	Ok		0.221	3.86	0.456
39	125	3.665	model0039	Ok		0.293	4.131	0.526
40	125	3.865	model0040	Failure	(CTOD)	0.446	4.501	0.654
41	120	3.673	model0041	Ok		0.295	4.141	0.528
42	120	3.873	model0042	Failure	(CTOD)	0.446	4.508	0.654
43	115	3.684	model0043	Ok		0.297	4.155	0.53
44	115	3.884	model0044	Failure	(CTOD)	0.449	4.523	0.657
45	110	3.693	model0045	Failure	(CTOD)	0.298	4.165	0.53
46	110	3.493	model0046	Ok		0.221	3.873	0.456
47	105	3.699	model0047	Ok		0.295	4.168	0.528
48	105	3.899	model0048	Failure	(CTOD)	0.437	4.526	0.648
49	100	3.716	model0049	Ok		0.286	4.176	0.519

Analysis ID	2c	a	Directory	Status	Stop Criteria	Crackgrowth	CrackDepth	CTOD
50	100	3.916	model0050	Failure	(CTOD)	0.418	4.525	0.633
51	95	3.776	model0051	Failure	(CTOD)	0.308	4.263	0.54
52	95	3.576	model0052	Ok		0.228	3.967	0.463
53	90	3.761	model0053	Ok		0.29	4.225	0.523
54	90	3.961	model0054	Failure	(CTOD)	0.421	4.573	0.635
55	85	3.798	model0055	Failure	(CTOD)	0.3	4.275	0.533
56	85	3.598	model0056	Ok		0.225	3.985	0.46
57	80	3.805	model0057	Ok		0.292	4.273	0.525
58	80	4.005	model0058	Failure	(CTOD)	0.415	4.611	0.63
59	75	3.841	model0059	Failure	(CTOD)	0.298	4.315	0.531
60	75	3.641	model0060	Ok		0.225	4.028	0.46
61	70	3.862	model0061	Ok		0.291	4.328	0.525
62	70	4.062	model0062	Failure	(CTOD)	0.404	4.655	0.622
63	65	3.914	model0063	Ok		0.297	4.385	0.53
64	65	4.114	model0064	Failure	(CTOD)	0.403	4.705	0.621
65	60	3.959	model0065	Failure	(CTOD)	0.3	4.432	0.532
66	60	3.759	model0066	Ok		0.224	4.144	0.459
67	55	3.991	model0067	Ok		0.284	4.445	0.518
68	55	4.191	model0068	Failure	(CTOD)	0.371	4.744	0.595
69	50	4.109	model0069	Failure	(CTOD)	0.31	4.588	0.541
70	50	3.909	model0070	Ok		0.237	4.304	0.472
71	45	4.12	model0071	Ok		0.268	4.55	0.503
72	45	4.32	model0072	Failure	(CTOD)	0.333	4.825	0.562
73	40	4.39	model0073	Failure	(CTOD)	0.303	4.858	0.536
74	40	4.19	model0074	Ok		0.253	4.599	0.488
75	35	4.529	model0075	Failure	(CTOD)	0.299	4.984	0.531
76	35	4.329	model0076	Ok		0.264	4.743	0.499
77	30	4.674	model0077	Ok		0.259	5.075	0.494
78	30	4.874	model0078	Failure	(CTOD)	0.298	5.319	0.53
79	25	5.321	model0079	Failure	(CTOD)	0.301	5.755	0.533
80	25	5.121	model0080	Ok		0.268	5.519	0.503

Table B.7 ECA Simulation Results Log (for **Figure 7.19** – Weld Under-match)

Analysis ID	2c	a	Directory	Status	Stop Criteria	Crackgrowth	CrackDepth	CTOD
1	200	2	model0001	Ok		0.06	2.248	0.246
2	200	2.2	model0002	Ok		0.075	2.479	0.272
3	200	2.4	model0003	Ok		0.101	2.724	0.312
4	200	2.6	model0004	Ok		0.143	2.973	0.368
5	200	2.8	model0005	Ok		0.217	3.221	0.452
6	200	3	model0006	Failure	(CTOD)	0.322	3.477	0.552
7	195	2.956	model0007	Ok		0.294	3.415	0.527
8	195	3.156	model0008	Failure	(CTOD)	0.43	3.74	0.642
9	190	2.966	model0009	Ok		0.297	3.422	0.529
10	190	3.166	model0010	Failure	(CTOD)	0.433	3.753	0.644
11	185	2.973	model0011	Failure	(CTOD)	0.299	3.413	0.531
12	185	2.773	model0012	Ok		0.201	3.168	0.435
13	180	2.973	model0013	Ok		0.297	3.411	0.529
14	180	3.173	model0014	Failure	(CTOD)	0.43	3.759	0.642
15	175	2.977	model0015	Ok		0.296	3.414	0.529
16	175	3.177	model0016	Failure	(CTOD)	0.429	3.761	0.641
17	170	2.984	model0017	Failure	(CTOD)	0.302	3.427	0.534
18	170	2.784	model0018	Ok		0.204	3.165	0.438
19	165	2.968	model0019	Ok		0.294	3.403	0.527
20	165	3.168	model0020	Failure	(CTOD)	0.424	3.748	0.638
21	160	2.971	model0021	Ok		0.294	3.406	0.527
22	160	3.171	model0022	Failure	(CTOD)	0.424	3.751	0.638
23	155	2.982	model0023	Ok		0.291	3.415	0.525
24	155	3.182	model0024	Failure	(CTOD)	0.417	3.755	0.632
25	150	3.013	model0025	Failure	(CTOD)	0.304	3.46	0.536
26	150	2.813	model0026	Ok		0.208	3.156	0.442
27	145	3.007	model0027	Ok		0.296	3.446	0.529
28	145	3.207	model0028	Failure	(CTOD)	0.421	3.786	0.635
29	140	3.017	model0029	Ok		0.297	3.458	0.53
30	140	3.217	model0030	Failure	(CTOD)	0.418	3.794	0.633
31	135	3.025	model0031	Ok		0.296	3.464	0.529
32	135	3.225	model0032	Failure	(CTOD)	0.415	3.798	0.63
33	130	3.039	model0033	Failure	(CTOD)	0.302	3.487	0.535
34	130	2.839	model0034	Ok		0.21	3.18	0.444
35	125	3.026	model0035	Ok		0.294	3.465	0.527
36	125	3.226	model0036	Failure	(CTOD)	0.41	3.796	0.626
37	120	3.036	model0037	Ok		0.295	3.475	0.528
38	120	3.236	model0038	Failure	(CTOD)	0.411	3.806	0.627
39	115	3.048	model0039	Failure	(CTOD)	0.298	3.491	0.53
40	115	2.848	model0040	Ok		0.209	3.189	0.444
41	110	3.056	model0041	Ok		0.297	3.499	0.529
42	110	3.256	model0042	Failure	(CTOD)	0.408	3.825	0.625
43	105	3.068	model0043	Ok		0.295	3.509	0.528
44	105	3.268	model0044	Failure	(CTOD)	0.404	3.833	0.622
45	100	3.088	model0045	Ok		0.285	3.52	0.519
46	100	3.288	model0046	Failure	(CTOD)	0.386	3.836	0.607
47	95	3.168	model0047	Failure	(CTOD)	0.31	3.631	0.542
48	95	2.968	model0048	Ok		0.228	3.335	0.463
49	90	3.154	model0049	Ok		0.296	3.601	0.529
50	90	3.354	model0050	Failure	(CTOD)	0.396	3.915	0.615

Analysis ID	2c	a	Directory	Status	Stop Criteria	Crackgrowth	CrackDepth	CTOD
51	85	3.172	model0051	Ok		0.294	3.617	0.527
52	85	3.372	model0052	Failure	(CTOD)	0.39	3.927	0.61
53	80	3.202	model0053	Ok		0.295	3.649	0.528
54	80	3.402	model0054	Failure	(CTOD)	0.386	3.955	0.607
55	75	3.24	model0055	Failure	(CTOD)	0.299	3.692	0.531
56	75	3.04	model0056	Ok		0.23	3.409	0.465
57	70	3.264	model0057	Ok		0.291	3.707	0.524
58	70	3.464	model0058	Failure	(CTOD)	0.369	3.999	0.593
59	65	3.335	model0059	Ok		0.297	3.788	0.53
60	65	3.535	model0060	Failure	(CTOD)	0.371	4.075	0.594
61	60	3.395	model0061	Ok		0.296	3.847	0.529
62	60	3.595	model0062	Failure	(CTOD)	0.368	4.132	0.592
63	55	3.462	model0063	Ok		0.287	3.906	0.521
64	55	3.662	model0064	Failure	(CTOD)	0.354	4.185	0.58
65	50	3.606	model0065	Failure	(CTOD)	0.31	4.076	0.541
66	50	3.406	model0066	Ok		0.253	3.808	0.488
67	45	3.621	model0067	Ok		0.264	4.04	0.499
68	45	3.821	model0068	Failure	(CTOD)	0.322	4.308	0.553
69	40	3.96	model0069	Failure	(CTOD)	0.316	4.438	0.547
70	40	3.76	model0070	Ok		0.259	4.173	0.494
71	35	4.047	model0071	Failure	(CTOD)	0.306	4.507	0.538
72	35	3.847	model0072	Ok		0.263	4.257	0.498
73	30	4.098	model0073	Ok		0.251	4.489	0.486
74	30	4.298	model0074	Ok		0.279	4.722	0.513
75	30	4.498	model0075	Failure	(CTOD)	0.312	4.96	0.544
76	25	4.951	model0076	Failure	(CTOD)	0.304	5.391	0.537
77	25	4.751	model0077	Ok		0.273	5.156	0.507

Table B.8 ECA Simulation Results Log (for **Figure 7.22** – Max Misalignment and Residual Stress with Enabled Relaxation)

Analysis ID	2c	a	Directory	Status	Stop Criteria	Crackgrowth	CrackDepth	CTOD
1	200	2	model0001	Ok		0.103	2.776	0.315
2	200	2.2	model0002	Ok		0.162	3.057	0.39
3	200	2.4	model0003	Ok		0.256	3.324	0.491
4	200	2.6	model0004	Failure	(CTOD)	0.387	3.653	0.608
5	195	2.467	model0005	Ok		0.294	3.417	0.527
6	195	2.667	model0006	Failure	(CTOD)	0.439	3.792	0.649
7	190	2.475	model0007	Failure	(CTOD)	0.3	3.451	0.532
8	190	2.275	model0008	Ok		0.193	3.166	0.426
9	185	2.469	model0009	Ok		0.295	3.438	0.528
10	185	2.669	model0010	Failure	(CTOD)	0.437	3.792	0.647
11	180	2.475	model0011	Failure	(CTOD)	0.298	3.425	0.531
12	180	2.275	model0012	Ok		0.192	3.155	0.425
13	175	2.474	model0013	Ok		0.296	3.417	0.529
14	175	2.674	model0014	Failure	(CTOD)	0.437	3.8	0.648
15	170	2.479	model0015	Failure	(CTOD)	0.298	3.407	0.531
16	170	2.279	model0016	Ok		0.192	3.145	0.425
17	165	2.48	model0017	Ok		0.297	3.427	0.53
18	165	2.68	model0018	Failure	(CTOD)	0.436	3.805	0.647
19	160	2.483	model0019	Failure	(CTOD)	0.301	3.416	0.533
20	160	2.283	model0020	Ok		0.195	3.13	0.428
21	155	2.472	model0021	Ok		0.291	3.391	0.525
22	155	2.672	model0022	Failure	(CTOD)	0.428	3.787	0.64
23	150	2.488	model0023	Failure	(CTOD)	0.299	3.42	0.532
24	150	2.288	model0024	Ok		0.195	3.141	0.428
25	145	2.486	model0025	Ok		0.296	3.415	0.529
26	145	2.686	model0026	Failure	(CTOD)	0.43	3.808	0.642
27	140	2.495	model0027	Failure	(CTOD)	0.298	3.428	0.531
28	140	2.295	model0028	Ok		0.195	3.147	0.429
29	135	2.496	model0029	Ok		0.295	3.426	0.528
30	135	2.696	model0030	Failure	(CTOD)	0.426	3.816	0.639
31	130	2.507	model0031	Failure	(CTOD)	0.299	3.444	0.531
32	130	2.307	model0032	Ok		0.197	3.106	0.43
33	125	2.509	model0033	Ok		0.295	3.443	0.528
34	125	2.709	model0034	Failure	(CTOD)	0.421	3.827	0.635
35	120	2.521	model0035	Failure	(CTOD)	0.298	3.46	0.53
36	120	2.321	model0036	Ok		0.199	3.104	0.432
37	115	2.529	model0037	Ok		0.296	3.469	0.529
38	115	2.729	model0038	Failure	(CTOD)	0.418	3.849	0.633
39	110	2.541	model0039	Failure	(CTOD)	0.302	3.49	0.535
40	110	2.341	model0040	Ok		0.205	3.154	0.439
41	105	2.528	model0041	Ok		0.288	3.458	0.522
42	105	2.728	model0042	Failure	(CTOD)	0.403	3.831	0.621
43	100	2.563	model0043	Failure	(CTOD)	0.299	3.513	0.532
44	100	2.363	model0044	Ok		0.205	3.162	0.439
45	95	2.574	model0045	Ok		0.297	3.524	0.53
46	95	2.774	model0046	Failure	(CTOD)	0.406	3.891	0.623
47	90	2.59	model0047	Ok		0.295	3.541	0.528
48	90	2.79	model0048	Failure	(CTOD)	0.402	3.905	0.62
49	85	2.615	model0049	Ok		0.297	3.573	0.53

Analysis ID	2c	a	Directory	Status	Stop Criteria	Crackgrowth	CrackDepth	CTOD
50	85	2.815	model0050	Failure	(CTOD)	0.401	3.935	0.62
51	80	2.638	model0051	Ok		0.296	3.6	0.529
52	80	2.838	model0052	Failure	(CTOD)	0.396	3.957	0.615
53	75	2.67	model0053	Failure	(CTOD)	0.298	3.641	0.531
54	75	2.47	model0054	Ok		0.217	3.304	0.452
55	70	2.693	model0055	Ok		0.296	3.665	0.529
56	70	2.893	model0056	Failure	(CTOD)	0.396	4.021	0.615
57	65	2.726	model0057	Ok		0.29	3.698	0.524
58	65	2.926	model0058	Failure	(CTOD)	0.388	4.049	0.608
59	60	2.794	model0059	Ok		0.294	3.783	0.527
60	60	2.994	model0060	Failure	(CTOD)	0.393	4.135	0.612
61	55	2.867	model0061	Failure	(CTOD)	0.304	3.879	0.536
62	55	2.667	model0062	Ok		0.234	3.558	0.469
63	50	2.892	model0063	Ok		0.289	3.888	0.522
64	50	3.092	model0064	Failure	(CTOD)	0.365	4.215	0.59
65	45	2.992	model0065	Ok		0.288	4.002	0.521
66	45	3.192	model0066	Failure	(CTOD)	0.359	4.321	0.585
67	40	3.14	model0067	Failure	(CTOD)	0.302	4.186	0.534
68	40	2.94	model0068	Ok		0.243	3.882	0.479
69	35	3.231	model0069	Ok		0.286	4.265	0.52
70	35	3.431	model0070	Failure	(CTOD)	0.336	4.557	0.565
71	30	3.455	model0071	Ok		0.288	4.514	0.521
72	30	3.655	model0072	Failure	(CTOD)	0.32	4.786	0.551
73	25	3.792	model0073	Ok		0.273	4.871	0.508
74	25	3.992	model0074	Failure	(CTOD)	0.319	5.152	0.55

Appendix C

LINKpipe ECA Simulation Results Sample for Clad Pipes

LINKpipe ECA Simulation Results Sample for Clad Pipes

(First Reeling Cycle)

Input data	
ID	BaseCaseCladPipeWithFCG.lpp
Project File	BaseCaseCladPipeWithFCG.lpp
Base material	
E-modulus	200000.0
Poisson Ratio	0.3
Yield Stress	500.00
Tensile Stress	553.83
Stress strain curve type	Power Law
Hardening Exponent	0.051
Stress strain curve	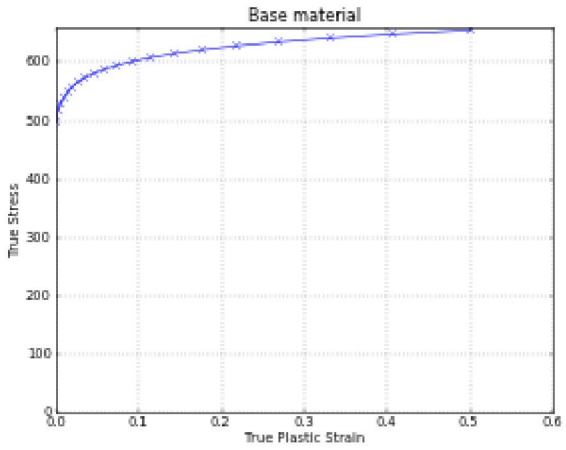
Weld material	
E-modulus	170000.0
Poisson Ratio	0.3
Yield Stress	310.00
Tensile Stress	752.90
Stress strain curve type	Power Law
Hardening Exponent	0.232
Stress strain curve	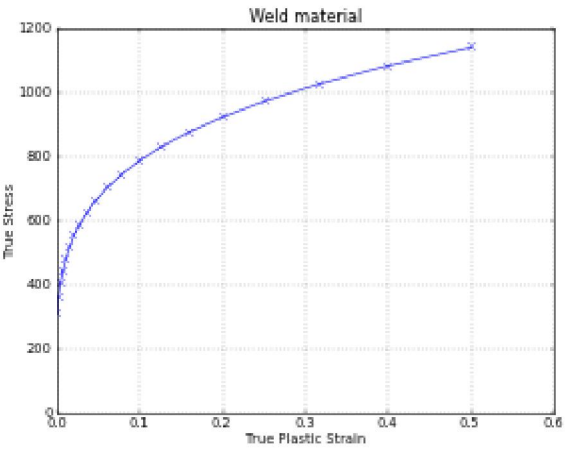
Ductile Crack Growth	
CTODi	0.001
c1	0.752
c2	0.786
Crack resistance curve	

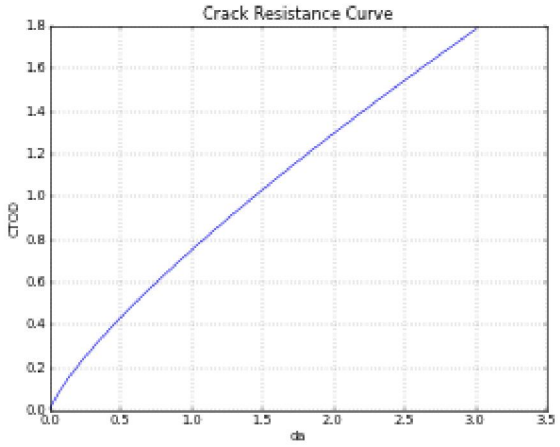

Pipe	
Outer Diameter	273.1
Wall Thickness	17.7
Length	1638.6
Misalignment	
No Misalignment	
Crack	
Crack Depth	2.9
Crack Length	45.0
Orientation	Circumferential
Type	Outside
Shape	Rectangular
Offset angle from centric crack	0.0
Weld	
Width Top	0.0
Width Bottom	0.0
Crack Position	Middle of Weld
Mesh Parameters	
DX1	75.0
DX2	3.0
DY1	10.0
DY2	2.0
DY	1.5
Minimum number of line-spring elements	0
Maximum number of line-spring elements	0
Residual Stresses	
No Residual Stresses	
Load Station	
Name	Reel Cycle 2
Type	Rotation
Pi	0.0
Pe	0.0
Total Global Rotation	0.1062
Max Global Increment	0.01
Number of times to store results	2000

Results

Calculation status	OK

Overview

Load station	Crack type	Crack Depth	Crack Length	CTOD	Ductile crack growth
		2.90	45.00	0.00	0.00
Reel Cycle 2	Surface	3.19	45.00	0.21	0.19

Calculation details

Result Directory	C:\Users\SS7N1346\Documents\Master Thesis\19 Simulation File LINKpipe3-001\Analysis1
Start Time	2013-06-05 10:40:41
End Time	10:41:30
CPU Seconds	48.843

LINKpipe ECA Simulation Results Sample for Clad Pipes

(Second Reeling Cycle)

Input data	
ID	BaseCaseCladPipeWithFCG.lpp
Project File	BaseCaseCladPipeWithFCG.lpp
Base material	
E-modulus	200000.0
Poisson Ratio	0.3
Yield Stress	500.00
Tensile Stress	553.83
Stress strain curve type	Power Law
Hardening Exponent	0.051
Stress strain curve	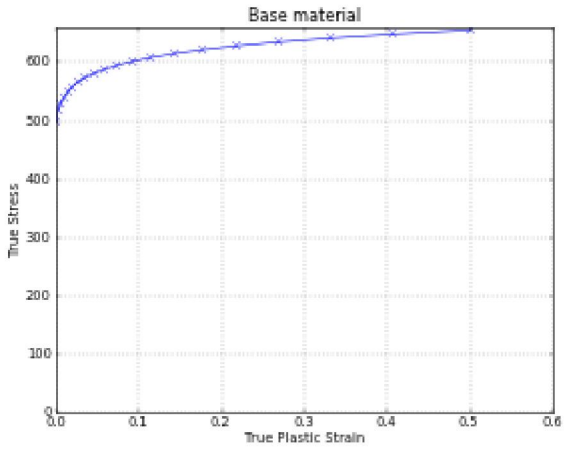
Weld material	
E-modulus	170000.0
Poisson Ratio	0.3
Yield Stress	310.00
Tensile Stress	752.90
Stress strain curve type	Power Law
Hardening Exponent	0.232
Stress strain curve	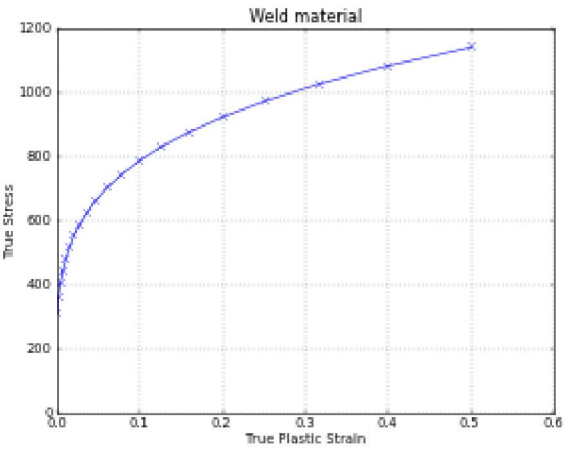
Ductile Crack Growth	
CTODi	0.001
c1	0.752
c2	0.786
Crack resistance curve	

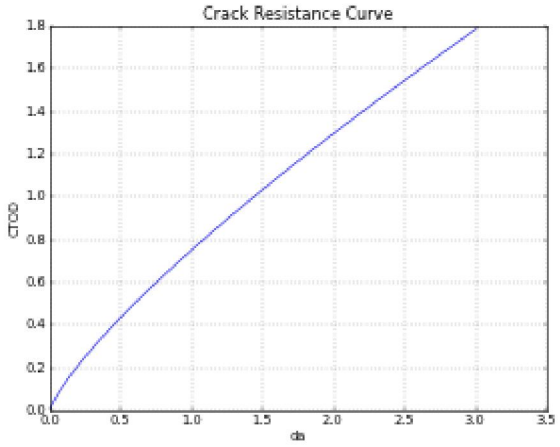

Pipe	
Outer Diameter	273.1
Wall Thickness	17.7
Length	1638.6
Misalignment	
No Misalignment	
Crack	
Crack Depth	3.19
Crack Length	45.0
Orientation	Circumferential
Type	Outside
Shape	Rectangular
Offset angle from centric crack	0.0
Weld	
Width Top	0.0
Width Bottom	0.0
Crack Position	Middle of Weld
Mesh Parameters	
DX1	75.0
DX2	3.0
DY1	10.0
DY2	2.0
DY	1.5
Minimum number of line-spring elements	0
Maximum number of line-spring elements	0
Residual Stresses	
No Residual Stresses	
Load Station	
Name	Reel Cycle 2
Type	Rotation
Pi	0.0
Pe	0.0
Total Global Rotation	0.0852
Max Global Increment	0.01
Number of times to store results	2000

Results

Calculation status	OK

Overview

Load station	Crack type	Crack Depth	Crack Length	CTOD	Ductile crack growth
		3.19	45.00	0.00	0.00
Reel Cycle 2	Surface	3.50	45.00	0.22	0.20

Calculation details

Result Directory	C:\Users\SS7N1346\Documents\Master Thesis\19 Simulation File LINKpipe3-002\Analysis1
Start Time	2013-06-05 10:42:01
End Time	10:42:43
CPU Seconds	41.714

LINKpipe ECA Simulation Results Sample for Clad Pipes

(Third Reeling Cycle)

Input data	
ID	BaseCaseCladPipeWithFCG.lpp
Project File	BaseCaseCladPipeWithFCG.lpp
Base material	
E-modulus	200000.0
Poisson Ratio	0.3
Yield Stress	500.00
Tensile Stress	553.83
Stress strain curve type	Power Law
Hardening Exponent	0.051
Stress strain curve	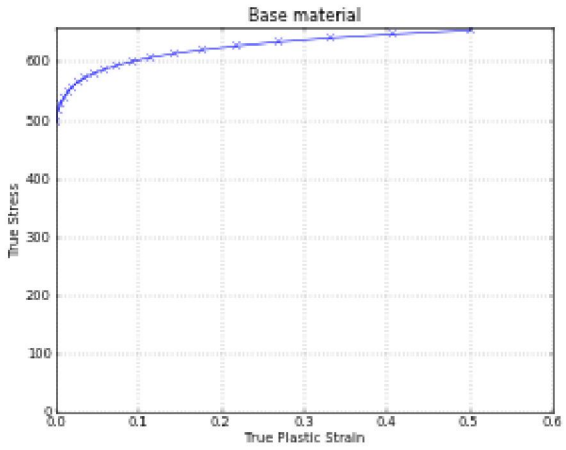
Weld material	
E-modulus	170000.0
Poisson Ratio	0.3
Yield Stress	310.00
Tensile Stress	752.90
Stress strain curve type	Power Law
Hardening Exponent	0.232
Stress strain curve	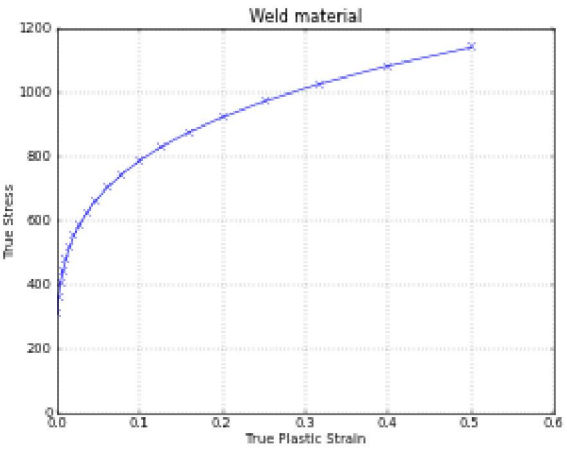
Ductile Crack Growth	
CTODi	0.001
c1	0.752
c2	0.786
Crack resistance curve	

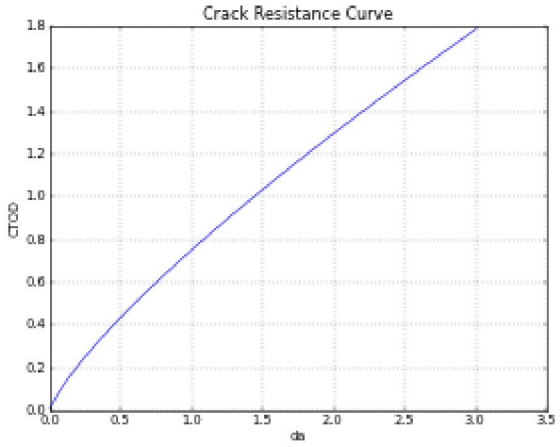

Pipe	
Outer Diameter	273.1
Wall Thickness	17.7
Length	1638.6
Misalignment	
No Misalignment	
Crack	
Crack Depth	3.5
Crack Length	45.0
Orientation	Circumferential
Type	Outside
Shape	Rectangular
Offset angle from centric crack	0.0
Weld	
Width Top	0.0
Width Bottom	0.0
Crack Position	Middle of Weld
Mesh Parameters	
DX1	75.0
DX2	3.0
DY1	10.0
DY2	2.0
DY	1.5
Minimum number of line-spring elements	0
Maximum number of line-spring elements	0
Residual Stresses	
No Residual Stresses	
Load Station	
Name	Reel Cycle 2
Type	Rotation
Pi	0.0
Pe	0.0
Total Global Rotation	0.0972
Max Global Increment	0.01
Number of times to store results	2000

Results

Calculation status	OK

Overview

Load station	Crack type	Crack Depth	Crack Length	CTOD	Ductile crack growth
		3.50	45.00	0.00	0.00
Reel Cycle 2	Surface	3.88	45.00	0.26	0.26

Calculation details

Result Directory	C:\Users\SS7N1346\Documents\Master Thesis\19 Simulation File LINKpipe3-003\Analysis1
Start Time	2013-06-05 10:43:11
End Time	10:43:57
CPU Seconds	45.801

LINKpipe ECA Simulation Results Sample for Clad Pipes

(Fatigue Crack Growth)

Input data	
ID	BaseCaseCladPipeWithFCG.lpp
Project File	BaseCaseCladPipeWithFCG.lpp
Base material	
E-modulus	200000.0
Poisson Ratio	0.3
Yield Stress	500.00
Tensile Stress	553.83
Stress strain curve type	Power Law
Hardening Exponent	0.051
Stress strain curve	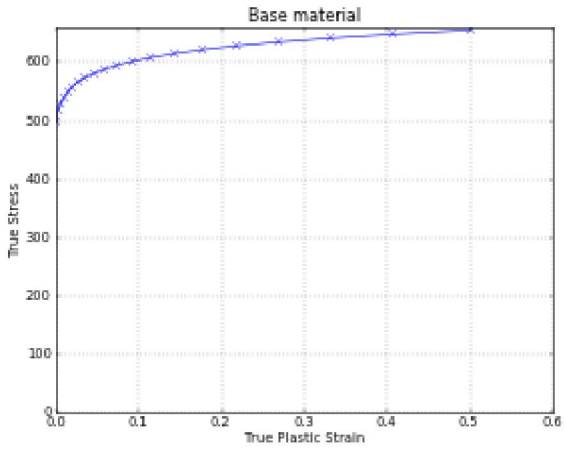
Weld material	
E-modulus	170000.0
Poisson Ratio	0.3
Yield Stress	310.00
Tensile Stress	752.90
Stress strain curve type	Power Law
Hardening Exponent	0.232
Stress strain curve	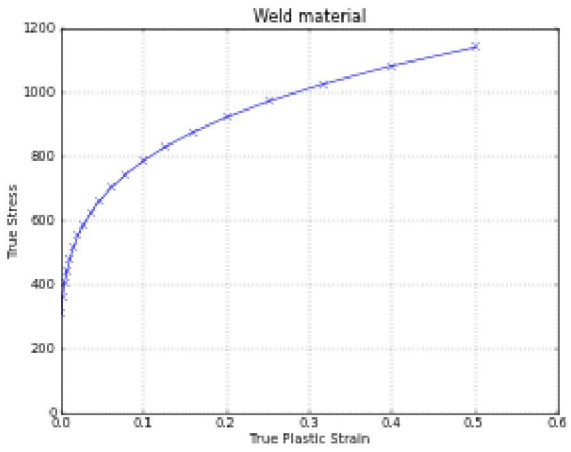
Ductile Crack Growth	
CTODi	0.001
c1	0.752
c2	0.786
Crack resistance curve	

	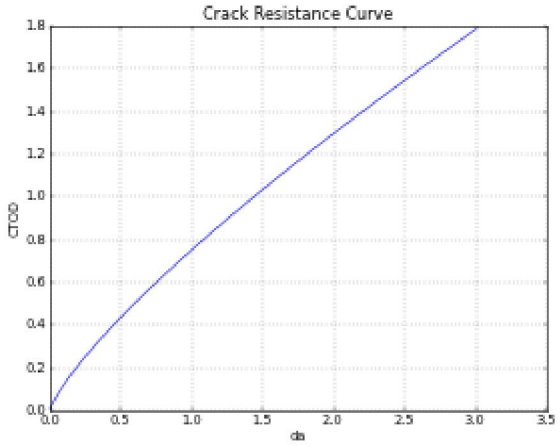
High cycle fatigue growth	
Curve name	Paris
Curve data	**deltaK0 C m** 63.0 2.1e-17 5.1 144.0 1.29e-12 2.88
Paris curve	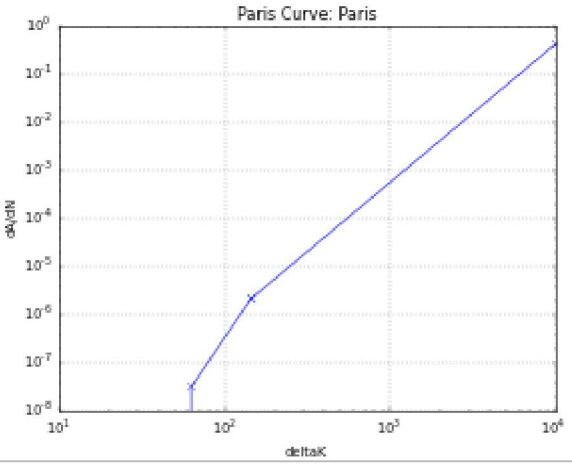
Pipe	
Outer Diameter	273.1
Wall Thickness	17.7
Length	1638.6
Misalignment	
No Misalignment	
Crack	
Crack Depth	3.88
Crack Length	45.0
Orientation	Circumferential
Type	Outside
Shape	Rectangular
Offset angle from centric crack	0.0
Weld	
Width Top	0.0
Width Bottom	0.0
Crack Position	Middle of Weld
Mesh Parameters	

DX1	75.0
DX2	5.0
DY1	20.0
DY2	3.0
DY	1.5
Minimum number of line-spring elements	0
Maximum number of line-spring elements	0

Residual Stresses

No Residual Stresses	

Load Station

Name	Installation Fatigue
Type	BS7910 Fatigue
Geometry	Cylinder
Crack type	Previous
Paris curve for Outside crack	Paris
Recategorisation	No recategorisation
Number of increments in Paris integration	1000
Number of times to store results	1000

Stress sprectrum>

Cycles	Membran stress	Bending stress
510	26.8	4.87
845	52.8	9.61
995	79.6	14.48
941	105.6	19.21
708	132.3	24.09
623	158.4	28.82
426	185.1	33.69
390	211.1	38.43
234	237.9	43.3
251	264.7	48.17
132	290.7	52.91
126	317.5	57.78
24	343.5	62.51
36	370.3	67.39
30	396.3	72.12
12	423.0	76.99
0	449.1	81.73
12	475.8	86.6
12	502.6	91.47
6	528.6	96.21

Results

Calculation status	OK

Overview

Load station	Crack type	Crack Depth	Crack Length	CTOD	Fatigue crack growth	Cycles
		3.88	45.00	0.00	0.00	0
Installation Fatigue	Surface	6.75	46.15	0.00	2.87	6313

Calculation details

Result Directory	C:\Users\SS7N1346\Documents\Master Thesis\19 Simulation File LINKpipe3-001\Analysis1
Start Time	2013-06-05 11:22:45
End Time	11:28:28

CPU Seconds	336.275